

MR11-03
(14 April - 5 May 2011)
Preliminary Cruise Report



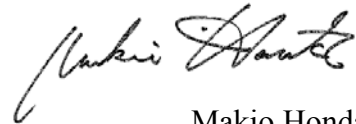
June 2011
JAMSTEC

Note

This cruise report is a preliminary documentation published in approximately a month after the end of this cruise. It may not be corrected even if changes on contents are found after publication. It may also be changed without notice. Data on the cruise report may be raw or not processed. Please ask the principal investigator and persons in charge of respective observations for the latest information and permission before using. Users of data are requested to submit their results to JAMSTEC Data Integration and Analysis Group (DIAG).

June 2011

Principal Investigator of MR11-03

A handwritten signature in black ink, appearing to read 'Makio Honda', written in a cursive style.

Makio Honda
JAMSTEC

Cruise Report ERRATA of the Nutrients part

page	Error	Correction
66	potassium nitrate CAS No. 7757-91-1	potassium nitrate CAS No. 7757-79-1
64	1N H ₂ SO ₄	1M H ₂ SO ₄

Cruise Report ERRATA of the Photosynthetic Pigments part

page	Error	Correction
92	Ethyl-apo-8'-carotenoate	trans-β-Apo-8'-carotenal

Contents of MR11-03 Preliminary Cruise Report

A. Cruise summary

1. Cruise information

A1

- (1) Cruise designation
- (2) Cruise title
- (3) Principal investigator
- (4) Science proposal of cruise
- (5) Cruise period (port call)
- (6) Cruise region (geographical boundary)
- (7) Cruise track and stations

2. Overview of MR11-03

A3

- (1) Objective
- (2) Overview of MR11-03

B. Text

1. Outline of MR11-03

- 1.1 Cruise summary
 - (1) Introduction of principal science proposal 1
 - (2) Objective of this cruise 1
 - (3) Overview of MR11-03 2
 - (4) Scientific gears 6
- 1.2 Track and log 7
- 1.3 Cruise participants 14

2. General observation

- 2.1 Meteorological observations
 - 2.1.1 Surface meteorological observation 16
 - 2.1.2 Ceilometer observation 23
 - 2.1.3 Lidar observations of clouds and aerosols 25
 - 2.1.4 Optical characteristics of aerosol observed by ship-borne sky-radiometer 27
 - 2.1.5 Tropospheric aerosol and gas profile observations by MAX-DOAS on a research vessel 28
 - 2.1.6 Rain, water vapor and surface water sampling 30
 - 2.1.7 Air-Sea surface eddy flux measurement 34
- 2.2 Physical oceanographic observations
 - 2.2.1 CTD cast and water sampling 35
 - 2.2.2 Salinity measurement 40

2.2.3 Shipboard ADCP	45
2.3 Sea surface water monitoring	49
2.4 Dissolved oxygen	54
2.5 Nutrients	58
2.6 pH	75
2.7 Dissolved inorganic carbon –DIC-	78
2.8 Total alkalinity	81
2.9 Underway pCO ₂	84
3. Special observation	
3.1 Phytoplankton	
3.1.1 Chlorophyll a measurements by fluorometric determination	86
3.1.2 HPLC measurements of marine phytoplankton pigments	91
3.1.3 Phytoplankton abundance	96
3.1.4 Primary production and new production	99
3.1.5 P vs E curve	105
3.1.6 Oxygen evolution (gross primary production) and FRRF observation	108
3.2 Drifting sediment trap of JAMSTEC	
3.2.1 Drifting mooring system	111
3.2.2 JAMSTEC drifting sediment trap	114
3.2.3 Vertical changes of fecal pellets	115
3.3 Po-210 and export flux	118
3.4 Zooplankton	
3.4.1 Community structure and ecological roles	119
3.4.2 Grazing pressure of microzooplankton	122
3.4.3 Biological study of phytoplankton and zooplankton	124
3.5 Active carbon flux	129
3.6 Community structures and metabolic activities of microbes	131
3.7 Dissolved organic carbon	133
3.8 Chlorofluorocarbon	134
3.9 Argo float	137
3.10 Optical measurement of marine snow: Visual Plankton Recorder (VPR)	141
3.11 Absolute salinity measurements of seawater	144
3.12 Validation of GOSAT products over the sea using a ship-borne high-resolution Fourier transform spectrometer	146

3.13	Observational research on air-sea interaction in the Kuroshio-Oyashio Extension region	149
3.14	The Tohoku Earthquake impact on deep-sea environment	153
3.15	Sampling for radiation monitoring	154
4. Geophysical observation		
4.1	Swath bathymetry	158
4.2	Sea surface gravity	160
4.3	Sea surface magnetic field	161
5.	Satellite image acquisition (MCSST from NOAA/HPRT)	164 - 165

Cover sheet: the first prize of “MR11-03 CRUISE REPORT COVER SHEET CONTEST” by M.C Honda. Photo was taken by using fish-eye camera when radiosonde observation was conducted. What? Red balloon?

A. Cruise summary

1. Cruise information

(1) Cruise designation (research vessel)

MR11-03 (R/V MIRAI)

(2) Cruise title (principal science proposal) and introduction

Change in material cycles and ecosystem by the climate change and its feedback

Introduction

Some disturbing effects are progressively coming to the fore in the ocean by climate change, such as rising water temperature, intensification of upper ocean stratification and ocean acidification. It is supposed that these effects result in serious damage to the ocean ecosystems. Disturbed ocean ecosystems will change a material cycle through the change of biological pump efficiency, and it will be fed back into the climate. We are aimed at clarifying the mechanisms of changes in the ocean structure in ocean ecosystems derived from the climate change,

We arranged the time-series observation stations in the subarctic gyre (K2: 47°N 160°E) and the subtropical gyre (S1: 30°N, 145°E) in the western North Pacific. In general, biological pump is more efficient in the subarctic gyre than the subtropical gyre because large size phytoplankton (diatom) is abundant in the subarctic gyre by its eutrophic oceanic condition. It is suspected that the responses against climate change are different for respective gyres. To elucidate the oceanic structures in ocean ecosystems and material cycles at both gyres is important to understand the relationship between ecosystem, material cycle and climate change in the global ocean.

There are significant seasonal variations in the ocean environments in both gyres. The seasonal variability of oceanic structures will be estimated by the mooring systems and by the seasonally repetitive ship observations scheduled for next several years.

(3) Principal Investigator (PI)

Makio Honda

Research Institute for Global Change (RIGC)

Japan Agency for Marine-Earth Science and Technology (JAMSTEC)

(4) Science proposals of cruise

Affiliation	PI	Proposal titles
AORI / The Univ. Tokyo	Koji HAMASAKI	Studies on the microbial-geochemical processes that regulate the operation of the biological pump in the subarctic and subtropical regions of the western North Pacific
JAMSTEC RIGC	Hiroshi UCHIDA	1. Absolute salinity measurements of seawater 2. Temporal changes in water properties of abyssal water in the western North Pacific
JAXA	Hiroshi OHYAMA	Validation of GOSAT products over the sea using a ship-borne high-resolution Fourier transform spectrometer
JAMSTEC RIGC	Yoshimi KAWAI	Observational research on air-sea interaction in the Kuroshio-Oyashio Extension region
JAMSTEC BioGeoss / KCC	Ken TAKAI / Weiren LIN	The Tohoku Earthquake impact on deep-sea environment

not onboard study		
Kagoshima Univ.	Toru KOBARI	Effects of meso-zooplankton on food web and vertical flux
Okayama Univ.	Osamu TSUKAMOTO	Onboard continuous air-sea eddy flux measurement
JAMSTEC	Hisanori TAKASHIMA	Tropospheric aerosol and gas profile observations by MAX-DOAS on a research vessel
Toyama Univ.	Kazuma AOKI	Maritime aerosol optical properties from measurements of Ship-borne sky radiometer
JAMSTEC	Toshio SUGA	Study of ocean circulation and heat and freshwater transport and their variability, and experimental comprehensive study of physical, chemical, and biochemical processes in the western North Pacific by the deployment of Argo floats and using Argo data
NIES	Nobuo SUGIMOTO	Study of distribution and optical characteristics of ice/water clouds and marine aerosols
Chiba Univ.	Masao NAKANISHI	Tectonics of the mid-Cretaceous Pacific Plate
Ryukyu Univ.	Takeshi MATSUMOTO	Standardization of marine geophysical data and its application to the ocean floor geodynamics studies
JAMSTEC	Yoshimi KAWAI	Observational research on air-sea interaction in the Kuroshio-Oyashio Extension region
JAMSTEC	Naoyuki KURITA	Rain and seawater sampling for stable isotopes

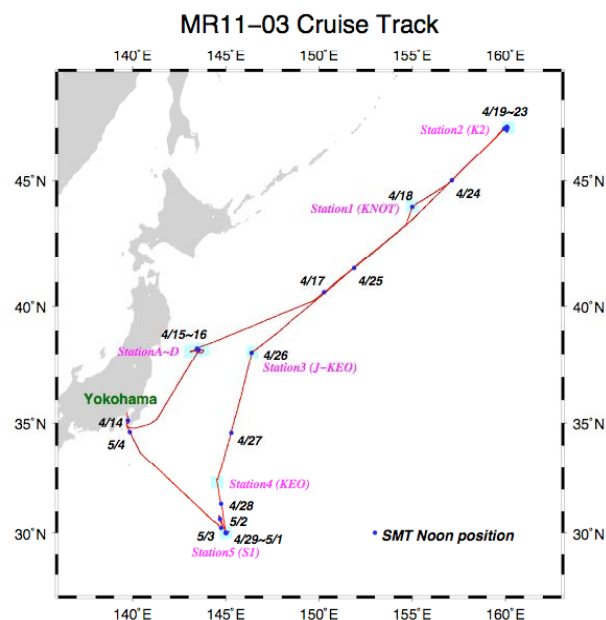
(5) Cruise period (port call)

14 April 2011 (Yokohama) – 5 May 2011 (Yokohama)

(6) Cruise region (geographical boundary)

The western North Pacific (50°N – 30°N, 140°E – 160°W)

(7) Cruise track and stations



2. Overview of MR11-03

(1) Objective

Objective of this cruise is to collect biological, biogeochemical and physical data in winter at our western Pacific time-series stations K2 (sub-arctic gyre) and S1 (sub-tropical data).

(2) Overview of MR11-03

1) Urgent research relating the great East Japan Earthquake

On 11 March 2011, the great earthquake of magnitude 9 occurred off Miyagi prefecture, Japan. This earthquake and the relevant tsunami with its height of more than 10 m attacked mainly the Pacific coastline of Tohoku district and approximately thirty thousand people were killed, missing or injured. What is worse is that Fukushima No.1 nuclear power plant was seriously damaged by this earthquake and the tsunami, resulting that a gigantic radiation has been leaking to the atmosphere, land and ocean. After this record crisis, the Ministry of Education, Culture, Sports, Science and Technology (MEXT) requested JAMSTEC to send JAMSTEC fleets to 30 km off Fukushima in order to monitor level of radiation of seawater, air and aerosol. R/V Mirai also participated this monitoring activity for approximately two weeks. After this contribution, it was decided that R/V Mirai starts original scientific cruise (MR11-03) in the western North Pacific with additional mission. This is water sampling near seafloor of earthquake and the tsunami source (Fig.1). This is based on the hypothesis that gasses and bacteria might be emitted from seafloor after the earthquake. We conducted four hydrocasts there. As a result, low beam transmittance layer was discovered near seafloor (Fig.2). It is suspected that this is attributed to re-suspension of seafloor sediment by the earthquake. In future, results of chemical and biological analysis of collected seawater will supply new insights, and more precise geological / geophysical / biological / geochemical researches will be conducted by JAMSTEC research vessels, deep-tow, ROV and Shinkai submersible.

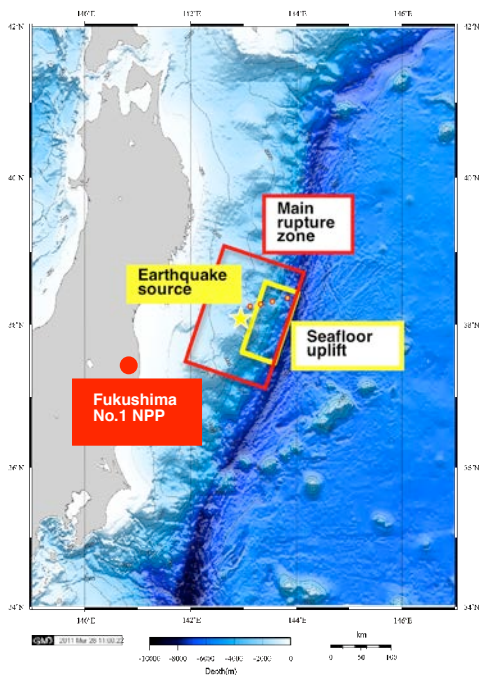


Fig. 1 Urgent research area near the earthquake / tsunami source

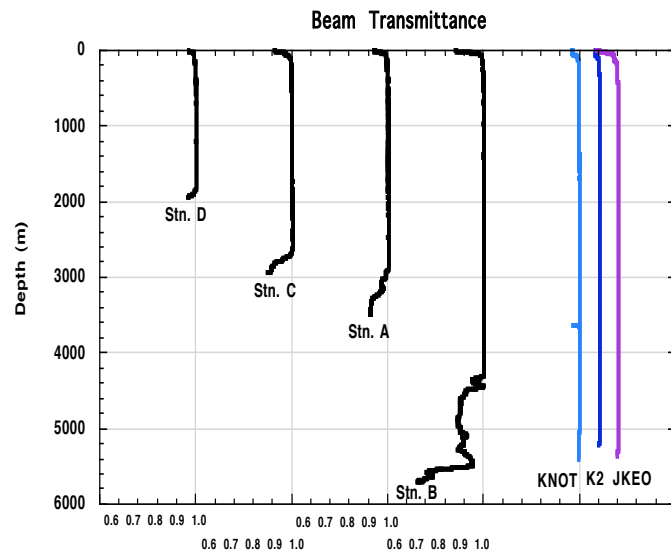


Fig. 2 Vertical profile of beam transmittance at urgent investigation area: stations A, B, C, D. For comparison, vertical profiles at our time-series stations are also shown

2) Outline of time-series observation at station K2 and S1

In order to certify seasonal and annual variability in ecosystem and biogeochemistry in the western North Pacific, biological and biogeochemical observation were conducted at time-series stations: K2 and S1 succeeding cruises of MR10-06 (September-October 2010) and MR11-02 (January-February 2011). Followings are main features during this cruise.

2-1) Station K2

Surface seawater temperature was approximately 1.7°C and less than that during last winter cruise: MR11-02 (approximately 2°C) (Fig. 3a). However temperature minimum layer with 1°C was observed at around 100 m and, thus, the maximum winter condition was likely over. Concentration of Si(OH)₄ in the surface seawater was approximately 42 μmol kg⁻¹ and constant upper 100 m (Fig. 3b). Based on previous reports, this concentration was almost the annual maximum at station K2. Concentration of chlorophyll-*a* was slightly higher than or comparable to that during the last winter cruise (MR11-02) (Fig. 3c). Integrated primary productivity was approximately 200 mg-C m⁻² day⁻¹ and higher than that during MR11-02 (Fig. 3d).

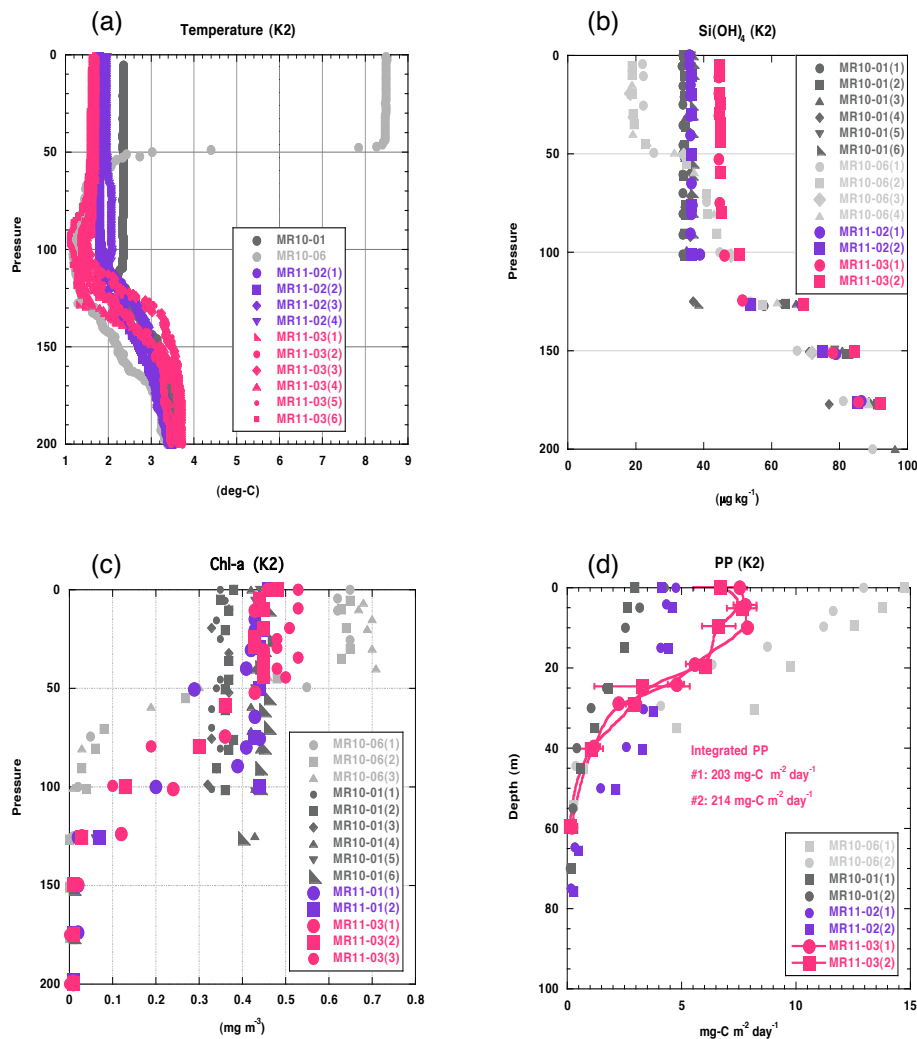


Fig. 3 Vertical profiles of (a) water temperature, (b) Si(OH)₄, (c) chlorophyll-*a* and (d) primary productivity at station K2

It was notable that standing stocks of planktonic foraminifera were quite high at station K2 (Kimoto, personal communication). Maximum of standing stock was approximately 3,000 individuals m^{-3} above 100 m water depths. Most dominant species was *Globigerina bulloides* and occupied more than 60 % of total individuals. *G. bulloides* is well known as a carnivorous species and an upwelling indicator, therefore production of this species should be related with increasing of small zooplankton and nutrient supply by vertical mixing in this area. This remarkable foraminiferal production had never been recorded from other seasons' observations (i.e. February ~ March 2010 and October ~ November 2010), and their higher production should contribute to transportation of carbon to the intermediate/deep water and ocean carbonate chemistry in the north Pacific. This is supported by large foraminifera flux in spring observed by time-series sediment trap at station K2 previously.



Fig. 4 Planktonic foraminifera recovered by vertical plankton tow

Moreover, adult copepodite *Neocalanus cristatus* (stage c5) was observed upper 50m by IONESS sampling (Kitamura, personal communication) (Fig. 5). During the last winter cruise (MR11-02), adult copepodite was observed between 200 m and 300 m for resting or hibernation. It is reported that adult copepodite dies between 200 m and 500 m after egg laying. After hatching, larva ascends to upper layer and grows up gradually toward autumn. Thus, the existence of adult copepodite in April is indicative of that *Neocalanus cristatus* quickly grew up during the last few months or adult copepodite does not die below 200 m. If the former is true, grazing pressure might be higher in April than previous reports. If the latter is true, carbon flux by zooplankton ontogenetic migration might be smaller than we expected. Future biological analysis of the collected sample and additional onboard experiments will reveal the role of zooplankton in the carbon cycle at



Fig.5 Copepodite *Neocalanus cristatus* collected by IONESS

station K2.

2-2) Station S1

Water temperature near surface was approximately 19°C (Fig. 6a) and higher than that during the last cruise (MR11-02). The surface mixed layer was approximately 40 m and shallower than that during MR11-02 (~ 120 m). Concentration of nitrate (NO_3) near surface was nearly zero (Fig. 6b). Chlorophyll-a was variable and its average was comparable to that observed in January-February 2010 (Fig. 6c). Integrated chlorophyll-a was estimated to be 43 mg m^{-2} . Primary productivity at surface was 13 $\text{mg-C m}^{-3} \text{ day}^{-1}$ and decreased with depth (Fig. 6d). Integrated primary productivity was approximately 356 $\text{mg-C m}^{-2} \text{ day}^{-1}$. During the last cruise, high primary productivity higher than 1,000 $\text{mg-C m}^{-2} \text{ day}^{-1}$ was observed (see MR11-02 preliminary cruise report) and, thus, nutrients were almost consumed within the last two months. However standing stock of phytoplankton was not small and primary productivity still continues. It is one of scientific interests how to maintain primary productivity in the subtropical area, that is, how macro- and micro-nutrients (e.g. Fe) are supplied to sun-lit layer: horizontal transport from the land? via atmosphere? or from subsurface by diffusion?

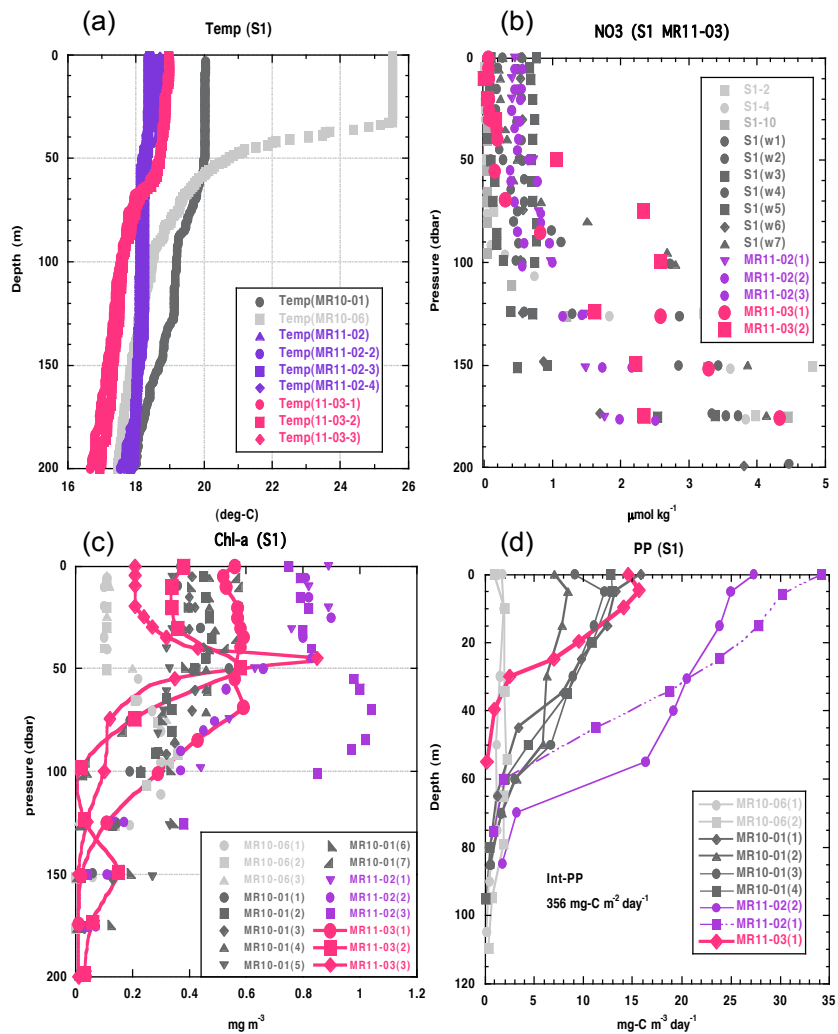


Fig. 6 Vertical profiles of (a) water temperature, (b) NO_3 , (c) chlorophyll-a, and (d) primary productivity at S1

B. Text

1. Outline of MR11-03

Makio HONDA (JAMSTEC RIGC)

Principal Investigator of MR11-03

1.1 Cruise summary

(1) Introduction of principal science proposal

Some disturbing effects are progressively coming to the fore in the ocean by climate change, such as rising water temperature, intensification of upper ocean stratification and oceanic acidification. It is supposed that these effects result in serious damage to the ocean ecosystems. Disturbed ocean ecosystems will change a material cycle through the change of biological pump efficiency, and it will be fed back into the climate. We are aimed at clarifying the mechanisms of changes in the oceanic structure in ocean ecosystems derived from the climate change,

We arranged the time-series observation stations in the subarctic gyre (K2: 47°N 160°E) and the subtropical gyre (S1: 30°N, 145°E) in the western North Pacific. In general, biological pump is more efficient in the subarctic gyre than the subtropical gyre because large size phytoplankton (diatom) is abundant in the subarctic gyre by its eutrophic oceanic condition. It is suspected that the responses against climate change are different for respective gyres. To elucidate the oceanic structures in ocean ecosystems and material cycles at both gyres is important to understand the relationship between ecosystem, material cycle and climate change in the global ocean.

There are significant seasonal variations in the ocean environments in both gyres. The seasonal variability of oceanic structures will be estimated by the mooring systems and by the seasonally repetitive ship observations scheduled for next several years.

(2) Objective of this cruise

Objective of this cruise is to collect biogeochemical and physical data in winter at our western Pacific time-series stations K2 (subarctic gyre) and S1 (subtropical data).

(3) Overview of MR11-03

1) Urgent research relating the great East Japan Earthquake

On 11 March 2011, the great earthquake of magnitude 9 occurred off Miyagi prefecture, Japan. This earthquake and the relevant tsunami with its height of more than 10 m attacked mainly the Pacific coastline of Tohoku district and approximately thirty thousand people were killed, missing or injured. What is worse is that Fukushima No.1 nuclear power plant was seriously damaged by this earthquake and the tsunami, resulting that a gigantic radiation has been leaking to the atmosphere, land and ocean. After this record crisis, the Ministry of Education, Culture, Sports, Science and Technology (MEXT) requested JAMSTEC to send JAMSTEC fleets to 30 km off Fukushima in order to monitor level of radiation of seawater, air and aerosol. R/V Mirai also participated this monitoring activity for approximately two weeks. After this contribution, it was decided that R/V Mirai starts original scientific cruise (MR11-03) in the western North Pacific with additional mission. This is water sampling near seafloor of earthquake and the tsunami source (Fig.1). This is based on the hypothesis that gasses and bacteria might be emitted from seafloor after the earthquake. We conducted four hydrocasts there. As a result, low beam transmittance layer was discovered near seafloor (Fig.2). It is suspected that this is attributed to re-suspension of seafloor sediment by the earthquake. In future, results of chemical and biological analysis of collected seawater will supply new insights, and more precise geological / geophysical / biological / geochemical researches will be conducted by JAMSTEC research vessels, deep-tow, ROV and Shinkai submersible.

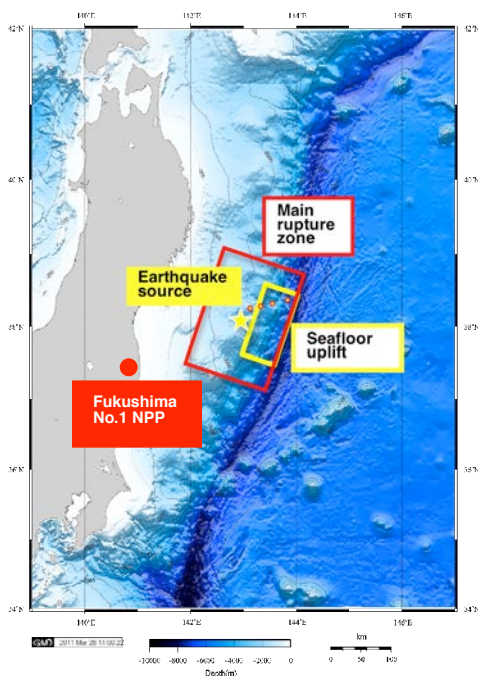


Fig. 1 Urgent research area near the earthquake / tsunami source

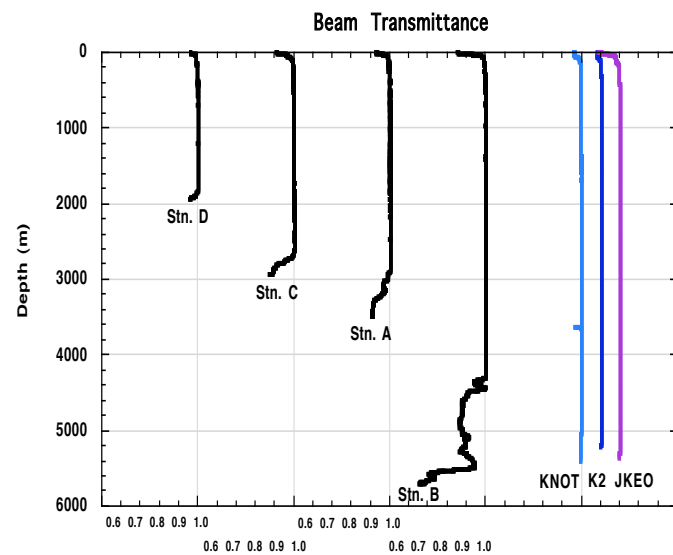


Fig. 2 Vertical profile of beam transmittance at urgent investigation area: stations A, B, C, D. For comparison, vertical profiles at our time-series stations are also shown

2) Outline of time-series observation at station K2 and S1

In order to certify seasonal and annual variability in ecosystem and biogeochemistry in the western North Pacific, biological and biogeochemical observation were conducted at time-series stations: K2 and S1 succeeding cruises of MR10-06 (September-October 2010) and MR11-02 (January-February 2011). Followings are main features during this cruise.

2-1) Station K2

Surface seawater temperature was approximately 1.7°C and less than that during last winter cruise: MR11-02 (approximately 2°C) (Fig. 3a). However temperature minimum layer with 1°C was observed at around 100 m and, thus, the maximum winter condition was likely over. Concentration of $\text{Si}(\text{OH})_4$ in the surface seawater was approximately 42 $\mu\text{mol kg}^{-1}$ and constant upper 100 m (Fig. 3b). Based on previous reports, this concentration was almost the annual maximum at station K2. Concentration of chlorophyll-*a* was slightly higher than or comparable to that during the last winter cruise (MR11-02) (Fig. 3c). Integrated primary productivity was approximately 200 $\text{mg-C m}^{-2} \text{day}^{-1}$ and higher than that during MR11-02 (Fig. 3d).

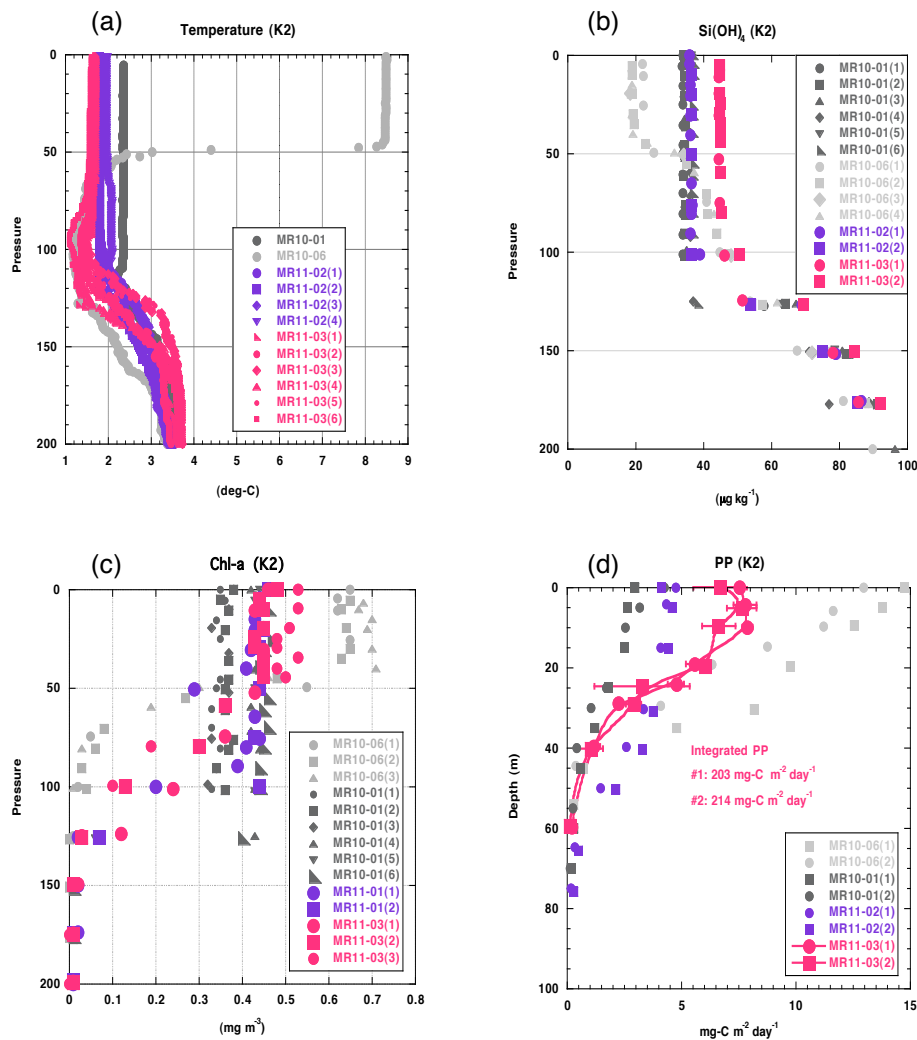


Fig. 3 Vertical profiles of (a) water temperature, (b) $\text{Si}(\text{OH})_4$, (c) chlorophyll-*a* and (d) primary productivity at station K2

It was notable that standing stocks of planktonic foraminifera were quite high at station K2 (Kimoto, personal communication). Maximum of standing stock was approximately 3,000 individuals m^{-3} above 100 m water depths. Most dominant species was *Globigerina bulloides* and occupied more than 60 % of total individuals. *G. bulloides* is well known as a carnivorous species and an upwelling indicator, therefore production of this species should be related with increasing of small zooplankton and nutrient supply by vertical mixing in this area. This remarkable foraminiferal production had never been recorded from other seasons' observations (i.e. February ~ March 2010 and October ~November 2010), and their higher production should contribute to transportation of carbon to the intermediate/deep water and ocean carbonate chemistry in the north Pacific. This is supported by large foraminifera flux in spring observed by time-series sediment trap at station K2 previously.



Fig. 4 Planktonic foraminifera recovered by vertical plankton tow

Moreover, adult copepodite *Neocalanus cristatus* (stage c5) was observed upper 50m by IONESS sampling (Kitamura, personal communication) (Fig. 5). During the last winter cruise (MR11-02), adult copepodite was observed between 200 m and 300 m for resting or hibernation. It is reported that adult copepodite dies between 200 m and 500 m after egg laying. After hatching, larva ascends to upper layer and grows up gradually toward autumn. Thus, the existence of adult copepodite in April is indicative of that *Neocalanus cristatus* quickly grew up during the last few months or adult copepodite does not die below 200 m. If the former is true, grazing pressure might be higher in April than previous reports. If the latter is true, carbon flux by zooplankton ontogenetic migration might be smaller than we expected. Future biological analysis of the collected sample and additional onboard experiments will reveal the role of zooplankton in the carbon cycle at



Fig.5 Copepodite *Neocalanus cristatus* collected by IONESS

station K2.

2-2) Station S1

Water temperature near surface was approximately 19°C (Fig. 6a) and higher than that during the last cruise (MR11-02). The surface mixed layer was approximately 40 m and shallower than that during MR11-02 (~ 120 m). Concentration of nitrate (NO_3) near surface was nearly zero (Fig. 6b). Chlorophyll-a was variable and its average was comparable to that observed in January-February 2010 (Fig. 6c). Integrated chlorophyll-a was estimated to be 43 mg m^{-2} . Primary productivity at surface was $13 \text{ mg-C m}^{-3} \text{ day}^{-1}$ and decreased with depth (Fig. 6d). Integrated primary productivity was approximately $356 \text{ mg-C m}^{-2} \text{ day}^{-1}$. During the last cruise, high primary productivity higher than $1,000 \text{ mg-C m}^{-2} \text{ day}^{-1}$ was observed (see MR11-02 preliminary cruise report) and, thus, nutrients were almost consumed within the last two months. However standing stock of phytoplankton was not small and primary productivity still continues. It is one of scientific interests how to maintain primary productivity in the subtropical area, that is, how macro- and micro-nutrients (e.g. Fe) are supplied to sun-lit layer: horizontal transport from the land? via atmosphere? or from subsurface by diffusion?

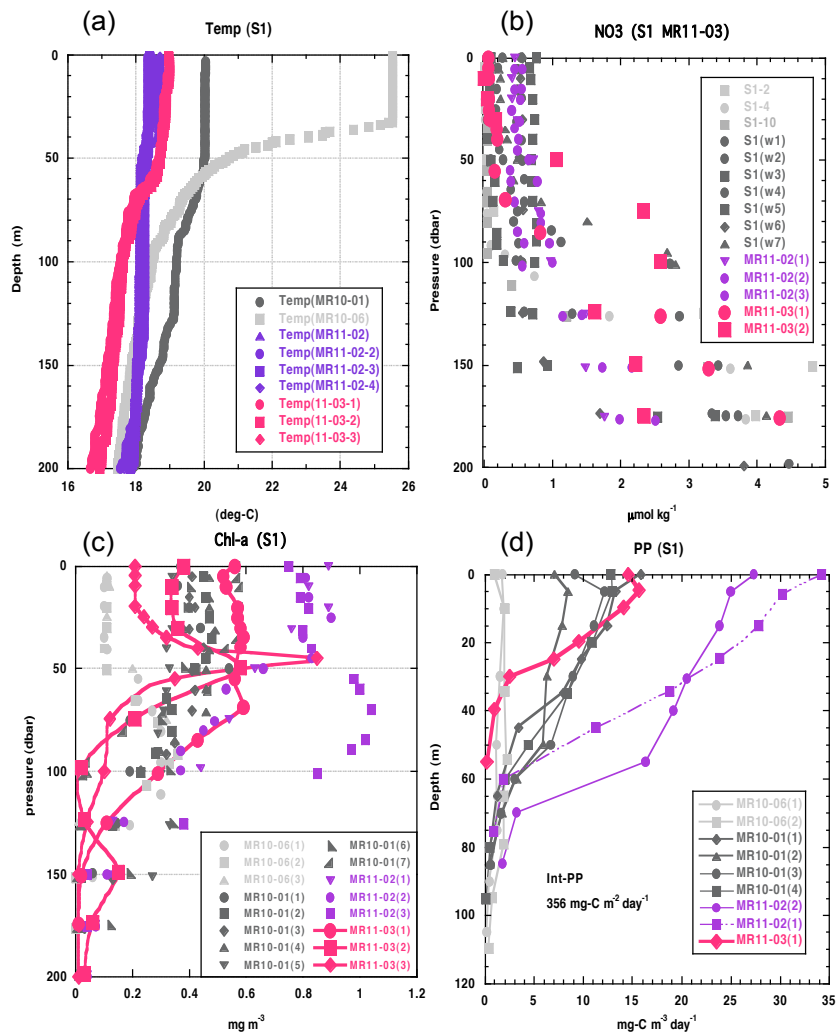


Fig. 6 Vertical profiles of (a) water temperature, (b) NO_3 , (c) chlorophyll-a, and (d) primary productivity at S1

(4) Scientific gears

All hydrocasts were conducted using 36-position 12 liter Niskin bottles carousel system with SBE CTD-DO system, fluorescence and transmission sensors. JAMSTEC scientists and MWJ (Marine Work Japan Co. Ltd.) technician group were responsible for analyzing water sample for salinity, dissolved oxygen, nutrients, CFCs, total carbon contents, alkalinity and pH. Cruise participants from JAMSTEC, University of Tokyo, and Kochi University helped to divide seawater from Niskin bottles to sample bottles for analysis. Surface water was collected with bucket.

Optical measurement in air and underwater was conducted with PAR sensor (RAMSES-ACC) and PAR sensor on CTD, respectively.

For collecting suspended particles at station K2 and S1, Large Volume Pump (LVP) was deployed. For observing in situ particles, optical sensor called LISSST (Laser In Situ Scattering and Transmissometer) and VPR (Visual Plankton recorder) were deployed by University of Tokyo and JAMSTEC, respectively.

GODI technicians group undertook responsibility for underway current direction and velocity measurements using an Acoustic Current Profiler (ADCP), geological measurements (topography, geo-magnetic field and gravity), and collecting meteorological data.

XCTD and Radio zonde observation were conducted by JAMSTEC and JAXA.

For collection of zooplankton, NORPAC plankton net, and IONESS were deployed.

For conducting in situ incubation for measurement of primary productivity and collecting sinking particles at station K2, drifter was deployed at station K2 and S1.

For observing vertical profile of primary productivity optically, FRRF was deployed.

In order to conduct time-series observation in biogeochemical cycle, JAMSTEC POPPS mooring was recovered and re-deployed at station S1.

For observation of atmospheric chemistry (aerosol and gas), various instruments including “sky-radiometer” and “MAX-DOAS” were onboard and automatic measurement was conducted.

Fourier Transform Spectrometry (FTS) was onboard and Greenhouse gas observation satellite (GOSAT or Ibuki in Japanese) products such as CO₂ over the sea was validated by Japan Aerospace Exploration Agency (JAXA).

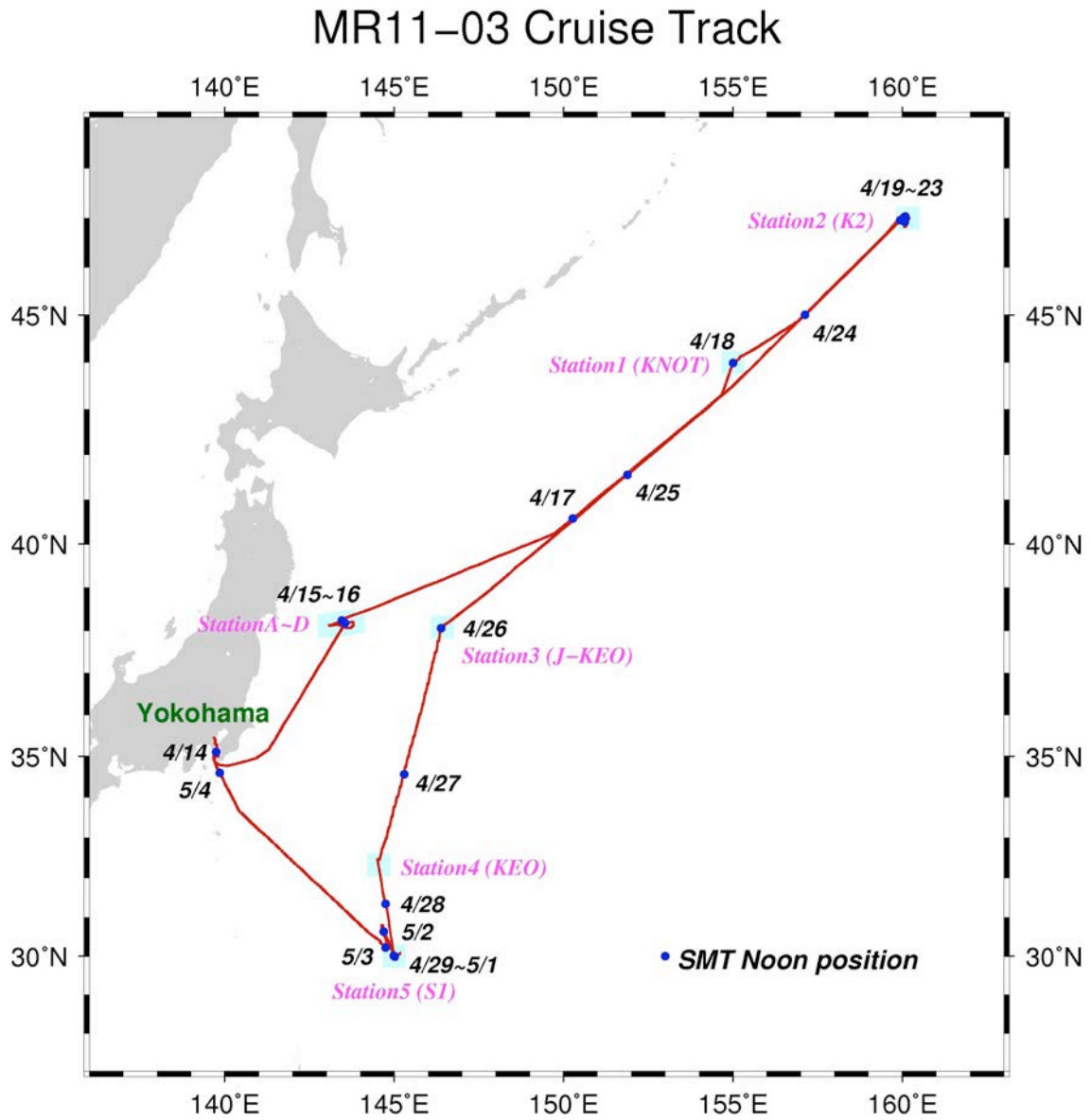
Please read text for more detail information and other instruments used for oceanographic and meteorological or atmospheric observation.

1.2 Track and log

1.2.1 Research Area

The western North Pacific (47°N – 30°N, 140°E – 160°W)

1.2.2 Cruise track



1.2.3 Cruise log

U.T.C.		S.M.T.		Position		Event logs
Date	Time	Date	Time	Latitude	Longitude	
4.14	0:50	4.14	9:50	35-27N	139-40E	Departure from Yokohama
	9:00		18:00	-	-	Continuous observations start
4.15	0:48	4.15	9:48	38-11N	143-33E	Arrival at Station A
	0:58		9:58	38-10.57N	143-33.00E	CTD cast #01 (3,493 m)
	4:06		13:06	-	-	Departure from Station A
	7:00		16:00	38-13N	143-47E	Arrival at Station B
	8:03		17:03	38-12.57N	143-47.13E	CTD cast #02 (5,700 m)
	12:08		21:08	38-12.53N	143-47.16E	IONESS #01 (150 m)
	15:00	4.16	0:00	-	-	Departure from Station B
	18:42		3:42	38-09N	143-19E	Arrival at Station C
	19:02		4:02	38-08.69N	143-18.99E	CTD cast #03 (2,943 m)
	21:36		6:36	-	-	Departure from Station C
	23:54		8:54	38-07N	143-05E	Arrival at Station D
	23:55		8:55	38-06.79N	143-04.99E	CTD cast #04 (1,964 m)
4.16	1:36		10:36	-	-	Departure from Station D
	3:00		12:00	38-14.96N	143-27.18E	Radiosonde observation #01
	13:00		22:00	-	-	Time adjustment +1 hour (SMT=UTC+10h)
4.17	12:00	4.17	22:00	-	-	Time adjustment +1 hour (SMT=UTC+11h)
	21:30	4.18	8:30	44-00N	155-00E	Arrival at Station #1 (KNOT)
	21:34		8:34	44-00.11N	154-59.94E	CTD cast #05 (5,292 m)
4.18	1:12		12:12	-	-	Departure from Station #1
	2:00		13:00	44-06.35N	155-11.40E	Radiosonde observation #02
4.19	1:00	4.19	12:00	47-00N	160-00E	Arrival at Station #2 (K2)
	6:57		17:57	46-59.93N	160-04.31E	CTD cast #06 (5,218 m)
	20:55	4.20	7:55	47-00.22N	160-11.59E	Drifting sediment trap buoy deployment #01
	23:05		10:05	46-59.93N	160-05.08E	LISST #01 (200 m)
4.20	0:04		11:04	46-59.74N	160-04.43E	CTD cast #07 (5,000 m)
	0:13		11:13	46-59.87N	160-04.80E	XBT observation #01
	2:00		13:00	46-59.69N	160-04.28E	Radiosonde observation #03
	4:02		15:02	47-00.00N	160-05.05E	Plankton net #01-1 (20-0 m)
	4:12		15:12	47-00.01N	160-05.00E	Plankton net #01-2 (50-20 m)
	4:25		15:25	47-00.00N	160-04.64E	Plankton net #01-3 (100-50 m)
	4:42		15:42	46-59.99N	160-04.88E	Plankton net #01-4 (100-50 m)
	5:02		16:02	46-59.96N	160-04.76E	Plankton net #01-5 (150-100 m)
	5:26		16:26	46-59.92N	160-04.67E	Plankton net #01-6 (200-150 m)
	5:45		16:45	46-59.89N	160-04.63E	Plankton net #01-7 (100-50 m)
	6:29		17:29	46-59.98N	160-05.02E	Large Volume Pump (LVP) #01 (200 m / 1 hour)

	9:53		20:53	47-00.06N	160-05.22E	IONESS #02 (400 m)
	13:00	4.21	0:00	47-03.63N	160-08.37E	Radiosonde observation #04
	14:40		1:40	46-59.53N	160-05.53E	Calibration for magnetometer #01
	16:28		3:28	47-00.00N	160-04.95E	CTD cast #08 (300 m)
	17:33		4:33	46-59.91N	160-04.50E	FRRF #01 (150 m)
	20:42		7:42	46-59.87N	160-04.87E	FRRF #02 (150 m)
	21:06		8:06	47-00.00N	160-04.73E	CTD cast #09 (200 m)
	22:26		9:26	47-00.02N	160-05.01E	CTD cast #10 (200 m)
4.21	0:07		11:07	47-00.02N	160-05.02E	FRRF #03 (150 m)
	0:33		11:33	47-00.21N	160-05.06E	LVP #02 (1,000 m / 5 hours)
	2:00		13:00	47-00.15N	160-05.04E	Radiosonde observation #05
	6:59		17:59	47-00.23N	160-05.24E	FRRF #04 (150 m)
	8:00		19:00	47-00.31N	160-04.69E	Plankton net #02-1 (20-0 m)
	8:07		19:07	47-00.31N	160-04.55E	Plankton net #02-2 (50-20 m)
	8:19		19:19	47-00.34N	160-04.49E	Plankton net #02-3 (50-20 m)
	8:29		19:29	47-00.34N	160-04.34E	Plankton net #02-4 (100-50 m)
	8:42		19:42	47-00.34N	160-04.18E	Plankton net #02-5 (150-100 m)
	8:51		19:51	47-00.32N	160-04.00E	Plankton net #02-6 (200-150 m)
	9:06		20:06	47-00.34N	160-03.84E	Plankton net #02-7 (300-200 m)
	9:45		20:45	47-00.36N	160-03.41E	Visual Plankton Recorder (VPR) #01 (500 m)
	10:20		21:20	47-00.39N	160-03.25E	Plankton net #03 (200 m)
	13:00	4.22	0:00	46-59.82N	160-04.67E	Radiosonde observation #06
	19:02		6:02	46-59.97N	160-04.55E	Plankton net #04-1 (500-300 m)
	19:35		6:35	46-59.89N	160-04.25E	Plankton net #04-2 (700-500 m)
	20:14		7:14	46-59.80N	160-03.93E	Plankton net #04-3 (1000-700 m)
	21:26		8:26	46-59.63N	160-03.43E	CTD cast #11 (1,000 m)
	22:48		9:48	47-00.00N	160-02.99E	Plankton net #05 (200 m)
	23:53		10:53	47-00.01N	160-04.96E	IONESS #03 (1,000 m)
4.22	2:00		13:00	47-03.89N	160-06.16E	Radiosonde observation #07
	3:02		14:02	47-05.63N	160-06.77E	Plankton net #06-1 (20-0 m)
	3:09		14:09	47-05.59N	160-06.71E	Plankton net #06-2 (50-20 m)
	3:19		14:19	47-05.55N	160-06.62E	Plankton net #06-3 (100-50 m)
	3:32		14:32	47-05.46N	160-06.48E	Plankton net #06-4 (150-100 m)
	3:47		14:47	47-05.43N	160-06.35E	Plankton net #06-5 (200-150 m)
	4:06		15:06	47-05.35N	160-06.17E	Plankton net #06-6 (300-200 m)
	4:48		15:48	47-05.00N	160-06.00E	LVP #03 (200 m / 2 hours)
	9:54		20:54	46-59.45N	160-03.57E	IONESS #04 (1,000 m)
	13:00	4.23	0:00	47-04.90N	160-03.24E	Radiosonde observation #08
	16:30		3:30	46-59.90N	160-04.83E	CTD cast #12 (300 m)
	17:22		4:22	47-00.00N	160-04.30E	FRRF #05 (150 m)
	20:26		7:26	46-49.56N	160-03.87E	FRRF #06 (150 m)
	21:15		8:15	46-50.55N	160-03.10E	Drifting sediment trap buoy recovery #01
	16:30		3:30	46-51.72N	160-03.23E	CTD cast #13 (200 m)
	23:53		10:53	46-55.01N	160-04.01E	FRRF #07 (150 m)
	0:35		11:35	46-55.15N	160-03.91E	IONESS #05 (1,000 m)
4.23	2:00		13:00	46-57.41N	160-03.84E	Radiosonde observation #09
	3:51		14:51	47-00.53N	160-03.51E	Plankton net #07-1 (300-250 m)
	4:15		15:15	47-00.38N	160-03.43E	Plankton net #07-2 (250-200 m)
	4:32		15:32	47-00.30N	160-03.32E	Plankton net #07-3 (200-180 m)
	4:46		15:46	47-00.21N	160-03.31E	Plankton net #07-4 (180-160 m)
	5:07		16:07	47-00.57N	160-03.55E	Plankton net #07-5 (160-140 m)
	5:21		16:21	47-00.10N	160-03.01E	Plankton net #07-6 (140-120 m)
	5:33		16:33	47-00.02N	160-02.91E	Plankton net #07-7 (120-100 m)
	5:46		16:46	46-59.83N	160-02.36E	Plankton net #07-8 (100-80 m)
	5:56		16:56	46-59.71N	160-02.59E	FRRF #08 (150 m)

	7:56		18:56	47-00.12N	160-04.77E	Plankton net #08-1 (Twin-NORPAC: 50 m)
	8:06		19:06	47-00.05N	160-04.76E	Plankton net #08-2 (Twin-NORPAC: 150 m)
	8:21		19:21	46-59.97N	160-04.74E	Plankton net #08-3 (Twin-NORPAC: 50 m)
	9:58		20:58	47-01.39N	160-05.12E	IONESS #06 (200 m)
	13:09	4.24	0:09	47-03.73N	159-59.69E	Radiosonde observation #10
	13:12		0:12	-	-	Departure from Station #2
	23:34		10:34	45-15.38N	157-25.50E	Cesium magnetometer towing start
4.24	5:31		16:31	44-18.30N	156-06.87E	Cesium magnetometer towing finish
			16:45	44-18.16N	156-06.49E	Cesium magnetometer towing start
4.25	7:15	4.25	18:15	40-42.15N	150-32.39E	Cesium magnetometer towing finish
	11:00		22:00	-	-	Time adjustment -1 hour (SMT=UTC+10h)
	18:49	4.26	4:49	39-00.03N	147-54.14E	Argo float #01 deployment
4.26	1:24		11:24	38-05N	146-25E	Arrival at Station #3 (JKEO)
	1:27		11:27	38-03.39N	146-22.67E	CTD cast #14 (5,371 m)
	5:15		15:15	38-03.00N	146-22.42E	Radiosonde observation #11
	5:27		15:27	38-02.78N	146-22.29E	Argo float #02 deployment
	5:28		15:28	38-02.64N	146-22.23E	XCTD #01
	5:30		15:30	-	-	Departure from Station #3
	6:57		16:57	37-46.12N	146-19.05E	XCTD #02
	7:00		17:00	37-46.03N	146-18.39E	Radiosonde observation #12
	8:29		18:29	37-30.31N	146-13.88E	XCTD #03
	8:30		18:30	37-30.19N	146-13.61E	Radiosonde observation #13
	9:58		19:58	37-14.53N	146-07.72E	XCTD #04
	10:00		20:00	37-14.84N	146-07.92E	Radiosonde observation #14
	11:27		21:27	37-00.31N	146-04.11E	Argo float #03 deployment
	11:30		21:30	37-00.30N	146-03.61E	Radiosonde observation #15
	11:34		21:34	36-59.81N	146-03.14E	XCTD #05
	13:02		23:02	36-45.10N	145-59.29E	Radiosonde observation #16
	13:07		23:07	36-44.32N	145-58.70E	XCTD #06
	14:30	4.27	0:30	36-30.39N	145-54.40E	Radiosonde observation #17
	14:32		0:32	36-30.28N	145-54.26E	XCTD #07
	16:00		2:00	36-15.35N	145-50.50E	Radiosonde observation #18
	16:05		2:05	36-15.18N	145-50.15E	XCTD #08
	17:44		3:44	36-00.04N	154-45.02E	Argo float #04 deployment
	17:31		3:31	36-01.22N	145-45.48E	Radiosonde observation #19
	17:38		3:38	36-00.90N	145-45.00E	XCTD #09
	19:00		5:00	35-45.55N	145-39.72E	Radiosonde observation #20
	19:08		5:08	35-45.37N	145-40.50E	XCTD #10
	20:26		6:26	35-29.56N	145-35.46E	XCTD #11
	20:30		6:30	35-30.07N	145-35.02E	Radiosonde observation #21
	22:00		8:00	35-15.75N	145-29.77E	Radiosonde observation #22
	22:05		8:05	35-15.44N	145-29.17E	XCTD #12
	23:29		9:29	34-59.78N	145-24.67E	Argo float #05 deployment
	23:30		9:30	34-59.91N	145-24.56E	Radiosonde observation #23
	23:34		9:34	34-59.60N	145-23.92E	XCTD #13
	1:00		11:00	34-44.96N	145-19.78E	Radiosonde observation #24
4.27	1:05		11:05	34-44.67N	145-19.14E	XCTD #14
	2:30		12:30	34-30.18N	145-15.83E	Radiosonde observation #25
	2:36		12:36	34-30.02N	145-14.61E	XCTD #15
	4:00		14:00	34-15.87N	145-10.89E	Radiosonde observation #26

	4:06		14:06	34-15.56N	145-10.15E	XCTD #16
	5:30		15:30	34-01.01N	145-05.46E	Radiosonde observation #27
	5:36		15:36	34-00.74N	145-04.79E	XCTD #17
	7:00		17:00	33-46.39N	144-59.83E	Radiosonde observation #28
	7:04		17:04	33-46.03N	144-59.27E	XCTD #18
	8:30		18:30	33-31.09N	144-55.72E	Radiosonde observation #29
	8:33		18:33	33-30.77N	144-55.25E	XCTD #19
	10:00		20:00	33-15.87N	144-50.72E	Radiosonde observation #30
	10:02		20:02	33-15.64N	144-50.46E	XCTD #20
	11:30		21:30	33-00.08N	144-46.02E	Radiosonde observation #31
	11:32		21:32	32-59.79N	144-45.77E	XCTD #21
	13:00		23:00	32-44.90N	144-38.70E	Radiosonde observation #32
	13:03		23:03	32-44.48N	144-38.30E	XCTD #22
	14:48	4.28	0:48	32-27.50N	144-32.58E	Radiosonde observation #33
	14:49		0:49	32-27.54N	144-32.47E	XCTD #23
	15:00		1:00	32-19N	145-00E	Arrival at Station #4 (KEO)
	15:58		1:58	32-27.66N	144-30.98E	CTD cast #15 (5,747 m)
	20:06		6:06	-	-	Departure from Station #4
4.28	1:24		11:24	-	-	Arrival at Station (Optical measurements #1)
	1:29		11:29	31-20.30N	144-44.50E	CTD cast #16 (200 m)
	1:51		11:51	31-20.38N	144-44.71E	FRRF #09 (150 m)
	2:36		12:36	-	-	Departure from the Station
	5:06		15:06	-	-	Arrival at Station (Optical measurements #2)
	5:12		15:12	30-49.06N	144-50.89E	CTD cast #17 (200 m)
	5:30		15:30	-	-	Departure from the Station
	9:24		19:24	30-00N	145-00E	Arrival at Station #5 (S1)
	9:24		19:24	30-00.29N	145-00.25E	CTD cast #18 (5,000 m)
	12:27		22:27	30-00.99N	145-00.82E	LISST #02 (200 m)
	14:00	4.29	0:00	30-00.88N	145-00.10E	Radiosonde observation #34
	14:05		0:05	30-00.80N	144-59.50E	Calibration for magnetometer #02
	17:26		3:26	30-00.25N	145-00.09E	CTD cast #19 (300 m)
	18:12		4:12	30-00.79N	145-00.77E	FRRF #10 (150 m)
	20:46		6:46	30-04.27N	145-10.36E	Drifting sediment trap buoy deployment #02
	22:01		8:01	30-02.46N	145-06.72E	FRRF #11 (150 m)
	22:39		8:39	30-02.82N	145-07.04E	CTD cast #20 (200 m)
4.29	0:53		10:53	29-59.86N	145-00.14E	FRRF #12 (150 m)
	1:31		11:31	29-59.78N	145-00.31E	LVP #04 (1,000 m / 5 hours)
	8:05		18:05	29-59.69N	145-00.29E	FRRF #13 (150 m)
	8:58		18:58	29-59.76N	145-00.01E	Plankton net #09-1 (20-0 m)
	9:04		19:04	29-59.69N	145-00.02E	Plankton net #09-2 (50-20 m)
	9:12		19:12	29-59.60N	145-00.03E	Plankton net #09-3 (100-50 m)
	9:22		19:22	29-59.49N	145-00.10E	Plankton net #09-4 (150-100 m)
	9:35		19:35	29-59.38N	145-00.18E	Plankton net #09-5 (200-150 m)
	9:48		19:48	29-59.29N	145-00.27E	Plankton net #09-6 (300-200 m)
	10:07		20:07	29-59.20N	145-00.40E	Plankton net #09-7 (300-200 m)
	10:29		20:29	20-59.14N	145-00.49E	VPR #02 (500 m)
	11:06		21:06	29-59.30N	145-00.66E	Plankton net #10 (200 m)
	20:00	4.30	6:00	30-00.00N	145-00.55E	CTD cast #21 (5,950 m)
	20:08		6:08	30-00.17N	145-00.27E	Water sampling for buckets #01
	23:13		9:13	29-59.81N	145-00.70E	Water sampling for buckets #02
4.30	0:10		10:10	29-59.60N	145-00.92E	LVP #05 (200m / 1 hour)

	23:13		9:13	29-59.61N	145-00.92E	Water sampling for buckets #03
	3:00		13:00	30-00.09N	144-59.99E	Radiosonde observation #35
	3:00		13:00	29-59.98N	145-00.27E	Plankton net #11-1 (1,000-700 m)
	3:53		13:53	29-59.97N	145-00.65E	Plankton net #11-2 (700-500 m)
	4:30		14:30	29-59.98N	145-00.83E	Plankton net #11-3 (500-300 m)
	5:02		15:02	29-59.91N	145-01.09E	CTD cast #22 (1,000 m)
	5:08		15:08	29-59.96N	145-00.96E	Water sampling for buckets #04
	7:58		17:58	29-59.66N	144-59.92E	Water sampling for buckets #05
	10:56		20:56	29-58.77N	144-59.46E	IONESS #07 (1,000 m)
	14:00	5.1	0:00	29-58.53N	145-05.39E	Radiosonde observation #36
	14:05		0:05	29-58.57N	145-05.25E	Water sampling for buckets #06
	17:28		3:28	30-00.24N	145-00.68E	CTD cast #23 (300 m)
	18:21		4:21	30-00.88N	145-00.89E	FRRF #14 (150 m)
	21:27		7:27	30-00.18N	145-00.35E	FRRF #15 (150 m)
	22:29		8:29	30-00.66N	145-00.91E	Plankton net #12 (200 m)
	22:53		8:53	30-00.88N	145-01.21E	CTD cast #24 (200 m)
5.1	0:54		10:54	30-00.19N	144-58.86E	FRRF #16 (150 m)
	1:34		11:34	30-01.37N	144-59.03E	IONESS #08 (1,000 m)
	3:00		13:00	30-00.37N	144-57.07E	Radiosonde observation #37
	4:36		14:36	29-59.13N	144-55.03E	Plankton net #13-1 (20-0 m)
	4:43		14:43	29-59.13N	144-55.13E	Plankton net #13-2 (50-20 m)
	4:51		14:51	29-59.14N	144-55.30E	Plankton net #13-3 (100-50 m)
	5:02		15:02	29-59.18N	144-55.50E	Plankton net #13-4 (150-100 m)
	5:15		15:15	29-59.21N	144-55.73E	Plankton net #13-5 (200-150 m)
	5:30		15:30	29-59.31N	144-55.96E	Plankton net #13-6 (300-200 m)
	5:50		15:50	29-59.42N	144-56.20E	Plankton net #13-7 (300-0 m)
	6:12		16:12	29-59.49N	144-56.54E	FRRF #17 (150 m)
	8:56		18:56	29-59.37N	144-57.00E	Plankton net #14-1 (50-0 m)
	9:06		19:06	29-59.39N	144-57.09E	Plankton net #14-2 (150-0 m)
	10:57		20:57	29-59.66N	145-00.78E	IONESS #09 (1,000 m)
	14:00	5.2	0:00	29-55.16N	145-03.25E	Radiosonde observation #38
	20:00		6:00	30-47-29N	144-37.03E	Drifting sediment trap buoy recovery #02
	21:57		7:57	30-44.28N	144-38.71E	Plankton net #15-1 (1,00-700 m)
	22:41		8:41	30-44.71N	144-38.70E	Plankton net #15-2 (700-500 m)
	23:18		9:18	30-45.04N	144-38.75E	Plankton net #15-3 (500-300 m)
5.2	1:04		11:04	30-39.32N	144-42.19E	IONESS #10 (1,000 m)
	2:57		12:57	30-36.48N	144-40.15E	Radiosonde observation #39
	4:27		14:27	30-35.41N	144-39.33E	Plankton net #16-1 (300-150 m)
	4:48		14:48	30-35.57N	144-39.39E	Plankton net #16-2 (300-150 m)
	5:09		15:09	30-35.65N	144-39.43E	Plankton net #16-3 (150-50 m)
	5:22		15:22	30-35.78N	144-39.53E	Plankton net #16-4 (150-50 m)
	5:36		15:36	30-35.83N	144-39.55E	Plankton net #16-5 (150-50 m)
	5:49		15:49	30-35.88N	144-39.57E	Plankton net #16-6 (50-0 m)
	5:55		15:55	30-35.91N	144-39.60E	Plankton net #16-7 (50-0 m)
	6:02		16:02	30-35.94N	144-39.61E	Plankton net #16-8 (50-0 m)
	6:12		16:12	30-35.99N	144-39.69E	Calibration for flow meter of Plankton net
	6:27		16:27	30-36.00N	144-39.79E	LVP #06 (200m / 2 hours)
	10:56		20:56	30-28.62N	144-44.06E	IONESS #11 (200 m)
	14:07	5.3	0:07	30-31.00N	144-46.44E	Radiosonde observation #40
5.3	0:34		10:34	30-13.88N	144-44.75E	Calibration for flow meter of IONESS
	2:06		12:06	30-13.84N	144-44.68E	Argo float #06 deployment
	2:07		12:07	30-13.88N	144-44.66E	Argo float #07 deployment
	2:12		12:12	-	-	Departure from Station #5
	3:01		13:01	30-22.25N	144-35.62E	Radiosonde observation #41
	12:00		22:00	-	-	Time adjustment -1 hour

(SMT=UTC+9h=JST)

5.4	0:30	5.4	9:30	-	-	Continuous observations finish
5.5	0:20	5.5	9:20	35-27N	139-40E	Arrival at Yokohama

1.3 Cruise Participants

	Name	Affiliation	Appointment
1	Makio HONDA (Principal Investigator)	Research Institute for Global Change (RIGC), Japan Agency for Marine-Earth Science and Technology (JAMSTEC)	Senior research scientist (II)
2	Kazuhiko MATSUMOTO (Deputy PI)	RIGC, JAMSTEC	Research scientist
3	Minoru KITAMURA	Institute of Biogeoscience (BIOGEOS) , JAMSTEC	Scientist
4	Hajime KAWAKAMI	Mutsu Institute for Oceanography (MIO), JAMSTEC	Research scientist
5	Masahide WAKITA	Same as above	Scientist
6	Tetsuichi FUJIKI	RIGC, JAMSTEC	Scientist
7	Katsunori KIMOTO	Same as above	Research scientist
8	Miho FUKUDA	Same as above	Graduate student
9	Hiroshi UCHIDA	Same as above	Research scientist
10	Hiroyuki TOMITA	Same as above	Technical staff
11	Shinsuke KAWAGUCHI	JAMSTEC, PEL	Postdoctoral researcher
12	Kaori YOSHIDA	JAMSTEC BIOGEOSS	Research scientist (II)
13	Akira KANEKO	University of Tokyo, AORI	Postdoctoral researcher
14	Mario UCHIMIYA	Same as above	Graduate student
15	Shuji KAWAKAMI	Japan Aerospace Exploration Agency (JAXA)	Associate senior engineer
16	Takuro NOGUCHI	Kochi University	Postdoctoral research fellow
17	Hideki YAMAMOTO (Principal Marine Tech.)	Marine Works Japan Inc. (MWJ)	Marin Technician
18	Atsushi OHHASHI	Same as above	Same as above
19	Kenichi KATAYAMA	Same as above	Same as above
20	Tatsuya TANAKA	Same as above	Same as above
21	Shinsuke TOYODA	Same as above	Same as above
22	Nagisa YAMAMOTO	Same as above	Same as above
23	Tamami UENO	Same as above	Same as above
24	Fujio KOBAYASHI	Same as above	Same as above
25	Ken-ichiro SATO	Same as above	Same as above
26	Masanori ENOKI	Same as above	Same as above
27	Yoshiko ISHIKAWA	Same as above	Same as above
28	Miyo IKEDA	Same as above	Same as above
29	Ayaka HATSUYAMA	Same as above	Same as above
30	Shoko TATAMISASHI	Same as above	Same as above
31	Misato KUWAHARA	Same as above	Same as above
32	Hiroyasu SATO	Same as above	Same as above
33	Hatsumi AOYAMA	Same as above	Same as above
34	Masahiro ORUI	Same as above	Same as above

35	Kanako YOSHIDA	Same as above	Same as above
36	Soichiro SUEYASHI (Principal Marine Tech.)	Global Ocean Development Inc. (GODI)	Same as above
37	Norio NAGAHAMA	Same as above	Same as above

2 General observation

2-1 Meteorological observations

2.1.1 Surface Meteorological Observation

Makio HONDA (JAMSTEC): Principal Investigator
Souichiro SUEYOSHI (Global Ocean Development Inc., GODI)
Norio NAGAHAMA (GODI)
Wataru TOKUNAGA (Mirai Crew)

(1) Objectives

Surface meteorological parameters are observed as a basic dataset of the meteorology. These parameters bring us the information about the temporal variation of the meteorological condition surrounding the ship.

(2) Methods

Surface meteorological parameters were observed throughout the MR11-03 cruise. During this cruise, we used three systems for the observation.

- i. MIRAI Surface Meteorological observation (SMet) system
- ii. Shipboard Oceanographic and Atmospheric Radiation (SOAR) system

i. MIRAI Surface Meteorological observation (SMet) system

Instruments of SMet system are listed in Table.2.1.1-1 and measured parameters are listed in Table.2.1.1-2. Data were collected and processed by KOAC-7800 weather data processor made by Koshin-Denki, Japan. The data set consists of 6-second averaged data.

ii. Shipboard Oceanographic and Atmospheric Radiation (SOAR) measurement system

SOAR system designed by BNL (Brookhaven National Laboratory, USA) consists of major three parts.

- a) Portable Radiation Package (PRP) designed by BNL – short and long wave downward radiation.
- b) Zeno Meteorological (Zeno/Met) system designed by BNL – wind, air temperature, relative humidity, pressure, and rainfall measurement.
- c) Scientific Computer System (SCS) developed by NOAA (National Oceanic and Atmospheric Administration, USA) – centralized data acquisition and logging of all data sets.

SCS recorded PRP data every 6 seconds, while Zeno/Met data every 10 seconds. Instruments and their locations are listed in Table.2.1.1-3 and measured parameters are listed in Table.2.1.1-4.

For the quality control as post processing, we checked the following sensors, before and after the cruise.

i. Young Rain gauge (SMet and SOAR)

Inspect of the linearity of output value from the rain gauge sensor to change Input value by adding fixed quantity of test water.

ii. Barometer (SMet and SOAR)

Comparison with the portable barometer value, PTB220CASE, VAISALA.

iii. Thermometer (air temperature and relative humidity) (SMet and SOAR)

Comparison with the portable thermometer value, HMP41/45, VAISALA.

(3) Preliminary results

Figure 2.1.1-1 shows the time series of the following parameters;

Wind (SMet)

Air temperature (SMet)

Relative humidity (SMet)

Precipitation (SOAR, rain gauge)

Short/long wave radiation (SOAR)

Pressure (SMet)

Sea surface temperature (SMet)

Significant wave height (SMet)

(4) Data archives

These meteorological data will be submitted to the Data Management Group (DMG) of JAMSTEC just after the cruise.

(5) Remarks

i. SST (Sea Surface Temperature) data were available in the following periods.

09:00UTC 14 Apr. - 00:30UTC 4 Mar.

ii. SMet ORG cleaning

02:17UTC 11 Apr., 03:44UTC 26 Apr.

iii. SMet Young rain gauge includes invalid data at the following time due to MF/HF transmit.

23:59UTC 16 Apr.

iv. Following period, SMet wave height and period data was invalid.

19:55UTC 18 Apr. - 07:55UTC 19 Apr.

v. SOAR optical rain gauge cleaning

05:28UTC 11 Apr.

vi. PRP cleaning

05:29UTC 11 Apr..

Table.2.1.1-1 Instruments and installations of MIRAI Surface Meteorological observation system

<u>Sensors</u>	<u>Type</u>	<u>Manufacturer</u>	<u>Location (altitude from surface)</u>
Anemometer	KE-500	Koshin Denki, Japan	foremast (24 m)
Tair/RH with 43408 Gill aspirated radiation shield	HMP45A	Vaisala, Finland R.M. Young, USA	compass deck (21 m) starboard side and port side
Thermometer: SST	RFN1-0	Koshin Denki, Japan	4th deck (-1m, inlet -5m)
Barometer	Model-370	Setra System, USA	captain deck (13 m) weather observation room
Rain gauge	50202	R. M. Young, USA	compass deck (19 m)
Optical rain gauge	ORG-815DR	Osi, USA	compass deck (19 m)
Radiometer (short wave)	MS-801	Eiko Seiki, Japan	radar mast (28 m)
Radiometer (long wave)	MS-200	Eiko Seiki, Japan	radar mast (28 m)
Wave height meter	MW-2	Tsurumi-seiki, Japan	bow (10 m)

Table.2.1.1-2 Parameters of MIRAI Surface Meteorological observation system

<u>Parameter</u>	<u>Units</u>	<u>Remarks</u>
1 Latitude	degree	
2 Longitude	degree	
3 Ship's speed	knot	Mirai log, DS-30 Furuno
4 Ship's heading	degree	Mirai gyro, TG-6000, Tokimec
5 Relative wind speed	m/s	6sec./10min. averaged
6 Relative wind direction	degree	6sec./10min. averaged
7 True wind speed	m/s	6sec./10min. averaged
8 True wind direction	degree	6sec./10min. averaged
9 Barometric pressure	hPa	adjusted to sea surface level 6sec. averaged
10 Air temperature (starboard side)	degC	6sec. averaged
11 Air temperature (port side)	degC	6sec. averaged
12 Dewpoint temperature (starboard side)	degC	6sec. averaged
13 Dewpoint temperature (port side)	degC	6sec. averaged
14 Relative humidity (starboard side)	%	6sec. averaged
15 Relative humidity (port side)	%	6sec. averaged
16 Sea surface temperature	degC	6sec. averaged
17 Rain rate (optical rain gauge)	mm/hr	hourly accumulation
18 Rain rate (capacitive rain gauge)	mm/hr	hourly accumulation
19 Down welling shortwave radiation	W/m ²	6sec. averaged
20 Down welling infra-red radiation	W/m ²	6sec. averaged
21 Significant wave height (bow)	m	hourly
22 Significant wave height (aft)	m	hourly
23 Significant wave period (bow)	second	hourly
24 Significant wave period (aft)	second	hourly

Table.2.1.1-3 Instruments and installation locations of SOAR system

<u>Sensors (Zeno/Met)</u>	<u>Type</u>	<u>Manufacturer</u>	<u>Location (altitude from surface)</u>
Anemometer	05106	R.M. Young, USA	foremast (25 m)
Tair/RH	HMP45A	Vaisala, Finland	
with 43408 Gill aspirated radiation shield		R.M. Young, USA	foremast (23 m)
Barometer	61202V	R.M. Young, USA	
with 61002 Gill pressure port		R.M. Young, USA	foremast (23 m)
Rain gauge	50202	R.M. Young, USA	foremast (24 m)
Optical rain gauge	ORG-815DA	Osi, USA	foremast (24 m)
<u>Sensors (PRP)</u>	<u>Type</u>	<u>Manufacturer</u>	<u>Location (altitude from surface)</u>
Radiometer (short wave)	PSP	Epply Labs, USA	foremast (25 m)
Radiometer (long wave)	PIR	Epply Labs, USA	foremast (25 m)
Fast rotating shadowband radiometer		Yankee, USA	foremast (25 m)

Table.2.1.1-4 Parameters of SOAR system

<u>Parameter</u>	<u>Units</u>	<u>Remarks</u>
1 Latitude	degree	
2 Longitude	degree	
3 SOG	knot	
4 COG	degree	
5 Relative wind speed	m/s	
6 Relative wind direction	degree	
7 Barometric pressure	hPa	
8 Air temperature	degC	
9 Relative humidity	%	
10 Rain rate (optical rain gauge)	mm/hr	
11 Precipitation (capacitive rain gauge)	mm	reset at 50 mm
12 Down welling shortwave radiation	W/m ²	
13 Down welling infra-red radiation	W/m ²	
14 Defuse irradiance	W/m ²	

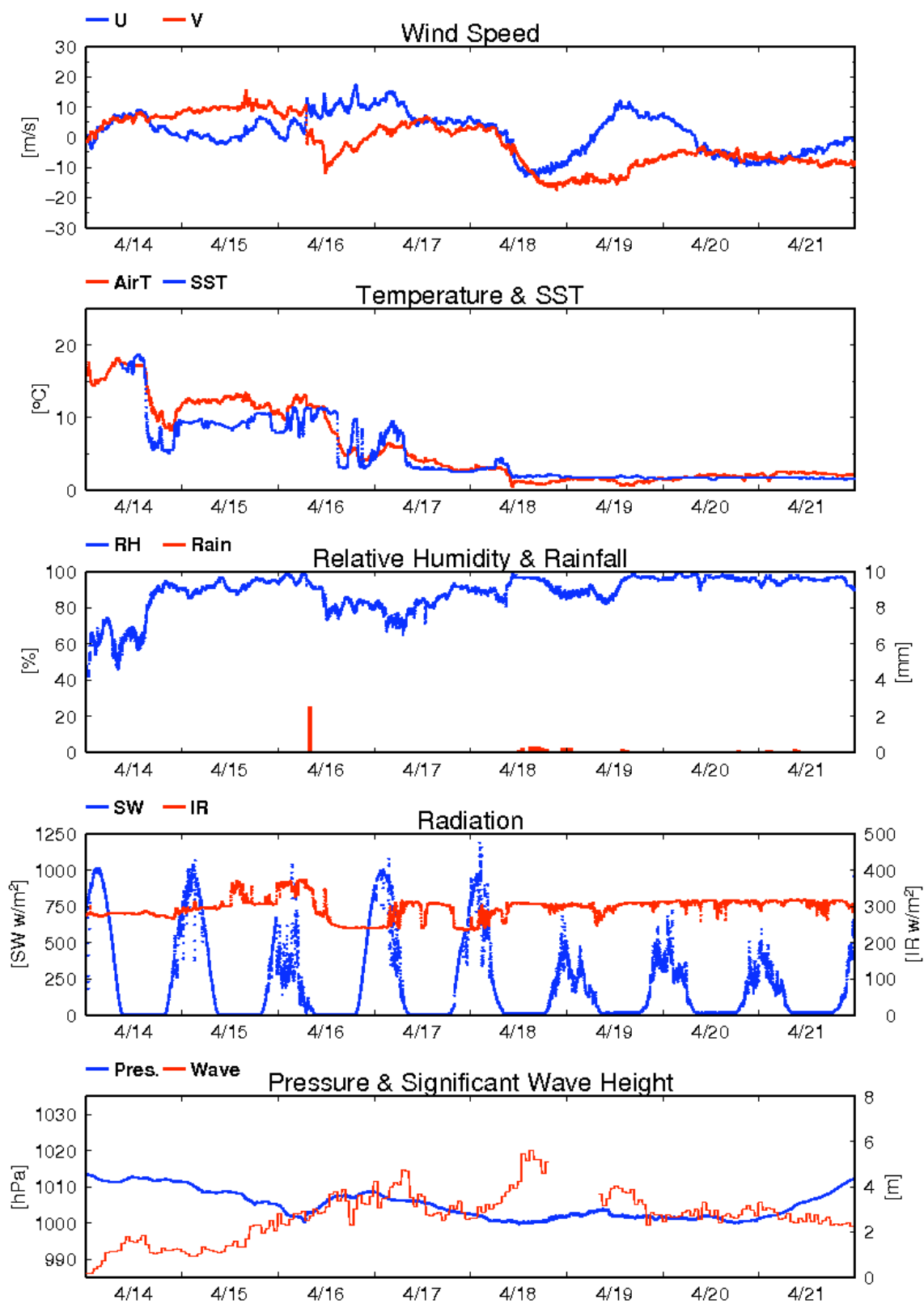


Fig.2.1.1-1 Time series of surface meteorological parameters during the MR11-03 cruise

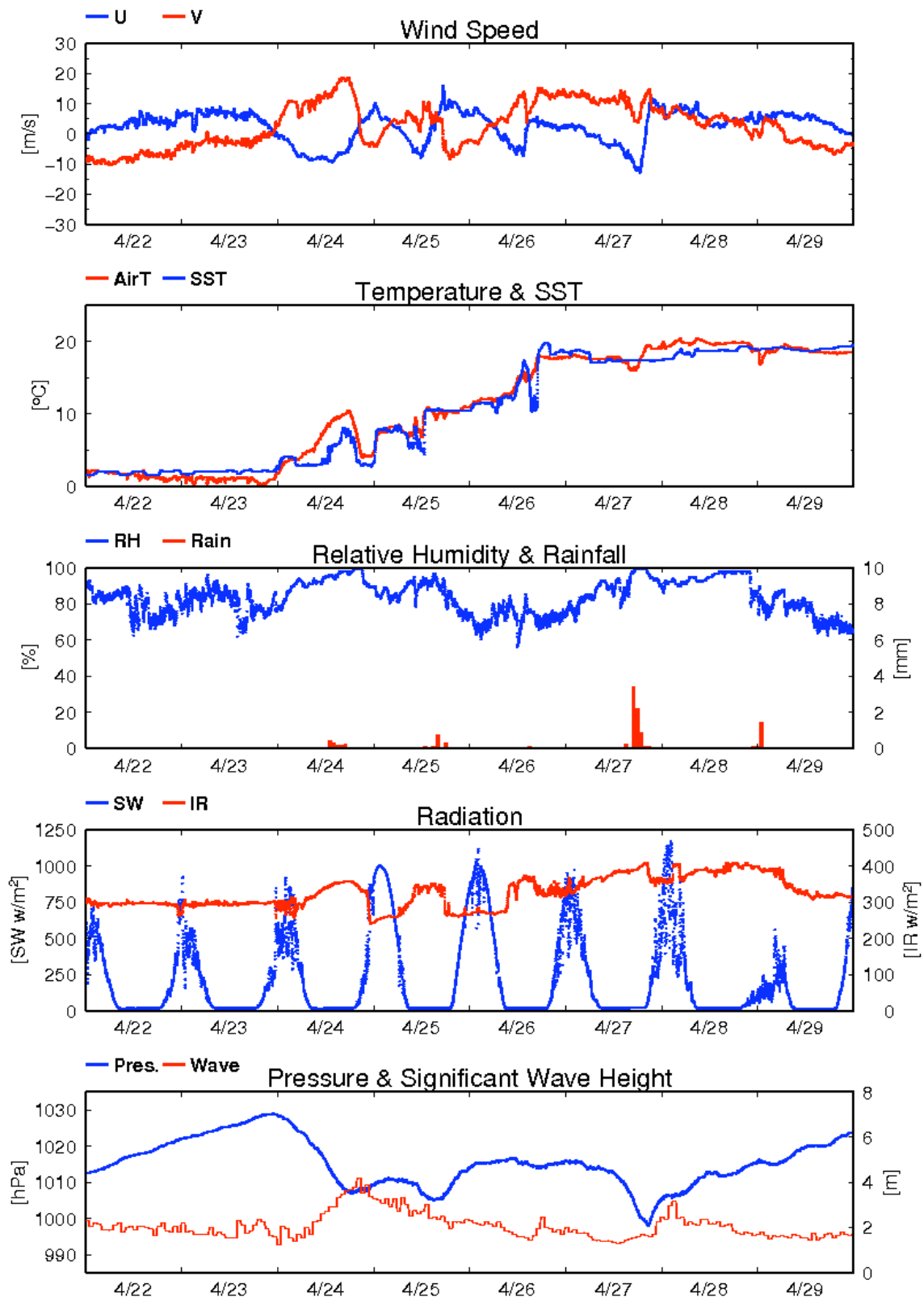


Fig.2.1.1-1 Continued

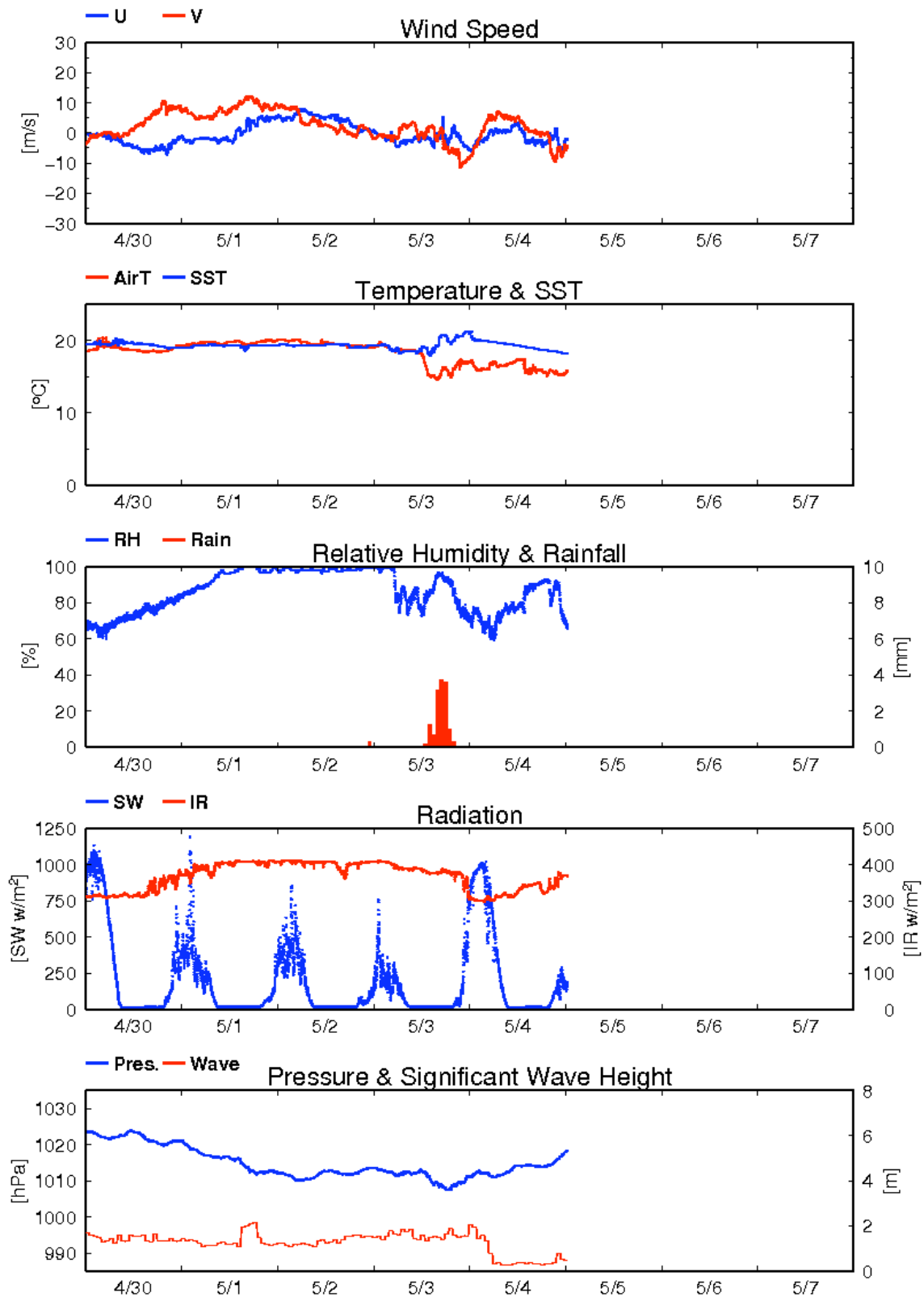


Fig.2.1.1-1 Continued

2.1.2 Ceilometer Observation

Makio HONDA (JAMSTEC): Principal Investigator
Souichiro SUEYOSHI (Global Ocean Development Inc., GODI)
Norio NAGAHAMA (GODI)
Wataru TOKUNAGA (Mirai Crew)

(1) Objectives

The information of cloud base height and the liquid water amount around cloud base is important to understand the process on formation of the cloud. As one of the methods to measure them, the ceilometer observation was carried out.

(2) Parameters

1. Cloud base height [m].
2. Backscatter profile, sensitivity and range normalized at 30 m resolution.
3. Estimated cloud amount [oktas] and height [m]; Sky Condition Algorithm.

(3) Methods

We measured cloud base height and backscatter profile using ceilometer (CT-25K, VAISALA, Finland) throughout the MR11-03 cruise from the departure of Yokohama on 14 April 2011 to arrival of Yokohama on 5 May 2011.

Major parameters for the measurement configuration are as follows;

Laser source:	Indium Gallium Arsenide (InGaAs) Diode
Transmitting wavelength:	905±5 nm at 25 degC
Transmitting average power:	8.9 mW
Repetition rate:	5.57 kHz
Detector:	Silicon avalanche photodiode (APD)
	Responsibility at 905 nm: 65 A/W
Measurement range:	0 ~ 7.5 km
Resolution:	50 ft in full range
Sampling rate:	60 sec
Sky Condition	0, 1, 3, 5, 7, 8 oktas (9: Vertical Visibility)
	(0: Sky Clear, 1:Few, 3:Scattered, 5-7: Broken, 8: Overcast)

On the archive dataset, cloud base height and backscatter profile are recorded with the resolution of 30 m (100 ft).

(4) Preliminary results

Figure 2.1.2-1 shows the time series of the lowest, second and third cloud base height.

(5) Data archives

The raw data obtained during this cruise will be submitted to the Data Management Group (DMG) in JAMSTEC.

(6) Remarks

1. Window cleaning;
05:43UTC 12 Apr., 22:15UTC 17 Apr., 03:43UTC 26 Apr.

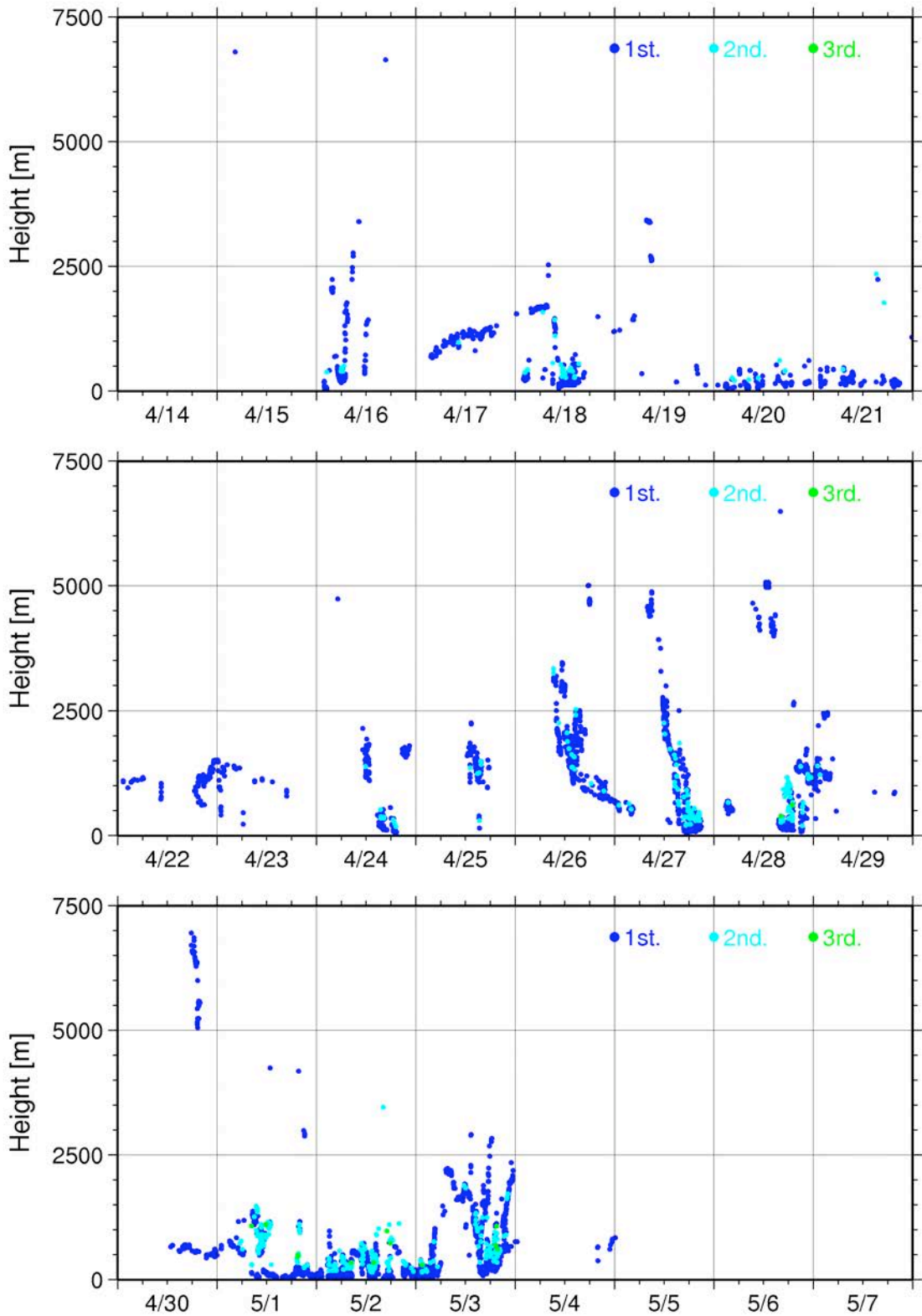


Fig.2.1.2-1 Lowest (blue), 2nd (green) and 3rd(red) cloud base height during the cruise.

2.1.3 Lidar observations of clouds and aerosols

Nobuo SUGIMOTO(NIES)

Ichiro MATSUI(NIES)

Atsushi SHIMIZU(NIES)

Tomoaki NISHIZAWA(NIES)

(1) Objectives

Objectives of the observations in this cruise is to study distribution and optical characteristics of ice/water clouds and marine aerosols using a two-wavelength lidar.

(2) Measured parameters

- Vertical profiles of backscattering coefficient at 532 nm
- Vertical profiles of backscattering coefficient at 1064 nm
- Depolarization ratio at 532 nm

(3) Method

Vertical profiles of aerosols and clouds were measured with a two-wavelength lidar. The lidar employs a Nd:YAG laser as a light source which generates the fundamental output at 1064 nm and the second harmonic at 532 nm. Transmitted laser energy is typically 30 mJ per pulse at both of 1064 and 532 nm. The pulse repetition rate is 10 Hz. The receiver telescope has a diameter of 20 cm. The receiver has three detection channels to receive the lidar signals at 1064 nm and the parallel and perpendicular polarization components at 532 nm. An analog-mode avalanche photo diode (APD) is used as a detector for 1064 nm, and photomultiplier tubes (PMTs) are used for 532 nm. The detected signals are recorded with a transient recorder and stored on a hard disk with a computer. The lidar system was installed in a container which has a glass window on the roof, and the lidar was operated continuously regardless of weather. Every 10 minutes vertical profiles of four channels (532 parallel, 532 perpendicular, 1064, 532 near range) are recorded.

(4) Results

Unfortunately a laser unit of the lidar system broke on April 20 and observation by the lidar was turned off. Time-height sections of lidar observation on during April 14-20, 2011 are shown in Figure 1. Temporal variation of atmospheric structure is clearly depicted. The depolarization ratio indicated that non-spherical particles were dominant at the beginning of observation period in lower atmosphere. In the middle there were dense surface aerosol layer which consist of spherical (anthropogenic) particles. After 18 April there were little information from lidar due to lower clouds or precipitation.

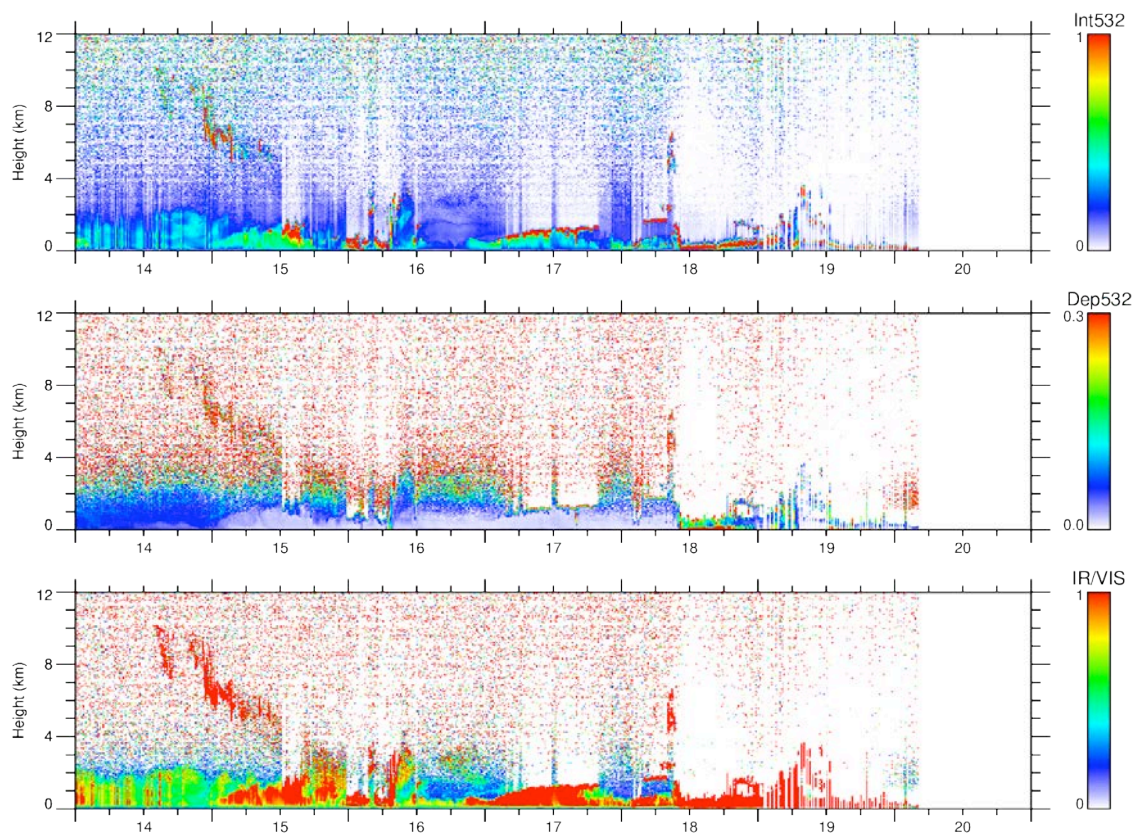


Figure 1: Time-height sections of (top) backscatter intensity at 532 nm, (middle) volume depolarization ratio at 532 nm, and (bottom) color ratio between 1064 nm and 532 nm during April 14-20, 2011.

(5) Data archive

- raw data

- lidar signal at 532 nm
- lidar signal at 1064 nm
- depolarization ratio at 532 nm
- temporal resolution 10min/ vertical resolution 6 m
- data period (UTC): April 14, 2011 - April 20, 2011

- processed data (plan)

- cloud base height, apparent cloud top height
- phase of clouds (ice/water)
- cloud fraction
- boundary layer height (aerosol layer upper boundary height)
- backscatter coefficient of aerosols
- particle depolarization ratio of aerosols

(6) Data policy and Citation

Contact NIES lidar team (nsugimot/i-matsui/shimizua/nisizawa@nies.go.jp) to utilize lidar data for productive use.

2.1.4 Optical characteristics of aerosol observed by Ship-borne Sky radiometer

Kazuma AOKI (University of Toyama) Principal Investigator / not onboard
Tadahiro HAYASAKA (Tohoku University) Co-worker / not onboard

(1) Objective

Objective of the observations in this aerosol is to study distribution and optical characteristics of marine aerosols by using a ship-borne sky radiometer (POM-01 MKII: PREDE Co. Ltd., Japan). Furthermore, collections of the data for calibration and validation to the remote sensing data were performed simultaneously.

(2) Methods and Instruments

Sky radiometer is measuring the direct solar irradiance and the solar aureole radiance distribution, has seven interference filters (0.34, 0.4, 0.5, 0.675, 0.87, 0.94, and 1.02 μm). Analysis of these data is performed by SKYRAD.pack version 4.2 developed by Nakajima *et al.* 1996.

@ Measured parameters

- Aerosol optical thickness at five wavelengths (400, 500, 675, 870 and 1020 nm)
- Ångström exponent
- Single scattering albedo at five wavelengths
- Size distribution of volume (0.01 μm – 20 μm)

GPS provides the position with longitude and latitude and heading direction of the vessel, and azimuth and elevation angle of sun. Horizon sensor provides rolling and pitching angles.

(3) Preliminary results

This study is not onboard. Data obtained in this cruise will be analyzed at University of Toyama.

(4) Data archives

Measurements of aerosol optical data are not archived so soon and developed, examined, arranged and finally provided as available data after certain duration. All data will archived at University of Toyama (K.Aoki, SKYNET/SKY: <http://skyrad.sci.u-toyama.ac.jp/>) after the quality check and submitted to JAMSTEC.

2.1.5 Tropospheric aerosol and gas observations on a research vessel by MAX-DOAS and auxiliary techniques

Hisahiro TAKASHIMA (PI, JAMSTEC/RIGC, not on board)

Fumikazu TAKETANI (JAMSTEC/RIGC, not on board)

Hitoshi IRIE (JAMSTEC/RIGC, not on board)

Yugo KANAYA (JAMSTEC/RIGC, not on board)

(1) Objectives

- To quantify typical background values of atmospheric aerosol and gas over the ocean
- To clarify transport processes from source over Asia to the ocean (and also clarify the gas emission from the ocean (including organic gas))
- To validate satellite measurements (as well as chemical transport model)

(2) Methods

(2-1) MAX-DOAS

Multi-Axis Differential Optical Absorption Spectroscopy (MAX-DOAS) is a passive remote sensing technique designed for atmospheric aerosol and gas profile measurements using scattered visible and ultraviolet (UV) solar radiation at several elevation angles. Our MAX-DOAS instrument for R/V *Mirai* consists of two main parts: an outdoor telescope unit and an indoor spectrometer (Acton SP-2358 with Princeton Instruments PIXIS-400B). These two parts are connected by a 10-m bundle cable that consists of 12 cores with 100-mm radii. On the roof top of the anti-rolling system of R/V *Mirai*, the telescope unit was installed on a gimbal mount, which compensates for the pitch and roll of the ship. A sensor measuring pitch and roll of the telescope unit (10Hz) is used together to measure an offset of elevation angle due to incomplete compensation by the gimbal. The line of sight was in directions of the starboard and portside of the vessel.

The MAX-DOAS system records spectra of scattered solar radiation every 0.2-0.4 second. Measurements were made at several elevation angles of 0, 1.5, 3, 5, 10, 20, 30, 70, 110, 150, 160, 170, 175, 177 and 178.5 degrees using a movable mirror, which repeated the same sequence of elevation angles every 30-min. The UV/visible spectra range was changed every minute (284-423 nm and 391-528 nm).

After measurements were made, we first selected spectrum data with an elevation angle offset less than ± 0.2 degrees. For those spectra, DOAS spectral fitting was performed to quantify the slant column density (SCD), defined as the concentration integrated along the light path, for each elevation angle. In this analysis, SCDs of NO₂ (and other gases) and O₄ (O₂-O₂, collision complex of oxygen) were obtained together. Next, O₄ SCDs were converted to the aerosol optical depth (AOD) and the vertical profile of aerosol extinction coefficient (AEC) at a wavelength of 476 nm using an optimal estimation inversion method with a radiative transfer model. Using derived aerosol information, another inversion is performed to retrieve the tropospheric vertical column/profile of NO₂ and other gases.

(2-2) CO, O₃, and aerosol size distribution

Carbon monoxide (CO), ozone (O₃), and aerosol size distribution measurements were also continually conducted during the cruise. For CO and O₃ measurements, ambient air was continually sampled on the compass deck and drawn through ~20-m-long Teflon tubes connected to gas filter correlation CO analyzer (Model 48C, Thermo Fisher Scientific) and UV photometric based ozone analyzer (Model 49C, Thermo Fisher Scientific) in the *Research Information Center*. For aerosol size distribution measurement, air was also sample on the compass deck and drawn through ~5-m-long tube connected to optical particle counter (KR-12A, Lion). All measurement data was recorded by both laptop and data logger.

(3) Preliminary results

These data for the whole cruise period will be analyzed.

(4) Data archives

The data will be submitted to the Marine-Earth Data and Information Department (MEDID) of JAMSTEC after the full analysis of the raw spectrum data is completed, which will be <2 years after the end of the cruise.

2.1.6 Rain, water vapor and surface water sampling

Naoyuki KURITA (JAMSTEC) Principal Investigator (not on-board)

Souichiro SUEYOSHI (Global Ocean Development Inc.: GODI) operator

(1) Objective

It is well known that the variability of stable water isotopes (HDO and H₂¹⁸O) is closely related with the moisture origin and hydrological processes during the transportation from the source region to deposition site. Thus, water isotope tracer is recognized as the powerful tool to study of the hydrological cycles in the atmosphere. However, oceanic region is one of sparse region of the isotope data, it is necessary to fill the data to identify the moisture sources by using the isotope tracer. In this study, to fill this sparse observation area, intense water isotopes observation was conducted along the cruise track of MR11-03.

(2) Method

Following observation was carried out throughout this cruise.

- Atmospheric moisture sampling:

Water vapor was sampled from the height about 20m above the sea level. The air was drawn at rate of 1.5-4.0L/min through a plastic tube attached to top of the compass deck. The flow rate is regulated according to the water vapor content to collect the sample amount 6-25ml. The water vapor was trapped in a glass trap submerged into an ethanol cooled to 100 degree C by radiator, and then they are collected every 12 hour during the cruise. After collection, water in the trap was subsequently thawed and poured into the 6ml glass bottle.

- Rainwater sampling

Rainwater samples gathered in rain/snow collector were collected just after precipitation events have ended. The collected sample was then transferred into glass bottle (6ml) immediately after the measurement of precipitation amount.

- Surface seawater sampling

Seawater sample taken by the pump from 4m depth were collected in glass bottle (6ml) around the noon at the local time.

(3) Results

Sampling of water vapor for isotope analysis is summarized in Table 2.1.6-1 (38 samples). The detail of rainfall sampling (7 samples) is summarized in Table 2.1.6-2. Described rainfall amount is calculated from the collected amount of precipitation. Sampling of surface seawater taken by pump from 4m depths is summarized in Table 2.1.6-3 (19 samples).

(4) Data archive

Isotopes (HDO, H₂¹⁸O) analysis will be done at RIGC/JAMSTEC, and then analyzed isotopes data will be submitted to JAMSTEC Data Integration and Analysis Group (DIAG).

Table 2.1.6-1 Summary of water vapor sampling for isotope analysis

Sample	Start		End		Lon	Lat	T.M. (m ³)	Sam. (ml)	H2O ppm
	Date	Time (UT)	Date	Time (UT)					
V-1	4.13	22:05	4.14	12:00	141-46.0E	35-49.3N	2.10	14.0	8296
V-2	4.14	12:04	4.15	0:00	143-30.8E	38-07.6N	1.78	12.0	8390
V-3	4.15	0:02	4.15	12:00	143-47.1E	38-12.6N	1.79	14.0	9733
V-4	4.15	12:03	4.16	0:00	143-05.0E	38-06.8N	1.79	14.0	9733
V-5	4.16	0:04	4.16	12:00	146-03.4E	39-04.5N	1.78	14.0	9788
V-6	4.16	12:03	4.17	0:00	149-46.2E	40-15.9N	1.79	7.5	5214
V-7	4.17	0:03	4.17	12:00	152-53.3E	42-12.9N	1.79	6.8	4727
V-8	4.17	12:02	4.18	0:00	155-00.1E	43-59.9N	2.31	8.5	4579
V-9	4.18	0:02	4.18	12:00	157-50.4E	45-31.1N	2.31	9.0	4848
V-10	4.18	12:03	4.19	0:00	159-48.5E	46-52.3N	2.31	7.9	4256
V-11	4.19	0:02	4.20	0:00	160-04.8E	46-59.9N	4.32	16.0	4609
V-12	4.20	0:02	4.21	0:00	160-05.0E	47-00.0N	4.32	19.5	5617
V-13	4.21	0:02	4.22	0:01	160-05.0E	47-00.2N	4.34	18.0	5161
V-14	4.22	0:04	4.23	0:00	160-04.0E	46-55.1N	4.33	14.0	4024
V-15	4.23	0:03	4.23	12:00	160-01.5E	47-02.9N	2.32	7.2	3862
V-16	4.23	12:02	4.24	0:00	157-22.2E	45-11.0N	2.32	6.0	3218
V-17	4.24	0:02	4.24	12:00	154-40.0E	43-17.7n	2.35	9.6	5084
V-18	4.24	12:03	4.25	0:00	152-06.3E	41-42.1N	2.43	15.0	7682
V-19	4.25	0:02	4.25	12:03	149-24.0E	39-58.4N	2.18	11.0	6279
V-20	4.25	12:06	4.26	0:00	146-39.9E	38-14.3N	2.14	14.0	8141
V-21	4.26	0:03	4.26	12:00	146-02.5E	36-54.9N	2.15	13.0	7525
V-22	4.26	12:02	4.27	0:00	145-22.6E	34-54.6N	2.16	18.0	10370
V-23	4.27	0:04	4.27	12:00	144-43.6E	32-54.8N	1.97	21.8	13771
V-24	4.27	12:03	4.28	0:01	144-39.9E	31-37.3N	1.80	22.0	15210
V-25	4.28	0:03	4.28	12:00	145-00.5E	30-00.4N	1.78	25.0	17478
V-26	4.28	12:02	4.29	0:00	145-03.3E	30-01.0N	1.79	24.0	16685
V-27	4.29	00:02	4.29	12:00	145-00.7E	29-59.3N	1.13	11.0	12114
V-28	4.29	12:02	4.30	0:00	145-00.8E	29-59.6N	1.13	9.2	10132
V-29	4.30	0:02	4.30	12:00	145-01.3E	29-58.1N	1.29	11.2	10804
V-30	4.30	12:02	5.1	0:00	145-00.4E	30-01.0N	1.29	12.6	12155
V-31	5.1	0:02	5.1	12:00	145-01.7E	29-58.0N	1.29	16.0	15435
V-32	5.1	12:02	5.2	0:00	144-39.5E	30-44.1N	1.29	18.0	17364
V-33	5.2	0:02	5.2	12:00	144-45.0E	30-29.4N	1.28	18.0	17500
V-34	5.2	12:03	5.3	0:00	144-44.9E	30-14.5N	1.28	17.6	17111
V-35	5.3	0:02	5.3	12:00	142-39.5E	31-53.2N	1.28	15.0	14583
V-36	5.3	12:02	5.4	0:00	140-14.8E	33-57.2N	1.28	11.6	11278
V-37	5.4	0:02	5.4	12:00	139-48.0E	35-00.7N	1.27	10.0	9799

Table 2.1.6-2 Summary of precipitation sampling for isotope analysis.

	Date	Time (UT)	Lon	Lat	Date	Time (UT)	Lon	Lat	Rain (mm)	R/S
R-1	4.14	00:00	139-39.85E	35-26.84N	4.16	09:41	145-21.40E	38-51.14N	3.7	S
R-2	4.16	09:48	145-23.58E	38-51.80N	4.18	23:15	159-42.30E	46-48.12N	1.4	R
R-3	4.18	23:15	159-42.32E	46-48.22N	4.22	02:00	160-06.20E	47-03.96N	4.1	R
R-4	4.22	02:00	160-06.20E	47-03.96N	4.25	19:50	147-40.34E	38-50.91N	1.4	R
R-5	4.25	19:50	147-40.34E	38-50.91N	4.27	21:19	144-33.22E	32-13.00N	9.0	R
R-6	4.27	21:19	144-33.22E	32-13.00N	4.30	04:38	145-00.81E	29-59.97N	0.9	R
R-7	4.30	04:38	145-00.81E	29-59.97N	5.03	23:52	140-15.76E	33-55.64N	13.4	S

Table 2.1.6-3 Summary of water vapor sampling for isotope analysis

Sampling No.	Date	Time (UTC)	Position LON	LAT
MR11-03 O-	1	4.15	03:04	143-33.0E 38-10.6N
MR11-03 O-	2	4.16	03:00	143-27.1E 38-15.0N
MR11-03 O-	3	4.17	02:00	150-16.6E 40-34.8N
MR11-03 O-	4	4.18	01:00	155-00.3E 43-59.8N
MR11-03 O-	5	4.19	01:00	159-56.1E 46-57.6N
MR11-03 O-	6	4.20	01:00	160-04.5E 46-59.8N
MR11-03 O-	7	4.21	01:00	160-05.1E 47-00.0N
MR11-03 O-	8	4.22	01:00	160-05.4E 47-02.0N
MR11-03 O-	9	4.23	01:00	160-03.9E 46-55.6N
MR11-03 O-	10	4.24	01:00	157-06.9E 45-00.5N
MR11-03 O-	11	4.25	01:00	151-52.5E 41-33.5N
MR11-03 O-	12	4.26	02:00	146-22.9E 38-03.6N
MR11-03 O-	13	4.27	02:00	145-17.2E 34-34.3N
MR11-03 O-	14	4.28	02:02	144-44.7E 31-20.4N
MR11-03 O-	15	4.29	02:01	145-00.3E 29-59.8N
MR11-03 O-	16	4.30	02:00	145-00.3E 29-59.6N
MR11-03 O-	17	5.1	02:00	144-58.7E 30-01.2N
MR11-03 O-	18	5.2	02:00	144-41.3E 30-38.1N
MR11-03 O-	19	5.3	02:00	144-44.8E 30-13.8N

2.1.7 Air-sea surface eddy flux measurement

Osamu TSUKAMOTO (Okayama University) Principal Investigator * not on board
Fumiyoshi KONDO (University of Tokyo) * not on board
Hiroshi ISHIDA (Kobe University) * not on board
Satoshi OKUMURA (Global Ocean Development Inc. (GODI))

(1) Objective

To better understand the air-sea interaction, accurate measurements of surface heat and fresh water budgets are necessary as well as momentum exchange through the sea surface. In addition, the evaluation of surface flux of carbon dioxide is also indispensable for the study of global warming. Sea surface turbulent fluxes of momentum, sensible heat, latent heat, and carbon dioxide were measured by using the eddy correlation method that is thought to be most accurate and free from assumptions. These surface heat flux data are combined with radiation fluxes and water temperature profiles to derive the surface energy budget.

(2) Instruments and Methods

The surface turbulent flux measurement system (Fig. 1) consists of turbulence instruments (Kaijo Co., Ltd.) and ship motion sensors (Kanto Aircraft Instrument Co., Ltd.). The turbulence sensors include a three-dimensional sonic anemometer-thermometer (Kaijo, DA-600) and an infrared hygrometer (LICOR, LI-7500). The sonic anemometer measures three-dimensional wind components relative to the ship. The ship motion sensors include a two-axis inclinometer (Applied Geomechanics, MD-900-T), a three-axis accelerometer (Applied Signal Inc., QA-700-020), and a three-axis rate gyro (Systron Donner, QRS-0050-100). LI7500 is a CO₂/H₂O turbulence sensor that measures turbulent signals of carbon dioxide and water vapor simultaneously. These signals are sampled at 10 Hz by a PC-based data logging system (Labview, National Instruments Co., Ltd.). By obtaining the ship speed and heading information through the Mirai network system it yields the absolute wind components relative to the ground. Combining wind data with the turbulence data, turbulent fluxes and statistics are calculated in a real-time basis. These data are also saved in digital files every 0.1 second for raw data and every 1 minute for statistic data.

(3) Observation log

The observation was carried out throughout this cruise.

(4) Data Policy and citation

All data are archived at Okayama University, and will be open to public after quality checks and corrections. Corrected data will be submitted to JAMSTEC Marine-Earth Data and Information Department.

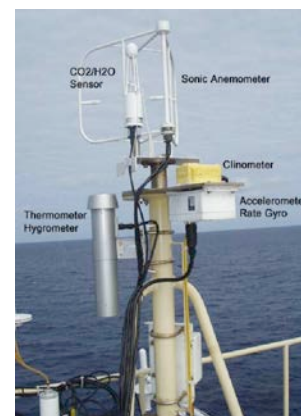


Fig. 1 Turbulent flux measurement system on the top deck of the foremast.

2.2 Physical oceanographic observations

2.2.1 CTD cast and water sampling

Masahide WAKITA (JAMSTEC MIO) : Principal investigator

Hiroshi UCHIDA (JAMSTEC RIGC)

Kenichi KATAYAMA (MWJ) : Operation leader

Tatsuya TANAKA (MWJ)

Tamami UENO (MWJ)

Nagisa YAMAMOTO (MWJ)

Fujio KOBAYASHI (MWJ)

Sinsuke TOYODA (MWJ)

(1) Objective

Investigation of oceanic structure and water sampling.

(2) Parameters

Temperature (Primary and Secondary)

Conductivity (Primary and Secondary)

Pressure

Dissolved Oxygen

Fluorescence

Beam Transmission Voltage

Dissolved Oxygen Voltage

Photosynthetically Active Radiation

Altimeter

(3) Instruments and Methods

CTD/Carousel Water Sampling System, which is a 36-position Carousel water sampler (CWS) with Sea-Bird Electronics, Inc. CTD (SBE9plus), was used during this cruise. 12-litter Niskin Bottles, which were washed by alkaline detergent and 1 N HCl, were used for sampling seawater. The sensors attached on the CTD were temperature (Primary and Secondary), conductivity (Primary and Secondary), pressure, fluorescence, beam transmission voltage, RINKO-III (dissolved oxygen sensor), dissolved oxygen, altimeter, PAR sensor and deep ocean standards thermometer. The Practical Salinity was calculated by measured values of pressure, conductivity and temperature. The CTD/CWS was deployed from starboard on working deck.

The CTD raw data were acquired on real time using the Seasave-V7 (ver.7.20g) provided by Sea-Bird Electronics, Inc. and stored on the hard disk of the personal computer. Seawater was sampled during the up cast by sending fire commands from the personal computer. We usually stop at each layer for 30 seconds to stabilize then fire.

24 casts of CTD measurements were conducted (table 2.2.1-1).

During the upcast of StAM01, data acquisition was stopped at 292 dbar due to communication error.

Data processing procedures and used utilities of SBE Data Processing-Win32 (ver.7.18d) and

SEASOFT were as follows:

(The process in order)

DATCNV: Convert the binary raw data to engineering unit data. DATCNV also extracts bottle information where scans were marked with the bottle confirm bit during acquisition. The duration was set to 4.4 seconds, and the offset was set to 0.0 seconds.

RINKOCOR (original module): Corrected the hysteresis of RINK-III voltage.

RINKOCORROS (original module): Corrected the hysteresis of RINKO-III voltage bottle data.

BOTTLESUM: Create a summary of the bottle data. The data were averaged over 4.4 seconds.

ALIGNCTD: Convert the time-sequence of sensor outputs into the pressure sequence to ensure that all calculations were made using measurements from the same parcel of water. Dissolved oxygen data are systematically delayed with respect to depth mainly because of the long time constant of the dissolved oxygen sensor and of an additional delay from the transit time of water in the pumped plumbing line. This delay was compensated by 6 seconds advancing dissolved oxygen sensor (SBE43) output (dissolved oxygen voltage) relative to the temperature data, RINKO-III data, and beam transmission voltage data are also delayed by slightly slow response time to the sensor. The delay was compensated by 1 second or 2 seconds advancing.

WILDEDIT: Mark extreme outliers in the data files. The first pass of WILDEDIT obtained an accurate estimate of the true standard deviation of the data. The data were read in blocks of 1000 scans. Data greater than 10 standard deviations were flagged. The second pass computed a standard deviation over the same 1000 scans excluding the flagged values. Values greater than 20 standard deviations were marked bad. This process was applied to pressure, depth, temperature, conductivity and dissolved oxygen voltage (SBE43).

CELLTM: Remove conductivity cell thermal mass effects from the measured conductivity. Typical values used were thermal anomaly amplitude $\alpha = 0.03$ and the time constant $1/\beta = 7.0$.

FILTER: Perform a low pass filter on pressure with a time constant of 0.15 second. In order to produce zero phase lag (no time shift) the filter runs forward first then backward.

WFILTER: Perform a median filter to remove spikes in the fluorescence data and beam transmission voltage data. A median value was determined by 49 scans of the window.

SECTIONU (original module of SECTION): Select a time span of data based on scan number in order to reduce a file size. The minimum number was set to be the starting time when the CTD package was beneath the sea-surface after activation of the pump. The maximum

number was set to be the end time when the package came up to the sea-surface.

LOOPEDIT: Mark scans where the CTD was moving less than the minimum velocity of 0.0 m/s (traveling backwards due to ship roll).

DESPIKE (original module): Remove spikes of the data. A median and mean absolute deviation was calculated in 1-dbar pressure bins for both down and up cast, excluding the flagged values. Values greater than 4 mean absolute deviations from the median were marked bad for each bin. This process was performed 2 times for temperature, conductivity, dissolved oxygen voltage (SBE43), RINKO-III voltage.

DERIVE: Compute dissolved oxygen (SBE43).

BINAVG: Average the data into 1-dbar pressure bins.

DERIVE: Compute the practical salinity, potential temperature, and sigma-theta.

SPLIT: Separate the data from an input .cnv file into down cast and up cast files.

Configuration file: MR1103A.con

Specifications of the sensors are listed below.

CTD: SBE911plus CTD system

Under water unit:

SBE9plus (S/N 09P21746-0575, Sea-Bird Electronics, Inc.)

Pressure sensor: Digiquartz pressure sensor (S/N 79492)

Calibrated Date: 08 Jul. 2010

Temperature sensors:

Primary: SBE03Plus (S/N 03P4815, Sea-Bird Electronics, Inc.)

Calibrated Date: 25 Jan. 2011

Secondary: SBE03-04/F (S/N 031359, Sea-Bird Electronics, Inc.)

Calibrated Date: 20 Jul. 2010

Conductivity sensors:

Primary: SBE04C (S/N 043036, Sea-Bird Electronics, Inc.)

Calibrated Date: 15 Dec. 2010

Secondary: SBE04-04/0 (S/N 042854, Sea-Bird Electronics, Inc.)

Calibrated Date: 02 Mar. 2011

Fluorescence:

Chlorophyll Fluorometer (S/N 3054, Seapoint Sensors, Inc.)

Transmissometer:

C-Star (S/N CST-1363DR, WET Labs, Inc.)

Altimeter:

Benthos PSA-916T (S/N 1100, Teledyne Benthos, Inc.)

Dissolved Oxygen sensor:

SBE43 (S/N 430394, Sea-Bird Electronics, Inc.)

Calibrated Date: 10 Dec. 2010

Dissolved Oxygen sensors:

RINK-III (S/N 0024, JFE Advantech Co., Ltd.)

RINK-III (S/N 0037, JFE Advantech Co., Ltd.)

Photosynthetically Active Radiation:

PAR sensor (S/N 0049, Satlantic Inc.)

Calibrated Date: 22 Jan. 2009

Deep Ocean Standards Thermometer:

SBE35 (S/N 0045, Sea-Bird Electronics, Inc.)

Calibrated Date: 10 Feb. 2011

Carousel water sampler:

SBE32 (S/N 3227443-0391, Sea-Bird Electronics, Inc.)

Deck unit: SBE11plus (S/N 11P7030-0272, Sea-Bird Electronics, Inc.)

(4) Preliminary Results

During this cruise, 24 casts of CTD observation were carried out. Date, time and locations of the CTD casts are listed in Table 2.2.1-1.

(5) Data archive

All raw and processed data files were copied onto CD-ROM. The data will be submitted to the Data Management Office (DMO), JAMSTEC, and will be opened to public via "JAMSTEC Data Site for Research Cruises".

Table 2.2.1-1 MR11-03 CTD Casttable

Stnbr	Castno	Date(UTC)	Time(UTC)		BottomPosition		Depth	Wire Out	HT Above Bottom	Max Depth	Max Pressure	CTD Filename	Remark
		(mmddyy)	Start	End	Latitude	Longitude							
StA	1	041511	01:05	04:00	38-10.56N	143-32.99E	3500.0	3495.0	9.2	3493.0	3548.5	StAM01	Hydrogen, Helium, pH/ORP Data acquisition stopped at upcast 292 dbar due to communication error.
StB	1	041511	08:08	11:50	38-12.56N	143-47.13E	5764.0	5708.0	15.3	5700.2	5822.3	StBM01	Hydrogen, Helium, pH/ORP
StC	1	041511	19:09	21:32	38-08.68N	143-18.99E	2965.0	2947.4	11.0	2943.0	2986.6	StCM01	Hydrogen, Helium, pH/ORP
StD	1	041611	00:01	01:31	38-06.78N	143-04.99E	1956.0	1941.3	8.7	1939.5	1964.5	StDM01	Hydrogen, Helium, pH/ORP
KNT	1	041711	21:40	01:07	43-59.99N	155-00.02E	5323.0	5301.7	10.5	5292.0	5400.5	KNTM01	Routine
K02	1	041911	07:02	10:36	46-59.93N	160-04.31E	5238.0	5225.6	9.8	5218.2	5325.6	K02M01	Routine
K02	2	042011	00:09	03:09	46-59.73N	160-04.42E	5234.0	5019.1	-	5000.8	5100.7	K02M02	Bacteria
K02	3	042011	16:33	17:08	46-59.99N	160-04.95E	5245.0	298.9	-	300.2	302.4	K02M03	P.P.
K02	4	042011	21:13	21:40	47-00.00N	160-04.73E	5240.0	197.3	-	201.5	203.3	K02M04	P.E., RI
K02	5	042011	22:32	22:59	47-00.02N	160-05.01E	5238.0	199.1	-	200.7	202.5	K02M05	Paleo
K02	6	042111	21:31	22:39	46-59.62N	160-03.43E	5227.0	1004.9	-	1003.7	1013.9	K02M06	RI
K02	7	042211	16:35	17:13	46-59.89N	160-04.81E	5239.0	299.7	-	300.1	303.2	K02M07	P.P.
K02	8	042211	22:32	22:56	46-51.70N	160-03.22E	5201.0	199.4	-	201.3	202.8	K02M08	POC, Paleo
JKO	1	042611	01:33	05:19	38-03.38N	146-22.66E	5383.0	5390.3	9.6	5371.5	5481.7	JKOM01	Routine
KEO	1	042711	16:02	19:59	32-27.66N	144-29.98E	5749.0	5752.8	10.2	5746.4	5866.5	KEOM01	Routine
001	1	042811	01:33	01:43	31-20.28N	144-44.38E	5635.0	204.8	-	200.2	203.9	001M01	PAR
002	1	042811	05:17	05:25	30-49.05N	144-50.88E	5967.0	199.7	-	200.5	201.5	002M01	PAR
S01	1	042811	09:30	12:18	30-00.28N	145-00.24E	5975.0	5003.4	-	5001.1	5095.4	S01M01	Bacteria
S01	2	042811	17:31	18:05	30-00.25N	145-00.09E	5968.0	300.9	-	301.5	303.4	S01M02	P.P.
S01	3	042811	22:42	23:08	30-02.82N	145-07.03E	5995.0	199.3	-	201.6	203.0	S01M03	P.E., RI, Paleo
S01	4	042911	20:07	00:07	30-00.00N	145-00.54E	5959.0	5953.6	9.4	5950.7	6076.4	S01M04	Routine
S01	5	043011	05:07	06:10	29-59.90N	145-01.08E	5953.0	1002.3	-	1001.6	1010.9	S01M05	RI
S01	6	043011	17:33	18:14	30-00.23N	145-00.67E	5971.0	300.6	-	301.4	303.4	S01M06	P.P.
S01	7	043011	22:59	23:24	30-00.87N	145-01.20E	5997.0	198.6	-	200.7	201.9	S01M07	POC, Paleo

Routine: Routine sampling cast

P.P.: Primary Production cast

RI: radioisotope cast

Bacteria: Bacteria sampling cast

P.E.: P vs. E curve cast

Paleo: Paleo sampling cast

POC: Particulate Organic Carbon sampling cast

2.2.2 Salinity measurement

Masahide WAKITA (JAMSTEC MIO)

Fujio Kobayashi (MWJ)

Shinsuke Toyoda (MWJ)

(1) Objective

To measure bottle salinity obtained by CTD casts, bucket sampling, and The Continuous Sea Surface Water Monitoring System (TSG).

(2) Methods

a. Salinity Sample Collection

Seawater samples were collected with 12 liter Niskin-X bottles, bucket, and TSG. The salinity sample bottles of the 250ml brown glass bottles with screw caps were used for collecting the sample water. Each bottle was rinsed three times with the sample water, and was filled with sample water to the bottle shoulder. The salinity sample bottles for TSG were sealed with plastic inner caps and screw caps because we took into consideration the possibility of storage for about a month. These caps were rinsed three times with the sample water before use. The bottle was stored for more than 24 hours in the laboratory before the salinity measurement.

The number of samples is shown as follows;

Table 2.2.2-1 The number of samples

Sampling type	Number of samples
CTD and Bucket	325
TSG	20
Total	345

b. Instruments and Method

The salinity analysis on R/V MIRAI was carried out during the cruise of MR11-03 using the salinometer (Model 8400B “AUTOSAL”; Guildline Instruments Ltd.: S/N 62827) with an additional peristaltic-type intake pump (Ocean Scientific International, Ltd.). A pair of precision digital thermometers (Model 9540; Guildline Instruments Ltd.: S/N 66528 and 62525) were used. The thermometer monitored the ambient temperature and the bath temperature of the salinometer.

The specifications of AUTOSAL salinometer and thermometer are shown as follows;

Salinometer (Model 8400B “AUTOSAL”; Guildline Instruments Ltd.)

Measurement Range : 0.005 to 42 (PSU)

Accuracy : Better than ± 0.002 (PSU) over 24 hours
without re-standardization

Maximum Resolution : Better than ± 0.0002 (PSU) at 35 (PSU)

Thermometer (Model 9540: Guildline Instruments Ltd.)

Measurement Range : -40 to +180 deg C
Resolution : 0.001
Limits of error \pm deg C : 0.01 (24 hours @ 23 deg C \pm 1 deg C)
Repeatability : \pm 2 least significant digits

The measurement system was almost the same as Aoyama *et al.* (2002). The salinometer was operated in the air-conditioned ship's laboratory at a bath temperature of 24 deg C. The ambient temperature varied from approximately 20 deg C to 25 deg C, while the bath temperature was very stable and varied within \pm 0.001 deg C on rare occasion.

The measurement for each sample was done with the double conductivity ratio and defined as the median of 31 readings of the salinometer. Data collection was started 5 seconds after filling the cell with the sample and it took about 10 seconds to collect 31 readings by a personal computer. Data were taken for the sixth and seventh filling of the cell after rinsing five times. In the case of the difference between the double conductivity ratio of these two fillings being smaller than 0.00002, the average value of the double conductivity ratio was used to calculate the bottle salinity with the algorithm for practical salinity scale, 1978 (UNESCO, 1981). If the difference was greater than or equal to 0.00003, an eighth filling of the cell was done. In the case of the difference between the double conductivity ratio of these two fillings being smaller than 0.00002, the average value of the double conductivity ratio was used to calculate the bottle salinity. In the case of the double conductivity ratio of eighth filling did not satisfy the criteria above, we measured a ninth filling of the cell and calculated the bottle salinity. The measurement was conducted in about 6 - 10 hours per day and the cell was cleaned with soap after the measurement of the day.

(3)Preliminary Result

a. Standard Seawater

Standardization control of the salinometer was set to 466 and all measurements were done at this setting. The value of STANDBY was 24+5394 \pm 0003 and that of ZERO was 0.0-0000 \pm 0001. The conductivity ratio of IAPSO Standard Seawater batch P152 was 0.99981 (the double conductivity ratio was 1.99962) and was used as the standard for salinity. We measured 31 bottles of P152.

The specifications of SSW used in this cruise are shown as follows ;

Batch : P152
conductivity ratio : 0.99981
salinity : 34.993
Use by : 5th May 2013

Fig.2.2.2-1 shows the history of the double conductivity ratio of the Standard Seawater batch P152 before correction. The average of the double conductivity ratio was 1.99960 and the standard deviation was 0.00002, which is equivalent to 0.0004 in salinity.

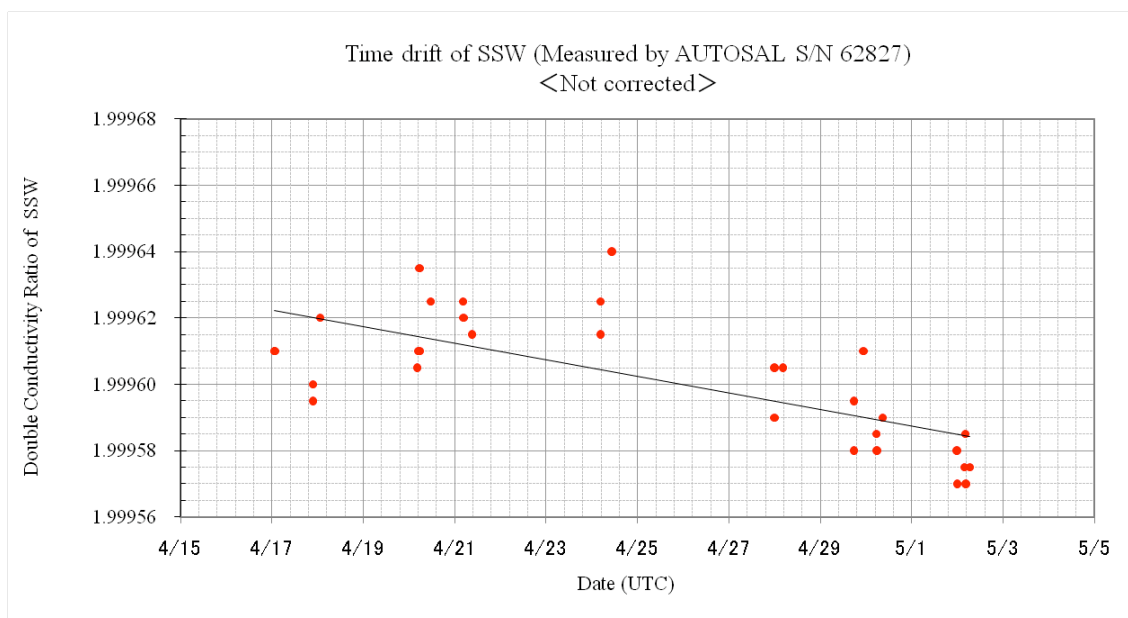


Fig. 2.2.2-1 The history of the double conductivity ratio for the Standard Seawater batch P152 (Before correction)

Fig.2.2.2-2 shows the history of the double conductivity ratio of the Standard Seawater batch P152 after correction. The average of the double conductivity ratio after correction was 1.99962 and the standard deviation was 0.00001, which is equivalent to 0.0001 in salinity.

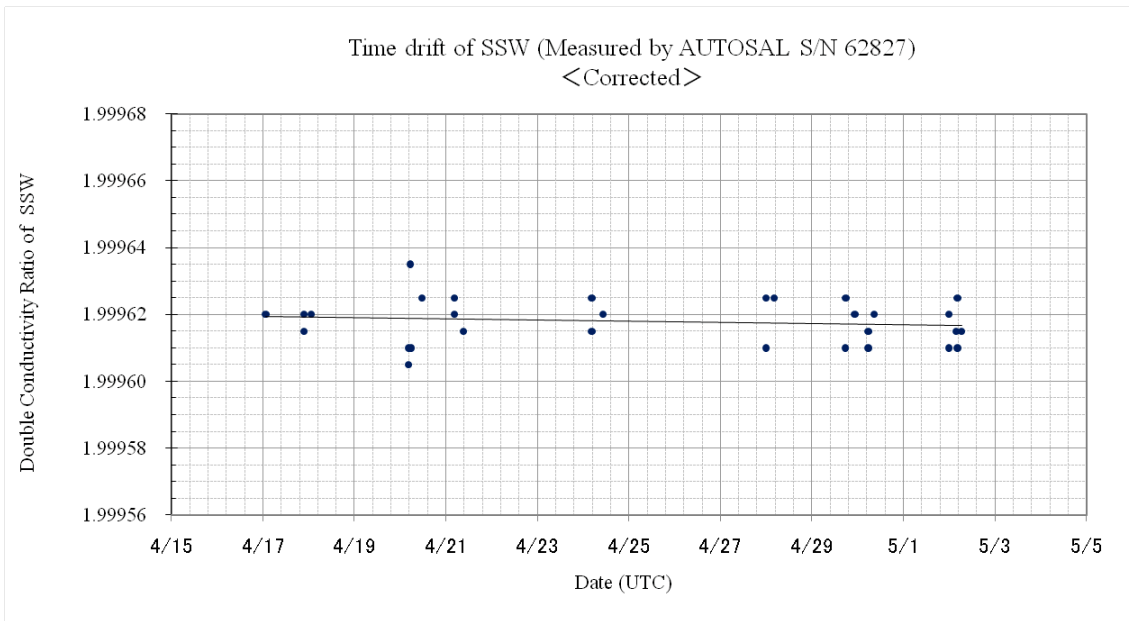


Fig. 2.2.2-2 The history of the double conductivity ratio for the Standard Seawater batch P152 (After correction)

b. Sub-Standard Seawater

Sub-standard seawater was made from deep-sea water filtered by a pore size of 0.45 micrometer and stored in a 20-liter container made of polyethylene and stirred for at least 24 hours before measuring. It was measured about every 6 samples in order to check for the possible sudden drifts of the salinometer.

c. Replicate Samples

We estimated the precision of this method using 34 pairs of replicate samples taken from the same Niskin bottle. Fig.2.2.2-3 shows the histogram of the absolute difference between each pair of the replicate samples. The average and the standard deviation of absolute difference among 34 pairs of replicate samples were 0.0002 and 0.0001 in salinity, respectively.

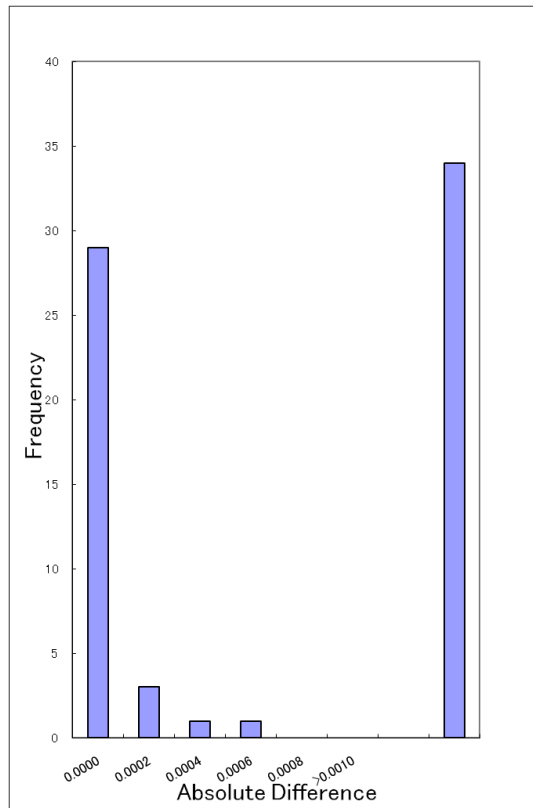


Fig. 2.2.2-3 The histogram of the double conductivity ratio for the absolute difference of replicate samples

(4) Data archive

These raw datasets will be submitted to JAMSTEC Data Management Office (DMO).

(5) Reference

- Aoyama, M. , T. Joyce, T. Kawano and Y. Takatsuki: Standard seawater comparison up to P129. Deep-Sea Research, I, Vol. 49, 1103~1114, 2002
- UNESCO : Tenth report of the Joint Panel on Oceanographic Tables and Standards. UNESCO Tech. Papers in Mar. Sci., 36, 25 pp., 1981

2.2.3 Shipboard ADCP

Makio HONDA (JAMSTEC RIGC)

Souichiro SUEYOSHI (Global Ocean Development Inc., GODI)

Norio NAGAHAMA (GODI)

Wataru TOKUNAGA (MIRAI Crew)

(1) Objective

To obtain continuous measurement of the current profile along the ship's track.

(2) Methods

Upper ocean current measurements were made in MR11-03 cruise, using the hull-mounted Acoustic Doppler Current Profiler (ADCP) system. For most of its operation the instrument was configured for water-tracking mode. Bottom-tracking mode, interleaved bottom-ping with water-ping, was made to get the calibration data for evaluating transducer misalignment angle in the shallow water. The system consists of following components;

1. R/V MIRAI has installed the Ocean Surveyor for vessel-mount ADCP (frequency 75 kHz; Teledyne RD Instruments, USA). It has a phased-array transducer with single ceramic assembly and creates 4 acoustic beams electronically. We mounted the transducer head rotated to a ship-relative angle of 45 degrees azimuth from the keel
2. For heading source, we use ship's gyro compass (Tokimec, Japan), continuously providing heading to the ADCP system directory. Additionally, we have Inertial Navigation System which provide high-precision heading, attitude information, pitch and roll, are stored in ".N2R" data files with a time stamp.
3. DGPS system (Trimble SPS751 & Fugro Multifix ver.5) providing precise ship's position.
4. We used VmDas software version 1.4.2 (TRDI) for data acquisition.
5. To synchronize time stamp of ping with GPS time, the clock of the logging computer is adjusted to GPS time every 1 minute
6. Fresh water is charged in the sea chest to prevent biofouling at transducer face.
7. The sound speed at the transducer does affect the vertical bin mapping and vertical velocity measurement, is calculated from temperature, salinity (constant value; 35.0 psu) and depth (6.5 m; transducer depth) by equation in Medwin (1975).

Data was configured for 8-m intervals starting 23-m below sea surface. Data was recorded every ping as raw ensemble data (.ENR). Also, 60 seconds and 300 seconds averaged data were recorded as short-term average (.STA) and long-term average (.LTA) data, respectively. Major parameters for the measurement, Direct Command, are shown in Table 2.2.3-1.

(3) Preliminary results

Fig.2.2.3-1 shows the current profile along the ship's track.

(4) Data archive

These data obtained in this cruise will be submitted to The Data Management Group (DMG) of JAMSTEC, and will be opened to the public via JAMSTEC home page.

(5) Remarks

Following periods, ship attitude (roll, pitch, heading) data was invalid, because of restarting the Inertial Navigation System.

01:08 – 01:13 UTC, 15 Apr.

01:33 – 01:38 UTC, 15 Apr.

02:04 – 02:09 UTC, 15 Apr.

Table 2.2.3-1 Major parameters

Bottom-Track Commands

BP = 001 Pings per Ensemble (almost less than 1000m depth)

Environmental Sensor Commands

EA = +04500 Heading Alignment (1/100 deg)

EB = +00000 Heading Bias (1/100 deg)

ED = 00065 Transducer Depth (0 - 65535 dm)

EF = +001 Pitch/Roll Divisor/Multiplier (pos/neg) [1/99 - 99]

EH = 00000 Heading (1/100 deg)

ES = 35 Salinity (0-40 pp thousand)

EX = 00000 Coord Transform (Xform:Type; Tilts; 3Bm; Map)

EZ = 10200010 Sensor Source (C; D; H; P; R; S; T; U)

C (1): Sound velocity calculates using ED, ES, ET (temp.)

D (0): Manual ED

H (2): External synchro

P (0), R (0): Manual EP, ER (0 degree)

S (0): Manual ES

T (1): Internal transducer sensor

U (0): Manual EU

Timing Commands

TE = 00:00:02.00 Time per Ensemble (hrs:min:sec.sec/100)

TP = 00:02.00 Time per Ping (min:sec.sec/100)

Water-Track Commands

WA = 255 False Target Threshold (Max) (0-255 count)

WB = 1	Mode 1 Bandwidth Control (0=Wid, 1=Med, 2=Nar)
WC = 120	Low Correlation Threshold (0-255)
WD = 111 100 000	Data Out (V; C; A; PG; St; Vsum; Vsum^2; #G; P0)
WE = 1000	Error Velocity Threshold (0-5000 mm/s)
WF = 0800	Blank After Transmit (cm)
WG = 001	Percent Good Minimum (0-100%)
WI = 0	Clip Data Past Bottom (0 = OFF, 1 = ON)
WJ = 1	Rcvr Gain Select (0 = Low, 1 = High)
WM = 1	Profiling Mode (1-8)
WN = 100	Number of depth cells (1-128)
WP = 00001	Pings per Ensemble (0-16384)
WS = 800	Depth Cell Size (cm)
WT = 000	Transmit Length (cm) [0 = Bin Length]
WV = 0390	Mode 1 Ambiguity Velocity (cm/s radial)

MR11-03 Cruise(2011/4/14-2011/5/4)
30min.Average / Layer : 100-140m

1.0m/s

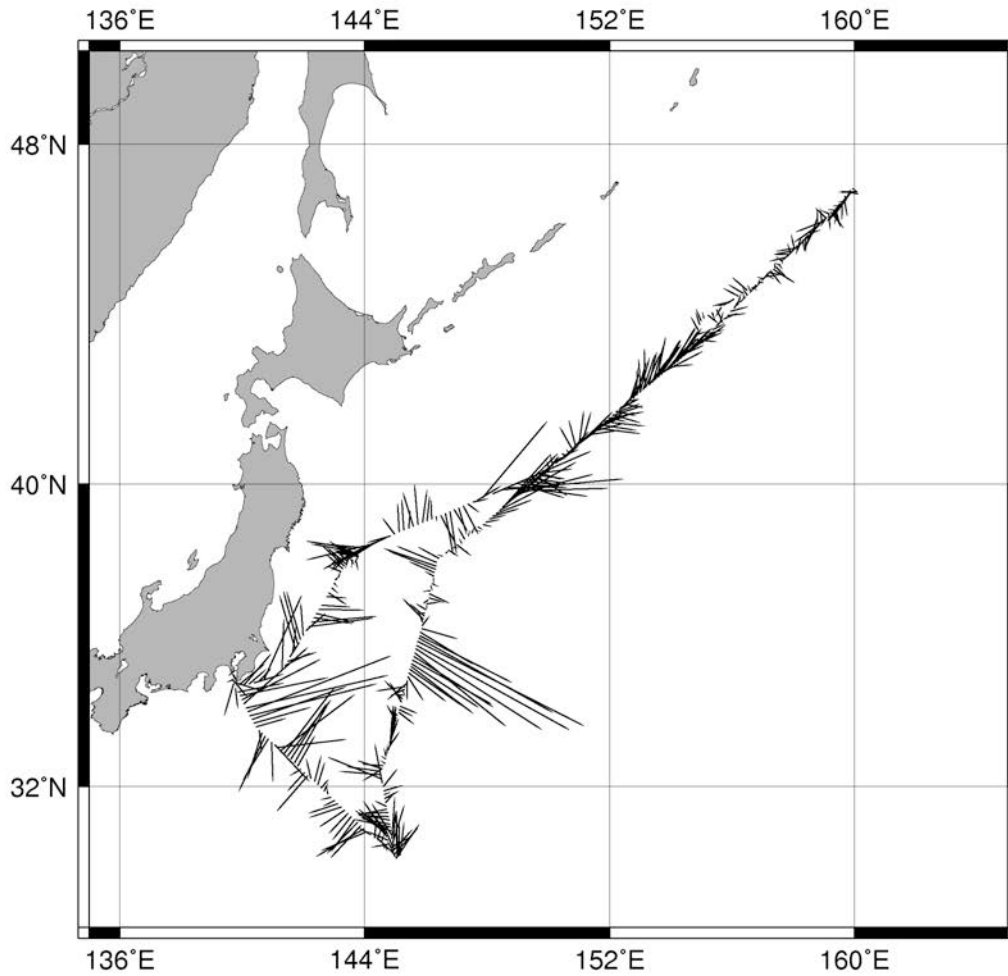


Fig 2.2.3-1. Current profile along the ship's track.

2.3 Sea surface water monitoring

Masahide WAKITA (JAMSTEC): Principal Investigator

Misato KUWAHARA (Marine Works Japan Co. Ltd): Operation Leader

Hideki YAMAMOTO (Marine Works Japan Co. Ltd)

(1) Objective

Our purpose is to obtain temperature, salinity, dissolved oxygen, and fluorescence data continuously in near-sea surface water.

(2) Parameters

Temperature (surface water)

Salinity (surface water)

Dissolved oxygen (surface water)

Fluorescence (surface water)

(3) Instruments and Methods

The Continuous Sea Surface Water Monitoring System (Marine Works Japan Co. Ltd.) has four sensors and automatically measures temperature, conductivity, dissolved oxygen and fluorescence in near-sea surface water every one minute. This system is located in the “*sea surface monitoring laboratory*” and connected to shipboard LAN-system. Measured data, time, and location of the ship were stored in a data management PC. The near-surface water was continuously pumped up to the laboratory from about 4.5 m water depth and flowed into the system through a vinyl-chloride pipe. The flow rate of the surface seawater was adjusted to be $5 \text{ dm}^3 \text{ min}^{-1}$.

a. Instruments

Software

Seamoni-kun Ver.1.10

Sensors

Specifications of the each sensor in this system are listed below.

1) Temperature and Conductivity sensor

Model:	SBE-45, SEA-BIRD ELECTRONICS, INC.
Serial number:	4552788-0264
Measurement range:	Temperature -5 to +35 °C Conductivity 0 to 7 S m ⁻¹
Initial accuracy:	Temperature 0.002 °C Conductivity 0.0003 S m ⁻¹
Typical stability (per month):	Temperature 0.0002 °C Conductivity 0.0003 S m ⁻¹
Resolution:	Temperatures 0.0001 °C

Conductivity 0.00001 S m⁻¹

2) Bottom of ship thermometer

Model: SBE 38, SEA-BIRD ELECTRONICS, INC.
 Serial number: 3852788-0457
 Measurement range: -5 to +35 °C
 Initial accuracy: ±0.001 °C
 Typical stability (per 6 month): 0.001 °C
 Resolution: 0.00025 °C

3) Dissolved oxygen sensor

Model: OPTODE 3835, AANDERAA Instruments.
 Serial number: 1519
 Measuring range: 0 - 500 µmol dm⁻³
 Resolution: <1 µmol dm⁻³
 Accuracy: <8 µmol dm⁻³ or 5% whichever is greater
 Settling time: <25 s

4) Fluorometer

Model: C3, TURNER DESIGNS
 Serial number: 2300123

b. Measurements

Periods of measurement during MR 11-03 are listed in Table 2.3-1.

Table 2.3-1 Events list of the Sea surface water monitoring during MR11-03

System Date [UTC]	System Time [UTC]	Events	Remarks
2011/4/14	10:16	All the measurements were started and data was available.	Cruise start
2011/04/23	06:05	All the measurements were stopped for seawater line maintenance	
2011/04/23	07:43	All the measurements were restarted and data was available.	
2011/04/29	18:14~18:16	The accident occurred when saving data.	
2011/05/04	0:22	All the measurements were stopped.	Cruise end

(5) Preliminary Result

Preliminary data of temperature, salinity, dissolved oxygen and fluorescence at sea surface is shown in Fig. 2.3-1.

Fig. 2.3-1. Spatial and temporal distribution of (a) temperature, (b) salinity, (c) dissolved oxygen and (d) fluorescence in MR11-03 cruise.

We took the surface water samples to compare sensor data with bottle data of salinity, dissolved oxygen and fluorescence. The results are shown in Figs. 2.3-2 - 4. All the salinity samples were analyzed by the Guideline 8400B “AUTOSAL” (see 2.2.2), and dissolve oxygen samples were analyzed by Winkler method (see 2.4), and fluorescence were analyzed by 10-AU (see 3.1.1).

(6) Data archive

All data will be submitted to Chief Scientist.

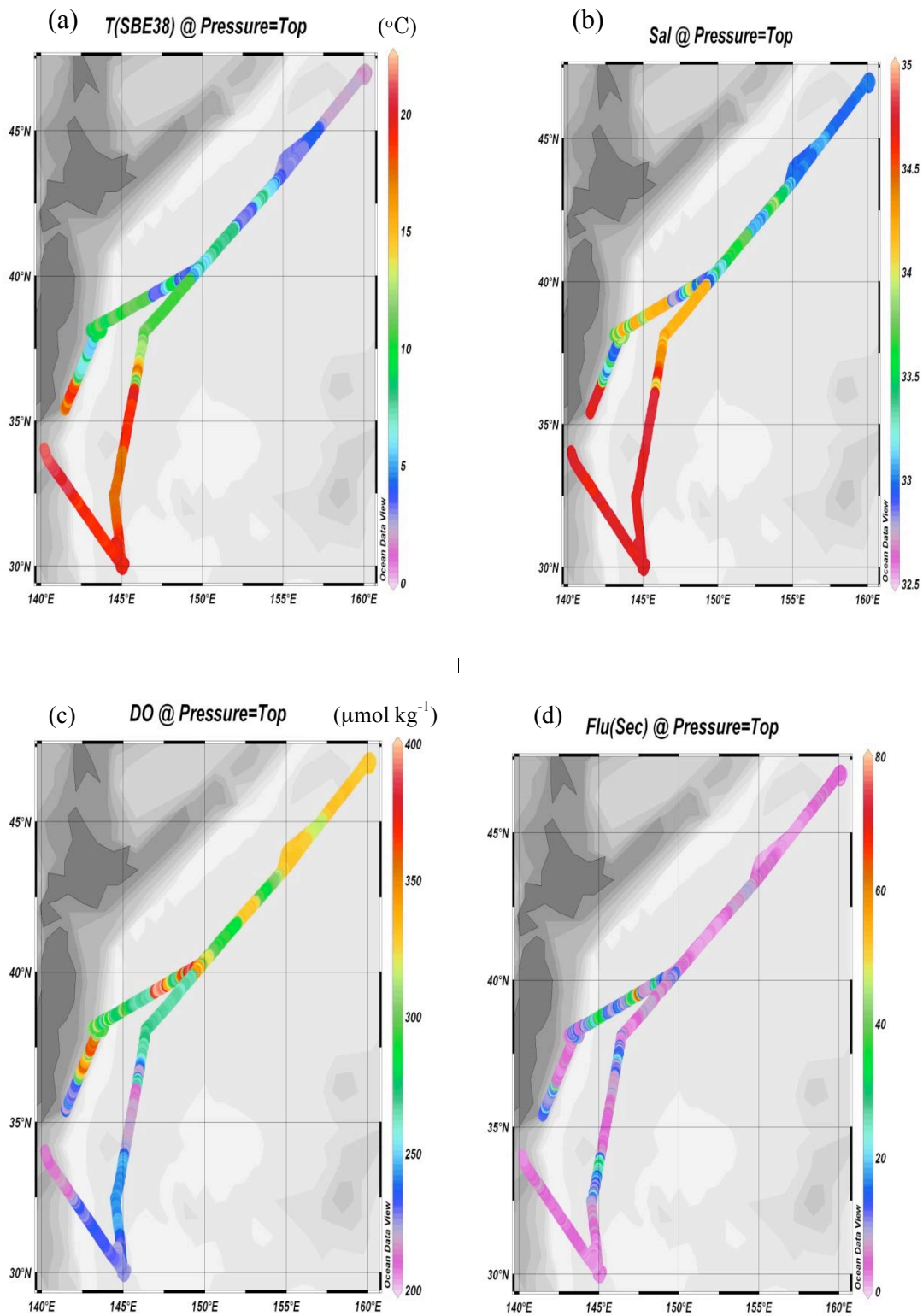


Fig. 2.3-1. Spatial and temporal distribution of (a) temperature, (b) salinity, (c) dissolved oxygen and (d) fluorescence in MR11-03 cruise.

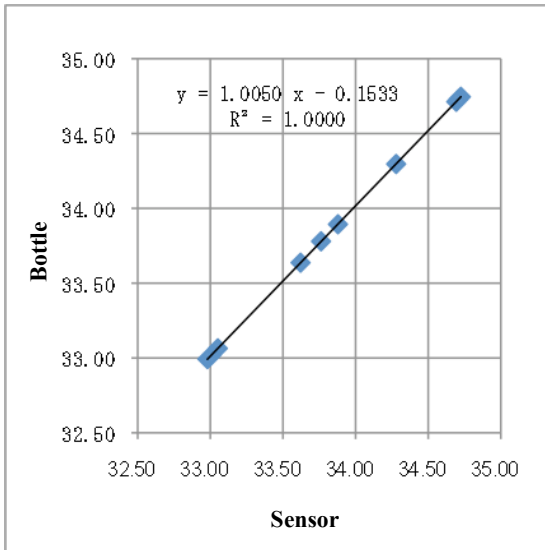


Fig. 2.3-2. Correlation of salinity between sensor and bottle data

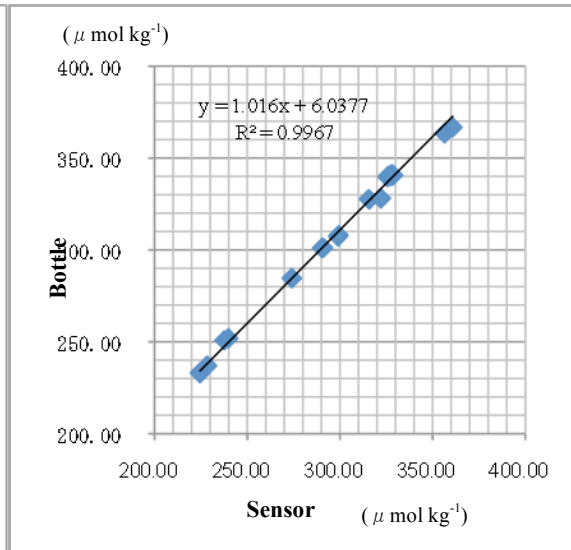


Fig. 2.3-3. Correlation of dissolved oxygen between sensor and bottle data

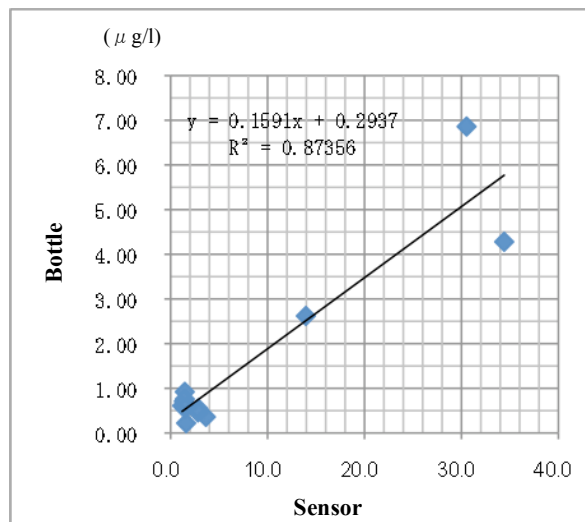


Fig. 2.3-4. Correlation of fluorescence between sensor and bottle data

2.4 Dissolved oxygen

Masahide WAKITA (JAMSTEC): Principal Investigator

Misato KUWAHARA (Marine Works Japan Co. Ltd): Operation Leader

Hideki YAMAMOTO (Marine Works Japan Co. Ltd)

(1) Objectives

Determination of dissolved oxygen in seawater by Winkler titration.

(2) Parameter

Dissolved Oxygen

(3) Instruments and Methods

Following procedure is based on an analytical method, entitled by “Determination of dissolved oxygen in sea water by Winkler titration”, in the WHP Operations and Methods (Dickson, 1996).

a. Instruments

Burette for sodium thiosulfate and potassium iodate;

APB-510 manufactured by Kyoto Electronic Co. Ltd. / 10 cm³ of titration vessel

Detector;

Automatic photometric titrator (DOT-01) manufactured by Kimoto Electronic Co. Ltd.

Software;

DOT controller Ver.2.2.1

b. Reagents

Pickling Reagent I: Manganese chloride solution (3 mol dm⁻³)

Pickling Reagent II: Sodium hydroxide (8 mol dm⁻³) / sodium iodide solution (4 mol dm⁻³)

Sulfuric acid solution (5 mol dm⁻³)

Sodium thiosulfate (0.025 mol dm⁻³)

Potassium iodide (0.001667 mol dm⁻³)

CSK standard of potassium iodide:

Lot EPJ3885, Wako Pure Chemical Industries Ltd., 0.0100N

c. Sampling

Seawater samples were collected with Niskin bottle attached to the CTD-system and surface bucket sampler. Seawater for oxygen measurement was transferred from sampler to a volume calibrated flask (ca. 100 cm³). Three times volume of the flask of seawater was overflowed. Temperature was measured by digital thermometer during the overflowing. Then two reagent solutions (Reagent I and II) of 0.5 cm³ each were added immediately into the sample flask and the stopper was inserted carefully into the flask. The sample flask was then shaken vigorously to mix the contents and to disperse the precipitate finely throughout. After

the precipitate has settled at least halfway down the flask, the flask was shaken again vigorously to disperse the precipitate. The sample flasks containing pickled samples were stored in a laboratory until they were titrated.

d. Sample measurement

At least two hours after the re-shaking, the pickled samples were measured on board. 1 cm³ sulfuric acid solution and a magnetic stirrer bar were added into the sample flask and stirring began. Samples were titrated by sodium thiosulfate solution whose morality was determined by potassium iodate solution. Temperature of sodium thiosulfate during titration was recorded by a digital thermometer. During this cruise, we measured dissolved oxygen concentration using 2 sets of the titration apparatus. Dissolved oxygen concentration ($\mu\text{mol kg}^{-1}$) was calculated by sample temperature during seawater sampling, salinity, flask volume, and titrated volume of sodium thiosulfate solution without the blank. When we measured low concentration samples, titration procedure was adjusted manually.

e. Standardization and determination of the blank

Concentration of sodium thiosulfate titrant was determined by potassium iodate solution. Pure potassium iodate was dried in an oven at 130 °C. 1.7835 g potassium iodate weighed out accurately was dissolved in deionized water and diluted to final volume of 5 dm³ in a calibrated volumetric flask (0.001667 mol dm⁻³). 10 cm³ of the standard potassium iodate solution was added to a flask using a volume-calibrated dispenser. Then 90 cm³ of deionized water, 1 cm³ of sulfuric acid solution, and 0.5 cm³ of pickling reagent solution II and I were added into the flask in order. Amount of titrated volume of sodium thiosulfate (usually 5 times measurements average) gave the morality of sodium thiosulfate titrant.

The oxygen in the pickling reagents I (0.5 cm³) and II (0.5 cm³) was assumed to be 3.8×10^{-8} mol (Murray *et al.*, 1968). The blank due to other than oxygen was determined as follows. 1 and 2 cm³ of the standard potassium iodate solution were added to two flasks respectively using a calibrated dispenser. Then 100 cm³ of deionized water, 1 cm³ of sulfuric acid solution, and 0.5 cm³ of pickling reagent solution II and I each were added into the flask in order. The blank was determined by difference between the first (1 cm³ of KIO₃) titrated volume of the sodium thiosulfate and the second (2 cm³ of KIO₃) one. The results of 3 times blank determinations were averaged.

Table 2.4-1 shows results of the standardization and the blank determination during this cruise.

Date	KIO ₃ ID	Na ₂ S ₂ O ₃	DOT-01(No.1)		DOT-01(No.2)		Stations
			E.P.	Blank	E.P.	Blank	
2011/4/15	20100630-02-07	20100702-07	3.942	0.000	3.943	0.000	StC, KNT
2011/4/15	CSK	20100702-07	3.935	0.000	3.937	0.000	
2011/4/16	CSK	20100702-07	3.934	0.000	3.935	0.000	
2011/4/19	20100630-02-08	20100702-07	3.940	0.000	3.939	0.001	K02 cast01,cast03,cast07
2011/4/23	20100630-02-09	20100702-07	3.942	0.000	3.941	0.000	
2011/4/24	20100630-02-10	20100702-07	3.940	0.000	3.940	0.000	

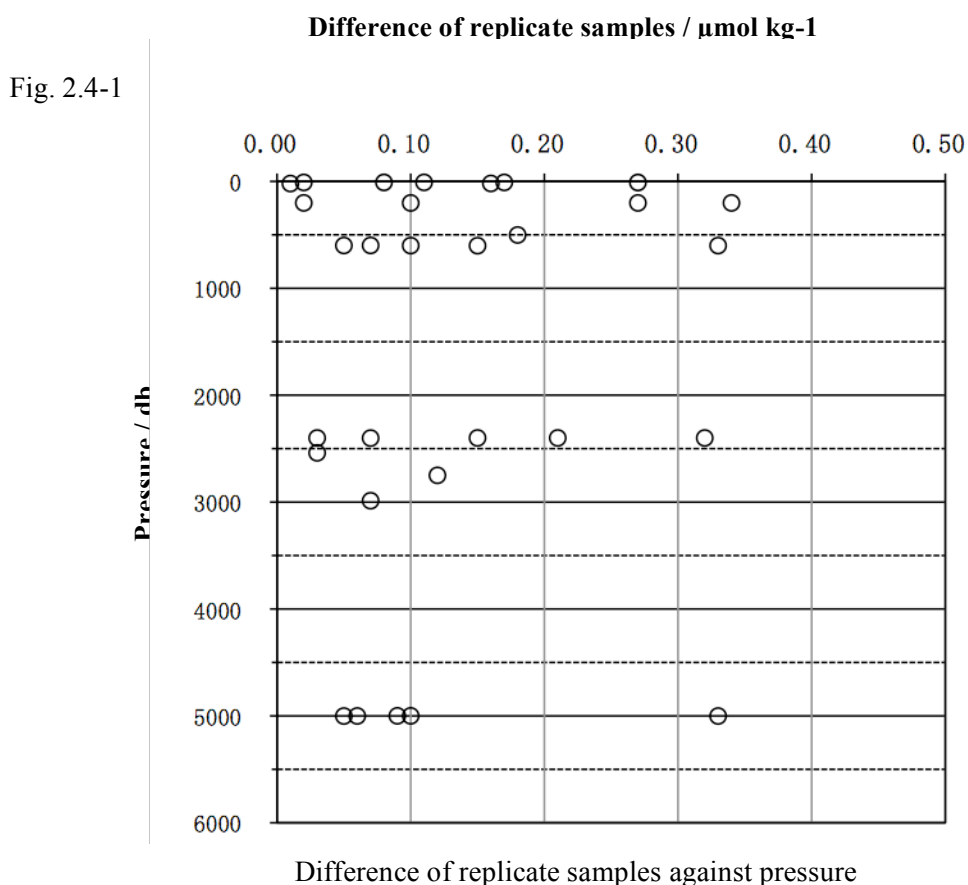
2011/4/25	20100630-03-01	20100702-07	3.944	0.000	3.946	0.000	JKO,KEO
2011/4/28	20100630-03-02	20100702-07	3.943	0.002	3.942	0.001	
2011/4/29	20100630-03-02	20100702-08	3.944	0.001	3.945	-0.001	S01 cast02, cast04, cast06
2011/5/2	20100630-03-03	20100702-08	3.943	0.000	3.944	-0.001	
2011/5/2	CSK	20100702-08	3.939	0.000	3.940	-0.001	

f. Repeatability of sample measurement

Replicate samples were taken at every CTD casts. Total amount of the replicate sample pairs of good measurement was 32. The standard deviation of the replicate measurement was 0.12 $\mu\text{mol kg}^{-1}$ that was calculated by a procedure in Guide to best practices for ocean CO_2 measurements Chapter4 SOP23 Ver.3.0 (2007). Results of replicate samples were shown in Table 2.4-2 and this diagram shown in Fig. 2.4-1and-2.

Layer	Number of replicate sample pairs	Oxygen concentration ($\mu\text{mol kg}^{-1}$) Standard Deviation.
1000m>=	19	0.13
>1000m	13	0.11
All	32	0.12

Table 2.4-2 Results of the standardization and the blank determinations during this cruise.



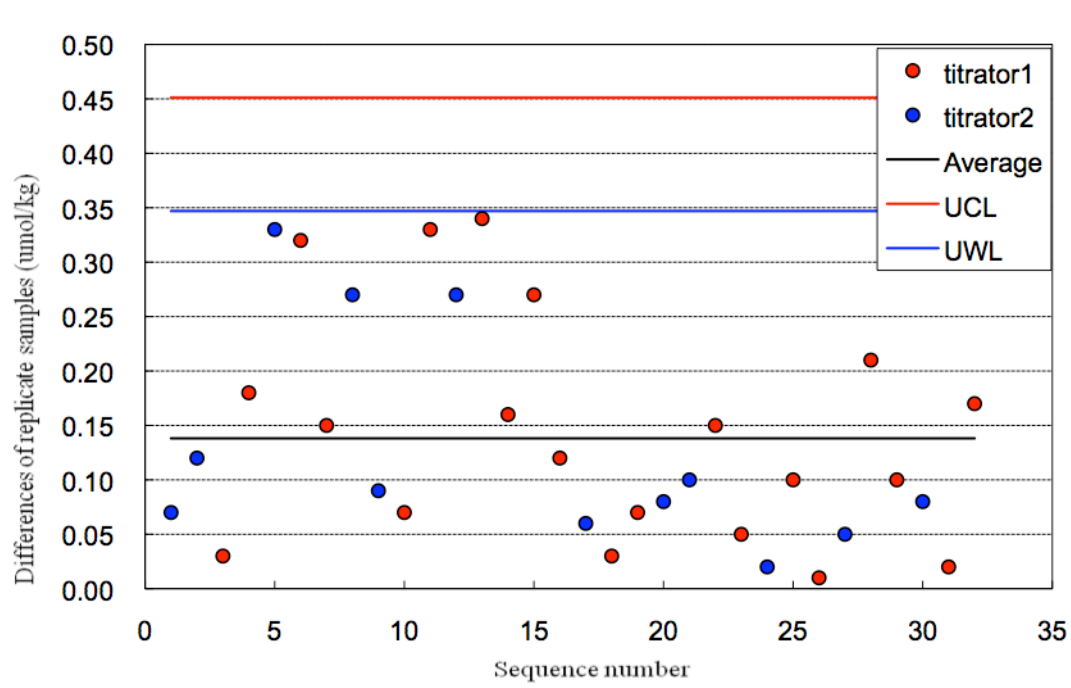


Fig. 2.4-2 Difference of replicate samples against sequence number

(4) Data archive

All data will be submitted to Chief Scientist.

(5) References

Dickson, A.G., Determination of dissolved oxygen in sea water by Winkler titration. (1996)

Dickson, A.G., Sabine, C.L. and Christian, J.R. (Eds.), Guide to best practices for ocean CO₂ measurements. (2007)

Culberson, C.H., WHP Operations and Methods July-1991 "Dissolved Oxygen", (1991)

Japan Meteorological Agency, Oceanographic research guidelines (Part 1). (1999)

KIMOTO electric CO. LTD., Automatic photometric titrator DOT-01 Instruction manual

2.5 Nutrients

Michio AOYAMA (Meteorological Research Institute) Principal investigator

Masahide WAKITA (JAMSTEC MIO)

Kenichiro SATO (Department of Marine Science, Marine Works Japan Ltd.)

Masanori ENOKI (Department of Marine Science, Marine Works Japan Ltd.)

(1) Objectives

The objectives of nutrients analyses during the R/V Mirai MR11-03 cruise in the Western North Pacific Ocean are as follows:

- Describe the present status of nutrients concentration with excellent comparability.
- Provide excellent nutrients data to biologist onboard MR11-03 to help their study.

(2) Parameters

The determinants are nitrate, nitrite, phosphate, silicate and ammonia in the western North Pacific Ocean.

(3) Summary of nutrients analysis

We made 10 runs for the samples at 9 stations (15 casts) in MR11-03. The total amount of layers of the seawater sample reached up to 299 for MR11-03. We made duplicate measurement at all layers (stn. A, B, C and D were single measurement). The station locations for nutrients measurement is shown in Figure 2.5.1

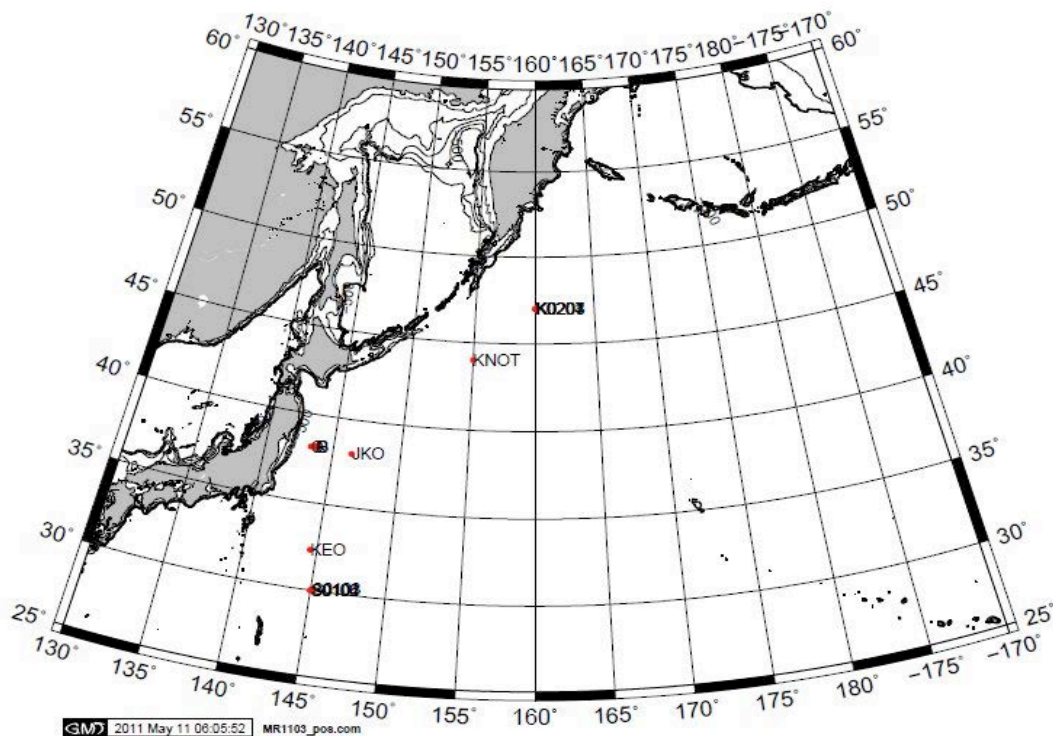


Figure 2.5.1 Sampling positions of nutrients sample.

(4) Instrument and methods

a). Analytical detail using QuAatro system

The phosphate analysis was a modification of the procedure of Murphy and Riley (1962). Molybdc acid was added to the seawater sample to form phosphomolybdc acid which was in turn reduced to phosphomolybdous acid using L-ascorbic acid as the reductant.

Nitrate + nitrite and nitrite were analyzed according to the modification method of Grasshoff (1970). The sample nitrate was reduced to nitrite in a cadmium tube inside of which was coated with metallic copper. The sample stream with its equivalent nitrite was treated with an acidic, sulfanilamide reagent and the nitrite forms nitrous acid which reacted with the sulfanilamide to produce a diazonium ion. N-1-Naphthylethylene-diamine added to the sample stream then coupled with the diazonium ion to produce a red, azo dye. With reduction of the nitrate to nitrite, both nitrate and nitrite reacted and were measured; without reduction, only nitrite reacted. Thus, for the nitrite analysis, no reduction was performed and the alkaline buffer was not necessary. Nitrate was computed by difference.

The silicate method was analogous to that described for phosphate. The method used was essentially that of Grasshoff et al. (1983), wherein silicomolybdc acid was first formed from the silicate in the sample and added molybdc acid; then the silicomolybdc acid was reduced to silicomolybdous acid, or "molybdenum blue" using ascorbic acid as the reductant. The analytical methods of the nutrients, nitrate, nitrite, silicate and phosphate, during this cruise were same as the methods used in (Kawano et al. 2009).

The details of modification of analytical methods used in this cruise are also compatible with the methods described in nutrients section in GO-SHIP repeat hydrography manual (Hydes et al., 2010)

The ammonia in seawater was mixed with an alkaline containing EDTA, ammonia as gas state was formed from seawater. The ammonia (gas) was absorbed in sulfuric acid by way of 0.5 μm pore size membrane filter (ADVANTEC PTFE) at the dialyzer attached to analytical system. The ammonia absorbed in sulfuric acid was determined by coupling with phenol and hypochlorite to form indophenols blue. Wavelength using ammonia analysis was 630 nm, which was absorbance of indophenols blue.

The flow diagrams and reagents for each parameter are shown in Figures 2.5.2 to 2.5.6.

b). Nitrate + Nitrite Reagents

Imidazole (buffer), 0.06 M (0.4 % w/v)

Dissolved 4 g imidazole, $C_3H_4N_2$, in ca. 1000 ml DIW; added 2 ml concentrated HCl. After mixing, 1 ml Triton®X-100 (50 % solution in ethanol) was added.

Sulfanilamide, 0.06 M (1 % w/v) in 1.2M HCl

Dissolved 10 g sulfanilamide, $4-NH_2C_6H_4SO_3H$, in 900 ml of DIW, added 100 ml concentrated HCl. After mixing, 2 ml Triton®X-100 (50 % solution in ethanol) was added.

N-1-Naphthylethylene-diamine dihydrochloride, 0.004 M (0.1 %f w/v)

Dissolved 1 g NED, $C_{10}H_7NHCH_2CH_2NH_2 \cdot 2HCl$, in 1000 ml of DIW and added 10 ml concentrated HCl. After mixing, 1 ml Triton®X-100 (50 % solution in ethanol) was added. This reagent was stored in a dark bottle.

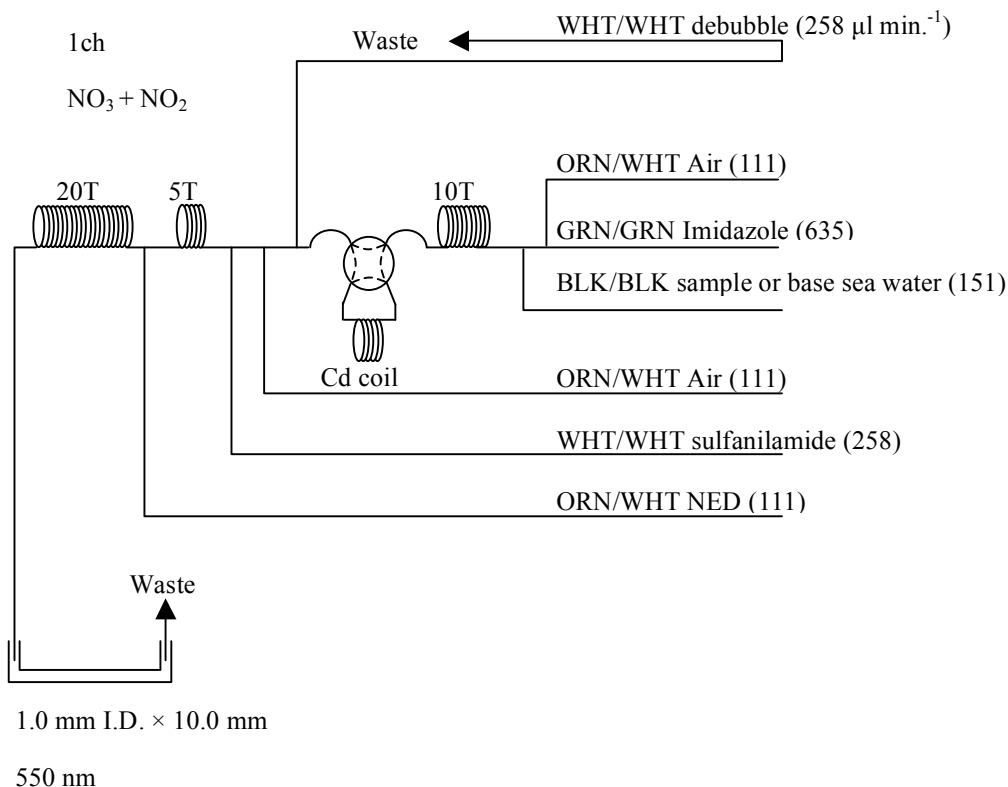


Figure 2.5.2 NO₃+NO₂ (1ch.) Flow diagram.

c). Nitrite Reagents

Sulfanilamide, 0.06 M (1 % w/v) in 1.2 M HCl

Dissolved 10g sulfanilamide, 4-NH₂C₆H₄SO₃H, in 900 ml of DIW, added 100 ml concentrated HCl. After mixing, 2 ml Triton®X-100 (50 % solution in ethanol) was added.

N-1-Naphthylethylene-diamine dihydrochloride, 0.004 M (0.1 % w/v)

Dissolved 1 g NED, C₁₀H₇NHCH₂CH₂NH₂•2HCl, in 1000 ml of DIW and added 10 ml concentrated HCl. After mixing, 1 ml Triton®X-100 (50 % solution in ethanol) was added. This reagent was stored in a dark bottle.

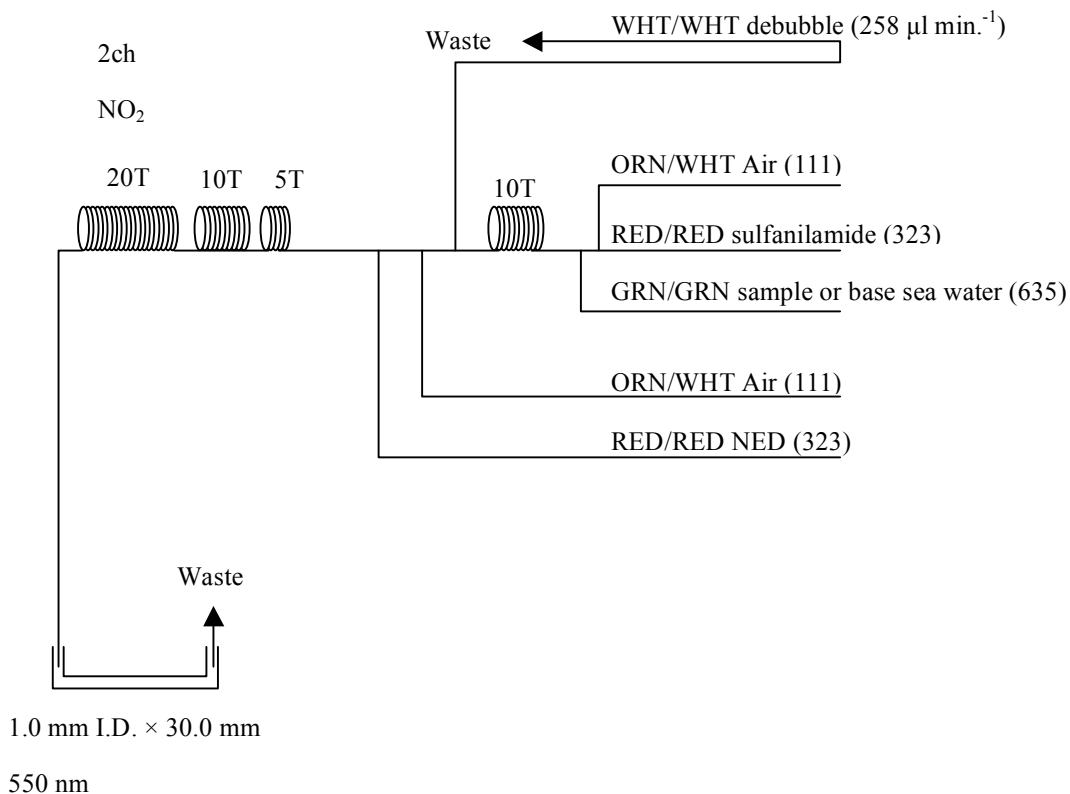


Figure 2.5.3 NO₂ (2ch.) Flow diagram.

d. Silicate Reagents

Molybdic acid, 0.06 M (2 % w/v)

Dissolved 15 g disodium molybdate (VI) dihydrate, $\text{Na}_2\text{MoO}_4 \cdot 2\text{H}_2\text{O}$, in 980 ml DIW, added 8 ml concentrated H_2SO_4 . After mixing, 20 ml sodium dodecyl sulphate (15 % solution in water) was added.

Oxalic acid, 0.6 M (5 % w/v)

Dissolved 50 g oxalic acid anhydrous, HOOC:COOH , in 950 ml of DIW.

Ascorbic acid, 0.01M (3 % w/v)

Dissolved 2.5g L (+)-ascorbic acid, $\text{C}_6\text{H}_8\text{O}_6$, in 100 ml of DIW. This reagent was freshly prepared before every measurement.

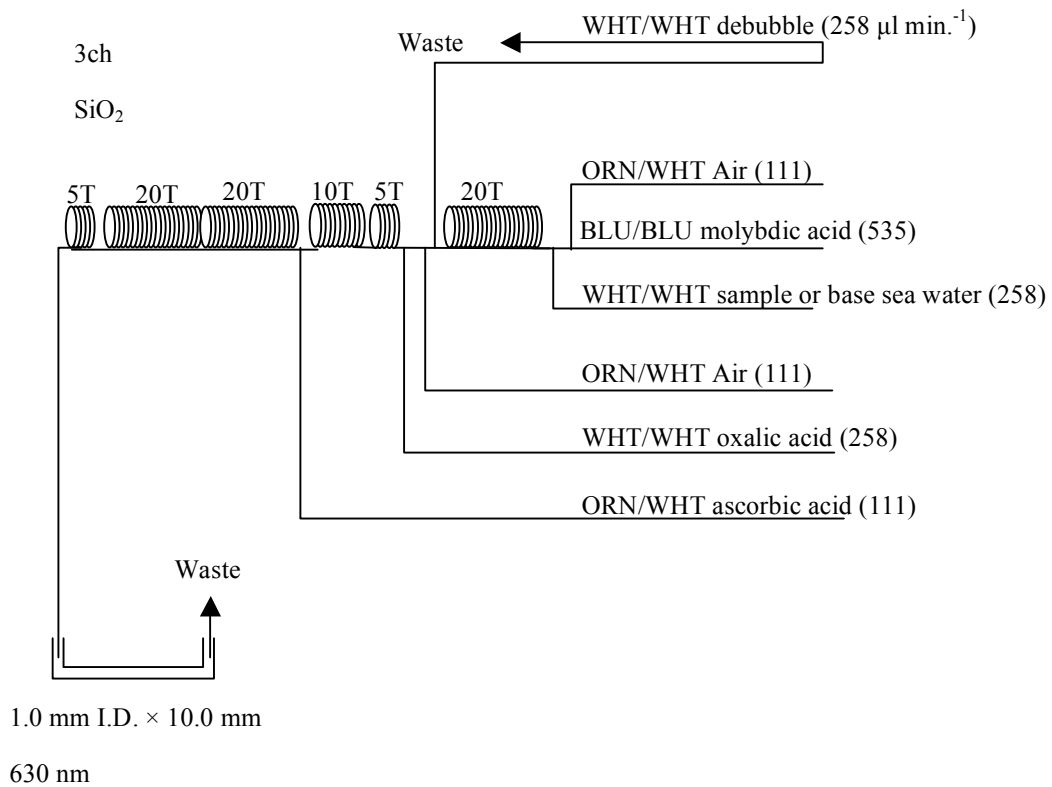


Figure 2.5.4 SiO_2 (3ch.) Flow diagram.

e). Phosphate Reagents

Stock molybdate solution, 0.03M (0.8 % w/v)

Dissolved 8 g disodium molybdate (VI) dihydrate, $\text{Na}_2\text{M}_6\text{O}_4 \cdot 2\text{H}_2\text{O}$, and 0.17 g antimony potassium tartrate, $\text{C}_8\text{H}_4\text{K}_2\text{O}_{12}\text{Sb}_2 \cdot 3\text{H}_2\text{O}$, in 950 ml of DIW and added 50 ml concentrated H_2SO_4 .

Mixed Reagent

Dissolved 1.2 g L (+)-ascorbic acid, $\text{C}_6\text{H}_8\text{O}_6$, in 150 ml of stock molybdate solution. After mixing, 3 ml sodium dodecyl sulphate (15 % solution in water) was added. This reagent was freshly prepared before every measurement.

Reagent for sample dilution

Dissolved sodium chloride, NaCl , 10 g in ca. 950 ml of DIW, added 50 ml acetone and 4 ml concentrated H_2SO_4 . After mixing, 5 ml sodium dodecyl sulphate (15 % solution in water) was added.

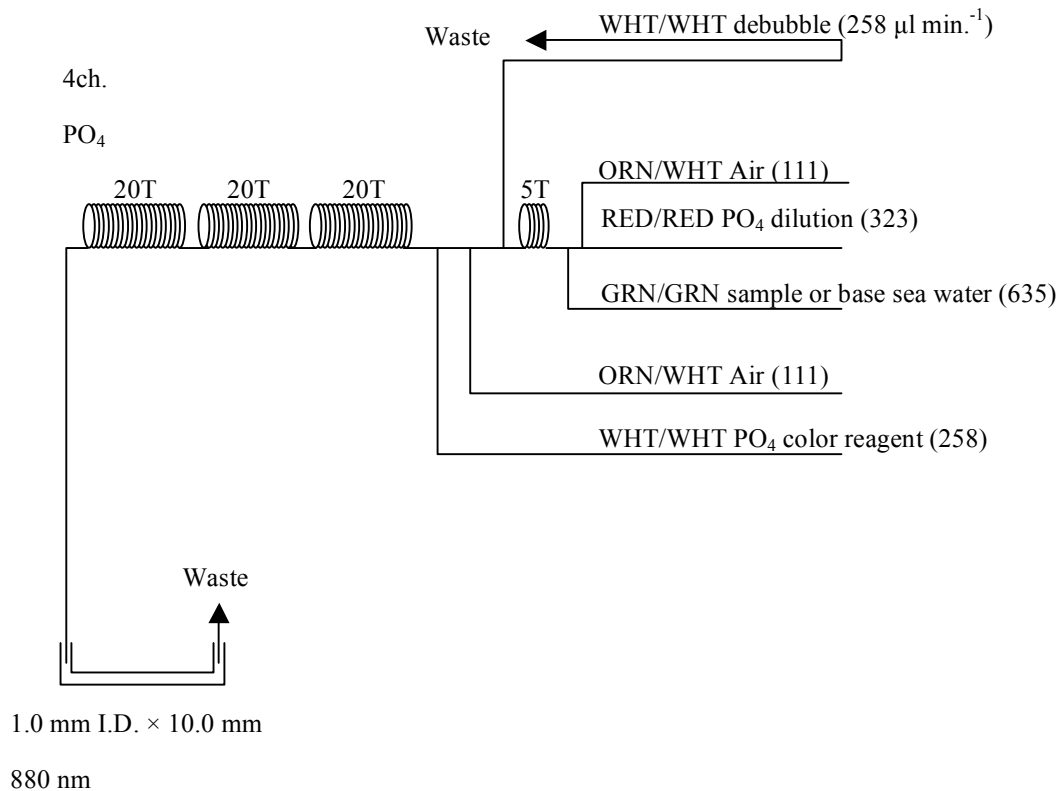


Figure 2.5.5 PO₄ (4ch.) Flow diagram.

f). Ammonia Reagents

EDTA

Dissolved 41 g EDTA (ethylenediaminetetraacetic acid tetrasodium salt), $C_{10}H_{12}N_2O_8Na_4 \cdot 4H_2O$, and 2 g boric acid, H_3BO_3 , in 200 ml of DIW. After mixing, 1 ml Triton®X-100 (30 % solution in DIW) was added. This reagent was prepared at a week about.

NaOH

Dissolved 5 g sodium hydroxide, NaOH, and 16 g EDTA in 100 ml of DIW. This reagent was prepared at a week about.

Stock Nitroprusside

Dissolved 0.25 g sodium pentacyanonitrosylferrate (II), $Na_2[Fe(CN)_5NO]$, in 100 ml of DIW and added 0.2 ml 1N H_2SO_4 . Stored in a dark bottle and prepared at a month about.

Nitroprusside solution

Mixed 4 ml stock nitroprusside and 5 ml 1N H_2SO_4 in 500 ml of DIW. After mixing, 1 ml Triton®X-100 (30 % solution in DIW) was added. This reagent was stored in a dark bottle and prepared at every 2 or 3 days.

Alkaline phenol

Dissolved 10 g phenol, C_6H_5OH , 5 g sodium hydroxide and citric acid, $C_6H_8O_7$, in 200 ml DIW. Stored in a dark bottle and prepared at a week about.

NaClO solution

Mixed 3 ml sodium hypochlorite solution, NaClO, in 47 ml DIW. Stored in a dark bottle and freshly prepared before every measurement. This reagent was prepared 0.3% available chlorine.

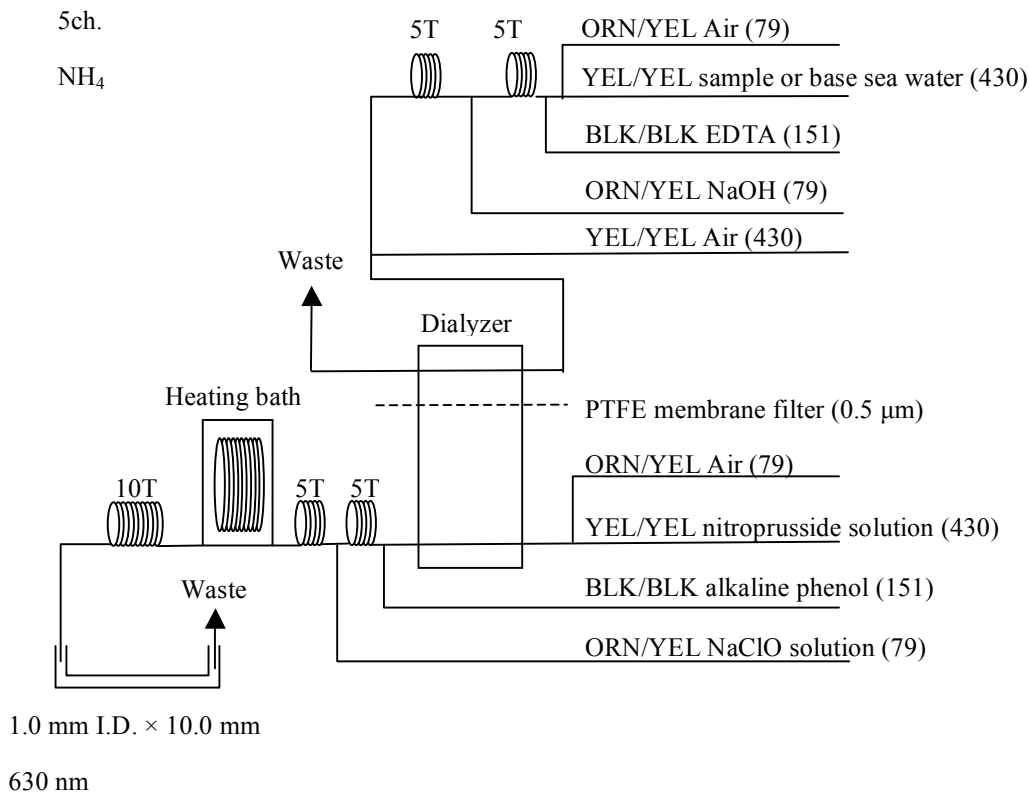


Figure 2.5.6 NH₄ (5ch.) Flow diagram.

g). Sampling procedures

Sampling of nutrients followed that oxygen, salinity and trace gases. Samples were drawn into two of virgin 10 ml polyacrylates vials without sample drawing tubes. These were rinsed three times before filling and vials were capped immediately after the drawing. The vials were put into water bath adjusted to ambient temperature, 24 ± 2 deg. C, in about 30 minutes before use to stabilize the temperature of samples in MR11-03.

No transfer was made and the vials were set an auto sampler tray directly. Samples were analyzed after collection basically within 24 hours in MR11-03.

h). Data processing

Raw data from QuAAtro was treated as follows:

- Checked baseline shift.
- Checked the shape of each peak and positions of peak values taken, and then changed the positions of peak values taken if necessary.
- Carry-over correction and baseline drift correction were applied to peak heights of each samples followed by sensitivity correction.
- Baseline correction and sensitivity correction were done basically using liner regression.

- Loaded pressure and salinity from CTD data to calculate density of seawater.
- Calibration curves to get nutrients concentration were assumed second order equations.

(5) Nutrients standards

a). Volumetric laboratory ware of in-house standards

All volumetric glass ware and polymethylpentene (PMP) ware used were gravimetrically calibrated. Plastic volumetric flasks were gravimetrically calibrated at the temperature of use within 0 to 4 K.

Volumetric flasks

Volumetric flasks of Class quality (Class A) were used because their nominal tolerances are 0.05 % or less over the size ranges likely to be used in this work. Class A flasks were made of borosilicate glass, and the standard solutions were transferred to plastic bottles as quickly as possible after they were made up to volume and well mixed in order to prevent excessive dissolution of silicate from the glass. PMP volumetric flasks were gravimetrically calibrated and used only within 0 to 4 K of the calibration temperature.

The computation of volume contained by glass flasks at various temperatures other than the calibration temperatures were done by using the coefficient of linear expansion of borosilicate crown glass.

Because of their larger temperature coefficients of cubical expansion and lack of tables constructed for these materials, the plastic volumetric flasks were gravimetrically calibrated over the temperature range of intended use and used at the temperature of calibration within 0 to 4 K. The weights obtained in the calibration weightings were corrected for the density of water and air buoyancy.

Pipettes and pipettors

All pipettes had nominal calibration tolerances of 0.1 % or better. These were gravimetrically calibrated in order to verify and improve upon this nominal tolerance.

b). Reagents, general considerations

Specifications

For nitrate standard, “potassium nitrate 99.995 suprapur®” provided by Merck, CAS No.: 7757-91-1, was used.

For phosphate standard, “potassium dihydrogen phosphate anhydrous 99.995 suprapur®” provided by Merck, CAS No.: 7778-77-0, was used.

For nitrite standard, “sodium nitrate” provided by Wako, CAS No.: 7632-00-0, was used. And assay of nitrite was determined according JIS K8019 and assays of nitrite salts were 97.75 %. We used that value to adjust the weights taken.

For the silicate standard, we use “Silicon standard solution SiO₂ in NaOH 0.5 mol/l CertiPUR®” provided by Merck, CAS No.: 1310-73-2, of which lot number HC074650 was used. The silicate concentration was certified by NIST-SRM3150 with the uncertainty of 0.5 %. Factor of HC074650 was signed 1.000, however we reassigned the factor as 0.975 from the result of comparison among HC814662, HC074650 and RMNS in MR10-05 cruise.

For ammonia standard, “ammonia sulfate” provided by Wako, CAS No.: 7783-20-2,

was used.

Ultra pure water

Ultra pure water (Milli-Q) freshly drawn was used for preparation of reagent, standard solutions and for measurement of reagent and system blanks.

Low-nutrients seawater (LNSW)

Surface water having low nutrient concentration was taken and filtered using 0.45 μm pore size membrane filter. This water was stored in 20 liter cubitainer with paper box. The concentrations of nutrient of this water were measured carefully in Jul 2008.

Treatment of silicate standard due to high alkalinity

Since the silicon standard solution Merck CertiPUR® is in NaOH 0.5 mol/l, we need to dilute and neutralize to avoid make precipitation of MgOH_2 etc. When we make B standard, silicon standard solution is diluted by factor 12 with pure water and neutralized by HCl 1.0 mol/l to be about 7. After that B standard solution is used to prepare C standards.

c). Concentrations of nutrients for A, B and C standards

Concentrations of nutrients for A, B and C standards (working standards) were set as shown in Table 2.5.1. The working standard was prepared according recipes as shown in Table 2.5.2. All volumetric laboratory tools were calibrated prior the cruise as stated in chapter (5). Then the actual concentration of nutrients in each fresh standard was calculated based on the ambient, solution temperature and determined factors of volumetric laboratory wares.

The calibration curves for each run were obtained using 5 levels working standards, C-1, C-2, C-3, C-4 and C-5.

Table 2.5.1 Nominal concentrations of nutrients for A, B and C standards.

	A	B	C-1	C-2	C-3	C-4	C-5
NO_3 (μM)	22000	900	0.03	9.2	18.3	36.6	55.0
NO_2 (μM)	4000	20	0.00	0.2	0.4	0.8	1.2
SiO_2 (μM)	36000	2800	0.80	28	56	111	167
PO_4 (μM)	3000	60	0.04	0.6	1.2	2.4	3.6
NH_4 (μM)	4000	200	0.00	0.0	2.0	4.0	6.0

Table 2.5.2 Working standard recipes.

C Std.	B-1 Std.	B-2 Std.	B-3 Std.	DIW
C-1	0 ml	0 ml	0 ml	75 ml
C-2	5 ml	5 ml	0 ml	65 ml
C-3	10 ml	10 ml	5 ml	40 ml
C-4	20 ml	20 ml	10 ml	25 ml
C-5	30 ml	30 ml	15 ml	0 ml

B-1 Std.: Mixture of nitrate, silicate and phosphate.

B-2 Std.: Nitrite.

B-3 Std.: Ammonia.

d). Renewal of in-house standard solutions

In-house standard solutions as stated in paragraph c) were renewed as shown in Table 2.5.3(a) to (c).

Table 2.5.3(a) Timing of renewal of in-house standards.

NO ₃ , NO ₂ , SiO ₂ , PO ₄ , NH ₄	Renewal
A-1 Std. (NO ₃)	maximum 1 month
A-2 Std. (NO ₂)	maximum 1 month
A-3 Std. (SiO ₂)	commercial prepared solution
A-4 Std. (PO ₄)	maximum 1 month
A-5 Std. (NH ₄)	maximum 1 month
B-1 Std. (mixture of NO ₃ , SiO ₂ , PO ₄)	8 days
B-2 Std. (NO ₂)	8 days
B-3 Std. (NH ₄)	8 days

Table 2.5.3(b) Timing of renewal of working calibration standards.

Working standards	Renewal
C Std. (mixture of B-1 , B-2 and B-3 Std.)	24 hours

Table 2.5.3(c) Timing of renewal of in-house standards for reduction estimation.

Reduction estimation	Renewal
----------------------	---------

D-1 Std. (3600 $\mu\text{M NO}_3$)	8 days
43 $\mu\text{M NO}_3$	when C Std. renewed
47 $\mu\text{M NO}_2$	when C Std. renewed

(6) Reference material of nutrients in seawater

To get the more accurate and high quality nutrients data to achieve the objectives stated above, huge numbers of the bottles of the reference material of nutrients in seawater (hereafter RMNS) are prepared (Aoyama et al., 2006, 2007, 2008, 2009). In the previous worldwide expeditions, such as CLIVAR cruises, the higher reproducibility and precision of nutrients measurements were required (Joyce and Corry, 1994). Since no standards were available for the measurement of nutrients in seawater at that time, the requirements were described in term of reproducibility. The required reproducibility was 1 %, 1 to 2 %, 1 to 3 % for nitrate, phosphate and silicate, respectively. Although nutrient data from the WOCE one-time survey was of unprecedented quality and coverage due to much care in sampling and measurements, the differences of nutrients concentration at crossover points are still found among the expeditions (Aoyama and Joyce, 1996, Mordy et al., 2000, Gouretski and Jancke, 2001). For instance, the mean offset of nitrate concentration at deep waters was $0.5 \mu\text{mol kg}^{-1}$ for 345 crossovers at world oceans, though the maximum was $1.7 \mu\text{mol kg}^{-1}$ (Gouretski and Jancke, 2001). At the 31 crossover points in the Pacific WHP one-time lines, the WOCE standard of reproducibility for nitrate of 1 % was fulfilled at about half of the crossover points and the maximum difference was 7 % at deeper layers below 1.6 deg. C in potential temperature (Aoyama and Joyce, 1996).

During the period from 2003 to 2010, RMNS were used to keep comparability of nutrients measurement among the 8 cruises of CLIVAR project (Sato et al., 2010), MR10-05 cruise for Arctic research (Aoyama et al., 2010) and MR10-06 cruise for “Change in material cycles and ecosystem by the climate change and its feedback” (Aoyama et al., 2011).

a). RMNS for this cruise

RMNS lots BA, AS, AY, BT, BD, BE, AZ and BF, which cover full range of nutrients concentrations in the North Pacific Ocean are prepared. These RMNS assignment were completely done based on random number. The RMNS bottles were stored at a room in the ship, REAGENT STORE, where the temperature was maintained 14 - 22 deg. C.

b). Assigned concentration for RMNSs

We assigned nutrients concentrations for RMNS lots BA, AS, AY, BT, BD, BE, AZ and BF as shown in Table 2.5.4.

Table 2.5.4 Assigned concentration of RMNSs.

	unit: $\mu\text{mol kg}^{-1}$				
	Nitrate	Phosphate	Silicate	Nitrite	Ammonia
BA	0.07	0.068	1.60	0.02	0.97
AS	0.11	0.077	1.58	0.02	-
AY	5.60	0.516	29.42	0.62	0.81
BT	17.99	1.310	40.85	0.44	-
BD	29.83	2.182	64.41	0.04	2.93
BE	36.70	2.662	99.20	0.03	-
AZ	42.36	3.017	133.93	0.03	-
BF	41.39	2.809	150.23	0.02	-

(7) Quality control

a). Precision of nutrients analyses during the cruise

Precision of nutrients analyses during the cruise was evaluated based on the 5 to 7 measurements, which are measured every 9 to 13 samples, during a run at the concentration of C-5 std. Summary of precisions are shown as shown in Table 2.5.5. Analytical precisions previously evaluated were 0.08 % for nitrate, 0.10 % for phosphate and 0.07 % for silicate in CLIVAR P21 revisited cruise of MR09-01 cruise in 2009, respectively. During this cruise, analytical precisions were 0.15 % for nitrate, 0.19 % for phosphate, 0.12 % for silicate, 0.10 % for nitrite and 0.39 % for ammonia in terms of median of precision, respectively. Then we can conclude that the analytical precisions for nitrate, phosphate and silicate were maintained throughout this cruise.

Table 2.5.5 Summary of precision based on the replicate analyses.

	Nitrate	Nitrite	Phosphate	Silicate	Ammonia
	CV %	CV %	CV %	CV %	CV%
Median	0.15	0.10	0.19	0.12	0.39
Mean	0.14	0.12	0.20	0.11	0.52
Maximum	0.18	0.24	0.30	0.16	0.95
Minimum	0.10	0.05	0.12	0.04	0.29
N	10	10	10	10	5

b). Carry over

We can also summarize the magnitudes of carry over throughout the cruise. These are

small enough within acceptable levels as shown in Table 2.5.6.

Table 2.5.6 Summary of carry over throughout MR11-03.

	Nitrate	Nitrite	Phosphate	Silicate	Ammonia
	%	%	%	%	%
Median	0.30	0.04	0.22	0.23	0.66
Mean	0.29	0.05	0.24	0.21	0.56
Maximum	0.39	0.16	0.61	0.35	0.88
Minimum	0.12	0.00	0.06	0.08	0.10
N	10	10	10	10	5

c). Estimation of uncertainty of phosphate, nitrate and silicate concentrations

Empirical equations, eq. (1), (2) and (3) to estimate uncertainty of measurement of phosphate, nitrate and silicate are used based on measurements of 140 sets of RMNSs during the cruise MR09-01 in 2009. These empirical equations are as follows, respectively.

Phosphate Concentration C_p in $\mu\text{mol kg}^{-1}$:

$$\text{Uncertainty of measurement of phosphate (\%)} = 0.000 + 0.378 * (1/C_p) + 0.00430 * (1/C_p) * (1/C_p) \quad \text{--- (1)}$$

where C_p is phosphate concentration of sample.

Nitrate Concentration C_n in $\mu\text{mol kg}^{-1}$:

$$\text{Uncertainty of measurement of nitrate (\%)} = 0.142 + 0.431 * (1/C_n) + 0.114 * (1/C_n) * (1/C_n) \quad \text{--- (2)}$$

where C_n is nitrate concentration of sample.

Silicate Concentration C_s in $\mu\text{mol kg}^{-1}$:

$$\text{Uncertainty of measurement of silicate (\%)} = 0.047 + 4.99 * (1/C_s) + 1.879 * (1/C_s) * (1/C_s) \quad \text{---(3)}$$

where C_s is silicate concentration of sample.

d). Empirical equation for uncertainty of ammonia

Since we do not have RM for ammonia, empirical equation of uncertainty of ammonia is created based on differences of duplicate measurements of samples taken from same niskin bottles during the cruise MR10-05. We got 875 pair of duplicate measurements and concentration of ammonia ranged from $0.00 \mu\text{mol kg}^{-1}$ to $5.15 \mu\text{mol kg}^{-1}$.

We got an empirical equation as follows;

Ammonia Concentration C_a in $\mu\text{mol kg}^{-1}$:

$$\text{Uncertainty of measurement of ammonia (\%)} = 2.53 * C_a^{0.847} \quad \text{---(4)}$$

where Ca is ammonia concentration of sample.

(8) Problems/improvements occurred and solutions.

From stn. JKO onward, we changed the pump tube of PO₄ dilution line from RED/RED to ORN/WHT to reduce baseline noise because we observe relatively larger noise due to rolling and pitching of the ship. We also reduce the gain from 181 to 158 without change the full range.

(9) Station list

Table 2.5.7 List of stations

Cruise	Station	Cast	Year	Month	Date	Latitude	Longitude		
MR11-03	A	01	2011	4	15	38.176	N	143.55	E
MR11-03	B	01	2011	4	15	38.209	N	143.786	E
MR11-03	C	01	2011	4	15	38.145	N	143.317	E
MR11-03	D	01	2011	4	16	38.113	N	143.083	E
MR11-03	KNT	01	2011	4	17	44.000	N	155.000	E
MR11-03	K02	01	2011	4	19	46.999	N	160.072	E
MR11-03	K02	03	2011	4	20	47.000	N	160.083	E
MR11-03	K02	04	2011	4	20	47.000	N	160.079	E
MR11-03	K02	07	2011	4	22	46.998	N	160.080	E
MR11-03	JKO	01	2011	4	26	38.056	N	146.378	E
MR11-03	KEO	01	2011	4	27	32.461	N	144.500	E
MR11-03	S01	02	2011	4	28	30.004	N	145.002	E
MR11-03	S01	03	2011	4	28	30.047	N	145.117	E
MR11-03	S01	04	2011	4	29	30.000	N	145.009	E
MR11-03	S01	06	2011	4	30	30.004	N	145.011	E

(10) Data archive

All data will be submitted to JAMSTEC Data Management Office (DMO) and is currently under its control.

References

- Aminot, A. and Kerouel, R. 1991. Autoclaved seawater as a reference material for the determination of nitrate and phosphate in seawater. *Anal. Chim. Acta*, 248: 277-283.
- Aminot, A. and Kirkwood, D.S. 1995. Report on the results of the fifth ICES intercomparison exercise for nutrients in sea water, ICES coop. Res. Rep. Ser., 213.
- Aminot, A. and Kerouel, R. 1995. Reference material for nutrients in seawater: stability of nitrate, nitrite, ammonia and phosphate in autoclaved samples. *Mar. Chem.*, 49: 221-232.

- Aoyama M., and Joyce T.M. 1996, WHP property comparisons from crossing lines in North Pacific. In Abstracts, 1996 WOCE Pacific Workshop, Newport Beach, California.
- Aoyama, M., 2006: 2003 Intercomparison Exercise for Reference Material for Nutrients in Seawater in a Seawater Matrix, Technical Reports of the Meteorological Research Institute No.50, 91pp, Tsukuba, Japan.
- Aoyama, M., Susan B., Minhan, D., Hideshi, D., Louis, I. G., Kasai, H., Roger, K., Nurit, K., Doug, M., Murata, A., Nagai, N., Ogawa, H., Ota, H., Saito, H., Saito, K., Shimizu, T., Takano, H., Tsuda, A., Yokouchi, K., and Agnes, Y. 2007. Recent Comparability of Oceanographic Nutrients Data: Results of a 2003 Intercomparison Exercise Using Reference Materials. *Analytical Sciences*, 23: 1151-1154.
- Aoyama M., J. Barwell-Clarke, S. Becker, M. Blum, Braga E. S., S. C. Coverly, E. Czobik, I. Dahllof, M. H. Dai, G. O. Donnell, C. Engelke, G. C. Gong, Gi-Hoon Hong, D. J. Hydes, M. M. Jin, H. Kasai, R. Kerouel, Y. Kiyomono, M. Knockaert, N. Kress, K. A. Kroglund, M. Kumagai, S. Leterme, Yarong Li, S. Masuda, T. Miyao, T. Moutin, A. Murata, N. Nagai, G. Nausch, M. K. Ngirchchol, A. Nybakk, H. Ogawa, J. van Ooijen, H. Ota, J. M. Pan, C. Payne, O. Pierre-Duplessix, M. Pujo-Pay, T. Raabe, K. Saito, K. Sato, C. Schmidt, M. Schuett, T. M. Shammon, J. Sun, T. Tanhua, L. White, E.M.S. Woodward, P. Worsfold, P. Yeats, T. Yoshimura, A. Youenou, J. Z. Zhang, 2008: 2006 Intercomparison Exercise for Reference Material for Nutrients in Seawater in a Seawater Matrix, Technical Reports of the Meteorological Research Institute No. 58, 104pp.
- Aoyama, M., Nishino, S., Nishijima, K., Matsushita, J., Takano, A., Sato, K., 2010a. Nutrients, In: R/V Mirai Cruise Report MR10-05. JAMSTEC, Yokosuka, pp. 103-122.
- Aoyama, M., Matsushita, J., Takano, A., 2010b. Nutrients, In: MR10-06 preliminary cruise report. JAMSTEC, Yokosuka, pp. 69-83
- Gouretski, V.V. and Jancke, K. 2001. Systematic errors as the cause for an apparent deep water property variability: global analysis of the WOCE and historical hydrographic data • REVIEW ARTICLE, *Progress In Oceanography*, 48: Issue 4, 337-402.
- Grasshoff, K., Ehrhardt, M., Kremling K. et al. 1983. *Methods of seawater analysis*. 2nd rev. Weinheim: Verlag Chemie, Germany, West.
- Hydes, D.J., Aoyama, M., Aminot, A., Bakker, K., Becker, S., Coverly, S., Daniel, A., Dickson, A.G., Grosso, O., Kerouel, R., Ooijen, J. van, Sato, K., Tanhua, T., Woodward, E.M.S., Zhang, J.Z., 2010. Determination of Dissolved Nutrients (N, P, Si) in Seawater with High Precision and Inter-Comparability Using Gas-Segmented Continuous Flow Analysers, In: *GO-SHIP Repeat Hydrography Manual: A Collection of Expert Reports and Guidelines*. IOCCP Report No. 14, ICPO Publication Series No 134.
- Joyce, T. and Corry, C. 1994. Requirements for WOCE hydrographic programmed data reporting. WHPO Publication, 90-1, Revision 2, WOCE Report No. 67/91.
- Kawano, T., Uchida, H. and Doi, T. WHP P01, P14 REVISIT DATA BOOK, (Ryoin Co., Ltd., Yokohama, 2009).
- Kirkwood, D.S. 1992. Stability of solutions of nutrient salts during storage. *Mar. Chem.*, 38 : 151-164.
- Kirkwood, D.S. Aminot, A. and Perttila, M. 1991. Report on the results of the ICES fourth intercomparison exercise for nutrients in sea water. ICES coop. Res. Rep. Ser., 174.
- Mordy, C.W., Aoyama, M., Gordon, L.I., Johnson, G.C., Key, R.M., Ross, A.A., Jennings, J.C.

- and Wilson. J. 2000. Deep water comparison studies of the Pacific WOCE nutrient data set. Eos Trans-American Geophysical Union. 80 (supplement), OS43.
- Murphy, J., and Riley, J.P. 1962. *Analytica chim. Acta* 27, 31-36.
- Sato, K., Aoyama, M., Becker, S., 2010. RMNS as Calibration Standard Solution to Keep Comparability for Several Cruises in the World Ocean in 2000s. In: Aoyama, M., Dickson, A.G., Hydes, D.J., Murata, A., Oh, J.R., Roose, P., Woodward, E.M.S., (Eds.), *Comparability of nutrients in the world's ocean*. Tsukuba, JAPAN: MOTHER TANK, pp 43-56.
- Uchida, H. & Fukasawa, M. WHP P6, A10, I3/I4 REVISIT DATA BOOK Blue Earth Global Expedition 2003 1, 2, (Aiwa Printing Co., Ltd., Tokyo, 2005).

2.6 pH measurement

Masahide WAKITA (JAMSTEC MIO): Principal Investigator
Yoshiko ISHIKAWA (MWJ)

(1) Objective

Since the global warming is becoming an issue world-widely, studies on the greenhouse gases such as CO₂ are drawing high attention. The ocean plays an important role in buffering the increase of atmospheric CO₂, and studies on the exchange of CO₂ between the atmosphere and the sea becomes highly important. Oceanic biosphere, especially primary production, has an important role concerned to oceanic CO₂ cycle through its photosynthesis and respiration. However, the diverseness and variability of the biological system make difficult to reveal their mechanism and quantitative understanding of CO₂ cycle. Dissolved CO₂ in water alters its appearance into several species, but the concentrations of the individual species of CO₂ system in solution cannot be measured directly. However, two of the four measurable parameters (alkalinity, total dissolved inorganic carbon, pH and pCO₂) can estimate each concentration of CO₂ system (Dickson et al., 2007). Seawater acidification associated with CO₂ uptake into the ocean possibly changes oceanic ecosystem and CO₂ garners in Ocean recently. We here report on board measurements of pH during MR11-03 cruise.

(2) Methods, Apparatus and Performance

(2)-1 Seawater sampling

Seawater samples were collected by 12 liter Niskin bottles mounted on the CTD/Carousel Water Sampling System and a bucket at 6 stations. Among these stations, deep and shallow casts were carried out for 2 stations. Seawater was sampled in a 100 ml glass bottle that was previously soaked in 5 % non-phosphoric acid detergent (pH13) solution at least 3 hours and was cleaned by fresh water for 5 times and Milli-Q ultrapure water for 3 times. A sampling silicone rubber tube with PFA tip was connected to the Niskin bottle when the sampling was carried out. The glass bottles were filled from the bottom smoothly, without rinsing, and were overflowed for 2 times bottle volume (about 10 seconds) with care not to leave any bubbles in the bottle. The water in the bottle was sealed by a glass made cap gravimetrically fitted to the bottle mouth without additional force. After collecting the samples on the deck, the bottles were carried into the lab and put in the water bath kept about 25 deg C before the measurement.

(2)-2 Seawater analyses

pH (-log[H⁺]) of the seawater was measured potentiometrically in the glass bottles. The pH / Ion meter (Radiometer PHM240) is used to measure the electromotive force (e.m.f.) between the glass electrode cell (Radiometer pHG201) and the reference electrode cell (Radiometer REF201) in the sample with its temperature controlled to 25 +/- 0.05 deg C.

Ag, AgCl reference electrode | solution of KCl || test solution | H⁺ -glass electrode.

To calibrate the electrodes, the TRIS buffer (Lot=100716-1: pH=8.0906 pH units at 25

deg C, Delvalls and Dickson, 1998) and AMP buffer (Lot=100716-1: pH=6.7838 pH units at 25 deg C, DOE, 1994) in the synthetic seawater (Total hydrogen ion concentration scale) were applied. pH_T of seawater sample (pH_{spl}) is calculated from the expression:

$$pH_{spl} = pH_{TRIS} + (E_{TRIS} - E_{spl}) / ER$$

where electrode response ER is calculated as follows:

$$ER = (E_{AMP} - E_{TRIS}) / (pH_{TRIS} - pH_{AMP})$$

ER value should be equal to the ideal Nernst value as follows:

$$ER = RT \ln(10) / F = 59.16 \text{ mV} / \text{pH units at 25 deg C}$$

(3) Preliminary results

A replicate analysis of seawater sample was made at 4 layers (ex. 50, 300, 1600, and 3500 dbar depth) of deep cast or 2 layers (ex. 25 and 125 dbar depth) of shallow cast. The difference between each pair of analyses was plotted on a range control chart (see Figure 2.6-1). The average of the difference was 0.000 pH units (n = 27 pairs) with its standard deviation of 0.001 pH units. These values were lower than the value recommended by Guide (Dickson et al., 2007).

(4) Data Archive

All data will be submitted to JAMSTEC and is currently under its control.

(5) Reference

DOE (1994), Handbook of methods for the analysis of the various parameters of the carbon dioxide system in sea water; version 2, A. G. Dickson & C. Goyet, Eds., ORNS/CDIAC-74

DelValls, T. A. and Dickson, A. G., 1998. The pH of buffers based on 2-amino-2-hydroxymethyl-1,3-propanediol ('tris') in synthetic sea water. Deep-Sea Research I 45, 1541-1554.

Dickson, A. G., C. L. Sabine and J. R. Christian, Eds. (2007): Guide to best practices for ocean CO₂ measurements, PICES Special Publication 3, 199pp.

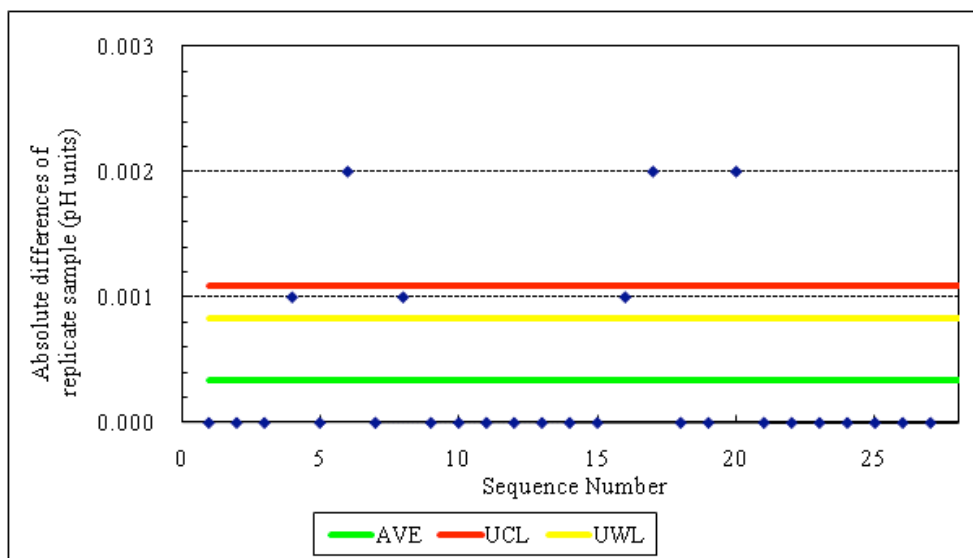


Figure 2.6-1 Range control chart of the absolute differences of replicate measurements of pH carried out during the cruise. AVE represents the average value, UCL upper control limit ($UCL = AVE * 3.267$), and UWL upper warning limit ($UWL = AVE * 2.512$) (Dickson et al., 2007).

2.7 Dissolved inorganic carbon-DIC

Masahide WAKITA (JAMSTEC MIO): Principal Investigator

Hatsumi AOYAMA (MWJ)

Ayaka HATSUYAMA (MWJ)

(1) Objective

Concentration of CO₂ in the atmosphere is now increasing at a rate of 1.5 ppmv yr⁻¹ owing to human activities such as burning of fossil fuels, deforestation, and cement production. The ocean plays an important role in buffering the increase of atmospheric CO₂, therefore the urgent tasks are to clarify the mechanism of the oceanic CO₂ absorption and to estimate of CO₂ absorption capacity of the oceans. Oceanic biosphere, especially primary production, has an important role concerned to oceanic CO₂ cycle through its photosynthesis and respiration. However, the diverseness and variability of the biological system make difficult to reveal their mechanism and quantitative understanding of the CO₂ cycle. When CO₂ dissolves in water, chemical reaction takes place and CO₂ alters its appearance into several species. Concentrations of the individual species of the CO₂ system in solution cannot be measured directly, but calculated from two of four parameters: total alkalinity, total dissolved inorganic carbon, pH and pCO₂ (Dickson et al., 2007). We here report on-board measurements of DIC performed during the MR11-03 cruise.

(2) Methods, Apparatus and Performance

(2)-1 Seawater sampling

Seawater samples were collected by 12 liter Niskin bottles mounted on the CTD/Carousel Water Sampling System and a bucket at 5 stations. Among these stations, deep and shallow casts were carried out for 2 stations. Seawater was sampled in a 300 ml glass bottle (SCHOTT DURAN) that was previously soaked in 5 % non-phosphoric acid detergent (pH = 13) solution at least 3 hours and was cleaned by fresh water for 5 times and Milli-Q deionized water for 3 times. A sampling silicone rubber tube with PFA tip was connected to the Niskin bottle when the sampling was carried out. The glass bottles were filled from the bottom, without rinsing, and were overflowed for 20 seconds. They were sealed using the polyethylene inner lids with its diameter of 29 mm with care not to leave any bubbles in the bottle. After collecting the samples on the deck, the glass bottles were carried to the laboratory to be measured. Within one hour after the sampling, 3 ml of the sample (1 % of the bottle volume) was removed from the glass bottle and poisoned with 100 µl of over saturated solution of mercury chloride. Then the samples were sealed by the polyethylene inner lids with its diameter of 31.9 mm and stored in a refrigerator at approximately 5 deg C until analyzed. Before the analysis, the samples were put in the water bath kept about 20 deg C for one hour.

(2)-2 Seawater analysis

Measurements of DIC were made with total CO₂ measuring system (Nippon ANS, Inc.). The system comprise of seawater dispensing unit, a CO₂ extraction unit and a coulometer (Model seacat2000, Nippon ANS, Inc.)

The seawater dispensing unit has an auto-sampler (6 ports), which dispenses the

seawater from a glass bottle to a pipette of nominal 21 ml volume. The pipette was kept at 20 ± 0.05 deg C by a water jacket, in which water circulated through a thermostatic water bath (RTE 10, Thermo) set at 20 deg C.

The CO₂ dissolved in a seawater sample is extracted in a stripping chamber of the CO₂ extraction unit by adding phosphoric acid (10 % v/v). The stripping chamber is made approx. 25 cm long and has a fine frit at the bottom. First, the certain amount of acid is taken to the constant volume tube and added to the stripping chamber from its bottom by pressurizing an acid bottle with nitrogen gas (99.9999 %). Second, a seawater sample kept in a pipette is introduced to the stripping chamber by the same method as that for an acid. The seawater and phosphoric acid are stirred by the nitrogen bubbles through a fine frit at the bottom of the stripping chamber. The CO₂ stripped in the chamber is carried by the nitrogen gas (flow rates of 140 ml min⁻¹) to the coulometer through two electric dehumidifiers (kept at 0.5 deg C) and a chemical desiccant (Mg(ClO₄)₂).

Measurements of 1.5 % CO₂ standard gas in a nitrogen base, system blank (phosphoric acid blank), and seawater samples (6 samples) were programmed to repeat. The variation of 1.5 % CO₂ standard gas signal was used to correct the signal drift results from chemical alternation of coulometer solutions.

(3) Preliminary results

During the cruise, 292 samples were analyzed for DIC. A replicate analysis was performed at the interval decided beforehand and the difference between each pair of analyses was plotted on a range control chart (Figure 2.7-1). The average of the differences was 0.9 μmol kg⁻¹ (n = 28). The standard deviation was 0.7 μmol kg⁻¹, which indicates that the analysis was accurate enough according to the Guide to best practices for ocean CO₂ measurements (Dickson et al., 2007).

(4) Data Archive

These data obtained in this cruise will be submitted to the Data Management Office (DMO) of JAMSTEC, and will be opened to the public via “R/V Mirai Data Web Page” in JAMSTEC home page.

(5) Reference

Dickson, A. G., Sabine, C. L. & Christian, J. R. (2007), Guide to best practices for ocean CO₂ measurements; PICES Special Publication 3, 199pp.

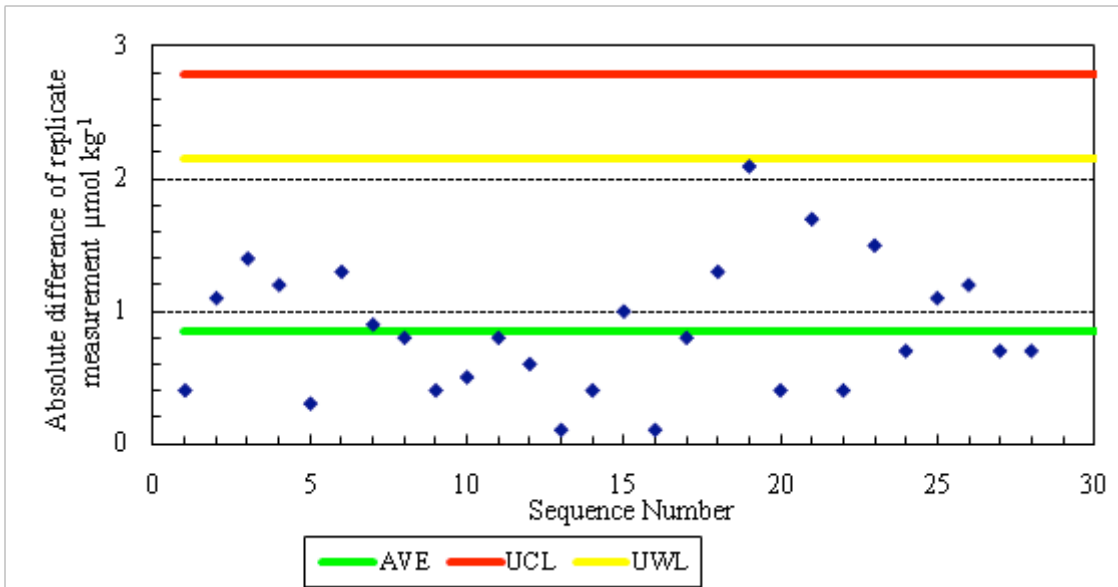


Figure 2.7-1 Range control chart of the absolute differences of replicate measurements of DIC carried out during this cruise. UCL and UWL represents the upper control limit ($UCL=AVE*3.267$) and upper warning limit ($UWL=AVE*2.512$), respectively.

2.8 Total Alkalinity

Masahide WAKITA (JAMSTEC MIO): Principal Investigator

Ayaka HATSUYAMA (MWJ)

Hatsumi AOYAMA (MWJ)

(1) Objective

Global warming is becoming an issue world-widely, therefore studies on green house gases, especially carbon dioxide (CO₂), are indispensable. The ocean currently absorbs one third of the 6 Gt of carbon emitted into the atmosphere each year by human activities, such as burning of fossil fuels, deforestation, and cement production. When CO₂ dissolves in sea water, chemical reaction takes place and CO₂ alters its appearance into several species and make the oceanic CO₂ cycle complicated. Furthermore, oceanic biological activity, especially oceanic primary production, plays an important role concerned to the CO₂ cycle through its photosynthesis and respiration. The concentrations of the individual CO₂ species cannot be measured directly, however, two of four measurable parameters: total alkalinity, total dissolved inorganic carbon, pH, and pCO₂, can clarify the whole distribution of the CO₂ species (Dickson et al., 2007). We here report on-board measurements of total alkalinity performed during the MR11-03 cruise.

(2) Methods, Apparatus and Performance

(2)-1 Seawater sampling

Seawater samples were collected by 12 liter Niskin bottles mounted on the CTD/Carousel Water Sampling System and a bucket at 5 stations. Among these stations, deep and shallow casts were carried out for 2 stations. A sampling silicone rubber tube with PFA tip was used to sample the seawater from the Niskin bottle. The 125 ml borosilicate glass bottles (SHOTT DURAN) were filled from the bottom smoothly, without rinsing, and were overflowed for 2 times bottle volume (10 seconds) with care not to leave any bubbles in the bottle. These bottles were pre-washed by soaking in 5 % non-phosphoric acid detergent (pH = 13) for more than 3 hours and then rinsed 5 times with tap water and 3 times with Milli-Q deionized water. After collecting the samples on the deck, the bottles were carried into the laboratory to be measured. The samples were stored in a refrigerator at approximately 5 deg C until being analyzed. Before the analysis, the samples were put in the water bath kept about 25 deg C for one hour.

(2)-2 Seawater analyses

The TA was measured using a spectrophotometric system (Nippon ANS, Inc.) using a scheme of Yao and Byrne (1998). The constant volume of sample seawater, with its value of approx. 42 ml, was transferred from a sample bottle into the titration cell kept at 25 deg C in a thermostated compartment. Then, the sample seawater was circulated through the tube connecting the titration cell and the pH cell in the spectrophotometer (Carry 50 Scan, Varian) by a peristaltic pump. The length and volume of the pH cell are 8 cm and 13 ml, respectively, and its temperature is also kept at 25 deg C in a thermostated compartment. The TA is calculated by measuring two sets of absorbance at three wavelengths (750, 616 and 444 nm). One is the

absorbance of seawater sample before injecting an acid with indicator solution (bromocresol green sodium) and another is the one after the injection. For mixing the acid with indicator solution and the seawater, and for degassing CO₂ from the mixed solution sufficiently, they are circulated between the titration and pH cell by a peristaltic pump for 7 and half minutes before the measurement.

The TA is calculated based on the following equation:

$$\begin{aligned} \text{pH}_T = & 4.2699 + 0.002578 * (35 - S) \\ & + \log ((R(25) - 0.00131) / (2.3148 - 0.1299 * R(25))) \\ & - \log (1 - 0.001005 * S), \end{aligned} \quad (1)$$

$$\begin{aligned} A_T = & (N_A * V_A - 10^{\text{pH}_T} * \text{DensSW}(T, S) * (V_S + V_A)) \\ & * (\text{DensSW}(T, S) * V_S)^{-1}, \end{aligned} \quad (2)$$

where R(25) represents the difference of absorbance at 616 and 444 nm between before and after the injection. The absorbance of wavelength at 750 nm is used to subtract the variation of absorbance caused by the system. DensSW (T, S) is the density of seawater at temperature (T) and salinity (S), N_A the concentration of the added acid, V_A and V_S the volume of added acid and seawater, respectively.

To keep the high analysis precision, some treatments were carried out during the cruise. The acid with indicator solution stored in 1 L DURAN bottle is kept in a bath with its temperature of 25 deg C, and about 10 ml of it is discarded at first before the batch of measurement. For mixing the seawater and the acid with indicator solution sufficiently, TYGON tube used on the peristaltic pump was periodically renewed. Absorbance measurements were done 10 times during each analysis, and the stable last five and three values are averaged and used for above listed calculation for before and after the injection, respectively.

(3) Preliminary results

A few replicate samples were taken at most of stations and the difference between each pair of analyses was plotted on a range control chart (see Figure 2.8-1). The average of the difference was 0.7 μmol kg⁻¹ (n = 28) with its standard deviation of 0.6 μmol kg⁻¹, which indicates that the analysis was accurate enough according to the Guide to best practices for ocean CO₂ measurements (Dickson et al., 2007).

(4) Data Archive

These data obtained in this cruise will be submitted to the Data Management Office (DMO) of JAMSTEC, and will be opened to the public via “R/V Mirai Data Web Page” in JAMSTEC home page.

(5) References

Yao, W. and Byrne, R. H. (1998), Simplified seawater alkalinity analysis: Use of linear array spectrometers. *Deep-Sea Research Part I*, Vol. 45, 1383-1392.

Dickson, A. G., Sabine, C. L. & Christian, J. R. (2007), Guide to best practices for ocean CO₂ measurements; PICES Special Publication 3, 199pp.

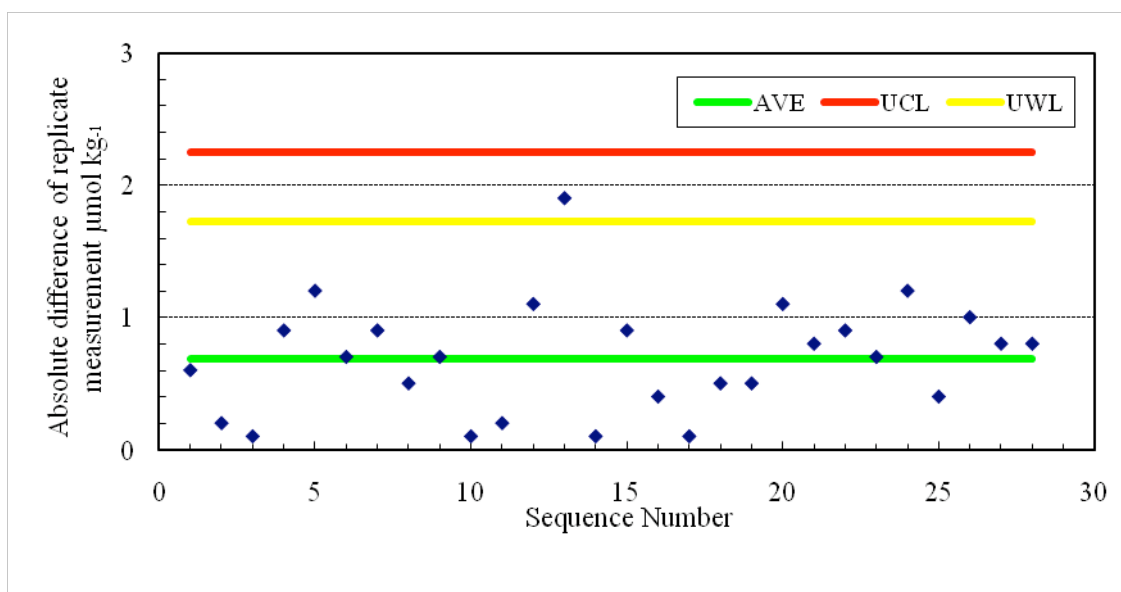


Figure 2.8-1 Range control chart of the absolute differences of replicate measurements carried out in the analysis of TA during the MR11-03 cruise. UCL and UWL represents the upper control limit ($UCL=AVE*3.267$) and upper warning limit ($UWL=AVE*2.512$), respectively.

2.9 Underway pCO₂

Masahide WAKITA (JAMSTEC MIO): Principal Investigator

Yoshiko ISHIKAWA (MWJ)

Ayaka HATSUYAMA (MWJ)

Hatsumi AOYAMA (MWJ)

(1) Objectives

Concentrations of CO₂ in the atmosphere are increasing at a rate of 1.5 ppmv yr⁻¹ owing to human activities such as burning of fossil fuels, deforestation, and cement production. Oceanic CO₂ concentration is also considered to be increased with the atmospheric CO₂ increase, however, its variation is widely different by time and locations. Underway pCO₂ observation is indispensable to know the pCO₂ distribution, and it leads to elucidate the mechanism of oceanic pCO₂ variation. We here report the underway pCO₂ measurements performed during MR11-03 cruise.

(2) Methods, Apparatus and Performance

Oceanic and atmospheric CO₂ concentrations were measured during the cruise using an automated system equipped with a non-dispersive infrared gas analyzer (NDIR; LI-7000, Li-Cor). Measurements were done every about one and a half hour, and 4 standard gasses, atmospheric air, and the CO₂ equilibrated air with sea surface water were analyzed subsequently in this hour. The concentrations of the CO₂ standard gases were 299.834, 350.002, 400.099 and 450.374 ppmv. Atmospheric air taken from the bow of the ship (approx.30 m above the sea level) was introduced into the NDIR by passing through a electrical cooling unit, a mass flow controller which controls the air flow rate of 0.5 L min⁻¹, a membrane dryer (MD-110-72P, perma pure llc.) and chemical desiccant (Mg(ClO₄)₂). The CO₂ equilibrated air was the air with its CO₂ concentration was equivalent to the sea surface water. Seawater was taken from an intake placed at the approximately 4.5 m below the sea surface and introduced into the equilibrator at the flow rate of 4 - 5 L min⁻¹ by a pump. The equilibrated air was circulated in a closed loop by a pump at flow rate of 0.7 - 0.8 L min⁻¹ through two cooling units, a membrane dryer, the chemical desiccant, and the NDIR.

(3) Preliminary results

Cruise track during pCO₂ observation is shown in Figure 2.9-1. Temporal variations of both oceanic and atmospheric CO₂ concentration (xCO₂) are shown in Fig. 2.9-2.

(4) Data Archive

Data obtained in this cruise will be submitted to the Data Management Office (DMO) of JAMSTEC, and will be opened to the public via “R/V Mirai Data Web Page” in JAMSTEC home page.

(5) Reference

Dickson, A. G., Sabine, C. L. & Christian, J. R. (2007), Guide to best practices for

ocean CO₂ measurements; PICES Special Publication 3, 199pp.

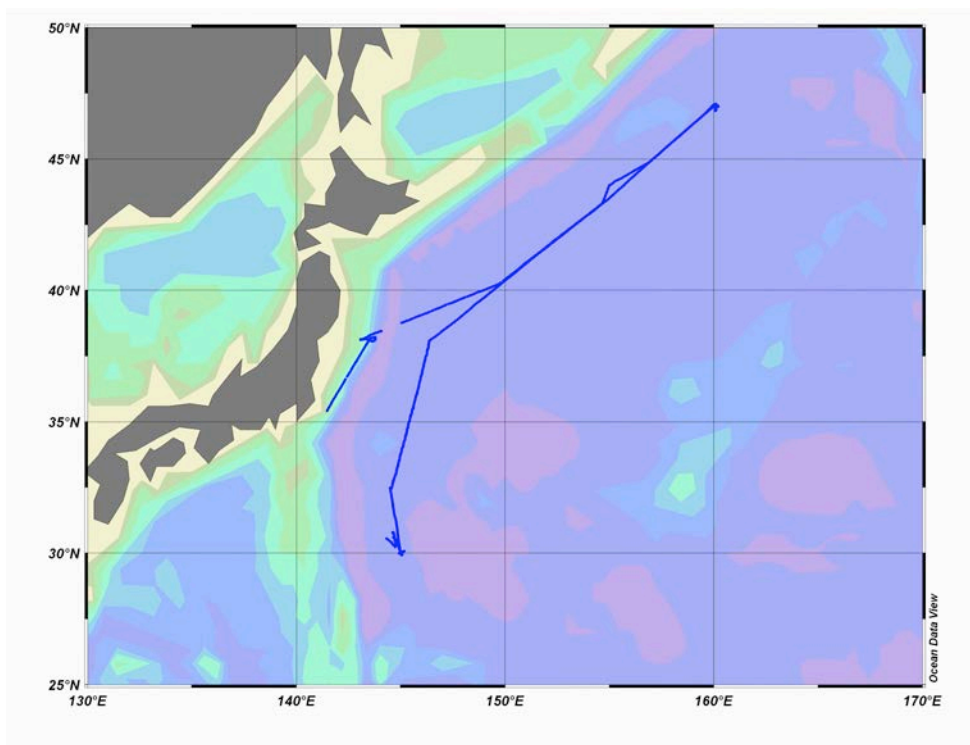


Figure 2.9-1 Observation map

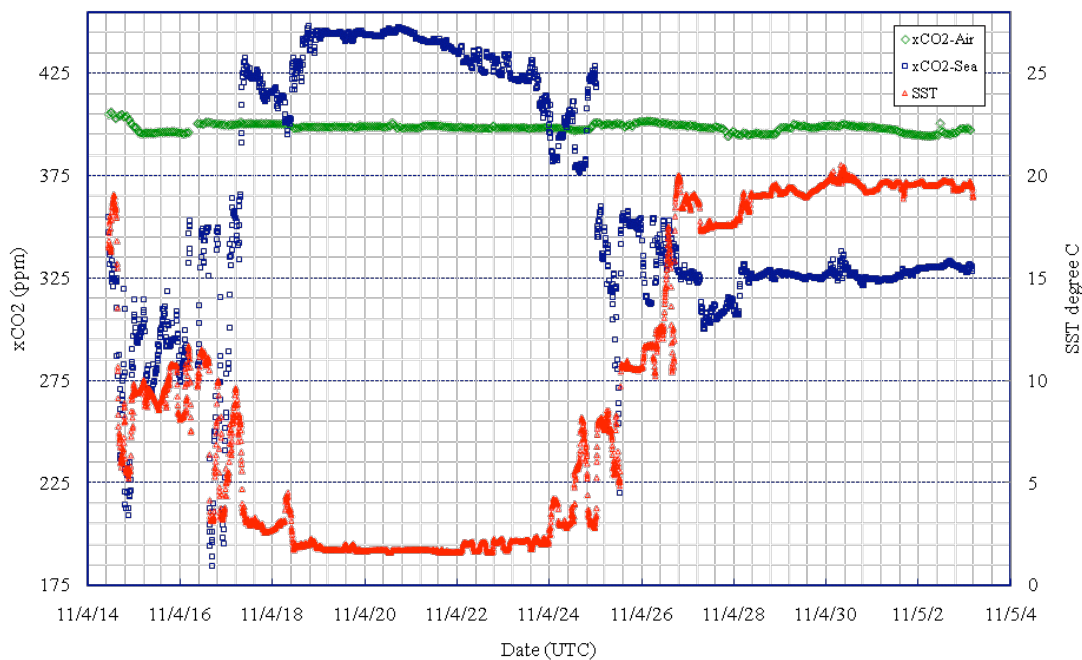


Figure 2.9-2 Temporal variations of oceanic and atmospheric CO₂ concentration (xCO₂). Blue dots represent oceanic xCO₂ variation and green atmospheric xCO₂. SST variation (red) is also shown.

3. Special observation

3.1 Phytoplankton

3.1.1 Chlorophyll *a* measurements by fluorometric determination

Kazuhiko MATSUMOTO (JAMSTEC)

Masahiro ORUI (MWJ)

1. Objective

Phytoplankton biomass can estimate as the concentration of chlorophyll *a* (chl-*a*), because all oxygenic photosynthetic plankton contain chl-*a*. Phytoplankton exist various species in the ocean, but the species are roughly characterized by their cell size. The objective of this study is to investigate the vertical distribution of phytoplankton and their size fractionations as chl-*a* by using the fluorometric determination.

2. Sampling

Samplings of total chl-*a* were conducted from 16 depths between the surface and 200 m at all observational stations. At the cast for primary production, water samples were collected at eight depths from among the surface, 1%, 3%, 5%, 7%, 13%, 35%, 60% light depths relative to the surface and at five other depths between the surface and 200 m at the station of S1 and K2.

3. Instruments and Methods

Water samples (0.5L) for total chl-*a* were filtered (<0.02 MPa) through 25mm-diameter Whatman GF/F filter. Size-fractionated chl-*a* were obtained by sequential filtration (<0.02 MPa) of 1-L water sample through 10- μ m, 3- μ m and 1- μ m polycarbonate filters (47-mm diameter) and Whatman GF/F filter (25-mm diameter). Phytoplankton pigments retained on the filters were immediately extracted in a polypropylene tube with 7 ml of N,N-dimethylformamide (Suzuki and Ishimaru, 1990). Those tubes were stored at -20°C under the dark condition to extract chl-*a* for 24 hours or more.

Fluorescences of each sample were measured by Turner Design fluorometer (10-AU-005), which was calibrated against a pure chl-*a* (Sigma-Aldrich Co.). We applied two kind of fluorometric determination for the samples of total chl-*a*: “Non-acidification method” (Welschmeyer, 1994) and “Acidification method” (Holm-Hansen *et al.*, 1965). Size-fractionated samples were applied only “Non-acidification method”. Analytical conditions of each method were listed in table 1.

4. Preliminary Results

The results of total chl-*a* at station K2 and S1 were shown in Figure 1 and 2. The results of total chl-*a* at station KNOT, JKEO and KEO were shown in Figure 3. The results of size fractionated chl-*a* were shown in Figure4.

6. Data archives

The processed data file of pigments will be submitted to the JAMSTEC Data Integration and Analysis Group (DIAG) within a restricted period. Please ask PI for the latest information.

7. Reference

Suzuki, R., and T. Ishimaru (1990), An improved method for the determination of phytoplankton chlorophyll using N, N-dimethylformamide, *J. Oceanogr. Soc. Japan*, 46, 190-194.

Holm-Hansen, O., Lorenzen, C. J., Holmes, R.W. and J. D. H. Strickland (1965), Fluorometric determination of chlorophyll. *J. Cons. Cons. Int. Explor. Mer.* 30, 3-15.

Welschmeyer, N. A. (1994), Fluorometric analysis of chlorophyll *a* in the presence of chlorophyll *b* and pheopigments. *Limnol. Oceanogr.* 39, 1985-1992.

Table 1. Analytical conditions of “Non-acidification method” and “Acidification method” for chlorophyll *a* with Turner Designs fluorometer (10-AU-005).

	Non-acidification method	Acidification method
Excitation filter (nm)	436	340-500
Emission filter (nm)	680	>665
Lamp	Blue Mercury Vapor	Daylight White

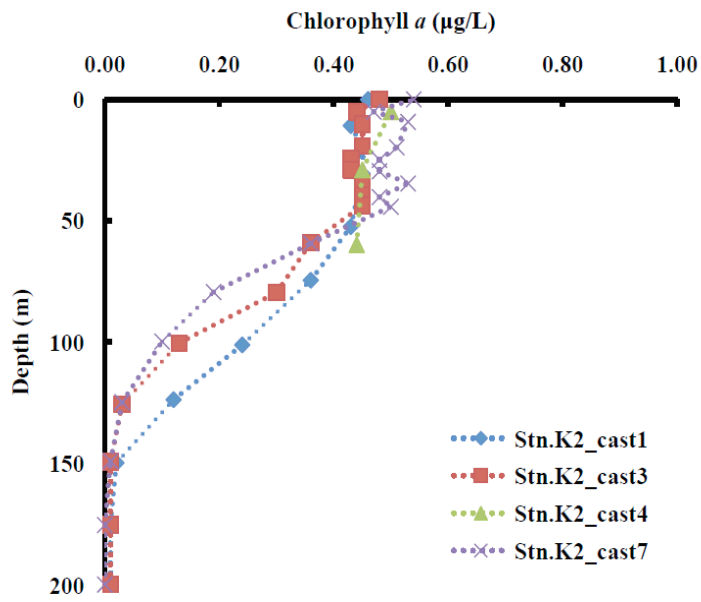


Figure 1. Vertical distribution of chlorophyll *a* at Stn.K2

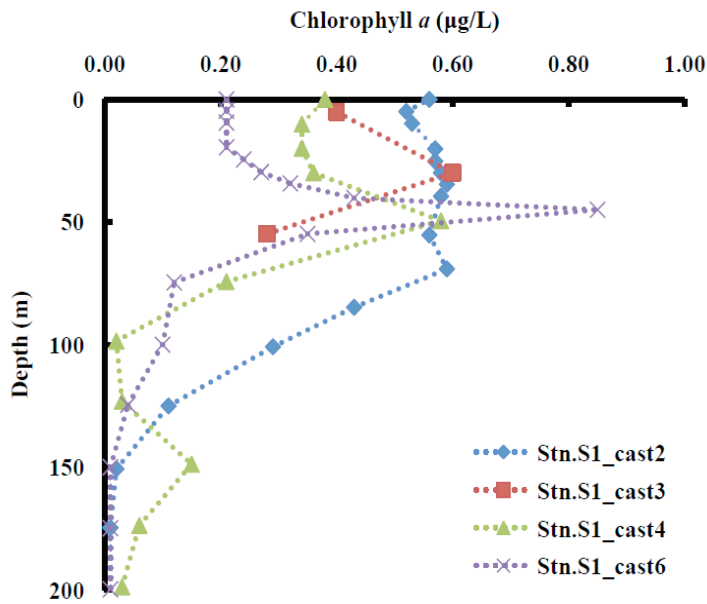


Figure 2. Vertical distribution of chlorophyll *a* at Stn.S1

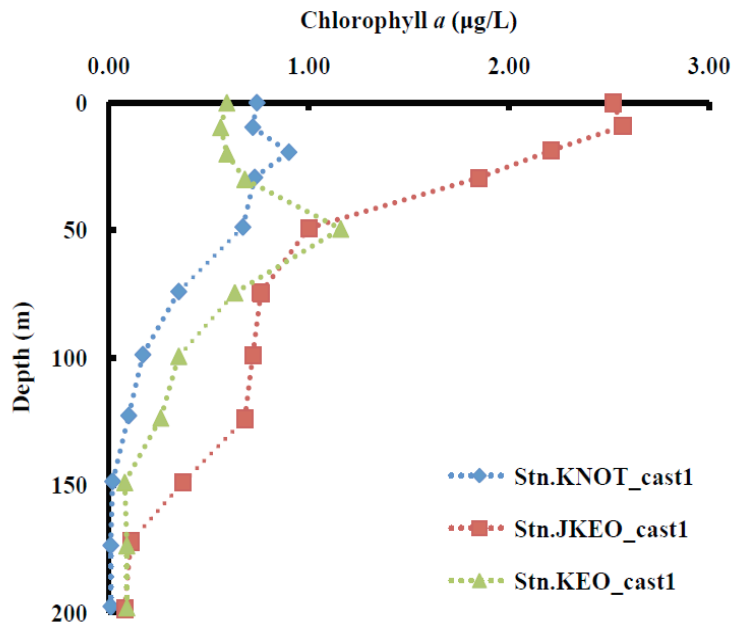


Figure 3. Vertical distribution of chlorophyll *a* at Stn.KNOT, JKEO and KEO

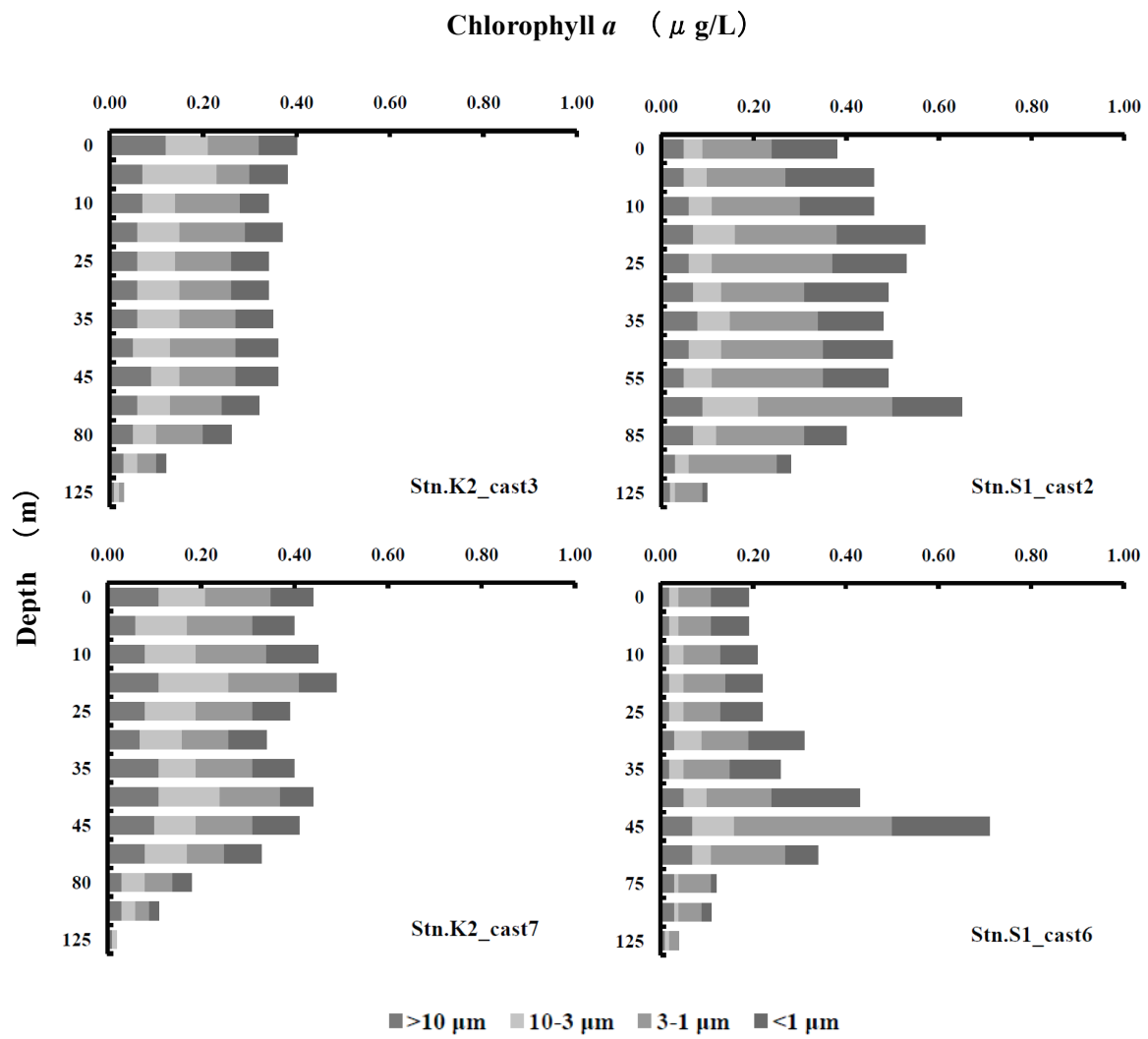


Figure 4. Vertical distribution of size-fractionated chlorophyll *a*

3.1.2. HPLC measurements of marine phytoplankton pigments

Kazuhiko MATSUMOTO (JAMSTEC RIGC)

Shoko TATAMISASHI (MWJ)

Hironori SATO (MWJ)

(1) Objective

The chemotaxonomic assessment of phytoplankton populations present in natural seawater requires taxon-specific algal pigments as good biochemical markers. A high-performance liquid chromatography (HPLC) measurement is an optimum method for separating and quantifying phytoplankton pigments in natural seawater. In this cruise, we measured the marine phytoplankton pigments by HPLC to investigate the marine phytoplankton community structure in the western North Pacific.

(2) Methods, Apparatus and Performance

Seawater samples were collected from 11 depths between the surface and 200 m at the cast for the primary production. Sampling depths were determined by the light intensity at eight depths from among the surface, 0.5%, 1%, 2.5%, 5%, 10%, 25%, 50% light depths relative to the surface and at three other depths between the surface and 200 m. Seawater samples were collected using Niskin bottles, except for the surface water, which was taken by a bucket. Seawater samples (5L) were filtered (<0.02 MPa) through the 47-mm diameter Whatman GF/F filter. To remove retaining seawater in the sample filters, GF/F filters were vacuum-dried in a freezer (0 °C) within 6 hours. Subsequently, phytoplankton pigments retained on a filter were extracted in a glass tube with 4 ml of N,N-dimethylformamide (HPLC-grade) for at least 24 hours in a freezer (-20 °C), and analyzed by HPLC within a few days.

Residua cells and filter debris were removed through polypropylene syringe filter (pore size: 0.2 µm) before the analysis. The samples injection of 500 µl was conducted by auto-sampler with the mixture of extracted pigments (350 µl), pure water (150 µl) and internal standard (10 µl). Phytoplankton pigments were quantified based on C₈ column method containing pyridine in the mobile phase (Zapata *et al.*, 2000).

(i) HPLC System

HPLC System was composed by Agilent 1200 modular system, G1311A Quaternary pump (low-pressure mixing system), G1329A auto-sampler and G1315D photodiode array detector.

(ii) Stationary phase

Analytical separation was performed using a YMC C₈ column (150×4.6 mm). The column was thermostatted at 35 °C in the column heater box.

(iii) Mobile phases

The eluant A was a mixture of methanol: acetonitrile: aqueous pyridine solution (0.25M pyridine), (50:25:25, v:v:v). The eluant B was a mixture of methanol: acetonitrile: acetone (20:60:20, v:v:v). Organic solvents for mobile phases were used reagents of

HPLC-grade.

(iv) Calibrations

HPLC was calibrated using the standard pigments (Table 1). The solvents of pigment standards were displaced to N,N-dimethylformamide, but the concentrations were determined with spectrophotometer by using its extinction coefficient in ethanol or acetone.

(v) Internal standard

Ethyl-apo-8'-carotenoate was added into the samples prior to the injection as the internal standard. The mean chromatogram area and its coefficient of variation (CV) of internal standard were estimated as the following two samples:

Standard samples (Figure 1): 249.4 ± 2.8 (n = 36), CV=1.1%

Seawater samples: 254.5 ± 6.8 (n = 111), CV=2.7%

(vi) Pigment detection and identification

Chlorophylls and carotenoids were detected by photodiode array spectroscopy (350~800 nm). Pigment concentrations were calculated from the chromatogram area at different five channels (Table 1). First channel was allocated at 409 nm of wavelength for the absorption maximum of Pheophorbide a and Pheophytin a. Second channel was allocated at 431 nm for the absorption maximum of chlorophyll a. Third channel was allocated at 440 nm for the absorption maximum of [3,8-divinyl]-protochlorophyllide. Fourth channel was allocated at 450 nm for other pigments. Fifth channel was allocated at 462 nm for chlorophyll b.

(3) Preliminary results

Vertical profiles of major pigments (Chlorophyll a, Chlorophyll b, Divinyl Chlorophyll a, Fucoxanthin 19'-hexanoyloxyfucoxanthin, 19'-butanoyloxyfucoxanthin, and zeaxanthin) at the station K2, S1 and JKEO were shown in Figure 2, 3 and 4.

(4) Data archives

The processed data file of pigments will be submitted to the JAMSTEC Data Integration and Analyses Group (DIAG) within a restricted period. Please ask PI for the latest information.

(5) Reference

Zapata M, Rodriguez F, Garrido JL (2000), Separation of chlorophylls and carotenoids from marine phytoplankton: a new HPLC method using a reversed phase C₈ column and pyridine-containing mobile phases, *Mar. Ecol. Prog. Ser.*, 195, 29-45.

Table 1. Retention time and wavelength of identification for pigment standards.

No.	Pigment	Productions	Retention Time (minute)	Wavelength of identification (nm)
1	Chlorophyll <i>c3</i>	DHI Co.	8.253	462
2	Chlorophyllide <i>a</i>	DHI Co.	10.375	431
3	[3,8-Divinyl]-Protochlorophyllide	DHI Co.	11.060	440
4	Chlorophyll <i>c2</i>	DHI Co.	11.610	450
5	Peridinin	DHI Co.	14.593	450
6	Pheophorbide <i>a</i>	DHI Co.	16.970	409
7	19'-butanoyloxyfucoxanthin	DHI Co.	18.151	450
8	Fucoxanthin	DHI Co.	19.397	450
9	Neoxanthin	DHI Co.	18.530	440
10	Prasinoxanthin	DHI Co.	21.083	450
11	19'-hexanoyloxyfucoxanthin	DHI Co.	21.901	450
12	Violaxanthin	DHI Co.	21.865	440
13	Diadinoxanthin	DHI Co.	28.156	450
14	Antheraxanthin	DHI Co.	25.932	450
15	Alloxanthin	DHI Co.	27.143	450
16	Diatoxanthin	DHI Co.	28.094	450
17	Zeaxanthin	DHI Co.	28.818	450
18	Lutein	DHI Co.	29.014	450
19	Ethyl-apo-8'-carotenoate	Sigma-Aldrich Co.	30.959	462
20	Crocoxanthin	DHI Co.	32.978	450
21	Chlorophyll <i>b</i>	Sigma-Aldrich Co.	33.468	462
22	Divinyl Chlorophyll <i>a</i>	DHI Co.	34.783	440
23	Chlorophyll <i>a</i>	Sigma-Aldrich Co.	35.110	431
24	Pheophytin <i>a</i>	DHI Co.	37.589	409
25	Alpha-carotene	DHI Co.	38.321	450
26	Beta-carotene	WAKO Ltd.	38.565	450

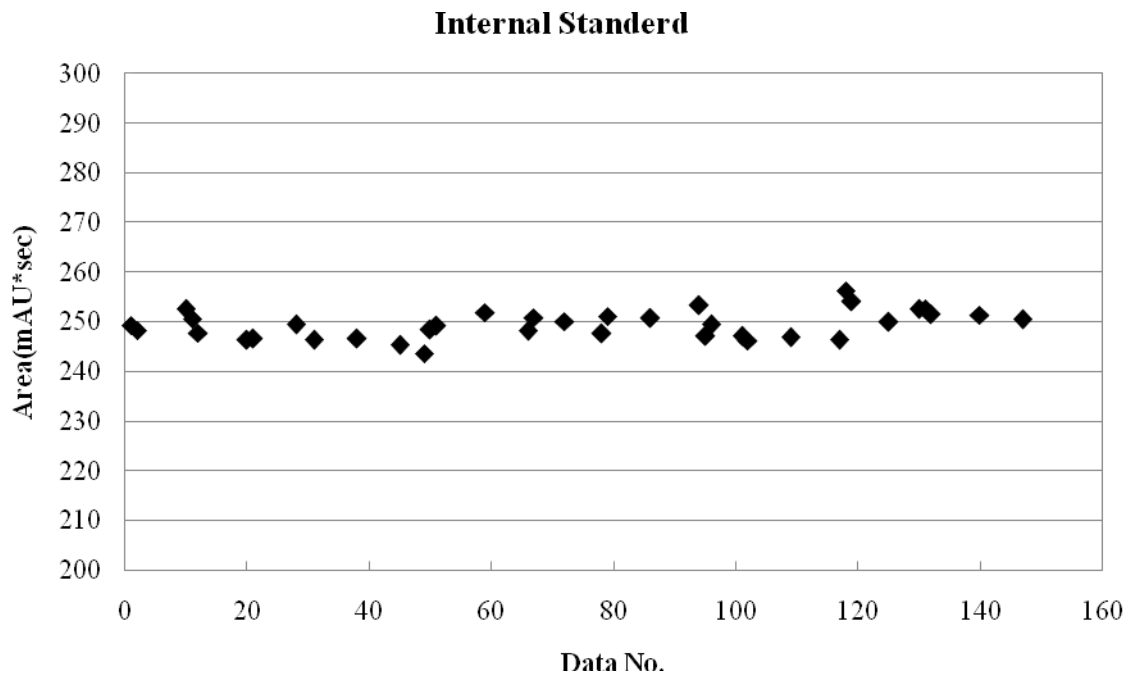


Figure 1. Variability of chromatogram areas for the internal standard.

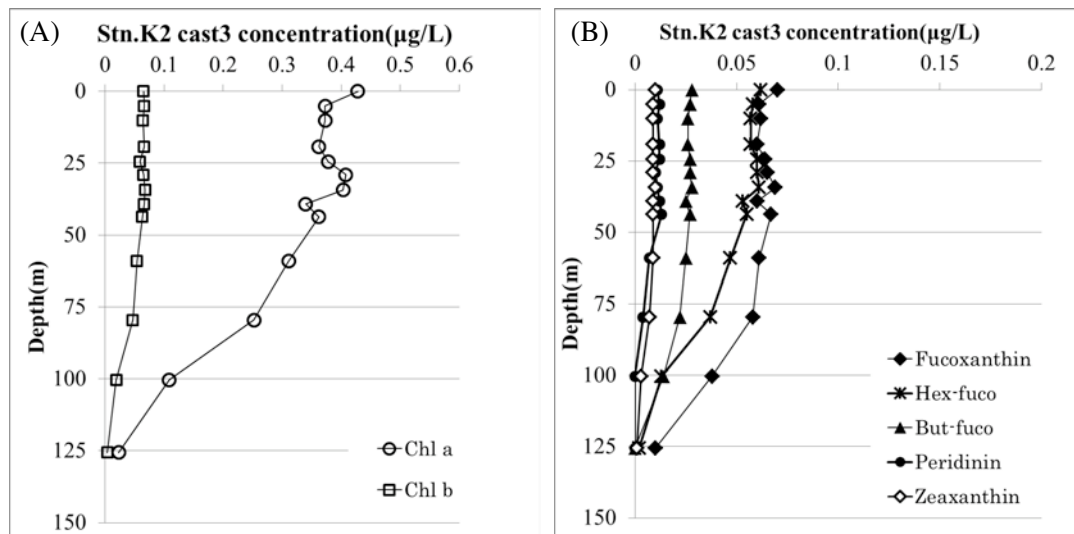


Figure 2-(A). Vertical distributions of major phytoplankton pigments (Chlorophyll *a*, Chlorophyll *b*) at Stn.K2 cast3.

Figure 2-(B). Vertical distributions of major phytoplankton pigments (Fucoxanthin, 19'-hexanoyloxyfucoxanthin, 19'-butanoyloxyfucoxanthin, Peridinin and Zeaxanthin) at Stn.K2 cast3.

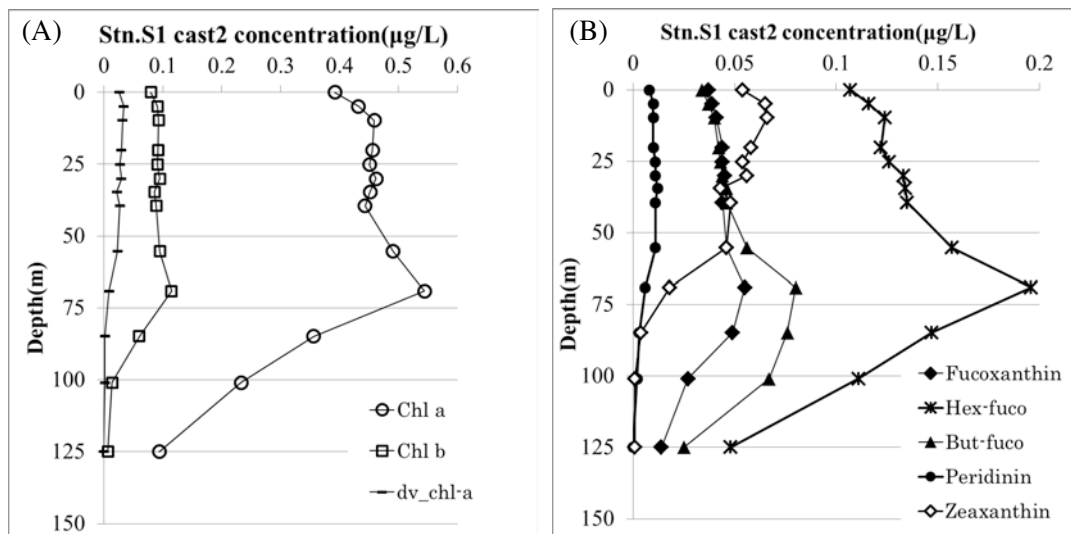


Figure 3-(A). Vertical distributions of major phytoplankton pigments (Chlorophyll *a*, Chlorophyll *b*, Divinyl Chlorophyll *a*) at Stn.S1 cast1.

Figure 3-(B). Vertical distributions of major phytoplankton pigments (Fucoxanthin, 19'-hexanoyloxyfucoxanthin, 19'-butanoyloxyfucoxanthin, Peridinin and Zeaxanthin) at Stn.S1 cast2.

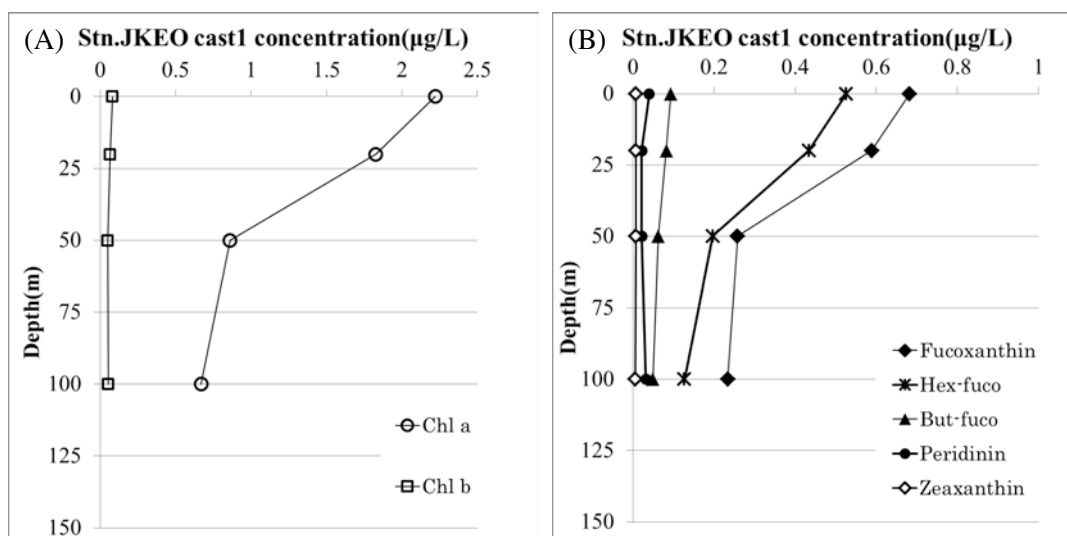


Figure 4-(A). Vertical distributions of major phytoplankton pigments (Chlorophyll *a*, Chlorophyll *b*,) at Stn.JKEO cast1.

Figure 4-(B). Vertical distributions of major phytoplankton pigments (Fucoxanthin, 19'-hexanoyloxyfucoxanthin, 19'-butanoyloxyfucoxanthin, Peridinin and Zeaxanthin) at Stn.JKEO cast1.

3.1.3 Phytoplankton abundance

Kazuhiko MATSUMOTO (JAMSTEC)

(1) Objectives

The main objective of this study is to estimate phytoplankton abundances and their taxonomy in the subarctic gyre and the subtropical gyre in the western North Pacific. Phytoplankton abundances were measured with two kinds of methods: microscopy for large size phytoplankton and flowcytometry for small size phytoplankton.

(2) Sampling

Samplings were conducted using Niskin bottles, except for the surface water, which was taken by a bucket. Samplings were carried out at the two observational stations of K2 and S1.

(3) Methods

1) Microscopy

Water samples were placed in 500 ml plastic bottle at station K2 and in 1000 ml plastic bottle at station S1. Samples were fixed with neutral-buffered formalin solution (1% final concentration). The microscopic measurements are scheduled after the cruise.

2) Flowcytometry

2)-1 Equipment

The flowcytometry system used in this research was BRYTE HS system (Bio-Rad Laboratories Inc). System specifications are follows:

Light source: 75W Xenon arc lamp

Excitation wavelength: 350-650 nm

Detector: high-performance PMT

Analyzed volume: 75 μ l

Flow rate: 10 μ l min⁻¹

Sheath fluid: Milli-Q water

Filter block: B2 as excitation filter block, OR1 as fluorescence separator block

B2 and OR1 have ability as follows:

B2: Excitation filter 390-490 nm

 Beam-splitter 510 nm

 Emission filter 515-720 nm

OR1: Emission filter 1 565-605 nm

 Beam-splitter 600 nm

 Emission filter 2 >615 nm

2)-2 Measurements

The water samples were fixed immediately with glutaraldehyde (1% final concentration) and stored in the dark at 4°C. The analysis by the flow cytometer was acquired on board within 24 hours after the sample fixation. Calibration was achieved with standard beads

of 0.356 – 9.146 μm (Polysciences, Inc.). Standard beads of 2.764 μm were added into each sample prior to the injection of flow cytometer as internal standard. Phytoplankton cell populations were estimated from the forward light scatter signal. Acquired data were stored in list mode file and analyzed with WinBryte software. Phytoplankton are classified with prokaryotic cyanobacteria (*Prochlorococcus* and *Synechococcus*) and other eukaryotes on the basis of scatter and fluorescence signals. *Synechococcus* is discriminated by phycoerythrin as the orange fluorescence, while other phytoplankton are recognized by chlorophylls as the red fluorescence without the orange fluorescence. *Prochlorococcus* and picoeukaryotes were distinguished with their cell size, but it was difficult to identify the abundance of *Prochlorococcus* accurately in the surface mixed layer due to its decreased chlorophyll fluorescence. The cell size was estimated using the empirically-determined relationship between cell diameter (d_{cell}) and bead diameter (d_{bead}) with the forward light scatter signal (FS) by Blanchot *et al.*, (2001) as follows.

$$d_{\text{cell}} = d_{\text{bead}} (\text{FS})^{1/5}$$

(4) Preliminary result

The vertical profile of phytoplankton group identified by flow cytometer at station K2 (cast 3) and station S1 (cast 2) are shown in Figure 1 and Figure 2, respectively.

K2:

Prochlorococcus was not observed in this station. The mean cell size of *Synechococcus* (SYN) was estimated to 0.9 μm . The mean cell size of eukaryotic phytoplankton of EUK-1 and EUK-2 were estimated to 1.3 – 1.4 μm and 1.6 – 1.8 μm , respectively. The population of EUK-3 was isolated in cell size of >3.1 μm .

S1:

The mean cell size of *Prochlorococcus* (PRO) and *Synechococcus* (SYN) were estimated to 0.4 – 0.5 μm and 0.7 – 0.8 μm , respectively. The mean cell size of eukaryotic phytoplankton of EUK-1 and EUK-2 were estimated to 0.9 – 1.1 μm and 1.5 – 1.6 μm , respectively. The population of EUK-3 was isolated in cell size of >2.7 μm .

(5) Data Archive

All data will be submitted to Data Integration and Analysis Group (DIAG), JAMSTEC.

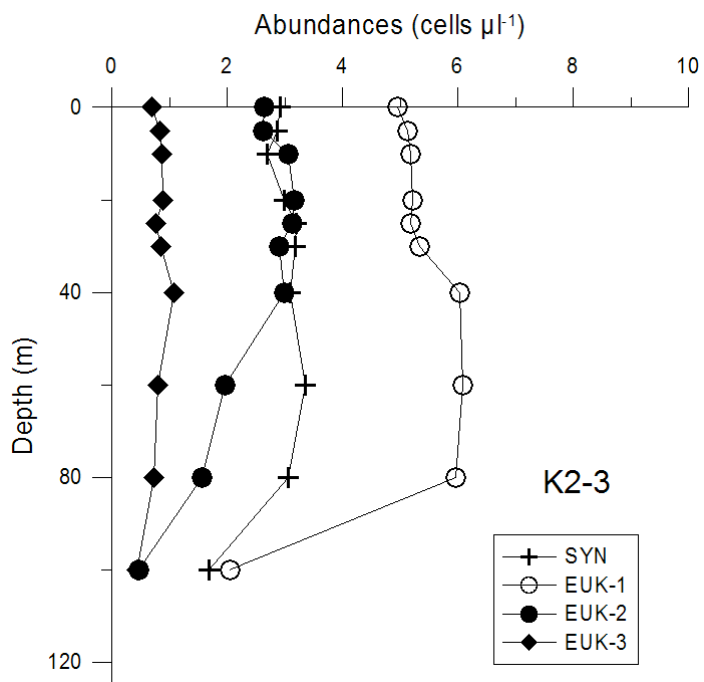


Figure 1. Vertical profile of phytoplankton abundances at K2

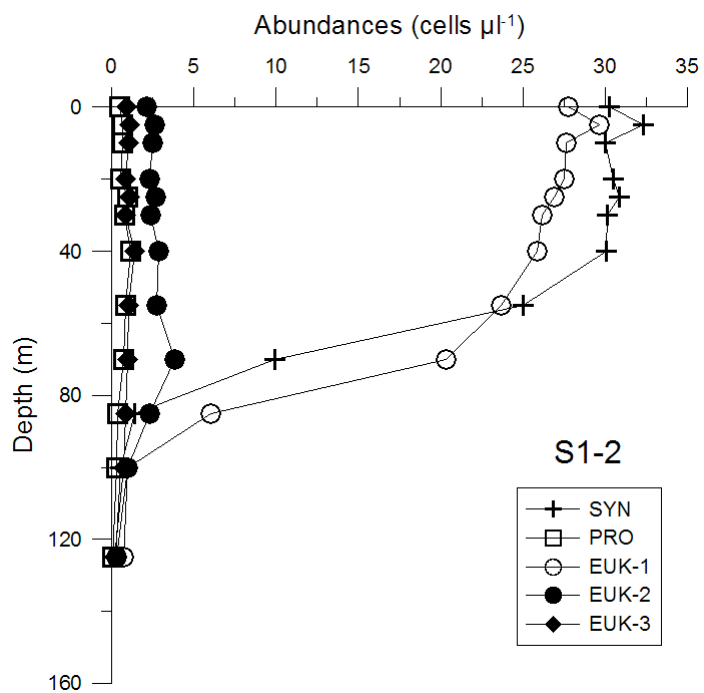


Figure 2. Vertical profile of phytoplankton abundances at S1

3.1.4 Primary production and new production

Kazuhiko MATSUMOTO (JAMSTEC RIGC)

Miyo IKEDA (MWJ)

Kanako YOSHIDA (MWJ)

Atsushi OHASHI (MWJ)

(1) Objective

Quantitative assessment of temporal and spatial variation in carbon and nitrate uptake in the surface euphotic layer should be an essential part of biogeochemical studies in the western North Pacific. Primary production (PP) was measured as incorporation of inorganic C¹³, and new production (NP), measurement of nitrate uptake rate was conducted with ¹⁵N stable isotope tracer at K2 and S1 stations.

(2) Methods

1) *Sampling, incubation bottle and filter*

Sampling was begun at predawn immediately before the incubation experiment. Seawater samples were collected using Teflon-coated and acid-cleaned Niskin bottles, except for the surface water, which was taken by a bucket. Samplings were conducted at eight depths between the surface and 1 % light depth in response to the light levels of the incubation containers adjusted with the blue acrylic plate. Two kinds of baths were prepared for PP and NP (bath-1), and for oxygen evolution (bath-2). The light levels of the incubation containers in each bath were shown in Table 3.1.4-1. The light depths relative to the surface had been estimated by a CTD-attached PAR sensor on the previous day of the sampling. The euphotic layers, that is defined as water depth with 0.5 % of surface PAR, were 65 – 87 m (Table 3.1.4-2). Seawater samples were placed into acid-cleaned clear polycarbonate bottles in duplicate for PP and NP, and in a single for the dark and the time-zero samples for bath-1. The time-zero sample was filtered immediately after the addition of ¹³C and ¹⁵N solution. The PP incubation was conducted in a single for bath-2. Filtration of seawater sample was conducted with pre-combusted glass fiber filters (Whatman GF/F 25 mm) with temperature of 450 degree C for at least 4 hours.

2) *Incubation*

All samples were incubated by simulated *in situ* method in this cruise. Each bottle was spiked with sufficient NaH¹³CO₃ just before incubation so that ¹³C enrichment was about 10% of ambient dissolved inorganic carbon as final concentration of 0.2 mmol dm⁻³ (Table 3.1.4-3). The ¹⁵N-enriched NO₃, K¹⁵NO₃ solution, was injected to the incubation bottles (except PP bottles), resulting that the final concentration of ¹⁵N enrichment was about 10% of ambient nitrate (Table 3.1.4-4). Incubation was begun at predawn and continued for 24 h. The simulated *in situ* method was conducted in the on-deck bath cooled by running surface seawater or by immersion cooler.

3) *Measurement*

After 24 hours incubation, samples were filtered though GF/F filter, and the filters

were kept in a freezer (-20 degree C) on board until analysis. Before analysis, the filters were dried in the oven (45 degree C) for at least 20 hours, and inorganic carbon was removed by acid treatment in a HCl vapor bath for 30 minutes. Several samples were measured by a mass spectrometer ANCA-SL system at MIRAI during this cruise. The remaining samples are scheduled to measure after the cruise.

Instruments: preprocessing equipment ROBOPLEP-SL (Europa Scientific Ltd.; now SerCon Ltd.)
stable isotope ratio mass spectrometer EUROPA20-20 (Europa Scientific Ltd.; now SerCon Ltd.)

Methods: Dumas method, Mass spectrometry

Precision: All specifications are for n=5 samples.

It is a natural amount and five time standard deviation of the analysis as for amount 100 µg of the sample. We measured repeatability 5 times in this cruise. ¹³C (0.2 – 0.5 ‰), ¹⁵N (0.3 – 0.8 ‰)

Reference Material: The third-order reference materials L-aspartic acid (SHOKO Co., Ltd.)

4) Calculation

(a) Primary Production

Based on the balance of ¹³C, assimilated organic carbon (ΔPOC) is expressed as follows (Hama *et al.*, 1983):

$$^{13}\text{C}_{(\text{POC})} * \text{POC} = ^{13}\text{C}_{(\text{sw})} * \Delta\text{POC} + (\text{POC} - \Delta\text{POC}) * ^{13}\text{C}_{(0)}$$

This equation is converted to the following equation;

$$\Delta\text{POC} = \text{POC} * (^{13}\text{C}_{(\text{POC})} - ^{13}\text{C}_{(0)}) / (^{13}\text{C}_{(\text{sw})} - ^{13}\text{C}_{(0)})$$

where ¹³C_(POC) is concentration of ¹³C of particulate organic carbon after incubation, *i.e.*, measured value(%). ¹³C₍₀₎ is that of particulate organic carbon before incubation, *i.e.*, that for samples as a blank.

¹³C_(sw) is concentration of ¹³C of ambient seawater with a tracer. This value for this study was determined based on the following calculation;

$$^{13}\text{C}_{(\text{sw})} (\%) = [(\text{TDIC} * 0.011) + 0.0002] / (\text{TDIC} + 0.0002) * 100$$

where TDIC is concentration of total dissolved inorganic carbon at respective bottle depth(mol dm⁻³) and 0.011 is concentration of ¹³C of natural seawater (1.1%). 0.0002 is added ¹³C (mol) as a tracer. Taking into account for the discrimination factor between ¹³C and ¹²C (1.025), primary production (PP) was, finally, estimated by

$$\text{PP} = 1.025 * \Delta\text{POC}$$

(b) New production

NO₃ uptake rate or new production (NP) was estimated with following equation:

$$\text{NP } (\mu\text{g dm}^{-3} \text{ day}^{-1}) = ({}^{15}\text{N}_{\text{excess}} * \text{PON}) / ({}^{15}\text{N}_{\text{enrich}}) / \text{day}$$

where ${}^{15}\text{N}_{\text{excess}}$, PON and ${}^{15}\text{N}_{\text{enrich}}$ are excess ${}^{15}\text{N}$ (measured ${}^{15}\text{N}$ minus ${}^{15}\text{N}$ natural abundance, 0.366 atom%) in the post-incubation particulate sample (%), particulate nitrogen content of the sample after incubation (mg dm^{-3}) and ${}^{15}\text{N}$ enrichment in the dissolved fraction (%), respectively.

(3) Preliminary results

Fig. 3.1.4.1 and 3.1.4.2 show the vertical profile of primary production (PP) and the diurnal change of photosynthetically available radiation (PAR) observed by PUV-510B (Biospherical Instruments Inc.).

(4) Data archives

All data will be submitted to JAMSTEC Data Integration and Analyses Group (DIAG).

Table 3.1.4-1 Light intensity of simulated *in situ* bath

Number	Bath 1	Bath 2 (with oxygen evolution)
#1	100%	96%
#2	59%	56%
#3	38%	33%
#4	17%	12%
#5	13%	7.8%
#6	7%	4.8%
#7	3.8%	3%
#8	1%	1%

Table 3.1.4-2 Locations of optical observation and principle characteristics

Date (UTC)	Station	Lat./Long.	Euphotic layer	CTD cast	Memo
2011.4.20	K2	47N/160E	73 m	K02M02	1 day before K2-PP#1
2011.4.21	K2	47N/160E	75 m	K02M06	1 day before K2-PP#2
2011.4.28	S1BF	30-53N/144-51E	65 m	002M01	1 day before S1-PP#1
2011.4.28	S1	30N/145E	87 m	S01M03	during S1-PP#1
2011.4.30	S1	30N/145E	68 m	S01M05	1 day before S1-PP#2

Table 3.1.4-3 Sampling cast table and spike ¹³C concentration

Incubation type	Station	CTD cast No.	NaH ¹³ CO ₃ (μmol dm ⁻³)
SIS	K2	3	200
SIS	K2	7	200
SIS	S1	2	200
SIS	S1	6	200

Table 3.1.4-4 Sampling cast table and spike ¹⁵N concentration

Incubation type	Station	CTD cast No.	Light Intensity	K ¹⁵ NO ₃ (μmol dm ⁻³)
SIS	K2	3	All layers	2.5
SIS	K2	7	All layers	2.5
SIS	S1	2	All layers	0.01
SIS	S1	6	100% - 7%	0.01
			3.8% - 1%	0.02

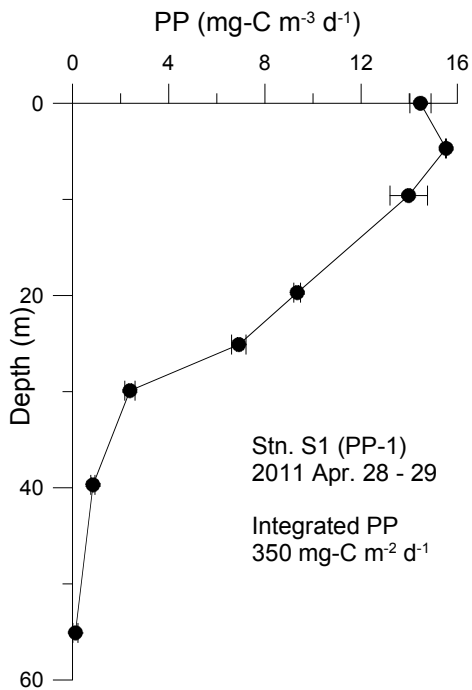
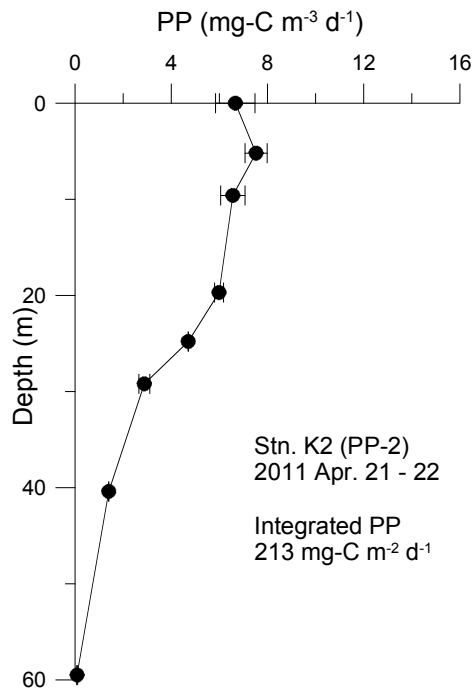
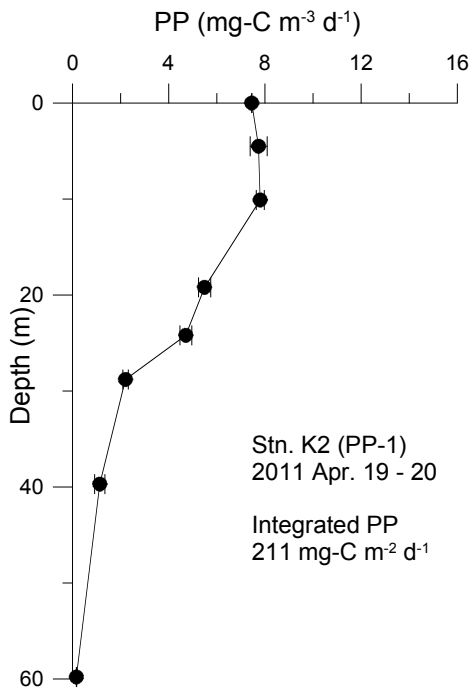


Figure 3.2.4.1 Vertical profile of primary production

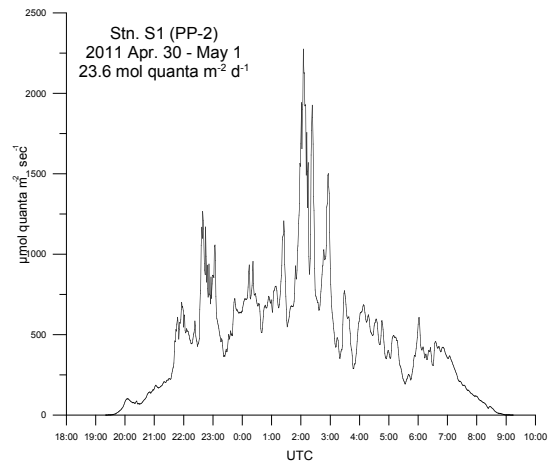
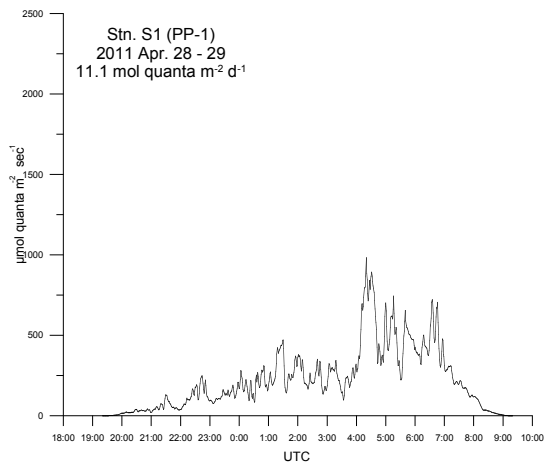
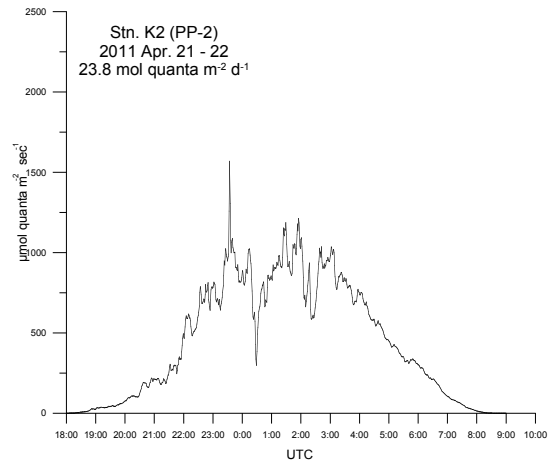
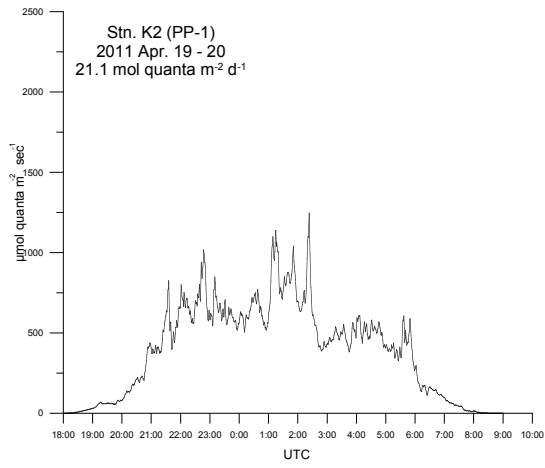


Figure 3.2.4.2 Photosynthetically available radiation (PAR) during incubation experiment

3.1.5 P vs. E curve

Kazuhiko MATSUMOTO (JAMSTEC RIGC)

Miyo IKEDA (MWJ)

Kanako YOSHIDA (MWJ)

Atsushi OHASHI (MWJ)

(1) Objectives

The objective of this study is to estimate the relationship between phytoplankton photosynthetic rate (P) and scalar irradiance (E) in the western North Pacific.

(2) Methods

1) Sampling

Samplings were carried out at two observational stations of K2 and S1. Sample water was collected at three depths of different irradiance level, using Teflon-coated and acid-cleaned Niskin bottles.

2) Incubation

Three incubators filled in water were used, illuminated at one end by a 500W halogen lamp. Water temperature was controlled by circulating water cooler (Fig. 3.1.5-1). Water samples were poured into acid-cleaned clear nine flasks (approx. 1 liter) and arranged in the incubator linearly against the lamp after adding the isotope solutions. The isotope solutions of 0.2 mmol dm⁻³ (final concentration) of NaH¹³CO₃ solution were spiked. All flasks were controlled light intensity by shielding with a neutral density filter on lamp side. The light intensities inside the flasks were shown in Table 3.1.5. The incubations were begun at about local noon and continued for 3 h. Filtration of seawater sample was conducted with glass fiber filters (Whatman GF/F 25 mm) which precombusted with temperature of 450 degree C for at least 4 hours.

3) Measurement

After the incubation, samples were treated as same as the primary production experiment. During the cruise, a set of one incubator samples were measured by a mass spectrometer ANCA-SL system at MIRAI, but the measurements of other samples are scheduled after the cruise. The analytical function and parameter values used to describe the relationship between the photosynthetic rate (P) and scalar irradiance (E) are best determined using a least-squares procedure from the following equation.

$$P = P_{\max}(1 - e^{-\alpha E/P_{\max}})e^{-b\alpha E/P_{\max}} : (\text{Platt et al., 1980})$$

where, P_{\max} is the light-saturated photosynthetic rate, α is the initial slope of the P vs. E curve, b is a dimensionless photoinhibition parameter.

(3) Preliminary results

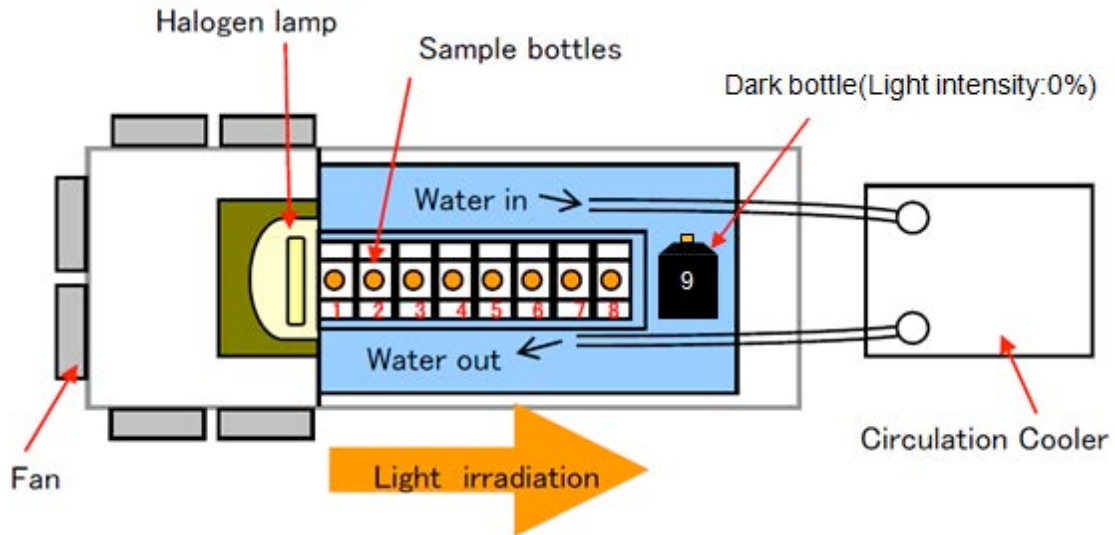
The P vs. E curve obtained at the station of K2 (5m) is shown in Fig. 3.1.5-2.

(4) Data archives

All data will be submitted to JAMSTEC Data Integration and Analyses Group (DIAG) .

(5) Reference

Platt, T., Gallegos, C.L. and Harrison, W.G., 1980. Photoinhibition of photosynthesis in natural assemblages of marine phytoplankton. *Journal of Marine Research*, 38, 687-701.



Fan: AC100V 50/60HZ 14/13W or 16/15W

Halogen lamp: 500W

Fig. 3.1.5-1 Look down view of Incubator for Photosynthesis and irradiation curve

Table 3.1.5 Light Intensity of P vs. E measurements

	Bath A	Bath B	Bath C
Bottle No.	Light intensity ($\mu\text{E m}^{-2} \text{sec}^{-1}$)		
1	2000	2000	2000
2	950	970	1050
3	420	520	480
4	190	260	230
5	90	110	100
6	41	46	43
7	17	22	18
8	7.3	9	7.5
9	0	0	0

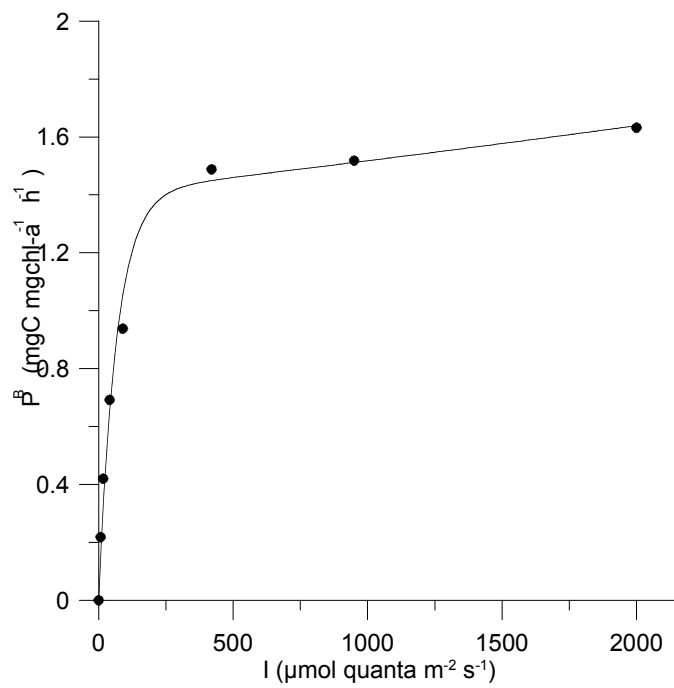


Fig. 3.1.5-2

3.1.6. Oxygen evolution (gross primary productivity) and FRRF observation

Tetsuichi FUJIKI (JAMSTEC)

Osamu ABE (Nagoya University)

Misato KUWAHARA (MWJ)

Hideki Yamamoto (MWJ)

(1) Objective

An understanding of the variability in phytoplankton productivity provides a basic knowledge of how aquatic ecosystems are structured and functioning. Primary productivity in the world's oceans has been measured mostly by the carbon tracer or oxygen evolution methods. In incubations of 24 hours, the former method provides the values closest to net primary productivity (NPP), while the latter comes closest to gross primary productivity (GPP). The GPP is defined as total amount of oxygen released by phytoplankton photosynthesis. The NPP/GPP ratio provides fundamental information on the metabolic balance and carbon cycle in the ocean. In the MR11-03, the GPP were measured using the light–dark bottle and ¹⁸O spike methods and fast repetition rate (FRR) fluorometry at the stations S1 and K2.

(2) Methods

Sampling

Seawater samples were collected from eight depths corresponding to light levels of approximately 100, 60, 35, 13, 7, 5, 3 and 1 % of surface light intensity, using a bucket (surface only) and 12-L Niskin-X bottles attached to a CTD rosette system. Seawater samples were carefully transferred from Niskin bottle into volume calibrated flasks (ca. 100 cm³).

Light-dark bottle method

At each light depth, three light and three dark bottles were incubated under light condition that simulated those of the original sampling depth. The dark bottles were wrapped with aluminum foil. After 24 h incubation, the light and dark bottles were fixed immediately. Fixing, storage, reagent preparation, measurement and standardization were followed the dissolve oxygen section. The GPP was estimated by adding the dark respiration in dark bottles to the net oxygen evolution in light bottles.

¹⁸O spike method

The samples were spiked with enriched ¹⁸O-labeled water (Cambridge Isotope Laboratories) and incubated for 24 h under light condition that simulated those of the original sampling depth as the light-dark bottle method. After incubation, ~100 mL of subsample were drawn into preevacuated gas extraction vessels and capped.

After measurements of the isotopic composition of O₂ in the laboratory on land, the GPP is calculated from the isotopic composition of dissolved oxygen in initial and incubated samples using the following equation (Bender et al. 2000).

$$GPP = \{[\delta^{18}\text{O}(\text{O}_2)_f - \delta^{18}\text{O}(\text{O}_2)_i] / [\delta^{18}\text{O}_{\text{water}} - \delta^{18}\text{O}(\text{O}_2)_i]\} \times (\text{O}_2)_i$$

where the subscripts i and f are the isotopic composition of O₂ in initial and final samples, (O₂)_i is the oxygen concentration of the initial water sample, and δ¹⁸O_{water} is the isotopic composition of the enriched water.

FRR fluorometry

The FRR fluorometer (Diving Flash, Kimoto Electric) consists of closed dark and open light chambers that measure the fluorescence induction curves of phytoplankton samples in darkness and under actinic illumination. To allow relaxation of photochemical quenching of fluorescence, the FRR fluorometer allows samples in the dark chamber to dark adapt for about 1 s before measurements. To achieve cumulative saturation of PSII within 150 μs — i.e., a single photochemical turnover — the instrument generates a series of subsaturating blue flashes at a light intensity of 25 mmol quanta m⁻² s⁻¹ and a repetition rate of about 250 kHz. The PSII parameters are derived from the single-turnover-type fluorescence induction curve by using the numerical fitting procedure described by Kolber et al. (1998). Analysis of fluorescence induction curves measured in the dark and light chambers provides PSII parameters such as fluorescence yields, photochemical efficiency and effective absorption cross section of PSII, which are indicators of the physiological state related to photosynthesis. Using the PSII parameters, the rate of photosynthetic electron transport and the GPP can be estimated. In the present study, we moved up and down a FRR fluorometer between surface and ~150 m using a ship winch, and measured the vertical and spatial variation in PSII parameters.

(3) Preliminary results

At stations S1 and K2, the vertical profiles of GPP measured with the light-dark bottle method were shown in figure 3.1.6.1.

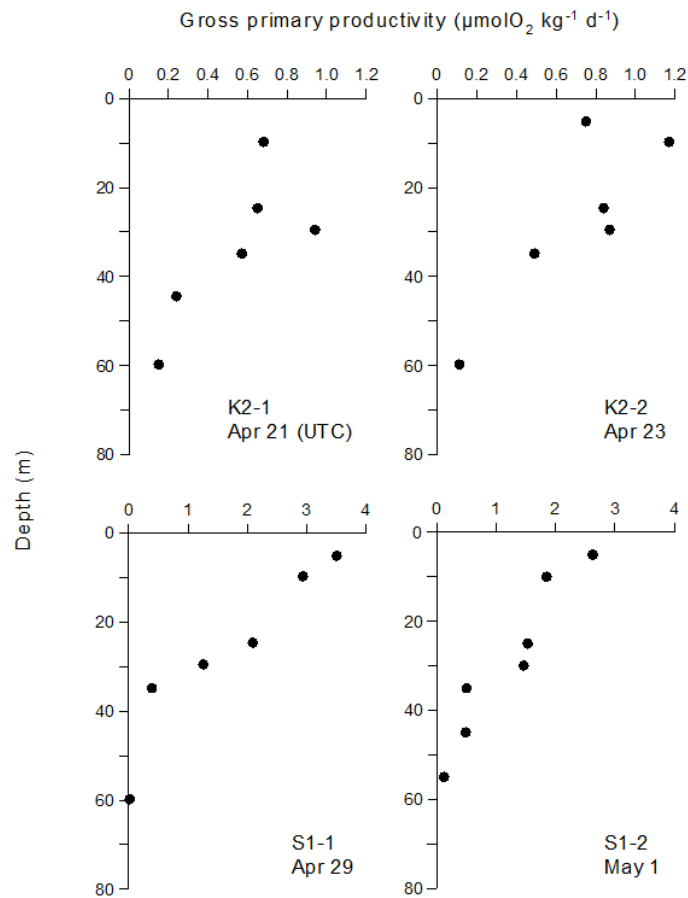


Figure 3.1.6.1. Vertical profiles of GPP at stations S1 and K2, measured with the light-dark bottle method.

(4) Data archives

The data will be submitted to Data Integration and Analyses Group (DIAG), JAMSTEC.

(5) References

Bender, M. L., M. L. Dickson and J. Orchardo. 2000. Net and gross production in the Ross Sea as determined by incubation experiments and dissolved O_2 studies. *Deep-Sea Res.* II 47: 3141–3158.

Kolber, Z. S., O. Prášil and P. G. Falkowski. 1998. Measurements of variable chlorophyll fluorescence using fast repetition rate techniques: defining methodology and experimental protocols. *Biochim. Biophys. Acta.* 1367: 88–106.

3.2 Drifting sediment trap

3.2.1 Drifting mooring system

Hajime KAWAKAMI (JAMSTEC MIO)

Makio C. HONDA (JAMSTEC RIGC)

Ryo KANEKO (University of Tokyo)

Mario UCHIMIYA (University of Tokyo)

Yoshihisa MINO (Nagoya University)

Chiho SUKIGARA (Nagoya University)

Miyo IKEDA (MWJ)

Kanako YOSHIDA (MWJ)

Fujio KOBAYASHI (MWJ)

Tamami UENO (MWJ)

In order to conduct drifting sediment trap experiment at stations K2 and S1, drifting mooring system (drifter) was deployed. This drifter consists of radar reflector, GPS radio buoy (Taiyo TGB-100), flush light, surface buoy, ropes and sinker. On this system, “Knauer” type sediment trap at 12 layers were installed together (Traps of JAMSTEC: 60, 100, 150, and 200 m; traps of Nagoya University: 85, 90, 95, 170, 180, and 190 m; traps of University of Tokyo: 105 and 210 m). Thanks to the effort by MWJ technicians, drifting mooring system was upgraded on board. The configuration is shown in Fig. 3.2.1-1.

The drifter was deployed at 21:50 on 19 April (UTC) at station K2 and at 20:40 on 28 April (UTC) at station S1. The drifter was recovered after 3 days at stations K2 and S1. The drifter’s position was monitored by using GPS radio buoy (Taiyo TGB-100). Fig. 3.2.1-2 shows tracks of the drifter. In general, the drifter tended to drift southwestward and northwestward at stations K2 and S1, respectively. The drifting distance at station S1 was about fourth longer than that at station K2.

Station: K2 & S1

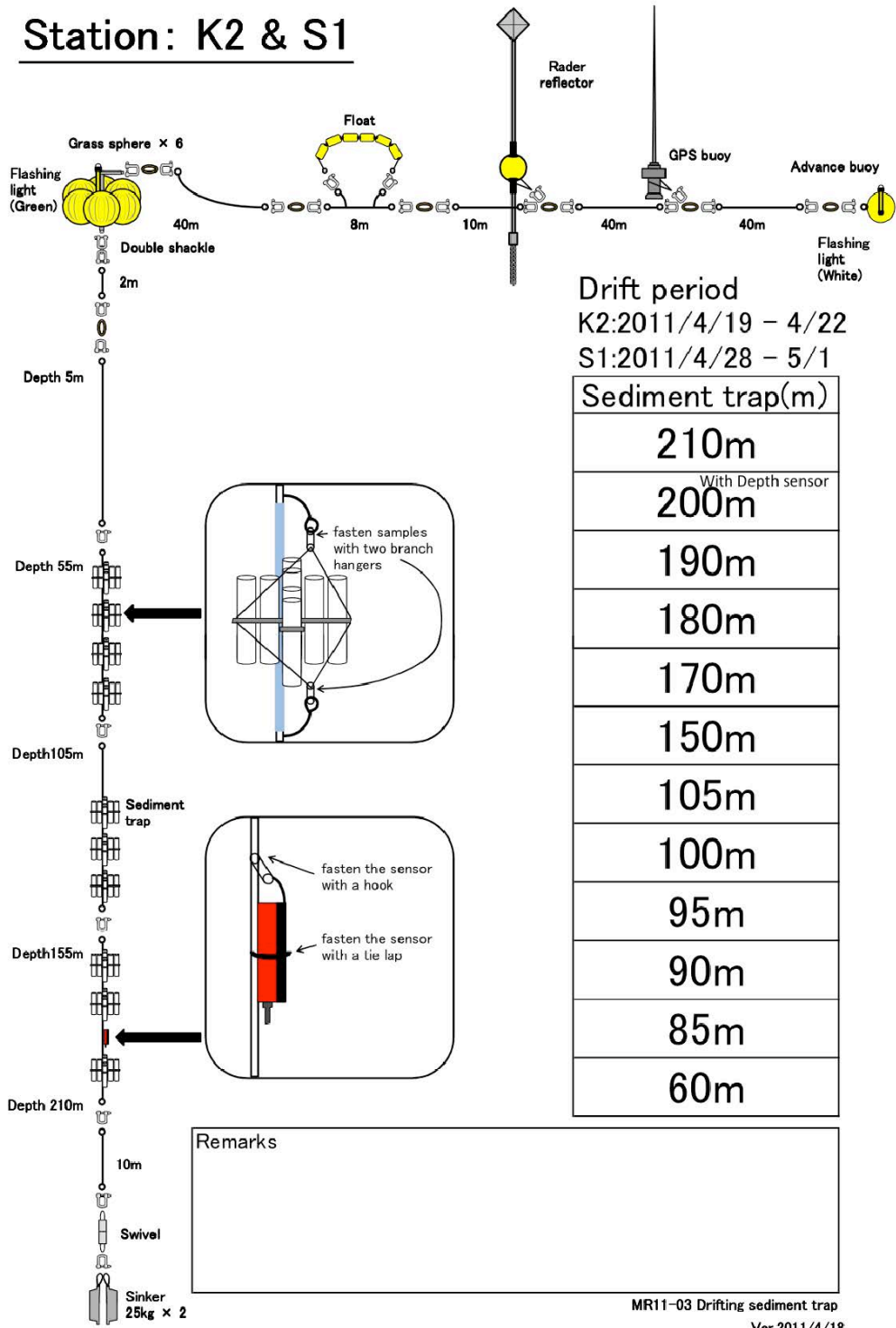


Fig. 3.2.1-1 Drifting mooring system at stations K2 and S1.

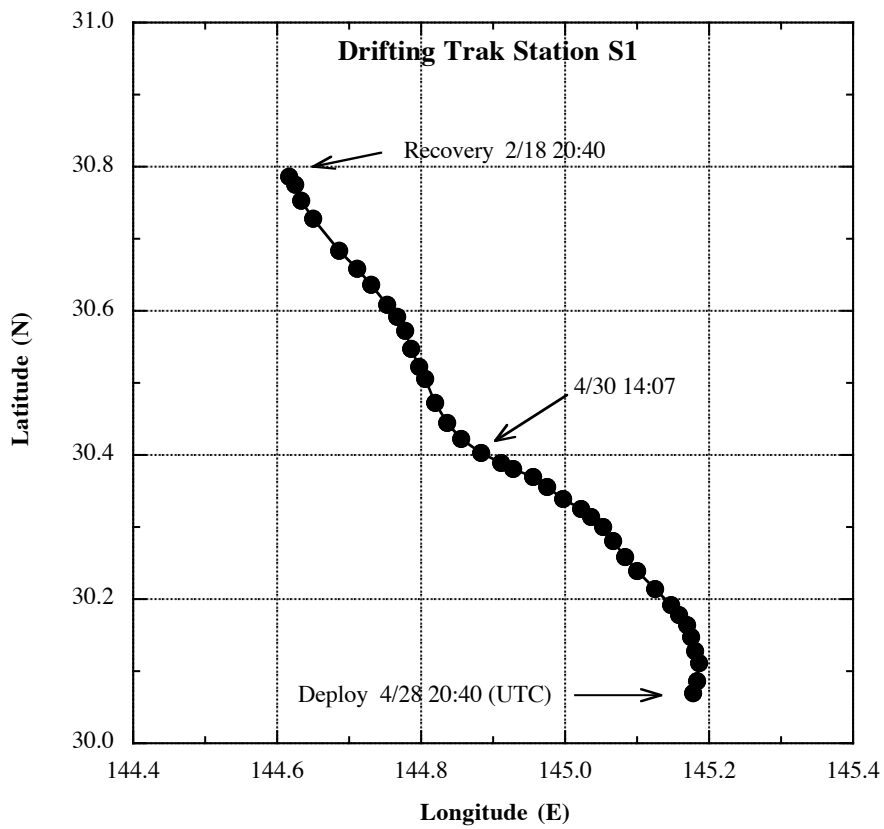
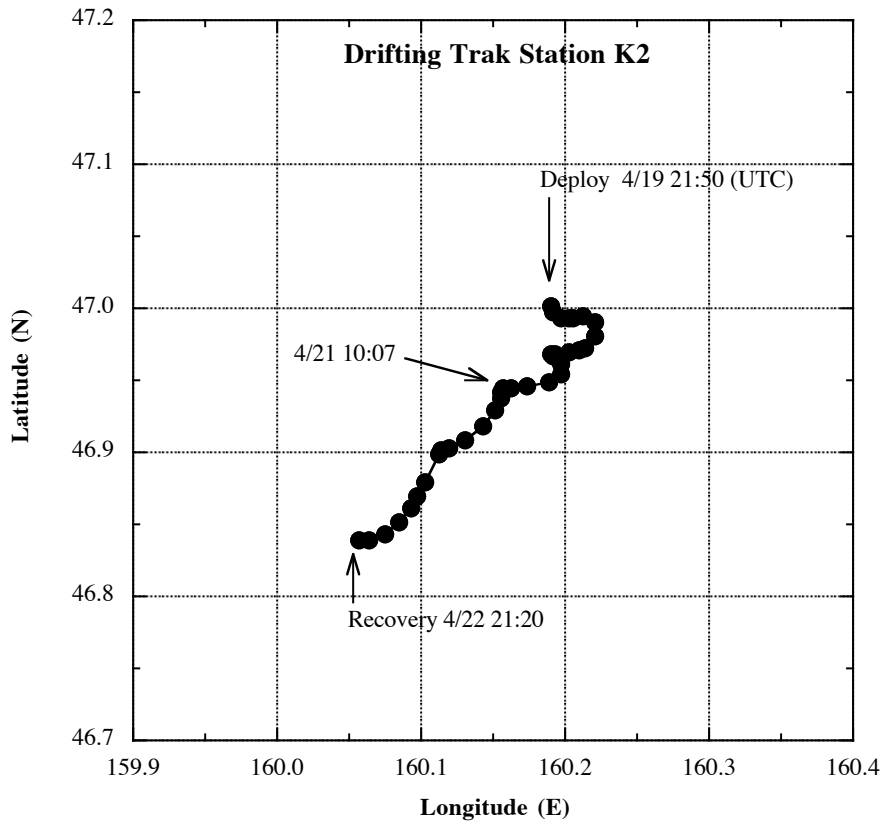


Fig. 3.2.1-2 Track of drifter (GPS buoy) at stations K2 and S1.

3.2.2 JAMSTEC Drifting sediment trap

Hajime KAWAKAMI (JAMSTEC MIO)
Makio C. HONDA (JAMSTEC RIGC)

In order to collect sinking particles and measure carbon flux, and zooplankton, “Knauer type” cylindrical sediment trap (Photo 3.2.2-1) was deployed at stations K2 and S1 where measurement of primary productivity was conducted. This trap consists of 8 individual transparent polycarbonate cylinders with baffle (collection area: ca. 0.0038 m², aspect ratio: 620 mm length / 75 mm width = 8.27), which was modified from Knauer (1979). Before deployment, each trap was filled with filtrated surface seawater, which salinity is adjusted to ~ 39 PSU by addition of NaCl (addition of 100 g NaCl to 20 L seawater) were placed in tubes. These were located at approximately 60, 100, 150, and 200 m. After recovery, sediment traps were left for half hour to make collected particles settle down to the bottle. After seawater in acrylic tube was dumped using siphonic tube, collecting cups were took off. Two cups of samples at each layer were given to the team of Kagoshima University to determine fecal pellets. Four cups of samples at each layer were filtered thorough Nuclepore filter with a nominal pore size of 0.4µm and GF/F filter by two cups, for respective purposes (total mass flux, trace elements, total particulate carbon, and particulate organic carbon). The other samples were added buffered formalin for archive. The filter and archive samples were kept in freezer and refrigerator by the day when these were analyzed, respectively.

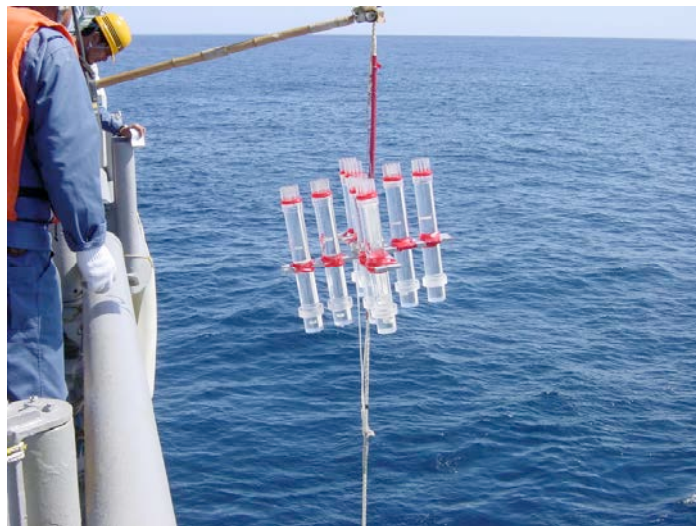


Photo 3.2.2-1 Drifting Sediment Trap.

3.2.3 Vertical changes of fecal pellets Toru KOBARI (Kagoshima University)

(1) Objective

Sinking particles includes phytoplankton aggregates, zooplankton fecal pellets, feeding mucus, carcass and crustacean molts (e.g. Flower and Knauer, 1986). Especially, fecal pellets significantly contribute to downward flux of particulate organic carbon (POC) and are a key component of the biological pump mediated by zooplankton community (Bishop et al., 1977; Lampitt et al., 1990; Silver and Gowing, 1991; Carroll et al., 1998; Turner, 2002). Fecal pellets are changed by zooplankton ingestion (coprophagy), fragmentation via sloppy feeding or swimming activity (coprorhexy) and loosening of membrane (coprochaly) during sinking (Paffenhöfer and Strickland, 1970; Lampitt et al., 1990; Noji et al., 1991). These processes largely affect transfer efficiency of POC flux (Wilson et al., 2008). It has been believed that fecal pellets are declined by bacterial decomposition (Honjo and Roman, 1978; Arístegui et al., 2002) and/or coprophagy/coprorhexy of small copepods such as cyclopoids and poecilostomatoids for last two decades (González and Smetacek, 1994; Suzuki et al., 2003; Svensen and Nejstgaard, 2003; Huskin et al., 2004; Poulsen and Kjørboe, 2006). In recent years, however, these copepods showed minor contributions to coprophagy/coprorhexy from the field observations (Iversen and Poulsen, 2007) and laboratory experiments (Reigstad et al., 2005). Alternatively, heterotrophic microbes consumed fecal pellets (Poulsen and Iversen, 2008). Thus, we should re-consider how fecal pellets are declined or changed during sinking from surface to mesopelagic depths.

In the present study, we investigated vertical changes in flux, shape and volume of fecal pellets from drifting sediment trap experiments to evaluate how fecal pellets were changed or declined.

(2) Methods

Knauer-type sediment traps were deployed at 60, 100, 150 and 200 m at K2 and S1 in the Northwestern Pacific Ocean for 48 hours during the Mirai cruise (MR11-02) from 9 February to 9 March 2011. The sediment traps were constructed from 8 cylinders (collection area: ca. 0.0038 m², aspect ratio: 620 mm length / 75 mm width = 8.27) with a baffle to reduce turbulence, mounted on a polyvinylchloride frame. Approximately 250-mL polycarbonate sample cup was attached to the bottom of each cylinder via screw threads. The sample cup was filled with a brine solution.

Once traps were recovered, samples for particle organic carbon (POC) flux were preserved at 4°C until filtration. To avoid pellet breakage during processing, samples for POC flux were not screened; i.e. swimmers were picked out under a stereo-dissecting microscope. These samples were filtered through a pre-combusted and pre-weighed Whatman GF/F filter under vacuum pressure less than 10kPa and rinsed with Milli-Q water. Samples for fecal pellet (FP) flux were fixed with 5% buffered formaldehyde solution.

(3) Preliminary results

During the cruise, we collected 8 samples for POC flux and 8 samples for FP flux (Table 1 and 2). In the land laboratory, carbon and nitrogen contents will be measured from these filter

samples. For fixed samples, number, shape and volume will be measured under a stereo dissecting microscope.

Samplings/Observations/Analyses	Stat	Start		End		Depth (m)	No. of samples	Reference	
		Date	Time	Date	Time				
Drifting Sediment Trap	FPD	19 Apr	21:50	21 Apr	21:20	60/100/150/200	4		
	CFlux						4		
Bucket	DE	21 Apr	-	23 Apr	-		48		
CTD-CMS	Pico	21 Apr	-	21 Apr	-	0/5/10/20/25/30/40/60	24		
	Nano						8		
	Micro						8		
Twin NORPAC	Macro + GP	21 Apr	21:22	21 Apr	21:32	0-200	1	GP sample was frozen	
	Macro + GP	22 Apr	09:50	22 Apr	10:00	0-200	1	GP sample was frozen	
IONESS	Macro+DM	20 Apr	Night	20 Apr	Night	0-400	14	1/4 sample for Macro and 1/8 sample for DM	
		22 Apr	Day	22 Apr	Day	0-1000	14	1/4 sample for Macro and 1/8 sample for DM	
		22 Apr	Night	22 Apr	Night		16	1/4 sample for Macro and 1/8 sample for DM	
		23 Apr	Day	23 Apr	Day		16	1/4 sample for Macro and 1/8 sample for DM	
Abbreviations	FPD	Fecal pellet analyses							
	DE	Dilution experiments							
	Pico	Microscopic analyses for picoplankton							
	Nano	Microscopic analyses for nanozooplankton							
	Micro	Microscopic analyses for microplankton							
	Macro	Microscopic analyses for macrozooplankton							
	GP	Gut pigment analyses							
	FPD	Fecal pellet decomposition							
	TC	Trophic cascading							
DM	Dry mass measurement								
CHL	Chlorophyll measurement								

Samplings/Observations/Analyses	Stat	Start		End		Depth (m)	No. of samples	Reference
		Date	Time	Date	Time			
Drifting Sediment Trap	FPD	28 Apr	20:40	02 May	20:40	60/100/150/200	4	
	CFlux						4	
Bucket	DE	28 Apr	-	29 Apr	-		57	
	DE	29 Apr	-	30 Apr	-		42	
	DE	29 Apr	-	30 Apr	-		57	
CTD-CMS	Pico	29 Apr	-	29 Apr	-	0/5/10/20/25/30/40/55	24	
	Nano						8	
	Micro						8	
Twin NORPAC	Macro + GP	29 Apr	21:09	29 Apr		0-200	2	GP sample was frozen
	Macro + GP	01 May	08:32	01 May		0-200	2	GP sample was frozen
IONESS	Macro+DM	30 Apr	Night	30 Apr	Night	0-1000	16	1/4 sample for Macro and 1/8 sample for DM
		01 May	Day	01 May	Day		16	1/4 sample for Macro and 1/8 sample for DM
		01 May	Night	01 May	Night		16	1/4 sample for Macro and 1/8 sample for DM
		02 May	Day	02 May	Day		16	1/4 sample for Macro and 1/8 sample for DM

(4) Reference

- Aristegui, J., Duarte, C.M., Agusti, S., Doval, M., Alvarez-Salgado, X.A., Hansell, D.A. (2002). Dissolved organic carbon support of respiration in the dark ocean. *Science*, 298, 1967-1967.
- Bishop, J.K., Edmond, J.M., Ketten, D.R., Bacon, M.P., Silker, W.B. (1977). The chemistry, biology, and vertical flux of particulate matter from the upper 400m of the equatorial Atlantic Ocean. *Deep-Sea Research*, 24, 511-548.
- Carroll, M.L., Miquel, J.-C., Fowler, S.W. (1998). Seasonal patterns and depth-specific trends of zooplankton fecal pellet fluxes in the Northwestern Mediterranean Sea. *Deep-Sea Research I*, 45, 1303-1318.
- González, H. E., Smetacek, V. (1994). The possible role of the cyclopoid copepod *Oithona* in retarding vertical flux of zooplankton fecal material. *Marine Ecology Progress Series*, 113, 233-246.
- Flower, S.W., Knauer, G.A. (1986). Role of large particles in the transport of elements and organic compounds through the oceanic water column. *Progress in Oceanography*, 16, 147-194.
- Honjo, S., Roman, M. R. (1978). Marine copepod fecal pellets: production, preservation and

- sedimentation. *Journal of Marine Research*, 36, 45-57.
- Huskin, I., Viesca, L., Anado' n, R. (2004). Particle flux in the Subtropical Atlantic near the Azores: influence of mesozooplankton. *Journal of Plankton Research*, 26, 403-415.
- Iversen, M. H., Poulsen, M. R. (2007). Coprorhexy, coprophagy, and coprochaly in the copepods *Calanus helgolandicus*, *Pseudocalanus elongates*, and *Oithona similis*. *Marine Ecology Progress Series*, 350, 79-89.
- Lampitt, R.S., Noji, T.T., von Bodungen, B. (1990). What happens to zooplankton faecal pellets? Implications for material flux. *Marine Biology*, 104, 15-23.
- Noji, T. T., Estep, K. W., MacIntyre, F., Norrbin, F. (1991). Image analysis of faecal material grazed upon by three species of copepods: evidence for coprohexy, coprophagy, and coprochaly. *Journal of the Marine Biological Association of the United Kingdom*, 71, 465-480.
- Paffenhöfer, G.-A ., Strickland, J. D. H. (1970). A note on the feeding of *Calanus helgolandicus* on detritus. *Marine Biology*, 5, 97-99.
- Poulsen, L. K., Kiørboe, T. (2006). Vertical flux and degradation rates of copepod fecal pellets in a zooplankton community dominated by small copepods. *Marine Ecology Progress Series*, 323, 195-204.
- Poulsen, M. R., Iversen, M. H. (2008). Degradation of copepod fecal pellets: key role of protozooplankton. *Marine Ecology Progress Series*, 367, 1-13.
- Reigstad, M., Riser, C. W., Svensen, C. (2005). Fate of copepod faecal pellets and the role of *Oithona* spp. *Marine Ecology Progress Series*, 304, 265-270.
- Silver, M.W., Gowing, M.M. (1991). The "particle" flux: origins and biological components. *Oceanography*, 26, 75-113.
- Suzuki, H., Sasaki, H., Fukuchi, M. (2003). Loss processes of sinking fecal pellets of zooplankton in the mesopelagic layers of the Antarctic marginal ice zone. *Journal of Oceanography*, 59, 809-818.
- Svensen, C., Nejstgaard, J. C. (2003). Is sedimentation of copepod faecal pellets determined by cyclopoids? Evidence from enclosed ecosystems. *Journal of Plankton Research*, 25, 917-926.
- Turner, J.T. (2002). Zooplankton fecal pellets, marine snow and sinking phytoplankton blooms. *Aquatic Microbial Ecology*, 27, 57-102.
- Wilson, S. E., Steinberg, D. K., Buesseler, K. O. (2008). Changes in fecal pellet characteristics with depth as indicators of zooplankton repackaging of particles in the mesopelagic zone of the subtropical and subarctic North Pacific Ocean. *Deep-Sea Research II*, 55, 1636-1647.

3.3 Po-210 and export flux

Hajime KAWAKAMI (JAMSTEC MIO)
Makio C. HONDA (JAMSTEC RIGC)

(1) Purpose of the study

The fluxes of POC were estimated from Particle-reactive radionuclide (^{210}Po) and their relationship with POC in the western North Pacific Ocean.

(2) Sampling

Seawater and suspended particulate sampling for ^{210}Po , ^{210}Pb , and POC: 2 stations (stations K2 and S1) and 16 depths (10, 20, 30, 50, 75, 100, 150, 200, 300, 400, 500, 600, 700, 800, 900, and 1000 m) at each station.

Seawater samples (10 L for ^{210}Po and ^{210}Pb) were taken from Hydrocast at each depth. The seawater samples for ^{210}Po were filtered through polypropylene cartridge filters with a nominal pore size of 0.8 μm on board immediately after water sampling.

In situ filtering (suspended particulate) samples were taken from large volume pump sampler (Large Volume Pump WTS-6-1-142 V, McLane Inc.). Approximately 200 and 1000 L seawater was filtered through glass-fiber filter with a nominal pore size of 0.7 μm at each station at 10–200m depths and 300–1000m depths, respectively. The filter samples were divided for ^{210}Po and POC.

(3) Chemical analyses

Dissolved and particulate ^{210}Po was absorbed on 25 mm silver disks electrically, and were measured by α -ray counter (Octéte, Seiko EG&G Co. Ltd.). For total (dissolved + particulate) ^{210}Pb measurement, the same procedure was applied to the seawater samples 18 months later, when ^{210}Po come to radioactive equilibrium with ^{210}Pb .

POC was measured with an elemental analyzer (Perkin-Elmer model 2400II) in land-based laboratory.

(4) Preliminary result

The distributions of ^{210}Po and POC will be determined as soon as possible after this cruise. This work will help further understanding of particle dynamics at the euphotic layer and twilight zone.

3.4 Zooplankton

3.4.1 Community structure and ecological roles

Minoru KITAMURA (JAMSTEC, BioGeos)

Kazuhiko MATSUMOTO (JAMSTEC, RIGC)

Toru KOBARI (Kagoshima Univ.)

(1) Objective

Subarctic western North Pacific is known to be a region with high biological draw down of atmospheric CO₂. And time-series biogeochemical observations conducted at the station K2 have revealed high annual material transportation efficiency to the deep compared to the other time-series sites set in the subtropical regions. Importance of not only sinking particle but also 'active transport' by zooplankton on vertical material transport is recently suggested in several area such as Oyashio region, the station BATS or Antarctic Ocean. However, biogeochemical role of zooplankton is not fully estimated in western subarctic gyre, North Pacific. With these backgrounds, goal of the research is to investigate roles of mesozooplankton and micronekton in vertical material transport in the station K2, western subarctic North Pacific. We deployed two types of plankton nets to investigate species and size composition of zooplankton from the surface to the greater deep.

Material transport through microbial food web is one of the pathways which is little understood. To estimate ecological roles of the nano- and microzooplankton we will also analyze abundance, vertical distribution and grazing pressure of them.

For comparison to K2 ecosystem, we also conducted same samplings at a new time-series station, S1

(2) Materials and methods

Mesozooplankton and micronekton samplings (IONESS Sampling)

For collection of stratified sample sets, multiple opening/closing plankton net system, IONESS, was used. This is a rectangular frame trawl with nine nets. Area of the net mouth is 1.5 m² when the net frame is towed at 45° in angle, and mesh pore size is 0.33-mm. Volume of filtering water of each net is estimated using area of net mouth, towing distance, and filtering efficiency. The area of net mouth is calibrated from frame angle during tow, the towing distance is calculated from revolutions of flow-meter, and the filtering efficiency is 96% which was directory measured. The net system is towed obliquely. Ship speed during net tow was about 2 knot, speeds of wire out and reeling were 0.1-0.7 m/s and 0.1-0.3 m/s, respectively.

Total eight tows (four at K2 and S1, respectively) of IONESS were done. The stratified sampling layers at stations K2 and S1 were as follows; 0-50, 50-100, 100-150, 150-200, 200-300, 300-500, 500-750, and 750-1000m. To understand diel vertical migration of mesozooplankton and micronekton, the samplings were conducted during both day and night. Towing data such as date, time, position, sampling layers are summarized in Table 3.5.1-1.

NORPAC net sampling

A twin-type NORPAC net with fine mesh (100 mm) and flow meters was used. The net was vertically towed 0-50 m and 0-150 m at the Stations K2 and S1 (Table 3.5.1-2). Zooplankton

collected were preserved in the 5% buffered formalin seawater for the later analysis.

Nano- and microzooplankton sampling

Seawater samples were collected at eight depths within the euphotic and three depths within the aphotic zones in both the stations K2 and S1. The former eight depths corresponded to nominal specific optical depths approximately 100, 50, 35, 17, 12, 7, 3 and 1% light intensity relative to the surface irradiance as determined from the optical profiles obtained by PAR sensor attached on CTD system. And the latter three depths were 200, 400 and 800 m.

Seawater samples were immediately treated with the final concentration of 1% glutaraldehyde and were kept at 4°C until filtering. Each seawater sample were filtered through 1µm pore size Nuclepore filter, pre-stained by irgalan black, at the low vacuum of 15 cmHg, and were double-stained using DAPI (4'6-diamidino-2-phenylindole dihydrochloride) and proflavine (3-6-diamidino-acridine hemisulfate). Just before the finish of filtering, DAPI was added to sample in filtering funnel for the staining DNA. After the DAPI staining, proflavine was also added for the staining of flagella. Both the staining time is five minute. The working solution of DAPI (10 µg/ml) and proflavine (0.033%) were pre-filtered through 0.45 µm pore size of non-pyrogenic Durapore membrane filter (Millipore, Millex-GX). After the filtering, sample filters put on a slide-glass with one drop of immersion oil, and covered with micro cover glass. All preparations were stored in the deep freezer (-80°C) until the observation.

Sampling data such as depths or filtering volume are summarized in Table 3.5.1-3.

Table 3.4.1-1. Summary of IONESS samplings.

MR11-03 IONESS Samplings
not including filtering efficiency, 96%, in calculations of filtering volume of water

Stn.	Tow ID	Local Time		Position	Sampling layer (upper, m) and filtering volume (lower, m ³)								Remarks		
		in	out		Net No. 0	1	2	3	4	5	6	7		8	
B	I110415A	2011.4.15	21:09	23:48	38° 12.10'N, 143° 47.20'E	0-150-100	100-40	40-15	15-0	0-120-100	100-40	40-15	15-0	0	RI samples
			23:48			1563.4	1962.6	1978.3	1658.5	1016.5	2384.1	1757.5	1193.3	37.1	
K2	I110420A	2011.4.20	20:57	23:18	47° 01.65'N, 160° 06.33'E	0-2496-400	400-300	300-200	200-150	150-100	100-50	50-0	0	CTD trouble	
			23:18											no sample	
	I110422A	2011.4.22	10:59	13:57	47° 05.64'N, 160° 06.80'E	0-1045-1000	1000-750	750-500	500-300	300-200	200-150	150-100	100-50	50-0	'trouble in release machinery
			13:57												
	I110422B	2011.4.22	20:59	23:56	47° 01.10'N, 160° 03.46'E	0-1045-1000	1000-750	750-500	500-300	300-200	200-150	150-100	100-50	50-0	
			23:56												
I110423A	2011.4.23	11:38	14:37	46° 56.74'N, 160° 03.84'E	0-1057-1000	1000-750	750-500	500-300	300-200	200-150	150-100	100-50	50-0		
		14:37													
I110423B	2011.4.23	21:00	0:00	47° 01.56'N, 160° 04.65'E	0-230-200	200-80	80-0	0-200	200-80	80-0	0-200	200-80	80-0	RI samples	
		0:00													
S1	I110430A	2011.4.30	21:00	0:00	29° 58.08'N, 145° 01.28'E	0-1040-1000	1000-750	750-500	500-300	300-200	200-150	150-100	100-50	50-0	
			0:00												
	I110501A	2011.5.1	11:40	14:22	30° 00.78'N, 144° 57.86'E	0-1045-1000	1000-750	750-500	500-300	300-200	200-150	150-100	100-50	50-0	
			14:22												
	I110501B	2011.5.1	21:00	23:51	29° 58.17'N, 145° 01.59'E	0-1050-1000	1000-750	750-500	500-300	300-200	200-150	150-100	100-50	50-0	
			23:51												
I110502A	2011.5.2	11:09	13:53	30° 38.16'N, 144° 41.38'E	0-1050-1000	1000-750	750-500	500-300	300-200	200-150	150-100	100-50	50-0		
		13:53													
I110502B	2011.5.2	21:12	0:03	30° 28.74'N, 144° 44.22'E	0-210-200	200-50	50-0	0-200	200-50	50-0	0-200	200-50	50-0	RI samples	
		0:03													

Table 3.4.1-2. Summary of NORPAC samplings

MRII-03
NORPAC net hauls
Rewind speed: 1.0 m / sec

Stn.	Date	Time	Position		Sampling Layer (m)	Wire out (m)	Wire angle (°)	Flow-meter readings		Filtering vol. (m ³)		Remarks
			Lat.	Long.				#1 net ID:2370	#2 net ID:3120	#1 net	#2 net	
K2	2011.4.21	21:22	47° 00.40'N	160° 03.28'E	200-0	202	8	2211	2119	28.7	27.5	Nighttime samplings for Kobari. #1 net; gut pigment (frozen). #2 net; community (formalin fix., bottle ID; 176)
	2011.4.22	9:50	46° 59.60'N	160° 03.03'E	200-0	200	0	2115	2042	27.5	26.5	Daytime samplings for Kobari. #1 net; gut pigment (frozen). #2 net; community (formalin fix., bottle ID; 177)
	2011.4.23	18:57	47° 00.13'N	160° 04.78'E	50-0	50	2	589	609	7.7	7.9	#1 net; <i>Oithona</i> sample for Chiba (frozen). #2 net: archive sample for Kitamura (formalin fix.)
	2011.4.23	18:57	47° 00.13'N	160° 04.78'E	150-0	150	0	1792	1650	23.3	21.5	#1 net; <i>Oithona</i> sample for Chiba (frozen). #2 net: archive sample for Kitamura (formalin fix.)
	2011.4.23	18:57	47° 00.13'N	160° 04.78'E	50-0	50	0	-	-	-	-	#1 and 2 nets; <i>N. cristatus</i> samplings for grazing experiments
S1	2011.4.29	21:09	29° 59.03'N	145° 00.65'E	200-0	204	11	2085	2030	27.1	26.4	Nighttime samplings for Kobari. #1 net; gut pigment (frozen). #2 net; community (formalin fix., bottle ID; 227)
	2011.5.1	8:32	30° 00.62'N	145° 00.84'E	200-0	200	3	1990	1943	25.9	25.3	Daytime samplings for Kobari. #1 net; gut pigment (frozen). #2 net; community (formalin fix., bottle ID:244)
	2011.5.1	18:58	29° 59.37'N	144° 56.98'E	50-0	50	0	541	532	7.0	6.9	#1 net; <i>Oithona</i> sample for Chiba (frozen). #2 net: archive sample for Kitamura (formalin fix.)
	2011.5.1	18:58	29° 59.37'N	144° 56.98'E	150-0	150	0	1481	1476	19.3	19.2	#1 net; <i>Oithona</i> sample for Chiba (frozen). #2 net: archive sample for Kitamura (formalin fix.)

Table 3.4.1-3. Summary of water samplings for nano- and microzooplankton abundance

MRII-03
Water samplings for analysis of nano- and microzooplankton abundance
* Local ship time

Stn.	Date*	Time*	CTD cast ID	Depth (m)	Irradiance (%)	Nanoozo for Kitamura			For Kagoshima Univ.				Remarks		
						Sample No.	Filtering vol. (ml)	Funnel No.	Micro zoo (ml)	bottle ID	Nano zoo (ml)	bottle ID		FCM (ml)	tube ID
K2	2011.4.19	18:00	K2_1 Deep cast (Routine)	200	-	K2-200	500	1	-	-	-	-	-		
				400	-	K2-400	500	2	-	-	-	-	-		
				800	-	K2-800	500	3	-	-	-	-	-		
K2	2011.4.21	8:00	K2_4 Shallow cast (PE/RI)	60	1	K2-0.5	260	1	500	24	250	24	1.5 x 3	634-636	
				40	3.8	K2-1	290	2	500	23	250	23	1.5 x 3	631-633	
				30	7	K2-2.5	295	3	500	22	250	22	1.5 x 3	628-630	
				25	12	K2-5	345	4	500	21	250	21	1.5 x 3	625-627	
				20	17	K2-10	295	1	500, <500	20*, 40	250	20	1.5 x 3	622-624	*no inner cap of sample bottle
				10	38	K2-25	325	2	500	19	250	19	1.5 x 3	619-621	
				5	50	K2-50	340	3	500	18	250	18	1.5 x 3	616-618	
				0	100	K2-100	345	4	500	17	250	17	1.5 x 3	613-615	
				S1	2011.4.28	19:30	S1_1 Deep cast (Bacteria)	200	-	S1-200	500	1	-	-	-
500	-	S1-500	500					2	-	-	-	-	-		
1000	-	S1-1000	500					3	-	-	-	-	-		
S1	2011.4.29	3:30	S1_2 Shallow cast (PP 1st)	55	1	S1-1	310	1	500	25	250	25	1.5 x 3	697-699	
				40	3	S1-2	280	2	500	26	250	26	1.5 x 3	700-702	
				30	7	S1-3	245	3	500	27	250	27	1.5 x 3	703-705	
				25	13	S1-4	260	4	500	28	250	28	1.5 x 3	706-708	
				20	17	S1-5	320	1	500	29	250	29	1.5 x 3	709-711	
				10	35	S1-6	305	2	500	30	250	30	1.5 x 3	712-714	
				5	60	S1-7	290	3	500	31	250	31	1.5 x 3	715-717	
				0	100	S1-S	325	4	500	32	250	32	1.5 x 3	718-720	

(3) Future plans and sample archives

Community structure and ecological role of mesozooplankton

Subsamples are stored at JAMSTEC or Kagoshima Univ. We will analyze as follows; (1) vertical distribution of zooplankton carbon mass, (2) vertical distribution of biomass in higher taxa level (copepods, euphausiids, etc.) and taxa composition based on the carbon weight, (3) vertical distribution, composition, biomass, and diel vertical migration for each species of dominant taxa such as copepods, euphausiids and chaetognaths, (4) estimation of carbon transport through diel or ontogenetic migration.

Environmental (T, S) and net status (net number, towing distance, etc.) data were recorded during each IONESS tow. All data is under Kitamura and Kobari.

Vertical distribution of microzooplankton

Sample analysis is consigned to Marine Biological Research Institute of Japan Co. LTD., Shinagawa, Tokyo.

3.4.2 Grazing pressure of microzooplankton

Minoru KITAMURA (JAMSTEC)

Kazuhiko MATSUMOTO (JAMSTEC)

(1) Objective

To understand material export from surface to deep ocean, not only estimations of primary productivity or vertical flux but also evaluation of grazing impacts at surface is needed. Grazing by larger organisms might bring about efficient vertical carbon transport through repackaging phytoplankton into fecal pellets or active carbon transport by diel and ontogenetic migrator. On the other hand, grazing by smaller organisms might have small or negative impact to vertical export. Identification of influential grazers and quantitative estimation of their grazing rates are essential to discuss the carbon cycle in the ocean. Recently, large grazing pressure of not only the crustacean plankton but also microzooplankton has been recognized in the several area. The grazing pressure by the micro organisms maybe important in the northwestern north Pacific in winter because large calanoid copepods migrate to midwater. Based on this background, we estimated grazing rate of them.

(2) Materials and methods

Four dilution incubation experiments were done through the cruise (Table 3.5.2-1). For each experiment 40 l of water were collected from Niskin bottle or bucket. Water was pre-screened through 200 μm mesh to exclude larger zooplankton. Dilution series were prepared with 25, 50, 75, and 100% of natural seawater. Filtered water was obtained by direct gravity flow through a compact cartridge filter (ADVANTEC, MCS-020-D10SR). Incubation of the dilute water was done in transparent polycarbonate bottle. Duplicate or triplicate bottle were prepared. Incubation lasted for 24 or 48 h in a tank with continuous flow of surface seawater under natural light conditions. All the water samplings, filtering, and incubate items were soaked in 10% HCl and rinsed Milli-Q water between each use on board. Nutrient was added in the incubation bottles. To measure initial and final chl. *a* concentration, experiment water were filtered onto GF/F filter and extracted 6 ml DMF at -20°C until measurement. Chl. *a* was measured fluorometrically (Welshmeyer method) with a Turner Design fluorometer. Phytoplankton cell numbers were also counted using flowcytometry.

Apparent phytoplankton growth rate (d^{-1}) were calculated using following equation:

$$\text{Apparent growth rate} = (1/t)\ln(P_t/P_0)$$

where t is incubation time (day), P_t and P_0 are final and initial Chl. *a* concentration or cell number, respectively. When the apparent phytoplankton growth rate is plotted as a function of dilution factor, the y-intercept and negative slope of the approximate line means true phytoplankton growth (k ; d^{-1}) and grazing coefficient of microzooplankton (g ; d^{-1}), respectively. According to Verity et al. (1993) and Zhang et al. (2006), microzooplankton grazing pressure on primary production (P_p ; %) is calculated as the following equation:

$$P_p = (e^{kt} - e^{(k-g)t}) / (e^{kt} - 1) * 100$$

Through the three incubation experiments, we tried to estimate true growth rate of phytoplankton, grazing rate of microzooplankton and grazing pressure of microzooplankton on primary production. Incubation states are summarized in Table 3.5.2-2.

Table 3.4.2-1. Dilution experiments, list of samplings.

MR11-03 Dilution incubation experiments

List of water samplings

Station	Date*	Exp. ID.	Water sampling								
			Time*	Position	Depth m	Irradiance %	Temp. °C	Chl. <i>a</i> µg/l	CTD cast No.	Sampler	
K2	2011.4.21-23	K2-1	7:40	46° 59.95'N, 160° 04.88'E	5	50	1.7	0.4	K2_4	Shallow cast (PE/RI)	Clean Niskin
S1	2011.4.28-29	S1-1	21:40	30° 02.64'N, 144° 59.66'E	0	100	19.0	0.35	S1_1	Deep cast (Bacteria)	Bucket
S1	2011.4.29-30	S1-2	3:30	30° 00.36'N, 145° 00.05'E	0	100	19.0	0.44	S1_2	Shallow cast (pp 1st)	Bucket
S1	2011.4.29-30	S1-3	8:30	30° 02.52'N, 145° 06.58'E	55	1	18.5	0.23	S1_3	Shallow cast (PE/RI)	Clean Niskin

*Local ship time

Table 3.4.2-2. Dilution experiments, summary of incubation states.

MR11-03 Dilution incubation experiments

Summary of incubation states

Station	Date*	Exp. ID.	Incubation						Remarks
			Time*		Incubation bottle	Temp. °C	Irradiance %	Nutrients addition	
start	end								
K2	2011.4.21-23	K2-1	21 Apr. 10:45	23 Apr. 9:30	1L		100	-	48h incubation, Matsumoto FCM, Kobari FCM
S1	2011.4.28-29	S1-1	28 Apr. 23:20	29 Apr. 23:20	1L		100	+	Kobari FCM
S1	2011.4.29-30	S1-2	29 Apr. 5:00	30 Apr. 5:45	1L		100	+	Matsumoto FCM, Kobari FCM
S1	2011.4.29-30	S1-3	29 Apr. 10:45	30 Apr. 11:00	1L		2.5	+	Matsumoto FCM, Kobari FCM

*Local ship time

(3) Preliminary results

All measurements of Chl. *a* and phytoplankton cell numbers were finished on board. Preliminary results of the experiments in the station K2 and S1 are shown in the Figures 3.5.2-1.

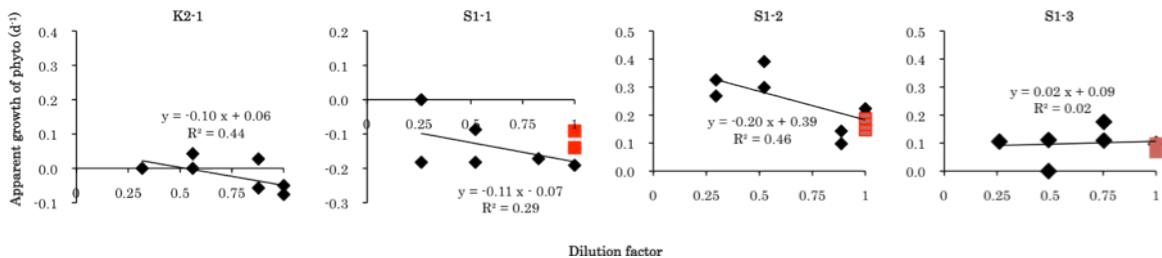


Fig.3.4.2. Correlation between apparent growth rates of phytoplankton community and dilution factors. Apparent growth rates were estimated from Chl. *a* measurements. Slops of the regression line means grazing rates (d^{-1}) of the microzooplankton community.

References

Verity, P.G., D.K. Stoecker, M.E. Sieracki & J.R. Nelson. 1996. Grazing, growth and mortality of microzooplankton during the 1989 North Atlantic spring bloom at 47°N, 18°W. *Deep-Sea Res.*, 40: 1793-1814.

Zhang, W., H. Li, T. Xiao, J. Zhang, C. Li & S. Sun. 2006. Impact of microzooplankton and copepods on the growth of phytoplankton in the Yellow Sea and East China Sea. *Hydrobiologia*, 553: 357-366.

3.4.3 Biological study for phytoplankton and zooplankton

Katsunori KIMOTO (RIGC, JAMSTEC)

Miho FUKUDA (RIGC, JAMSTEC/Tsukuba University)

3.4.3.1 Planktic foraminifers

(1) Objective

Planktic foraminifers, a kind of shell-bearing single cell plankton produce calcium carbonate test and contribute to the carbon cycle. Planktic foraminifers show wide distributions in the surface water. Recent molecular biological studies revealed the high genetic variations within many planktic foraminifera species. These intra-specific genetic variations considered be the indications of the cryptic speciation and their ecologies could be different among these cryptic species. Moreover, morphological variations which correspond to the genetic populations is confirmed on several species. The water mass structure is considered as one of the factors which affect the distribution of the genetic populations. However, the genetic variability of the planktic foraminifers is not fully understood. In this study, we collected living planktic foraminifer in order to reveal the genetic populations of the planktic foraminifera in the western North Pacific Subpolar gyre and the Subtropical gyre.

(2) Methods

Living planktic foraminifera samples were collected by vertical towing of a NORPAC (closing) net. The NORPAC net towing was conducted at station K2 and S1 during this cruise. A closing NORPAC net (63 μm opening) was used in order to obtain depth-stratified samples. Sampling depths of the NORPAC net tows are summarized in Table 1. A part of obtained NORPAC net samples were fixed by 100 % Ethyl alcohol and stored in the cold store (4°C) for faunal assemblage study. Others were processed for preparation of DNA analysis. Living planktic foraminifer individuals were picked under a stereomicroscope. Picked specimens were cleaned in filtered seawater with cleaned brushes. Specimens were air dried on the faunal slides at room temperature and then, stored at -80 °C.

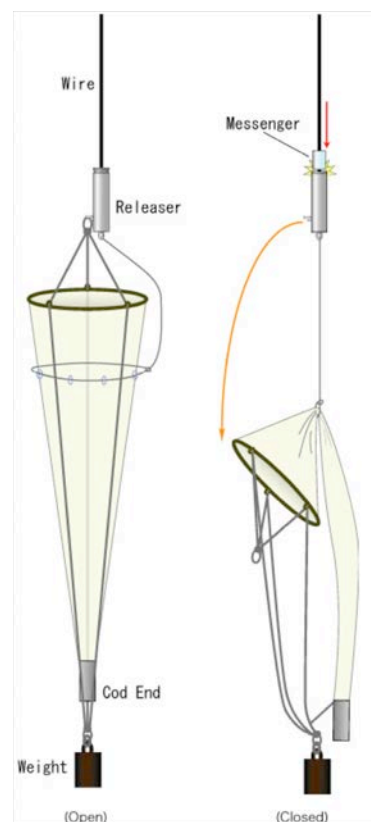


Fig.1 Schematic illustration of closing NORPAC net. Plankton net is open during towing (left), and closed at the top of the sampling depth range by deploying a messenger (right).

(3) Preliminary result

Species identifications under stereomicroscope showed that planktic foraminifer species at K2 consist of subpolar species while species at S1 consist of subtropical species. Samples collected at Stn. K2 contained just four species: *Globigerina bulloides*, *Neogloboquadrina pachyderma*, *Turborotalita quinqueloba*, *Globigerinita uvula*. We observed huge number of individuals of *G. bulloides* above 100m water depth at Stn. K2 during this cruise. Such higher production of *G. bulloides* should act carbon fixation effectively in surface water and contribute to carbon cycles of the ocean.

Planktic foraminifera species observed in the samples collected in Stn. S1 were consisted of *Globigerinoides ruber*, *Globigerinoides sacculifer*, *Globigerinoides conglobatus*, *Orbulina universa*, *Hastigerina pelagica*, *Globorotalia truncatulinoides*, *Globorotalia menardii* and *Globorotalia hirsuta*. The number of individuals collected at S1 was few compared to the samples collected at K2. It is particularly worth noting that we collected living biserial planktic foraminifer *Streptochilus globulosus* in Stn. S1. This is first report to collect living biserial planktic species in the Pacific. We will try to perform SSU rDNA analysis for this species on the onshore laboratory.

(4) Data archive

The planktic foraminifer samples are stored at JAMSTEC. Molecular phylogenetic analyses and morphological observations will be conducted.

Table 1. Plankton tow sampling locations and depths during MR11-03 cruise.

No.	Year	Month	Day	Time		towing depth m	Mesh Size	Apparatus
1	2011	Apr	20	15:00	JST	0-20	63um (NXX25)	45cm NORPAC
2	2011	Apr	20	15:10	JST	20-50	63um (NXX25)	45cm NORPAC
3	2011	Apr	20	16:16	JST	150-200	63um (NXX25)	45cm NORPAC
4	2011	Apr	20	16:40	JST	50-100	63um (NXX25)	45cm NORPAC
5	2011	Apr	21	19:01	JST	0-20	63um (NXX25)	45cm NORPAC
6	2011	Apr	21	19:09	JST	20-50	63um (NXX25)	45cm NORPAC
7	2011	Apr	21	19:29	JST	50-100	63um (NXX25)	45cm NORPAC
8	2011	Apr	21	19:37	JST	100-150	63um (NXX25)	45cm NORPAC
9	2011	Apr	21	19:52	JST	150-200	63um (NXX25)	45cm NORPAC
10	2011	Apr	21	20:07	JST	200-300	63um (NXX25)	45cm NORPAC
11	2011	Apr	22	6:04	JST	300-500	63um (NXX25)	45cm NORPAC
12	2011	Apr	22	14:50	JST	250-300	63um (NXX25)	45cm NORPAC
13	2011	Apr	22	15:12	JST	200-250	63um (NXX25)	45cm NORPAC
14	2011	Apr	22	15:35	JST	180-200	63um (NXX25)	45cm NORPAC
15	2011	Apr	22	15:50	JST	160-180	63um (NXX25)	45cm NORPAC
16	2011	Apr	22	16:10	JST	140-160	63um (NXX25)	45cm NORPAC
17	2011	Apr	22	16:21	JST	120-140	63um (NXX25)	45cm NORPAC
18	2011	Apr	22	16:35	JST	100-120	63um (NXX25)	45cm NORPAC
19	2011	Apr	22	16:45	JST	80-100	63um (NXX25)	45cm NORPAC
20	2011	Apr	29	19:00	JST	0-20	63um (NXX25)	45cm NORPAC
21	2011	Apr	29	19:05	JST	20-50	63um (NXX25)	45cm NORPAC
22	2011	Apr	29	19:15	JST	50-100	63um (NXX25)	45cm NORPAC
23	2011	Apr	29	19:22	JST	100-150	63um (NXX25)	45cm NORPAC
24	2011	Apr	29	19:35	JST	150-200	63um (NXX25)	45cm NORPAC
25	2011	Apr	29	19:50	JST	200-300	63um (NXX25)	45cm NORPAC
26	2011	Apr	29	20:08	JST	200-300	63um (NXX25)	45cm NORPAC
27	2011	Apr	30	13:01	JST	700-1000	63um (NXX25)	45cm NORPAC
28	2011	Apr	30	13:53	JST	500-700	63um (NXX25)	45cm NORPAC
29	2011	Apr	30	14:31	JST	300-500	63um (NXX25)	45cm NORPAC
30	2011	May	1	14:37	JST	0-20	63um (NXX25)	45cm NORPAC
31	2011	May	1	14:44	JST	20-50	63um (NXX25)	45cm NORPAC
32	2011	May	1	14:52	JST	50-100	63um (NXX25)	45cm NORPAC
33	2011	May	1	15:03	JST	100-150	63um (NXX25)	45cm NORPAC
34	2011	May	1	15:15	JST	150-200	63um (NXX25)	45cm NORPAC
35	2011	May	1	15:31	JST	200-300	63um (NXX25)	45cm NORPAC
36	2011	May	1	15:51	JST	0-300	63um (NXX25)	45cm NORPAC
37	2011	May	2	7:59	JST	700-1000	63um (NXX25)	45cm NORPAC
38	2011	May	2	8:48	JST	500-700	63um (NXX25)	45cm NORPAC
39	2011	May	2	9:22	JST	300-500	63um (NXX25)	45cm NORPAC
40	2011	May	2	14:28	JST	150-300	63um (NXX25)	45cm NORPAC
41	2011	May	2	14:48	JST	150-300	63um (NXX25)	45cm NORPAC
42	2011	May	2	15:10	JST	50-150	63um (NXX25)	45cm NORPAC
43	2011	May	2	15:23	JST	50-150	63um (NXX25)	45cm NORPAC
44	2011	May	2	15:36	JST	50-150	63um (NXX25)	45cm NORPAC
45	2011	May	2	15:50	JST	0-50	63um (NXX25)	45cm NORPAC
46	2011	May	2	15:56	JST	0-50	63um (NXX25)	45cm NORPAC
47	2011	May	2	16:03	JST	0-50	63um (NXX25)	45cm NORPAC

3.4.3.2 Shell-beared phytoplankton studies in the western North Pacific

(1) Objectives

Shell-beared phytoplanktons (Diatoms, Silicoflagellates, and Coccolithophorids) are one of the primary producers of the ocean, therefore it is important to know their seasonal distribution, interactions, and transgressions of assemblages among each seasons through the year. Furthermore, hard skeletons of phytoplankton remains in the deep sea sediments and it provide useful information for paleoceanographic changes of sea surface water conditions. In this study, we collected water samples from Stn. K2 and S1 to investigate vertical distributions and ecological features of each phytoplankton.

(2) Methods

Seawater samples were obtained from upper 200 m water depths at Stn. S1 and K2 by CTD/Niskin systems of 12L bottle capacity. Surface water (0 m) samples were collected by bucket. The locations that were collected seawater were listed in Table 2.

For coccolithophorid separations, maximally 10 litter seawaters were filtered using 0.45 μm membrane filter (ADVANTEC MFS, Inc., JAPAN) immediately after collection. For diatoms and silicoflagellates separations, maximally 10 litter seawaters were also filtered using 0.45 μm membrane filter. Filtered particulate samples were dried up at room temperature and stored in the desiccator.

(3) Future works

Collected samples were analyzed assemblages, diversities and spacial distributions for each taxon at onshore laboratory. These data will be compared with the sediment trap datasets that are moored at St. S1 and K2, same locations with water sampling points in this time. That should be provided the important information of seasonal and spacial variability of phytoplankton related with oceanographic changes in the western north Pacific.

Table 2. Sampling depths of seawater during MR11-03.

No.	Year	Month	Day	Time		water detph m	Apparatus	Latitude			Longitude			Station
1	2011	Apr	22	23:00	UTC	200	Niskin	47	0	N	160	0	E	K2
2	2011	Apr	22	23:00	UTC	150	Niskin	47	0	N	160	0	E	K2
3	2011	Apr	22	23:00	UTC	100	Niskin	47	0	N	160	0	E	K2
4	2011	Apr	22	23:00	UTC	75	Niskin	47	0	N	160	0	E	K2
5	2011	Apr	22	23:00	UTC	50	Niskin	47	0	N	160	0	E	K2
6	2011	Apr	22	23:00	UTC	30	Niskin	47	0	N	160	0	E	K2
7	2011	Apr	22	23:00	UTC	10	Niskin	47	0	N	160	0	E	K2
8	2011	Apr	22	23:00	UTC	0	Bucket	47	0	N	160	0	E	K2
9	2011	Apr	20	23:00	UTC	200	Niskin	47	0	N	161	1	E	K2
10	2011	Apr	20	23:00	UTC	150	Niskin	47	0	N	162	2	E	K2
11	2011	Apr	20	23:00	UTC	100	Niskin	47	0	N	163	3	E	K2
12	2011	Apr	20	23:00	UTC	75	Niskin	47	0	N	164	4	E	K2
13	2011	Apr	20	23:00	UTC	50	Niskin	47	0	N	165	5	E	K2
14	2011	Apr	20	23:00	UTC	30	Niskin	47	0	N	166	6	E	K2
15	2011	Apr	20	23:00	UTC	10	Niskin	47	0	N	167	7	E	K2
16	2011	Apr	20	23:00	UTC	0	Bucket	47	0	N	168	8	E	K2
17	2011	Apr	30	23:27	UTC	200	Niskin	30	00	N	145	00	E	S1
18	2011	Apr	30	23:27	UTC	150	Niskin	30	00	N	145	00	E	S1
19	2011	Apr	30	23:27	UTC	100	Niskin	30	00	N	145	00	E	S1
20	2011	Apr	30	23:27	UTC	75	Niskin	30	00	N	145	00	E	S1
21	2011	Apr	30	23:27	UTC	50	Niskin	30	00	N	145	00	E	S1
22	2011	Apr	30	23:27	UTC	30	Niskin	30	00	N	145	00	E	S1
23	2011	Apr	30	23:27	UTC	10	Niskin	30	00	N	145	00	E	S1
24	2011	Apr	30	23:27	UTC	0	Bucket	30	00	N	145	00	E	S1
25	2011	Apr	28	23:13	UTC	200	Niskin	30	00	N	145	00	E	S1
26	2011	Apr	28	23:13	UTC	150	Niskin	30	00	N	145	00	E	S1
27	2011	Apr	28	23:13	UTC	100	Niskin	30	00	N	145	00	E	S1
28	2011	Apr	28	23:13	UTC	75	Niskin	30	00	N	145	00	E	S1
29	2011	Apr	28	23:13	UTC	50	Niskin	30	00	N	145	00	E	S1
30	2011	Apr	28	23:13	UTC	30	Niskin	30	00	N	145	00	E	S1
31	2011	Apr	28	23:13	UTC	10	Niskin	30	00	N	145	00	E	S1
32	2011	Apr	28	23:13	UTC	0	Bucket	30	00	N	145	00	E	S1

3.5 Active carbon flux

Toru KOBARI (Kagoshima University)

(1) Objective

It has been long accepted that sinking particles are major pathway of vertical carbon flux into the ocean interior and support mesopelagic carbon demand (Fowler and Knauer, 1986; Zhang and Dam, 1997; Aristegui et al., 2002). In the past decade, a number of studies have also shown that diurnally vertical migrants significantly contribute to carbon flux by consuming POC in surface waters and respiring and excreting the metabolized POC at depth. This “actively transported carbon flux” is equivalent to 3 to 127%, of the sinking POC flux in tropical to subarctic waters (Al-Mutairi and Landry, 2001; Dam et al., 1995; Longhurst et al., 1990; Le Borgne and Rodier, 1997; Steinberg et al., 2000, 2008; Zhang and Dam, 1997). Thus, we should evaluate how mesozooplankton community transports carbon to mesopelagic depth as active carbon flux.

In the present study, we compare abundance, biomass and taxonomic composition of mesozooplankton community between day and night at K2 and S1 in Northwestern Pacific Ocean to estimate active carbon flux.

(2) Methods

Samplings were carried out during the RV Mirai cruise (MR11-02) from 9 February to 9 March 2011 at K2 and S1 in the Northwestern Pacific Ocean. Mesozooplankton were collected from 200 m to sea surface using Twin North Pacific Standard net (Motoda 1957: diameter 45 cm, mesh size 0.1 mm) at a speed of 1 m sec⁻¹. One sample was preserved in borax-buffered 5% formaldehyde for microscopic identification. Another sample was immediately anesthetized with soda water. Sample was frozen in liquid nitrogen after blotting adhering seawater on paper towels and stored at -80°C for measurement of gut pigments.

(3) Preliminary results

During the cruise, 6 samples for microscopic identification and 6 samples for gut pigments were collected (Table). In the land laboratory, major taxa and predominant copepods will be identified under a stereo dissecting microscope from fixed samples. For frozen samples, gut pigments of the predominant copepods will be measured by fluorometer.

(4) Reference

- Al-Mutairi, H., Landry, M.R. (2001). Active export of carbon and nitrogen at Station ALOHA by diel migrant zooplankton. *Deep-Sea Research II*, 48, 2083–2103.
- Aristegui, J., Duarte, C.M., Agusti, S., Doval, M., A'lvarez-Salgado, X.A., Hansell, D.A. (2002). Dissolved organic carbon support of respiration in the dark ocean. *Science*, 298, 1967.

- Dam, H.G., Roman, M.R., Youngbluth, M.J. (1995). Downward export of respiratory carbon and dissolved inorganic nitrogen by diel-migrant mesozooplankton at the JGOFS Bermuda time-series station. *Deep-Sea Research I*, 42, 1187–1197.
- Fowler, S.W. Knauer, G.A. (1986). Role of large particles in the transport of elements and organic compounds through the oceanic water column. *Progress in Oceanography*. 16, 147–194.
- Le Borgne, R., Rodier, M. (1997). Net zooplankton and the biological pump: a comparison between oligotrophic and mesotrophic equatorial Pacific. *Deep-Sea Research II*, 44, 2003–2023.
- Longhurst, A.R., Bedo, A.W., Harrison, W.G., Head, E.J.H., Sameoto, D.D. (1990). Vertical flux of respiratory carbon by oceanic diel migrant biota. *Deep-Sea Research*, 37, 685–694.
- Motoda, S., (1957). North Pacific standard net. *Information Bulletin of Planktology in Japan*, 4, 13-15.
- Steinberg, D.K., Carlson, C.A., Bates, N.R., Goldthwait, S.A., Madin, L.P., Michaels, A.F. (2000). Zooplankton vertical migration and the active transport of dissolved organic and inorganic carbon in the Sargasso Sea. *Deep-Sea Research I*, 47, 137–158.
- Steinberg, D.K., Cope, J.S., Wilson, S.E., Kobari, T. (2008). A comparison of mesopelagic mesozooplankton community structure in the subtropical and subarctic North Pacific Ocean. *Deep-Sea Research II*, 55, 1615– 1635.
- Zhang, X., Dam, H.G. (1997). Downward export of carbon by diel migrant mesozooplankton in the central equatorial Pacific. *Deep-Sea Research II*, 44, 2191–2202.

3.6 Community structures and metabolic activities of microbes

Ryo KANEKO

(AORI: Atmosphere and Ocean Research Institute, The University of Tokyo)

Mario UCHIMIYA (AORI)

Hideki FUKUDA (AORI)

Hiroshi OGAWA (AORI)

Toshi NAGATA (AORI)

Kazuhiro KOGURE (AORI)

Koji HAMASAKI (AORI)

(1) Objective

A significant fraction of dissolved and particulate organic matter produced in the euphotic layer of oceanic environments is delivered to meso- and bathypelagic layers, where substantial transformation and decomposition of organic matter proceeds due to the actions of diverse microbes thriving in these layers. Statio-temporal variations in organic matter transformation and decomposition in the ocean's interior largely affect patterns in carbon cycling in the global ocean. Thus elucidating diversity, activities and distribution patterns of microbes in deep oceanic waters is fundamentally important in order to better understand major controls of oceanic material cycling in the ocean.

The objective of this study is to determine seasonal variability of microbial diversity and activities during the time-series observation of vertical fluxes at the two distinctive oceanic stations located in the subarctic and subtropical western North Pacific. We investigated i) full-depth profiles of prokaryotic abundance and related biogeochemical parameters including dissolved organic carbon and nitrogen concentrations (potential resources of prokaryotes), and the abundances of viruses (potential predators of prokaryotes), ii) community structures of Bacteria and Archaea and their metabolic activities, iii) sinking velocity and physic-chemical properties of suspended particles in the mixing layer.

(2) Method

Seawater samples were collected from predetermined depths of two CTD casts, i.e. the Atmosphere and Ocean Research Institute (AORI) cast and the Routine cast, conducted at Stations K2 and S1 (see the meta-data sheet for details). Sinking particles were collected by drifting traps to determine fluxes of sinking POC/PON and their weight (see the meta-data sheet for details).

i) Full-depth profiles of prokaryotic activity and abundance and related biogeochemical parameters

- a) Prokaryotic abundance: Flow cytometry
- b) Prokaryotic production: ³H-leucine incorporation
- c) Virus abundance: Flow cytometry
- d) DOC/DON: Concentrations of dissolved organic carbon and total dissolved nitrogen were determined by the high temperature catalytic oxidation (HTCO) method. The concentration of dissolved organic nitrogen was calculated by subtracting the concentration of dissolved inorganic nitrogen (determined by Auto-analyzer) from that of total dissolved nitrogen.

ii) Relationship between community structures of Bacteria and Archaea and their

metabolic activities

- a) Bacterial community structures: PCR-DGGE method after extracting DNA from particles collected on 0.22 μm -pore-size filters (Sterivex).
- b) Activities of bacteria: Bromodeoxyuridine-incorporating methods

iii) Sinking velocity and physico-chemical properties of suspended particles

- a) Concentrations of particulate organic carbon and nitrogen: Determined using an elemental analyzer for samples collected on GF/F filters.
- b) Weight of suspended solid: Determined by weighing samples collected on pre-weighted GF/F filter.
- c) Particle size distribution of suspended particles in upper layer (0-200 m): Determined by an *in situ* particle sizing instrument, LISST-100 (Sequoia Scientific Inc., USA).

(3) All results will be submitted to Data Management Office, JAMSTEC after analysis and validation and be opened to public via the web site.

3.7 Dissolved Organic Carbon

Masahide WAKITA (Mutsu Institute for Oceanography, JAMSTEC)

(1) Purpose of the study

Fluctuations in the concentration of dissolved organic carbon (DOC) in seawater have a potentially great impact on the carbon cycle in the marine system, because DOC is a major global carbon reservoir. A change by < 10% in the size of the oceanic DOC pool, estimated to be ~ 700 GtC, would be comparable to the annual primary productivity in the whole ocean. In fact, it was generally concluded that the bulk DOC in oceanic water, especially in the deep ocean, is quite inert based upon ¹⁴C-age measurements. Nevertheless, it is widely observed that in the ocean DOC accumulates in surface waters at levels above the more constant concentration in deep water, suggesting the presence of DOC associated with biological production in the surface ocean. This study presents the distribution of DOC during early spring in the northwestern North Pacific Ocean.

(2) Sampling

Seawater samples were collected at stations K2 (Cast 1 and 7) and S1 (Cast 4 and 6) and brought the total to ~160. Seawater from each Niskin bottle was transferred into 60 ml High Density Polyethylene bottle (HDPE) rinsed with same water three times. Water taken from the surface to 250 m is filtered using precombusted (450°C) GF/F inline filters as they are being collected from the Niskin bottle. At depths > 250 m, the samples are collected without filtration. After collection, samples are frozen upright and preserved at ~ -20 °C cold until analysis in our land laboratory. Before use, all glassware was muffled at 550 °C for 5 hrs.

(3) Analysis

Prior to analysis, samples are returned to room temperature and acidified to pH < 2 with concentrated hydrochloric acid. DOC analysis was basically made with a high-temperature catalytic oxidation (HTCO) system improved a commercial unit, the Shimadzu TOC-V (Shimadzu Co.). In this system, the non-dispersive infrared was used for carbon dioxide produced from DOC during the HTCO process (temperature: 680 °C, catalyst: 0.5% Pt-Al₂O₃).

(4) Preliminary result

The distributions of DOC will be determined as soon as possible after this cruise.

(5) Data Archive

All data will be submitted to JAMSTEC Data Management Office (DMO) within 2 years.

3.8 Chlorofluorocarbons

Masahide WAKITA (JAMSTEC MIO)

Ken'ichi SASAKI (JAMSTEC MIO)

(1) Objective

Chlorofluorocarbons (CFCs) are chemically and biologically stable gases that have been synthesized at 1930's and 1960's, respectively. The atmospheric CFCs can slightly dissolve in sea surface water by air-sea gas exchange and then are spread into the ocean interior. The chemical species of CFCs (CFC-11 (CCl_3F), CFC-12 (CCl_2F_2) and CFC-113 ($\text{C}_2\text{Cl}_3\text{F}_3$)) can be used as transient chemical tracers for the ocean circulation on timescale of several decades. We measured concentrations of CFCs in seawater.

(2) Apparatus

Dissolved CFCs are measured by an electron capture detector (ECD) – gas chromatograph attached with a purging & trapping system.

Table 3-14-1 Instruments

Gas Chromatograph:	GC-14B (Shimadzu Ltd.)
Detector:	ECD-14 (Shimadzu Ltd)
Analytical Column:	
Pre-column:	Silica Plot capillary column [i.d.: 0.53mm, length: 8 m, film thickness: 0.25 μm]
Main column:	Connected two capillary columns (Pola Bond-Q [i.d.: 0.53mm, length: 9 m, film thickness: 6.0 μm] followed by Silica Plot [i. d.: 0.53mm, length: 14 m, film thickness: 0.25 μm])
Purging & trapping:	Developed in JAMSTEC. Cold trap columns are 1/16" SUS tubing packed with Porapak T.

(3) Procedures

3-1 Sampling

Seawater sub-samples for CFC measurements were collected from 12 liter Niskin bottles to 300 ml glass bottles at stations K2 (Cast 1) and S1 (Cast 4) and brought the total to ~80. The bottles were filled by nitrogen gas before sampling. Three times of the bottle volumes of seawater sample were overflowed. The bottles filled by seawater sample were kept in water bathes controlled at 5°C until analysis in our land-based laboratory. The CFCs concentrations

were determined as soon as possible after this cruise.

In order to confirm CFC concentrations of standard gases and their stabilities, CFC mixing ratios in air were also analyzed. Air samples were collected into a 200ml glass cylinder at outside of our laboratory.

3-2 Analysis

The analytical system is modified from the original design of Bullister and Weiss (1988). Constant volume of sample water (50ml) is taken into a sample loop. The sample is sent into stripping chamber and dissolved CFCs are de-gassed by N₂ gas purging for 8 minutes. The gas sample is dried by magnesium perchlorate desiccant and concentrated on a trap column cooled down to -50 °C. Stripping efficiencies of CFCs are confirmed by re-stripping of surface layer samples and more than 99.5 % of dissolved CFCs are extracted on the first purge. Following purging & trapping, the trap column is isolated and electrically heated to 140 °C. CFCs are desorbing by electrically heating the trap column, and lead into the pre-column. CFCs are roughly separated from other compounds in the pre-column and are sent to main analytical column. And then the pre-column is switched to another line and flushed by counter flow of pure nitrogen gas. CFCs sent into main column are separated further and detected by an electron capture detector (ECD). Nitrogen gases used in this system was filtered by gas purifier tube packed Molecular Sieve 13X (MS-13X).

Table 3-14-2 Analytical conditions of dissolved CFCs in seawater.

Temperature	
Analytical Column:	95 °C
Detector (ECD):	240°C
Trap column:	-50 °C (at adsorbing) & 140 °C (at desorbing)
Mass flow rate of nitrogen gas (99.99995%)	
Carrier gas:	15 ml/min
Detector make-up gas:	22 ml/min
Back flush gas:	20 ml/min
Sample purge gas:	130 ml/min

Standard gas (Japan Fine Products co. ltd.)

Base gas:	Nitrogen
CFC-11:	300 ppt (v/v)
CFC-12:	160 ppt (v/v)
CFC-113:	30 ppt (v/v)

(4) Preliminary result

The distributions of CFCs will be determined as soon as possible after this cruise. The standard gases used in this analysis will be calibrated with respect to SIO scale standard gases and then the data will be corrected.

(5) Data archive

All data will be submitted to JAMSTEC Data Management office (DMO) and under its control.

(6) Reference

Bullister, J.L and Weiss R.F. 1988. Determination of CCl_3F and CCl_2F_2 in seawater and air. Deep Sea Research, 35, 839-853.

3.9 Argo Float

Toshio SUGA (JAMSTEC/RIGC, not on board): Principal Investigator

Shigeki HOSODA (JAMSTEC/RIGC, not on board)

Kanako SATO (JAMSTEC/RIGC, not on board)

Mizue HIRANO (JAMSTEC/RIGC, not on board)

Tamani UENO (MWJ): Operation Leader

Fujio KOBAYASHI (MWJ)

(1) Objective

The objective of deployment is to clarify the structure and temporal/spatial variability of water masses in the North Pacific such as North Pacific Subtropical Mode Water and North Pacific Intermediate Water and their formation mechanism. To achieve the objective, profiling floats are launched to measure vertical profiles of temperature and salinity automatically every five days. As the vertical resolution of the profiles is very fine, the structure and variability of the water mass can be displayed well. Therefore, the profile data from the floats will enable us to understand the variability and the formation mechanism of the water mass.

We will implement the western North Pacific Integrated Physical-Biogeochemical Ocean Observation Experiment (INBOX) in July 2011. In this experiment, we will deploy 25 floats equipped with the dissolved oxygen sensor within the 150km-square region centered at S1. We deploy a few floats equipped with the dissolved oxygen sensor near S1 in this cruise in order to check the operation and data of floats and to capture the condition by analyzing preliminarily.

(2) Methods (Description of instruments deployed)

First, we launched five Provor floats manufactured by Nke. The float equips one SBE41cp CTD sensor manufactured by Sea-Bird Electronics Inc to measure temperature, salinity and pressure from surface to 2000 dbar. The float usually drifts at a depth of 1000 dbar (called the parking depth), then it dives to a depth of 2000 dbar. During the ascent to the sea surface with increasing its volume in order to change its buoyancy, the float measures sea water temperature, salinity, and pressure. To send the measured data to the Argo data center via the ARGOS transmitting system in real time, the float stays at the sea surface for enough time, approximately 11 hours. Finally the float returns to the parking depth with decreasing volume. The cycle of the float moving repeats each 5days for 3 or 4 years. The status of the float and the launch is shown in Table 3.13-1.

Second, we launched two NEMO floats manufactured by Optimare. The float equips one SBE41 CTD sensor manufactured by Sea-Bird Electronics Inc to measure temperature, salinity, pressure and measure dissolved oxygen from Aanderaa Data Instruments from surface to 2000 dbar. The float usually drifts at a depth of 1500 dbar (called the parking depth), then it dives to a depth of 2000 dbar. During the ascent to the sea surface with increasing its volume in order to change its buoyancy, the float measures sea water temperature, salinity, pressure and dissolved oxygen. To send the measured data to the Argo data center via the Iridium transmitting system in real time, the float stays at the sea surface for enough time, approximately 1 hour (the time out period). Finally the float returns to the parking depth with decreasing volume. The cycle of the float moving repeats each 2days for 3 or 4 years. The status of the float and the launch is shown in Table 3.13-2.

Table 3.10-1 Specification of launched float (Provor)

Float Type	Provor float manufactured by Nke.
CTD sensor	SBE41cp manufactured by Sea-Bird Electronics Inc.
Cycle	5days (approximately 11 hours at the sea surface)
ARGOS transmit interval	30 sec
Target Parking Pressure	1000 dbar
Sampling layers	115
	(2000,1950,1900,1850,1800,1750,1700,1650,1600,1550,1500,1450,1400,1350,1300,1250,1200,1150,1100,1050,1000,980,960,940,920,900,880,860,840,820,800,780,760,740,720,700,680,660,640,620,600,580,560,540,520,500,490,480,470,460,450,440,430,420,410,400,390,380,370,360,350,340,330,320,310,300,290,280,270,260,250,240,230,220,210,200,195,190,185,180,175,170,165,160,155,150,145,140,135,130,125,120,115,110,105,100,95,90,85,80,75,70,65,60,55,50,45,40,35,30,25,20,15,10,4 or surf, dbar)

Table 3.10-2 Specification of launched float (NEMO)

Float Type	Provor float manufactured by Optimare.
CTD sensor	SBE41 manufactured by Sea-Bird Electronics Inc.
Dissolved oxygen	Optode 3830 manufactured by Aanderaa Data Instruments
Cycle	2days
Iridium transmit timeout	90 minutes (The timeout period at the sea surface)
Target Parking Pressure	1500 dbar
Sampling layers	115
	(2000,1950,1900,1850,1800,1750,1700,1650,1600,1550,1500,1450,1400,1350,1300,1250,1200,1150,1100,1050,1000,980,960,940,920,900,880,860,840,820,800,780,760,740,720,700,680,660,640,620,600,580,560,540,520,500,490,480,470,460,450,440,430,420,410,400,390,380,370,360,350,340,330,320,310,300,290,280,270,260,250,240,230,220,210,200,195,190,185,180,175,170,165,160,155,150,145,140,135,130,125,120,115,110,105,100,95,90,85,80,75,70,65,60,55,50,45,40,35,30,25,20,15,10,6 dbar)

(3) Preliminary result

The Float S/N, ARGOS ID or IMEI Number, launched date/ time, launched position observation cycle of the float is summarized in Table. 3.10-3. The data will be measured automatically each observation cycle and can be obtained via internet promptly and freely.

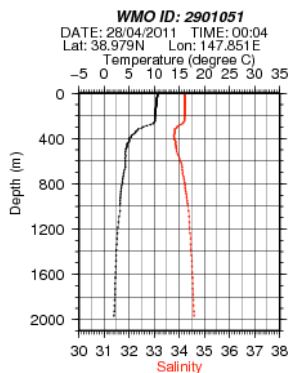
Table 3.10-3 Launching area and date/time

Float S/N	ARGOS /IMEI ID	Date and Time of Reset (UTC)	Date and Time of Launch(UTC)	Location of Launch	Observation Cycle	Remarks
10022	97933	2011/4/25	2011/4/25	39-00.03 [N]	5days	Provor

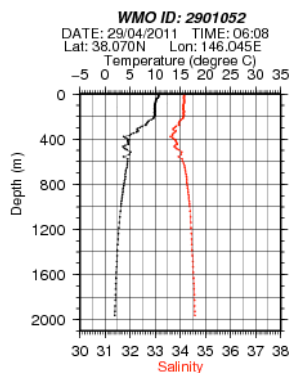
		17:37	18:49	147-54.14[E]		
09025	97920	2011/4/26 04:11	2011/4/26 05:27	38-02.78 [N] 146-22.29[E]	5days	Provovr
09014	97909	2011/4/26 10:38	2011/4/26 11:27	37-00.31 [N] 146-04.11[E]	5days	Provovr
10003	33353	2011/4/26 16:44	2011/4/26 17:44	36-00.04 [N] 145-45.02[E]	5days	Provovr
10008	34290	2011/4/26 22:43	2011/4/26 23:29	34-59.78 [N] 145-24.67[E]	5days	Provovr
159	3000 340 135 40640	2011/5/3 00:45	2011/05/03 02:06	30-13.84 [N] 144-44.68[E]	2days	NEMO
160	3000 340 135 40650	2011/5/3 00:55	2011/05/03 02:07	30-13.38[N] 144-44.66[E]	2days	NEMO

(4) Data archive

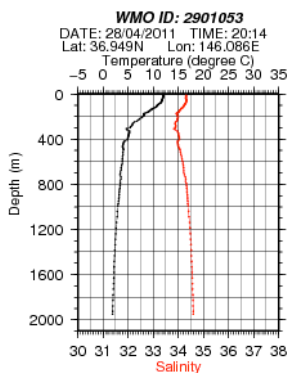
The real-time data are provided to meteorological organizations, research institutes, and universities via Global Data Assembly Center (GDAC: <http://www.usgodae.org/argo/argo.html>, <http://www.coriolis.eu.org/>) and Global Telecommunication System (GTS), and utilized for analysis and forecasts of the ocean conditions and the climates.



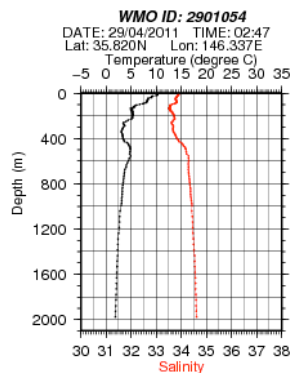
S/N10022



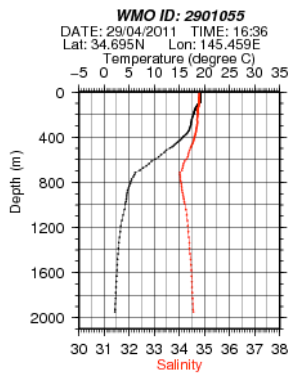
S/N09025



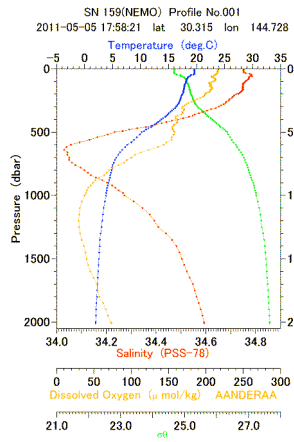
S/N09014



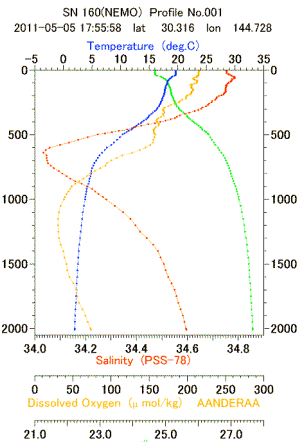
S/N10003



S/N10008



S/N 159



S/N 160

Figure 3.10-1 The first profiles of each float launched during MR11-03.

3.10 Optical measurement of marine snow: Visual Plankton Recorder (VPR)

Makio HONDA (JAMSTEC RIGC)

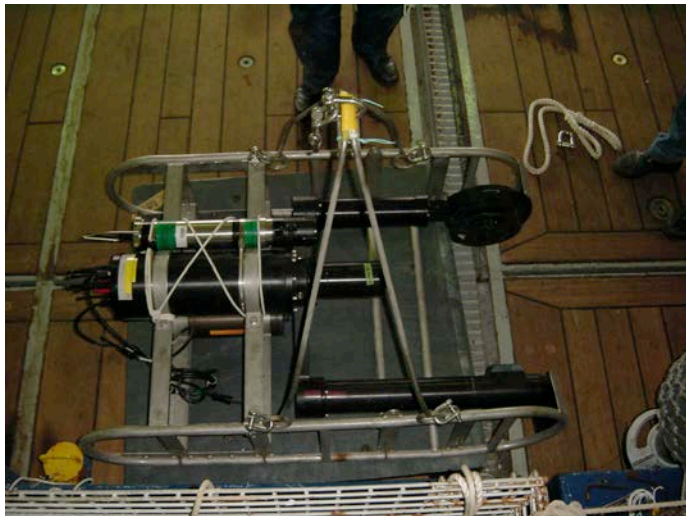
(1) Objective

Aggregated sinking particles, namely “marine snow”, play an important role in transporting atmospheric CO₂ to the ocean interior. The study of marine snow has been traditionally conducted by collecting these with “sediment trap” and by chemical and biological analysis in laboratory. On the other hand, in situ qualitative observations of marine snow such as measurement of turbidity and light attenuation have also been conducted. Bishop et al. (2009) tried to estimate abundance and flux of particulate organic carbon (POC) by using the “carbon explorer”, that is “ARGO float” type optical method. Recently application of visual plankton recorder (VPR) to marine snow observation (Lindsay et al., 2008) has been examined. In addition, in situ laser raman spectrometry (LR) has been also examined (Brewer et al., 2004) in order to know chemical composition of seawater and sea-floor sediment (see appendix). In order to conduct the research and development of optical measurement of marine snow, I have started to evaluate VPR and LR.

(2) Method

In this cruise, Visual Plankton Recorder (VPR) (picture 1) was deployed once at stations S1 and K2.

VPR takes approximately 12 dark-field images per second. Field of view is approximately 5 cm x 5 cm. In order to take pictures under same light condition, VPR was deployed at night. Deployment record is shown in Table 1. During this cruise, VPR descended to 500 m with downward velocity of 0.5 m/sec. Depth of VPR and vertical profiles in water temperature and salinity was monitored with CTD with sampling time of 0.5 seconds.



Station	K2	S1
Date (LST*)	21 April 2011	29 April 2011
Battery connect	20:26	20:18
CTD connect	20:28	20:20
Switch ON	20:36	20:25
Water In	20:46	21:31
Start Descend (0.5m/sec ↓)	20:47	20:32
Bottom (500m)	21:08	20:51
Start Ascend (1.0m/sec ↑)	21:08	20:52
Water out	21:15	21:01
On deck	21:16	21:02
Switch OFF	21:17	21:05

(K2) LST= JST + 2 hr = UTC + 11 hr

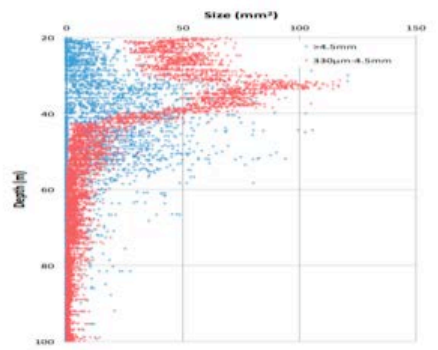
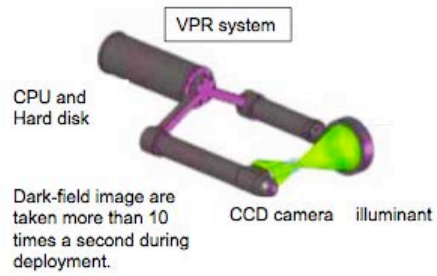
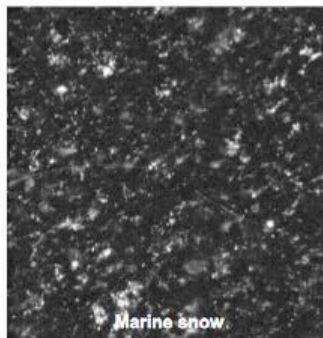
(S1) LST= JST + 1 hr = UTC + 10 hr

(3) Data analysis

Data stored in hard disk will be analyzed with image-analysis software (Image pro) on land.

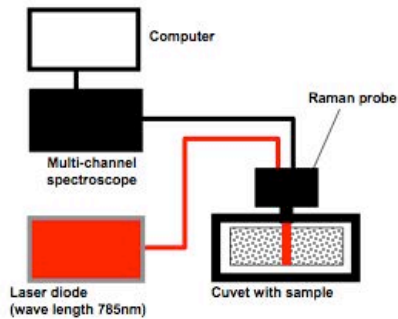
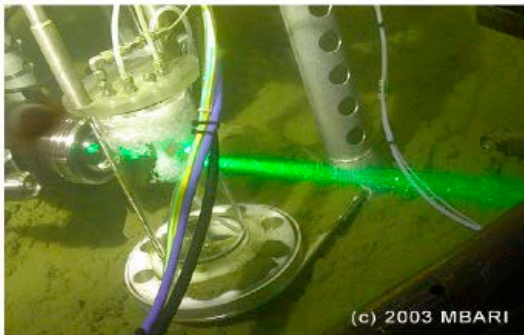
Visual Plankton Recorder

Image analysis of marine snow

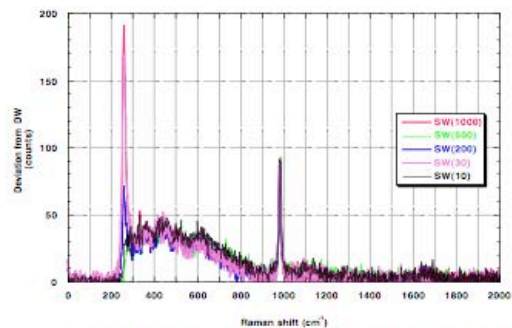


Vertical distribution of particulate materials

Laser Raman Spectrometry



Conceptual diagram of PLRS



Raman shift of seawater collected from 10 m to 1000m

3.11 Absolute salinity measurements of seawater

Hiroshi UCHIDA (JAMSTEC RIGC) (Principal Investigator)

Takeshi KAWANO (JAMSTEC RIGC) (not on board)

Akihiko MURATA (JAMSTEC RIGC) (not on board)

Michio AOYAMA (JMA MRI) (not on board)

(1) Objective

The objective of this study is to collect absolute salinity (also called “density salinity”) data, and to evaluate an algorithm to estimate absolute salinity provided along with TEOS-10 (the International Thermodynamic Equation of Seawater 2010).

(2) Materials and methods

Seawater densities were measured during the cruise with an oscillation-type density meter (DMA 5000M, serial no. 80570578, Anton-Paar GmbH, Graz, Austria) with a sample changer (Xsample 122, serial no. 80548492, Anton-Paar GmbH). The sample changer was used to load samples automatically from up to ninety-six 12-mL glass vials. AC power was supplied to the density meter through a frequency conversion AC power supply unit (AA500F, Takasago, Ltd., Japan).

The water samples were collected in 50-mL I-BOY polyethylene bottles and densities of the samples were measured at 20 °C by the density meter three to five times for each bottle.

Time drift of the density meter was monitored by periodically measuring the density of ultra-pure water (Milli-Q water, Millipore, Billerica, Massachusetts, USA) prepared from Yokosuka (Japan) tap water in July 2010. The true density at 20 °C of the Milli-Q water was estimated to be 998.2038 kg m⁻³ from the isotopic composition and International Association for the Properties of Water and Steam (IAPWS)-95 standard. The true density of International Association of the Physical Sciences of the Ocean (IAPSO) Standard Seawater (SSW) batch P152 was estimated from the Reference-Composition Salinity calculated from the labeled Practical Salinity with the slight correction (+0.0011 g kg⁻¹) of Pawlowicz et al. (2010) for absolute salinity and TEOS-10 (IOC et al., 2010). An offset correction was applied to the measured density by using the Milli-Q water measurements ($\rho_{\text{Milli-Q}}$) with a slight modification of the density dependency (Uchida et al., 2011). The offset (ρ_{offset}) of the measured density (ρ) was estimated from the following equation:

$$\rho_{\text{offset}} = (\rho_{\text{Milli-Q}} - 998.2038) - (\rho - 998.2038) \times 0.000241 \text{ [kg m}^{-3}\text{]}.$$

The offset correction was verified by measuring Reference Material for Nutrients in Seawater (RMNS) lot BF (Kanso Technos Co., Ltd., Osaka, Japan) along with the Milli-Q water. Mean density of eight bottles of the RMNS was 1024.4826 ± 0.0014 kg m⁻³.

Density salinity can be back calculated from measured density and TEOS-10.

(3) Preliminary result

Density salinities of the water samples were plotted against pressure (Fig. 3.11.1). Data obtained in the Bering Sea at the cruise MR10-06 were also shown. Salinity anomalies from the Reference-Composition Salinity were from 0.01 to 0.02 for the deep ocean (> 1000 m). The largest anomalies were seen not in the Bering Sea but at station KNOT (44°N, 155°E), contrary to some algorithms (IOC et al., 2010; Pawlowicz et al., 2010) to estimate absolute salinity.

(4) Data archive

The bottle-sampled data file (SEA file) includes the quality-controlled density salinity data (DNSSAL). The SEA file will be submitted to JAMSTEC Data Integration and Analyses Group (DIAG).

(5) References

IOC, SCOR and IAPSO (2010): The international thermodynamic equation of seawater – 2010: Calculation and use of thermodynamic properties. Intergovernmental Oceanographic Commission, Manuals and Guides No. 56, United Nations Educational, Scientific and Cultural Organization (English), 196 pp.

Pawlowicz, R., D. G. Wright and F. J. Millero (2010): The effects of biogeochemical processes on oceanic conductivity/salinity/density relationships and the characterization of real seawater. *Ocean Sci. Discuss.*, 7, 773–836.

Uchida, H., T. Kawano, M. Aoyama and A. Murata (2011): Absolute salinity measurements of standard seawaters for conductivity and nutrients. submitted to *La mer*.

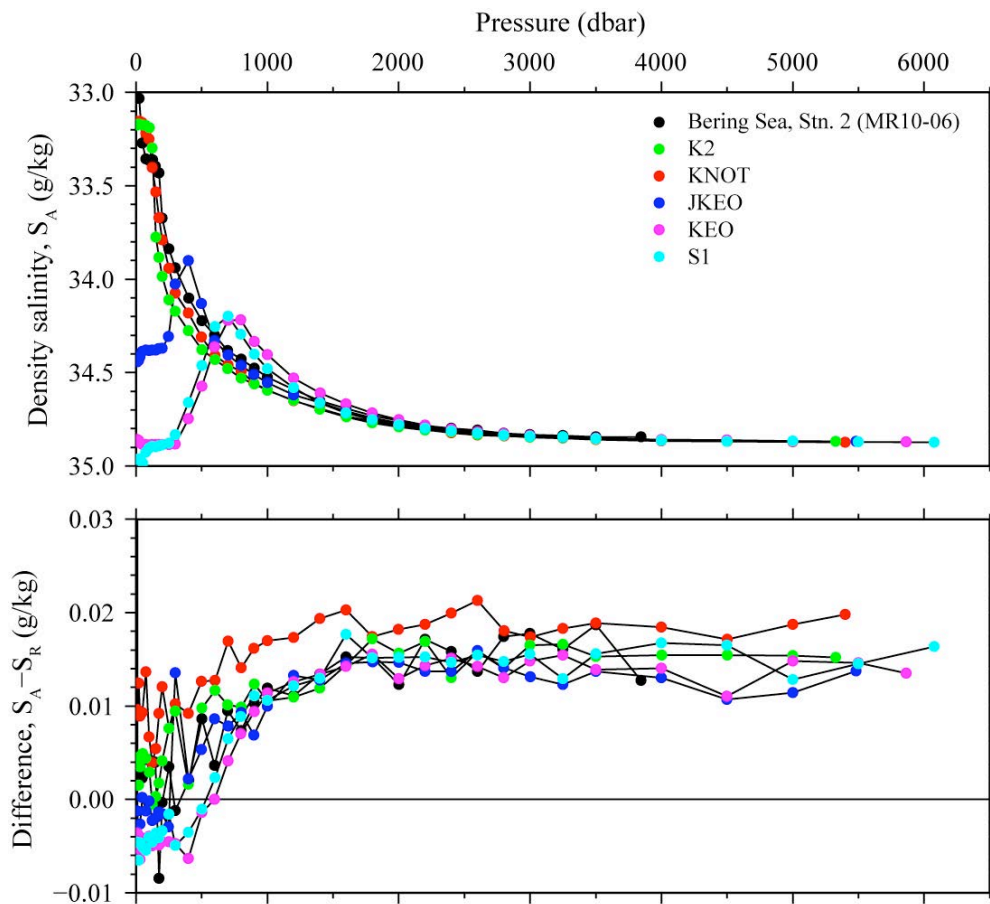


Fig. 3.11.1. Profiles of measured density salinity (S_A) and difference between the density salinity and Reference-Composition Salinity (S_R) obtained from the CTD data.

3.12 Validation of GOSAT products over sea using a ship-borne high-resolution Fourier transform spectrometer

Hirofumi OHYAMA (JAXA EORC)

Shuji KAWAKAMI (JAXA EORC)

(1) Objective

Greenhouse gases Observing SATellite (GOSAT) was launched on 23 January 2009 in order to monitor the global distributions of greenhouse gases, carbon dioxide (CO₂) and methane (CH₄). A network of ground-based high-resolution Fourier transform spectrometers (FTSs) provides essential validation data for GOSAT and vertical CO₂ profiles near airports are obtained during ascents and descents of commercial airliners instrumented with the in-situ CO₂ measuring instrument. The most validation data are obtained over land and validation data over sea is insufficient to validate GOSAT product over sea. The objective of this measurement is to validate CO₂ column averaged volume mixing ratios of GOSAT products over sea using a ship-borne high-resolution FTS.

(2) Description of instruments deployed

The high-resolution FTS records direct solar spectra in the near-infrared spectral region and CO₂ column averaged volume mixing ratios are retrieved from the spectra. The FTS is installed in a thermostated container at the aft right side on the upper deck with a Solar tracker on the roof(Figure 1). The essential observation is made for an hour including 12:50 (local time) which corresponds to the daytime overpass of the GOSAT satellite. The observation keep continuing during daytime while the strength of the solar spectra is enough for the measurements. Collocated radiosonde observations are made to obtain vertical profiles of temperature and water(Figure 2).

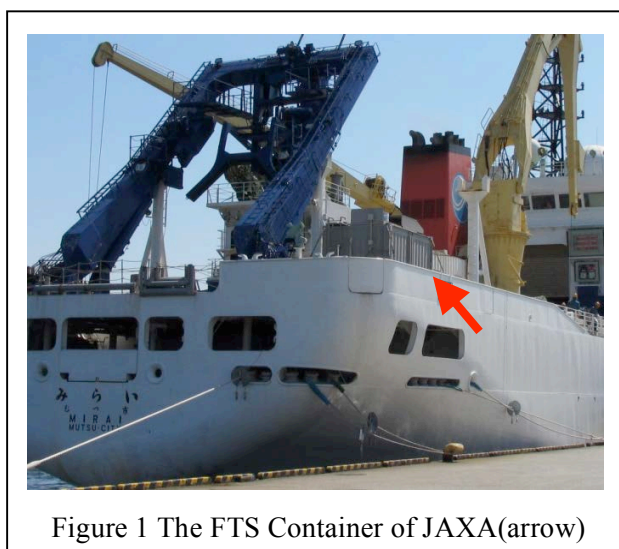
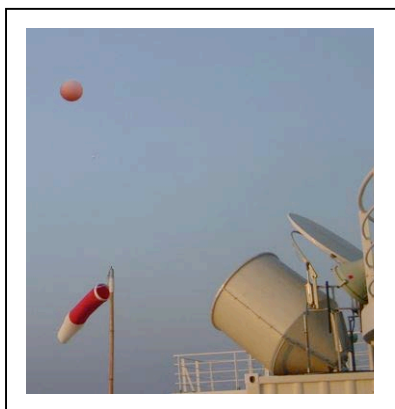


Figure 1 The FTS Container of JAXA(arrow)



(3) Preliminary result

The FTS observations were made on April 13, 14, 15, 17, and May 5 including while the ship is in port. The opportunity of observations were limited mainly by the weather condition and the status of the instruments during the cruise. Radiosonde data were obtained on April 16, 18, 20-23, 28, 30, May 1-3(Table 1).

(4) Data archive

Preliminary analysis results of the CO₂ column

averaged volume mixing ratios data were filed. These final data files will be submitted to JAMSTEC Data Integration and Analyses Group (DIAG).

Table 1 Schedule of CO₂ column averaged volume mixing ratios by gFTS

Date		GOSAT Path	FTS and Radiosode measurement	Ship Schedule
April 12	Tue.	4,25	Transport to Yokohama port/get onboard on 11:00	
April 13	Wed.	5,26	Meas. : 11:00-15:00 (393.5)* Clear 15:00-19:00 Gas-cell meas.	Yamashita berth, Yokohama port
April 14	Thur.	3,24	Meas. : 9:30-16:00 (395)	Departure at 10:00
April 15	Fri.	4,25	Meas. : 10:00-16:00 (395) partial cloud	Fukushima off shore
April 16	Sat.	5,26	No. Meas. Cloudy. Radiosonde(D)	Fukushima off shore
April 17	Sun.	3,24	Meas. : 7:49-15:00(394) Clear/partial cloud	
April 18	Mon.	4,25	No. Meas.(Trouble of Solar tr tracker) Radiosonde(D)	KNOT
April 19	Tue.	5,26	No. Meas. Rain/ Overcast	
April 20	Wed.	3,24	No. Meas. Rain/ Overcast Radiosonde(D/N)	K2
April 21	Thur.	4,25	No. Meas. Rain/ Overcast Radiosonde(D/N)	
April 22	Fri.	5,26	No. Meas. Overcast Radiosonde(D/N)	
April 23	Sat.	3,24	No. Meas. Overcast .12:00-18:00 Gas-cell meas. Radiosonde(D/N)	
April 24	Sun.	4,25	No. Meas. Overcast.	
April 25	Mon.	5,26	No. Meas. Clear.	
April 26	Tue.	3,24	No. Meas.Clear. Radiosonde(Kuroshio Special)	JKEO
April 27	Wed.	4,25	No. Meas.Clear/partail Cloud. Radiosonde(Kuroshio Special)	
April 28	Thur.	5,26	No. Meas. partail Cloud. Radiosonde(N)	KEO
April 29	Fri.	3,24	No. Meas. Rain.	S1
April 30	Sat.	4,25	No. Meas.Clear/ partail Cloud. Radiosonde(D/N)	
May 1	Sun.	5,26	No. Meas. Overcast. 13:00- 17:00 Gas-cell meas. Radiosonde(D/N))	
May 2	Mon.	3,24	No. Meas. Overcast/Rain. Radiosonde(D/N))	
May 3	Tue.	4,25	No. Meas. Overcast/Rain.	

			Radiosonde(D)	
May 4	Wed.	5,26	No. Meas.	
May 5	Thur.	3,24	Gas-cell meas.	Yokohama port at 9:00
May 6	Fri.	4,25	Transport to Tsukuba	

* A quicklook value of XCO₂ (ppm) at about local noon.

3.13 Observational research on air-sea interaction in the Kuroshio-Oyashio Extension region

Yoshimi KAWAI (JAMSTEC, PI/not on board)

Hiroyuki TOMITA (JAMSTEC)

Souichirou SUEYOSHI (GODI)

Norio NAGAHAMA (GODI)

Wataru TOKUNAGA (GODI)

(1) Background

Air-sea interaction processes in the mid-latitude region are one of the key factors to understand global climate system because the upward air-sea heat flux is considerably large and it might have significant role on the ocean and atmosphere. In particular, ocean and atmosphere near the oceanic front in the Kuroshio-Oyashio extension region are quite variable modulated by the front. In order to capture a cross frontal variation of the ocean, the atmosphere and the air-sea flux, we have conducted simultaneous XCTD, GPS radiosonde and surface meteorological observations between JKEO and KEO sites in the cruise. We provide brief description of the observations and preliminary results here.

(2) Parameters

According to the manufacturer, the range and accuracy of parameters measured by the XCTD (eXpendable Conductivity, Temperature & Depth profiler) are as follows;

Parameter	Range	Accuracy
Conductivity	0~60 mS	+/- 0.03 mS/cm
Temperature	-2~35 °C	+/- 0.02 °C
Depth	0~1000 m	5 m or 2 % at depth, whichever is greater

According to the manufacturer, the range and accuracy of parameters measured by the GPS radiosonde sensor (Vaisala RS92-SGPD) are as follows;

Parameter	Range	Accuracy
Pressure	3~1080 hPa	+/- 1 hPa (1080-100 hPa), +/- 0.6 hPa (100-3 hPa)
Temperature	-90~60 °C	+/- 0.5 °C
Humidity	0~100 %	5 %

(3) Methods

We observed the vertical profiles of the sea water temperature and salinity by using the XCTD-1 manufactured by Tsurumi-Seiki Co. The signal was converted by MK 130, Tsurumi-Seiki Co. and was recorded by MK-130 software (version 3.07) made by Tsurumi-Seiki Co. We dropped 23 probes between the JKEO and KEO sites across the Kuroshio Extension by using automatic launcher and hand launcher (Table 3.13.1).

Atmospheric sounding by GPS radiosonde was carried out between the JKEO and KEO sites in the northwestern Pacific Ocean. In total, 23 soundings were carried out (Table 3.13-2). The main system consists of processor (Vaisala, DigiCORA III), GPS antenna

(GA20), UHF antenna (RB21), ground check kit (GC25), balloon launcher (ASAP), and GPS radiosonde sensor (RS92-SGPD).

(4) Preliminary results

We show cross front sections of atmospheric potential temperature, specific humidity, air-sea turbulent heat flux and ocean temperature (Figure 3.13.1). The significant oceanic front was observed at about 36.25°N at surface. The maximum sea surface temperature (about 20°C) was found the south of the front. The air-sea heat flux shows significant variation corresponding the oceanic front. The minimum is about -100 W/m^2 and it shows a warming of ocean surface north of the front. On the other hand, the maximum is cooling about 300 W/m^2 south of the front. This is resulted form large variations in air-sea temperature difference and surface wind speed caused by the presence of the front. The atmosphere looks to be influenced by the oceanic front and air-sea flux. Potential temperature profiles show thick boundary layer south of front. The cross frontal advection might be important because southerly wind is observed during the period. More detailed analysis is indispensable.

(5) Data and archives

These XCTD and GPS radiosonde data will be submitted to the Data Integration and Analysis Group (DIAG) of JAMSTEC just after the cruise.

Table 3.13.1: Launch log of XCTD between JKEO and KEO sites.

Station No.	Date [YYYY/MM/DD]	Time [hh:mm]	Latitude	Longitude	Depth [m]	SST [deg-C]	SSS [PSU]
JKEO	2015.04.27	05:28	38-02.65N	146-22.23E	5387	11.780	34.269
2	2015.04.27	06:57	37-46.12N	146-19.05E	5530	10.389	34.021
3	2015.04.27	08:28	37-30.31N	146-13.88E	5537	12.487	34.339
4	2015.04.27	09:58	37-15.00N	146-08.00E	5571	12.454	34.335
5	2015.04.27	11:34	36-59.81N	146-03.14E	5468	13.142	34.388
6	2015.04.27	13:05	36-44.78N	145-58.78E	5480	15.929	34.625
7	2015.04.27	14:32	36-30.23N	145-54.25E	5485	16.219	34.616
8	2015.04.27	16:04	36-15.18N	145-50.15E	5581	12.424	34.201
9	2015.04.27	17:37	36-00.90N	145-45.00E	5696	19.054	34.742
10	2015.04.27	19:07	35-45.37N	145-40.50E	5816	19.985	34.778
11	2015.04.27	20:26	35-29.56N	145-35.46E	5844	18.415	34.763
12	2015.04.27	22:04	35-15.44N	145-29.17E	5935	18.783	34.780
13	2015.04.27	23:34	34-59.60N	145-23.92E	5874	18.830	34.786
14	2015.04.28	01:05	34-44.67N	145-19.14E	5835	18.479	34.770
15	2015.04.28	02:36	34-30.22N	145-14.61E	5824	19.017	34.781
16	2015.04.28	04:05	34-15.56N	145-10.15E	5783	18.877	34.778
17	2015.04.28	05:35	34-00.74N	145-04.79E	5778	18.647	37.754
18	2015.04.28	07:04	33-46.03N	144-59.27E	5756	17.274	34.697
19	2015.04.28	08:38	33-30.77N	144-55.25E	5712	17.426	34.700
20	2015.04.28	10:02	33-15.66N	144-50.47E	5723	17.421	34.684
21	2015.04.28	11:32	32-59.82N	144-45.79E	5646	17.649	34.701
22	2015.04.28	13:03	32-44.48N	144-38.30E	5405	17.537	34.684
KEO	2015.04.28	14:48	32-27.54N	144-32.47E	5723	17.582	34.696

Table 3.13.2: Launch log of GPS radiosonde between the JKEO and KEO sites.

Sounding Number	Date (YYYYMMDDHH)	Lat. (deg.N)	Lon. (deg.E)	SLP (hPa)	TA (deg.C)	RH (%)	WD (deg.)	WS (m/s)	SST (deg.C)	Max. P (hPa)
RS011	2011042605	38.051	146.377	1012.8	12.2	69	230	5.1	11.689	149.6
RS012	2011042607	37.820	146.332	1013.3	12.2	74	191	5.2	10.647	149.9
RS013	2011042608	37.557	146.255	1013.6	12.6	82	169	4.5	12.496	162.5
RS014	2011042610	32.290	146.153	1014.0	12.6	80	143	7.3	12.501	135.3
RS015	2011042611	37.037	147.079	1014.0	13.8	74	145	9.3	12.923	114.3
RS016	2011042613	36.798	146.018	1013.2	15.0	72	149	14.0	15.801	196.1
RS017	2011042615	36.560	145.933	1012.7	15.7	76	200	8.8	16.309	112.8
RS018	2011042616	36.311	145.863	1011.8	15.8	76	199	9.6	12.281	173.8
RS019	2011042617	36.059	145.785	1011.9	18.0	72	178	15.9	19.054	144.9
RS020	2011042619	35.803	145.690	1012.0	18.0	75	201	13.8	19.983	168.5
RS021	2011042620	35.525	145.607	1012.7	17.7	76	198	13.4	18.408	144.9
RS022	2011042622	35.299	145.524	1012.9	17.9	75	190	14.9	18.792	169.9
RS023	2011042623	35.042	145.437	1013.1	18.0	76	178	14.7	18.702	161.6
RS024	2011042701	34.793	145.355	1013.5	18.0	80	192	14.2	18.460	160.7
RS025	2011042702	34.547	145.280	1013.4	18.3	73	193	12.3	18.996	134.9
RS026	2011042704	34.312	145.207	1013.1	18.0	82	192	13.3	18.894	141.4
RS027	2011042706	34.066	145.124	1011.6	17.8	86	181	14.5	18.641	159.4
RS028	2011042707	33.808	145.026	1011.8	17.6	83	178	12.1	17.279	154.7
RS029	2011042708	33.567	144.952	1011.8	17.6	90	170	10.7	17.434	137.2
RS030	2011042710	33.320	144.873	1011.0	17.6	92	156	10.8	17.420	90.7
RS031	2011042712	33.062	144.789	1010.8	17.8	91	165	12.0	17.612	127.2
RS032	2011042713	32.799	144.677	1009.0	17.7	94	160	9.8	17.535	155.2
RS033	2011042715	32.489	144.576	1007.3	17.3	84	150	17.3	17.588	64.3

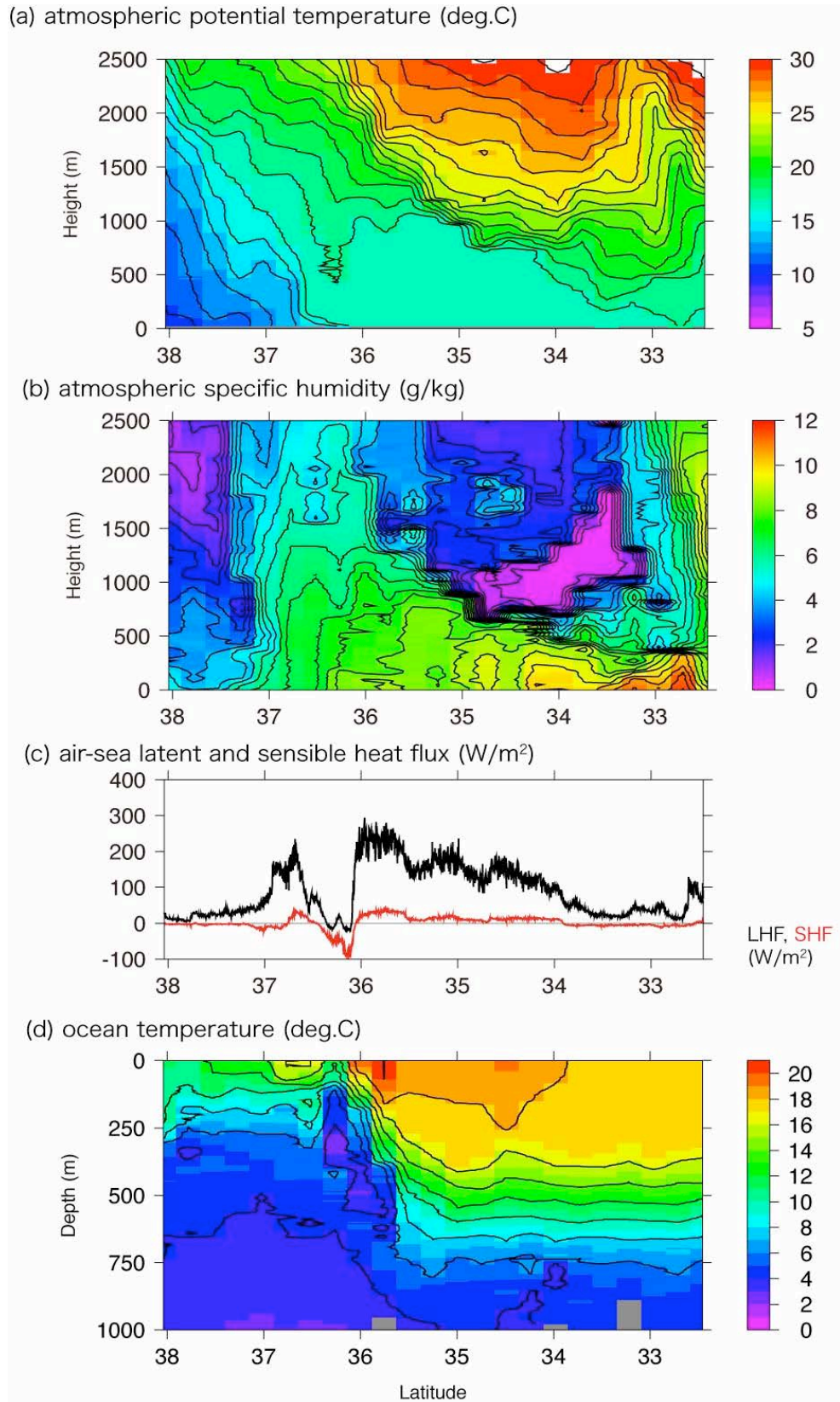


Figure 3.13.1: Cross front section of (a) atmospheric potential temperature, (b) specific humidity, (c) air-sea latent and sensible heat flux and (d) ocean temperature.

3.14 The Tohoku Earthquake impact on deep-sea environment

Shinsuke KAWAGUCCI (JAMSTEC - PEL)

Yukari T. YOSHIDA (JAMSTEC - Biogeos)

Takuroh NOGUCHI (Kochi Univ., JAMSTEC - KCC)

Ken TAKAI (JAMSTEC - Biogeos)

Weiren LIN (JAMSTEC - KCC)

(1) Objective

The Tohoku Earthquake (M=9.0) and the relevant Tsunami occurred on March 11 2011. The objective of our observation is to detect and understand geochemical and microbiological changes in deep-seawater environment induced by the mega earthquake, which implies activation of seafloor geofluid systems and exhaust of earthquake-energy-based ecosystem if it exists.

(2) Analyses

Four CTD-CMS hydrocasts were carried out at off Tohoku region (Stns. A-D, see *Section 1.7*). Sampled deep-sea water were subsampled adequately for each analysis. At onboard laboratory, H₂ concentration and fluid turbidity were determined. In addition to these, we plan to determine ³He/⁴He ratio and tritium concentration (Prof. Y. Sano, Univ. Tokyo), CH₄ and N₂O concentration and their stable isotope ratios (Dr. U. Tsunogai, Hokkaido Univ.), cation concentration including dissolved Mn and nutrients (Dr. K. Okamura, Kochi Univ.), and prokaryotic and viral abundances and their community structure (Drs. T. Nunoura and K. Takai, JAMSTEC).

3.15 Sampling for radiation monitoring

Makio HONDA (JAMSTEC)
Hajime KAWAKAMI (JAMSTEC)
Minoru KITAMURA (JAMSTE)

Fukushima No. 1 nuclear power plant (Fukushima #1 NPP) was seriously damaged by the earthquake and relevant tsunami on 11 March 2011. As a result, a large amount of radiation has been leaking from Fukushima #1 NPP to the atmosphere, land and ocean. It is great concern that radiation emitted to the ocean might affect aquatic resources and how this contamination will extend over the Pacific Ocean. Japanese government such as MEXT and Fishery Agency started to monitor radiation of seawater and creature off Fukushima. On the other hand, Japanese scientific societies, mainly the Oceanographic Society of Japan, started to organize scientific community and to conduct systematic marine radiation monitoring from off Fukushima to the pelagic ocean. In order to contribute this later monitoring network, surface water, suspended materials, phytoplankton and aerosol were collected.

(1) Water sampling

Water samples were collected along cruise track during this cruise. Sampling positions and date and time are shown in Fig. 1 and Table 1. Surface seawater pumped up at the bow to the laboratory of 20 L was collected in “cubitainer”. For first fourteen sample collected from Yokohama to K2, hydrochloric acid (HCl) of 20 ml and ammonium phosphomolybdate (AMP) of 10 mg were add to precipitate radioisotope of cesium (^{137}Cs). After station K2, only HCl of 20 ml was add to collected seawater. At stations K2 and S1, seawater samples at 10 m (surface mixed layer) and 200 m (subsurface water) were collected by carousel water sampling system.

After cruise, these water sample will be send to mainly the National Institute of Radiological Sciences (NIRS) in Chiba prefecture and concentration of ^{137}Cs will be determined by gamma-spectrometry after sample preparation.

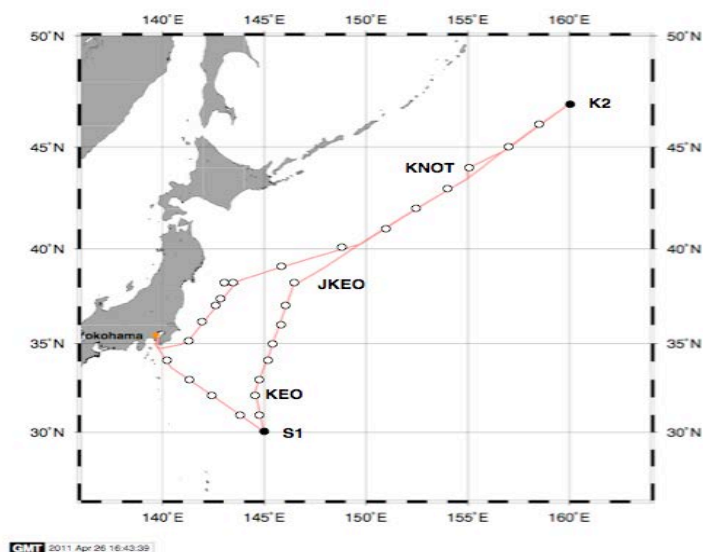


Fig. 1 Water sampling position

Table 1 Record of water sampling position

S/N	Date and Time (UTC)	Lat	Long	SST (deg-C)	Sal	Total Cs	Memo
1	2011.4.14 9:18	35-11.33610N	141-18.29610E	16.3	-		AMP add 10:51 / HCl add 11:27
2	2011.4.14 13:30	36-09.43930N	142-01.62750E	18.8	34.74		
3	2011.4.14 17:38	37-05.47720N	142-43.24320E	6.3	33.18		
4	2011.4.14 21:35	37-51.73670N	143-18.51000E	5.6	32.94		
5	2011.4.15 9:00	38-12.63300N	143-47.12210E	9.3	33.76	○	Stn. A
6	2011.4.16 0:08	38-06.82920N	143-04.97920E	8.1	33.60	○	Stn. D
7	2011.4.16 11:06	38-59.29000N	145-46.91750E	11.3	34.15	○	~ 39N
8	2011.4.16 21:38	40-01.56110N	149-03.08950E	3.2	32.83	○	~ 40N
9	2011.4.17 4:23	40-57.64740N	150-52.09970E	9.6	34.06	○	~ 41N
10	2011.4.17 10:23	41-57.39130N	152-27.74150E	3.1	32.95	○	~ 42N
11	2011.4.17 16:33	42-58.50390N	154-08.32240E	3.0	33.00	○	~ 43N
12	2011.4.17 21:26	43-59.63070N	154-59.85610E	2.6	32.98	○	KNOT
13	2011.4.18 8:34	44-57.67860N	157-03.00420E	3.6	33.06	○	~ 45N
14	2011.4.18 15:35	45-58.02430N	158-30.21060E	1.9	32.98	○	~ 46N
	2011.4.20 21:00	47N	160N			○	K2 10m only HCl (20ml) add
	2011.4.20 21:00	47N	160N			○	K2 200m only HCl (20ml) add
15-1	2011.4.21 2:45	47N	160N	1.7	33.01		K2 only HCl (20ml) add
15-2	2011.4.21 2:45	47N	160N	1.7	33.01		K2 only HCl (20ml) add
15-3	2011.4.21 2:45	47N	160N	1.7	33.01		K2 only HCl (20ml) add
15-4	2011.4.21 2:45	47N	160N	1.7	33.01		K2 only HCl (20ml) add
15-5	2011.4.21 2:45	47N	160N	1.7	33.01		K2 only HCl (20ml) add
16	2011.4.26 2:11	38-05N	146-25E	11.7	34.27	○	JKEO only HCl (20ml) add
17	2011.4.26 11:34	36-59.84660N	146-03.14340E	13.1	34.39	○	~ 37N only HCl (20ml) add
18	2011.4.26 17:25	36-01.20440N	145-46.11780E	18.9	34.74	○	~ 36N only HCl (20ml) add. Kuroshio extension?!
19	2011.4.26 23:32	35-00.02470N	145-24.20370E	18.8	34.78	○	~ 35N only HCl (20ml) add Kuroshio extension?!
20	2011.4.27 5:19	34-02.40360N	145-06.96700E	18.6	34.76	○	~ 34N only HCl (20ml) add
21	2011.4.27 11:22	33-00.98500N	144-47.02620E	17.7	34.73	○	~ 33N only HCl (20ml) add
22	2011.4.27 19:23	32-28.27530N	144-30.05910E	17.6	34.68	○	KEO only HCl (20ml) add
23	2011.4.28 4:03	31-02.10030N	144-49.01800E	18.6	34.70	○	~ 31N only HCl (20ml) add
	2011.4.28 22:00	30N	145E			○	S1 10m only HCl (20ml) add
	2011.4.28 22:00	30N	145E			○	S1 200m only HCl (20ml) add
24	2011.5.3 7:01	31-00.77120N	143-44.65610E	18.6	34.72	○	~ 31N only HCl (20ml) add
25							
26	2011.5.3 12:28	31-58.03760N	142-33.20380E	19.4	34.77	○	~ 32N only HCl (20ml) add
27	2011.5.3 18:29	33-00.48630N	141-15.96450E	20.3	34.65	○	~ 33N only HCl (20ml) add
28	2011.5.3 23:59	33-57.02580N	140-14.85750E	21.2	34.74	○	~ 34N only HCl (20ml) add

(2) Suspended particles

Suspended particles at two layers were collected at stations K2 and S1. In situ pumping / filtration system (McLane WTS-6-1-142V) was used.

	K2	S1
Sampling date and time (UTC)	2011.4.22 5:30 – 7:30	2011. 5. 2 7:00 – 9:00
Sampling depth (m)	10, 200	10, 200
Filter	Membrane (0.45 μm) *PALL Super membrane filter, materials: polysulfone Glass fiber (0.7 μm) *PALL TCLP GF filter	Membrane (0.45 μm) *PALL Super membrane filter, materials: polysulfone Glass fiber (0.7 μm) *PALL TCLP GF filter
Sampling volume (m^3) (filtration volume)	10 m, Membrane: 0.190 10 m, Glass fiber: 0.140 200 m, Membrane: 0.324 200 m, Glass fiber: 0.418	10 m, Membrane: 0.178 10 m, Glass fiber: 0.343 200 m, Membrane: 0.336 200 m, Glass fiber: 0.427

Sample on filters were frozen immediately onboard.

(3) Zooplankton sample

Zooplankton samples were also collected at station K2 and S1. Multiple opening / closing net system, IONESS, was used.

	K2	S1
Sampling date and time (UTC)	2011. 4. 23 10:00 – 13:00	2011. 5. 2 11:00 – 14:00
Sampling depth (m)	200-80, 80-0	200-50, 50-0
Sampling volume (m^3) (filtration volume)	4029.7, 1793.8	7205.7, 3393.4

Sample collected were frozen onboard.

(4) Aerosol

Ambient aerosol particles were collected along cruise track. High-Volume air Sampler (SHIBATA HV-525PM) was used. HVS was installed on the flying bridge and air was vacuumed up with speed of 500L min^{-1} . Start and stop of pumping were planned to be controlled automatically by “Wind-direction selection system” in order to avoid collecting the particle emitted by ship’s funnel. However, pumping was manually controlled because of malfunction of instrument.

By setting particle size selector for the HVS, two types of particles (larger or smaller than diameter of $2.5\ \mu\text{m}$) were separately collected on the filters (glass fiber filter for larger particle and quartz filter for smaller particle. Trapping efficiency of these filters is $> 99.9\%$ using $0.3\ \mu\text{m}$ standard particles). After sampling, two filters collected larger and smaller than $2.5\ \mu\text{m}$ were stored in plastic Petri dish and glass bottle under room temperature, respectively. Sampling log is shown in Table 2.

Table 2 Aerosol sampling log

Sample Name	A		B	C		
	Start	Stop	sampling volume (m ³)	power supply time (h)	memo	
MR03- 1 (Lat/Long)	2011.4.13 11:35	2011.4.14 8:56	331.9	11	Yokohama Date and Time are JST.	330
MR03- 2 (Lat/Long)	2011.4.14 9:09	2011.4.14 22:50	169.3	6.2	2011.4.14 10:00 Lv. Yokohama	186
MR03- 3 (Lat/Long)	2011.4.14 23:00	2011.4.15 10:08	0	3.2	No data ? Pumping was off when filter was changed although power was supplied.	96
MR03- 4 (Lat/Long)	2011.4.15 10:19	2011.4.16 9:44	431.1	21.1	Start at stn. A. / Stop at Stn. D Pumping was off when filter was changed although power was supplied.	633
MR03- 5 (Lat/Long)	2011.4.16 9:55	2011.4.17 6:11	48	6.2	Start at Stn. D / Stop at 40° N	186
MR03- 6 (Lat/Long)	2011.4.16 21:22	2011.4.18 1:06	51.5	9.5	Start at 40N / Stop at KNOT Lv. Restart once. Most sample obtained at KNOT. From this sampling, Date and Time are expressed as UTC.	285
MR03- 7 (Lat/Long)	2011.4.18 1:18	2011.4.19 1:53	568.7	22.1	Start KNOT Lv./Stop K2 Arv. Restart twice	663
MR03- 8 (Lat/Long)	2011.4.19 2:01	2011.4.23 12:45	2,850.7	-	Start K2 Arv. / Stop K2 Lv.	-
MR03- 9 (Lat/Long)	2011.4.23 12:57	2011.4.24 7:24	553.4	18.45	Start K2 Lv. / Stop East of KNOT	553.5
MR03- 10 (Lat/Long)	2011.4.24 7:33	2011.4.26 3:37	1321.8	44.07	Start East of KNOT / Stop JKEO	1322
MR03- 11 (Lat/Long)	2011.4.26 3:48	2011.4.28 9:50	1618.8	54.03	Start JKEO / Stop S1 Arv.	1621
MR03- 12 (Lat/Long)	2011.4.28 9:59	2011.5.3 2:05	3363.6	112.10	Start S1 Arv. / Stop S1 Lv.	3363
MR03- 13 (Lat/Long)	2011.5.3 2:05	2011.5.4 23:24	1355.1	45.31	Start S1 Lv. / Stop Yokohama	1359

$$C = B * 60 * 500 / 1000 (\sim = A)$$

4. Geophysical observation

4.1 Swath Bathymetry

Takeshi MATSUMOTO (University of the Ryukyus): Principal Investigator (not on-board)

Masao NAKANISHI (Chiba University): Principal Investigator (not on-board)

Souichiro SUEYOSHI (Global Ocean Development Inc.: GODI)

Norio NAGAHAMA (GODI)

Wataru TOKUNAGA (Mirai Crew)

(1) Introduction

R/V MIRAI is equipped with a Multi narrow Beam Echo Sounding system (MBES), SEABEAM 2112.004 (SeaBeam Instruments Inc.). The objective of MBES is collecting continuous bathymetric data along ship's track to make a contribution to geological and geophysical investigations and global datasets.

(2) Data Acquisition

The "SEABEAM 2100" on R/V MIRAI was used for bathymetry mapping during the MR11-03 cruise from 14 April to 4 May 2011.

To get accurate sound velocity of water column for ray-path correction of acoustic multibeam, we used Surface Sound Velocimeter (SSV) data to get the sea surface (6.2m) sound velocity, and the deeper depth sound velocity profiles were calculated by temperature and salinity profiles from CTD and XCTD data by the equation in Del Grosso (1974) during the cruise.

Table 4.1-1 shows system configuration and performance of SEABEAM 2112.004 system.

Table 4.1-1 System configuration and performance

SEABEAM 2112.004 (12 kHz system)

Frequency:	12 kHz
Transmit beam width:	2 degree
Transmit power:	20 kW
Transmit pulse length:	3 to 20 msec.
Depth range:	100 to 11,000 m
Beam spacing:	1 degree athwart ship
Swath width:	150 degree (max) 120 degree to 4,500 m 100 degree to 6,000 m 90 degree to 11,000 m
Depth accuracy:	Within < 0.5% of depth or +/-1m, whichever is greater, over the entire swath. (Nadir beam has greater accuracy; typically within < 0.2% of depth or +/-1m, whichever is greater)

(3) Preliminary Results

The results will be published after primary processing.

(4) Data Archives

Bathymetric data obtained during this cruise will be submitted to the Data Management Group (DMG) in JAMSTEC, and will be archived there.

4.2 Sea surface gravity

Takeshi MATSUMOTO (University of the Ryukyus): Principal Investigator (not on-board)

Masao NAKANISHI (Chiba University): Principal Investigator (not on-board)

Souichiro SUEYOSHI (Global Ocean Development Inc.: GODI)

Norio NAGAHAMA (GODI)

Wataru TOKUNAGA (Mirai Crew)

(1) Introduction

The local gravity is an important parameter in geophysics and geodesy. We collected gravity data at the sea surface.

(2) Parameters

Relative Gravity [CU: Counter Unit]

$$[\text{mGal}] = (\text{coef1: } 0.9946) * [\text{CU}]$$

(3) Data Acquisition

We measured relative gravity using LaCoste and Romberg air-sea gravity meter S-116 (Micro-g LaCoste, LLC) during the MR11-03 cruise from 14 April 2011 to 5 May 2011.

To convert the relative gravity to absolute one, we measured gravity using portable gravity meter (Scintrex gravity meter CG-5), at Yokohama as the reference points.

(4) Preliminary Results

Absolute gravity table is shown in Tabel 4.2-1.

Table 4.2-1

No.	Date	U.T.C.	Port	Absolute Gravity [mGal]	Sea Level [cm]	Draft [cm]	Gravity at Sensor * ¹ [mGal]	L&R * ² Gravity [mGal]
#1	13 Apr.	23:43	Yokohama	979742.21	258	620	979743.05	12023.91
#2	05 May	03:20	Yokohama	979742.19	338	590	979743.27	12024.22

*¹: Gravity at Sensor = Absolute Gravity + Sea Level*0.3086/100 + (Draft-530)/100*0.0431

*²: LaCoste and Romberg air-sea gravity meter S-116

(5) Data Archives

Surface gravity data obtained during this cruise will be submitted to the Data Management Group (DMG) in JAMSTEC, and will be archived there.

5. Satellite Image Acquisition (MCSST from NOAA/HRPT)

Makio HONDA (JAMSTEC)
Souichiro SUEYOSHI (Global Ocean Development Inc.: GODI)
Norio NAGAHAMA (GODI)
Wataru TOKUNAGA (Mirai Crew)

(1) Objectives

It is our objectives to collect data of sea surface temperature in a high spatial resolution mode from the Advance Very High Resolution Radiometer (AVHRR) on the NOAA polar orbiting satellites and to build a time and depth resolved primary productivity model.

(2) Method

We receive the down link High Resolution Picture Transmission (HRPT) signal from NOAA satellites. We processed the HRPT signal with the in-flight calibration and computed the sea surface temperature by the Multi-Channel Sea Surface Temperature (MCSST) method. A daily composite map of MCSST data is processed for each day on the R/V MIRAI for the area, where the R/V MIRAI located.

We received and processed NOAA data throughout MR11-03 cruise from 14 April 2011 to 5 May 2011.

The sea surface temperature data will be applied for the time and depth resolved primary productivity model to determine a temperature field for the model.

(3) Preliminary results

Fig.5-1 showed MCSST composite image during this cruise from 14 April 2011 to 3 May 2011 at the Northern-west Pacific Ocean.

(5) Data archives

The raw data obtained during this this cruise will be submitted to the Data Management Group (DMG) in JAMSTEC, and will be archived there.

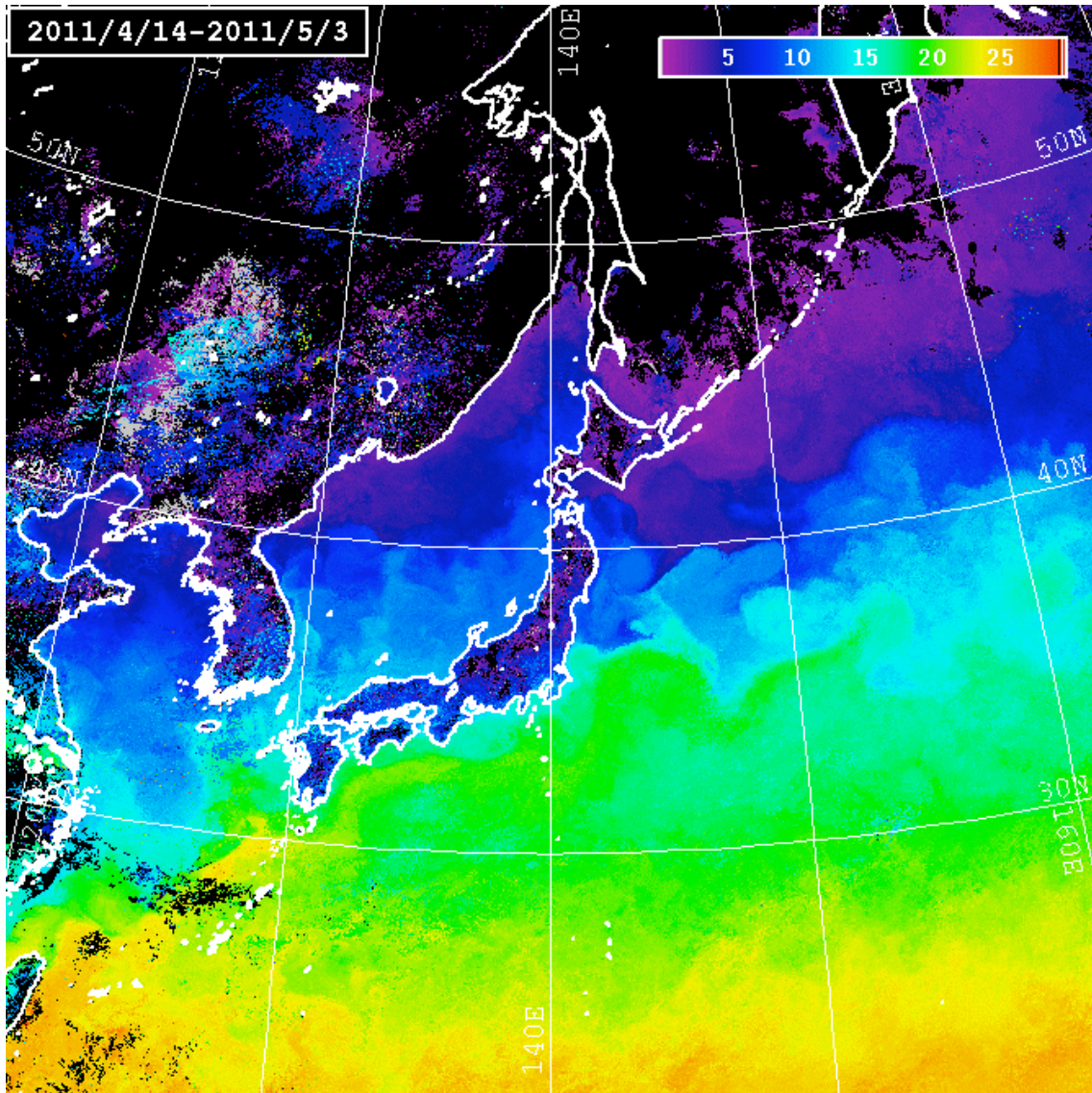


Fig.5-1 MCSST composite image at Northern-west Pacific Ocean.
from 14 April 2011 to 3 May 2011